Josip Juraj Strossmayer University of Osijek, Croatia
University of Dubrovnik, Croatia
Ruđer Bošković Institute, Zagreb, Croatia

University Postgraduate Interdisciplinary Doctoral Study
Molecular Biosciences

Lana Vujica

UNDERSTANDING THE ECOTOXICOLOGICAL ROLE OF THE OATP1D1 TRANSMEMBRANE TRANSPORTER USING A ZEBRAFISH (*DANIO RERIO* HAMILTON, 1822) *OATP1D1* MUTANT LINE

DOCTORAL THESIS

Ocjena rada u tijeku

Osijek, 2025.

TEMELJNA DOKUMENTACIJSKA KARTICA

Sveučilište Josipa Jurja Strossmayera u Osijeku **Doktorski rad**
Sveučilište u Dubrovniku
Institut Ruđer Bošković
Doktorski studij Molekularne bioznanosti

Znanstveno područje: Interdisciplinarno područje znanosti
Znanstvena polja: Biologija i Kemija

Razumijevanje ekotoksikološke uloge Oatp1d1 transmembranskog prijenosnika korištenjem *oatp1d1* mutantne linije ribe zebrice (*Danio rerio* Hamilton, 1822)

Lana Vujica

Doktorski rad je izrađen u: Laboratoriju za molekularnu ekotoksikologiju, Zavod za istraživanje mora i okoliša, Institut Ruđer Bošković
Mentor/i: dr.sc. Tvrtko Smital, dr.sc. Ivan Mihaljević

Kratki sažetak doktorskog rada:
Transmembranski prijenosnici organskih aniona (eng. *Organic Anion Transporting Polypeptides*; OATPs) posreduju u unosu brojnih spojeva u eukariotske stanice. *In vitro* istraživanja na Oatp1d1 prijenosniku ribe zebrice (*Danio rerio*) snažno upućuju na njegovu ekotoksikološku važnost, dok su fiziološke posljedice nedostatka Oatp1d1 proteina još uvijek nepoznate. Stoga je cilj ovog istraživanja detaljna *in vivo* karakterizacija Oatp1d1 prijenosnika u svrhu razumijevanja njegove fiziološke i ekotoksikološke uloge. Fenotipskom karakterizacijom Oatp1d1 mutanata dobivenih CRISPR-Cas9 metodologijom, toksikološkim eksperimentima izlaganja, te analizom ekspresijskih profila srodnih prijenosnika, uočena je moguća fiziološka uloga Oatp1d1 prijenosnika u regulaciji razvoja pigmentacije, kao i dvostruka uloga Oatp1d1 prijenosnika ovisno o metabolizmu supstrata kroz različitu osjetljivost WT i Oatp1d1 embrija zeborice pri izlaganju modelnim zagađivalima diklofenaku i PFOS-u. Provedene analize dodatno ukazuju na kompleksnost uloge membranskih prijenosnika te pružaju temelj za daljnja *in vivo* istraživanja važnosti Oatp1d1 prijenosnika u staničnoj detoksifikaciji i obrani organizma.

Broj stranica: 196
Broj slika: 59
Broj tablica: 9
Broj literaturnih navoda: 311
Jezik izvornika: engleski
Ključne riječi: ADME, *Danio rerio*, Oatp1d1, Fenotip, Diclofenac, PFOS

Datum javne obrane:
Povjerenstvo za javnu obranu:
1.
2.
3.
4. (zamjena)

Doktorski rad je pohranjen u: Nacionalnoj i sveučilišnoj knjižnici Zagreb, Ul. Hrvatske bratske zajednice 4, Zagreb;Gradskoj i sveučilišnoj knjižnici Osijek, Europska avenija 24, Osijek; Sveučilištu Josipa Jurja Strossmayera u Osijeku, Trg sv. Trojstva 3, Osijek

Ocjena rada u tijeku

BASIC DOCUMENTATION CARD

Josip Juraj Strossmayer University of Osijek **PhD thesis**
University of Dubrovnik
Ruđer Bošković Institute
Doctoral Study of Molecular biosciences

Scientific Area: Interdisciplinary area of science
Scientific Fields: Biology and Chemistry

Understanding the ecotoxicological role of the Oatp1d1 transmembrane transporter using a zebrafish (*Danio rerio* Hamilton, 1822) *oatp1d1* mutant line

Lana Vujica

Thesis performed at: Laboratory for molecular ecotoxicology, Division for Marine and Environmental Research, Ruđer Bošković Institute, Zagreb
Supervisor/s: Dr. Tvrtko Smital, Dr. Ivan Mihaljević

Short abstract:
Organic anion-transporting polypeptides (OATPs) mediate the uptake of various compounds into eukaryotic cells. *In vitro* studies on the zebrafish (*Danio rerio*) Oatp1d1 transporter strongly suggest its ecotoxicological importance, while the physiological consequences of Oatp1d1 deficiency are still largely unknown. Therefore, this study aims at a detailed *in vivo* characterisation of Oatp1d1 to better understand its physiological and ecotoxicological role. Through phenotypic characterisation of CRISPR-Cas9-generated mutants, toxicological exposure experiments and expression profiling of related transporters, we observed a potential role of Oatp1d1 in pigment development and a dual function depending on substrate metabolism, reflected in the different sensitivity of WT and Oatp1d1 mutant embryos to model environmental contaminants diclofenac and PFOS. These results highlight the complex role of membrane transporters and form the basis for further *in vivo* research on the role of Oatp1d1 in cellular detoxification and organismal defence.

Number of pages: 196
Number of figures: 59
Number of tables: 9
Number of references: 311
Original in:
Key words: ADME, *Danio rerio*, Oatp1d1, Phenotype, Diclofenac, PFOS

Date of the thesis defense:
Reviewers:
1.
2.
3.
4. (substitute)

Thesis deposited in: National and University Library in Zagreb, Ul. Hrvatske bratske zajednice 4, Zagreb; City and University Library of Osijek, Europska avenija 24, Osijek; Josip Juraj Strossmayer University of Osijek, Trg sv. Trojstva 3, Osijek

Ocjena rada u tijeku

Acknowledgments

Ocjena rada u tijeku

Table of contents

Ocjena rada u tijeku

Ocjena rada u tijeku

Ocjena rada u tijeku

List of abbreviations

17β-E2 – 17β-Estradiol

ABC – ATP-binding cassette

ADME – Absorption, Distribution, Metabolism, and Elimination

AKR – Aldo-keto reductase

AO – Acridine Orange

ASBT – Apical sodium-dependent bile acid transporter

ATG – Start Codon (Adenine-Thymine-Guanine)

ATP – Adenosine Triphosphate

ATP50 - ATP synthase, H+ transporting, mitochondrial F1 complex, beta polypeptide

BBB – Blood-brain barrier

Bco1/Bco2 – β-Carotene Oxygenase 1/2

BCRP – Breast cancer resistance protein

BSA – Bovine Serum Albumin

CAT – Catalase

Cas9 – CRISPR-associated protein 9

COMT – Catechol-O-methyltransferase

COX – Cyclooxygenase

CRISPR - Clustered Regularly Interspaced Short Palindromic Repeats

CT – Citrate Buffer

CYP – Cytochrome P450

DAPI – 4′,6-Diamidino-2-Phenylindole

Ocjena rada u tijeku

DCF – 2′,7′-Dichlorofluorescein

DCFH-DA – 2′,7′-Dichlorodihydrofluorescein Diacetate

DCT – Deparaffinisation and Citrate Treatment

DHEAS – Dehydroepiandrosterone sulfate

DMSO – Dimethyl Sulfoxide

dpf – Days Post Fertilization

dpe – Days Post-Exposure

E1 – Estrone

E2 – Estradiol

E17β-glucuronide - Estradiol-17β-glucuronide

E3S – Estrone-3-sulfate

ECL – Extracellular loop

EE2 – Ethinylestradiol

EF1α – Elongation Factor 1 Alpha

EPHX – Epoxide hydrolase

ER – Endoplasmic reticulum

EVL – Enveloping Layer

F3 – Filial Generation 3

FBS – Fetal Bovine Serum

FET – Fish Embryo Toxicity

FITC - Fluorescein Isothiocyanate

FMO – Flavin-containing monooxygenase

GAR-CY3 – Goat Anti-Rabbit IgG Conjugated with Cy3

GFP – Green Fluorescent Protein

GHB – Gamma-hydroxybutyric acid

GPX – Glutathione peroxidase

Ocjena rada u tijeku

GST – Glutathione S-transferase

GTPCH – GTP Cyclohydrolase I

HAB – Harmful algal bloom

HEK / HEK293T – Human Embryonic Kidney (293T)

HRMA – High-Resolution Melting Analysis

hpf – Hours Post Fertilization

IC_{50} – Half maximal inhibitory concentration

IL – Intracellular loop

IPTM – Interface Predicted Template Modeling Score

K_m – Michaelis constant (enzyme kinetics)

LB – Lysogeny Broth

LC_{50} – Lethal Concentration 50%

Log POW - Octanol-water partition coefficient (log Partition coefficient)

LY – Lucifer Yellow

MATE – Multidrug and Toxic Compound Extrusion

MCT – Monocarboxylate Transporter

MC – Microcystin

MDR – Multidrug Resistance

MFS – Major Facilitator Superfamily

MNE – Mean Normalized Expression

MO – Morpholino Oligonucleotide

MRP – Multidrug Resistance-Associated Protein

NAT – N-acetyltransferase

NGS – Normal Goat Serum

NaN3 – Sodium Azide

NQO – NAD(P)H-quinone oxidoreductase

Ocjena rada u tijeku

NSAID – Non-steroidal Anti-inflammatory Drug

OAT – Organic Anion Transporter

OATP – Organic Anion Transporting Polypeptide

OCT / OCTN – Organic Cation Transporter / Organic Cation/Carnitine Transporter

OCT (medium) – Optimal Cutting Temperature

OECD – Organisation for Economic Co-operation and Development

PAE – Predicted Aligned Error

PBS – Phosphate Buffered Saline

PBSt – Phosphate Buffered Saline with Tween-20

PFA – Paraformaldehyde

PFAS – Per- and Polyfluoroalkyl Substances

PFOA – Perfluorooctanoic Acid

PFOS – Perfluorooctanesulfonic Acid

pLDDT – Predicted Local Distance Difference Test

Plin6 – Perilipin 6

PPAR – Peroxisome Proliferator-Activated Receptor

PVF – Perivitelline Fluid

qPCR – Quantitative Polymerase Chain Reaction

ROS – Reactive Oxygen Species

RT – Room Temperature

RT-PCR – Reverse Transcription Polymerase Chain Reaction

scarb1 – Scavenger Receptor Class B Member 1

SDS – Sodium Dodecyl Sulfate

SLC – Solute Carrier

SLCO – Solute Carrier Organic Anion Transporter Family

sgRNA – Single Guide RNA

Ocjena rada u tijeku

SOD – Superoxide Dismutase

SULT – Sulfotransferase

T3 – Triiodothyronine

T4 – Thyroxine

TCDC – Taurochenodeoxycholate

TMD – Transmembrane Domain

TPMT – Thiopurine S-methyltransferase

T-X-100 – Triton X-100

TBSt – Tris Buffered Saline with Tween-20

TXN – Thioredoxin

UGT – UDP-glucuronosyltransferase

URAT1 – Uric Acid Transporter 1

UTR – Untranslated Region

V_{max} – Maximum Rate of Enzyme-Catalyzed Reaction

Vtg – Vitellogenin

WT – Wild-Type

ZFNs – Zinc Finger Nucleases

Ocjena rada u tijeku

1. INTRODUCTION

1.1. ADME at the cellular level, the role of biological membranes and membrane transporters

Biological membranes, thin barriers composed of amphipathic molecules, define both the boundaries of all cells as well as the diversity of the internal compartments in eukaryotes. Despite their fluid nature, membranes are crucial for maintaining the internal organization, functional identity and integrity of cells (Gould, 2018). They are composed of lipids, proteins, and carbohydrates (in the form of glycolipids and post-translationally modified proteins). The current understanding is best represented by the "fluid mosaic model" (Singer & Nicolson, 1972). This model emphasizes the dynamic nature of membranes, highlighting the lateral mobility of lipids and proteins. Membrane proteins play a vital role in biological membranes, as they help to maintain the structural integrity, organization and flow of material through membranes (Watson, 2015). In addition, considering their role in regulating cellular entry and exit, biological membranes and embedded transport proteins directly impact absorption, distribution, metabolism, and elimination (ADME) processes at the cellular level. Synthesis of membrane proteins in eukaryotic cells, destined for the plasma membrane, endoplasmic reticulum (ER) or any other membrane-bound compartment begins on cytosolic ribosomes. After a short segment of protein has been synthesized, the ribosome, mRNA and nascent protein chain associate with the ER, where the rest of the protein is made and simultaneously inserted into the membrane, the process is referred to as co-translational targeting (Watson, 2015).

The acronym "ADME" was first presented in English by Nelson in 1961, who rephrased resorption, distribution, consumption and elimination used by Teorell in 1937 (Nelson, 1961; Teorell, 1937). Traditionally, ADME at the cellular level is described in three main phases (phases I, II and III). However, “phase 0,” which encompasses the entry of a drug into the cell via influx (uptake) transporters has been more recently proposed as integral phase of cellular detoxification machinery (Petzinger & Geyer, 2006). Therefore, the ADME on the cellular level includes:

(i) Phase 0: influx (uptake) of endo- and xenobiotics by uptake transporters;

Ocjena rada u tijeku

(ii) Phase I: Introduction of a reactive group into the molecule, oxidative, reductive and hydrolytic drug metabolism which includes CYP enzymes and flavin-containing monooxygenases;

(iii) Phase II: drugs and phase I metabolites further detoxified by enzymes and conjugation reactions, and

(iv) Phase III: Transport of water-soluble phase I and II metabolites out of the cell, mediated by efflux transporters (Zaïr et al., 2008).

The main function and physiological goal of all elements of the ADME process is elimination of endo- and/or xenobiotics that might be potentially toxic for the cell and/or organism, or are simply not useful as the source of energy, building material for cellular structures or signaling molecules. Yet, the main problem that should be addressed at the cellular level is the fact that many endo- or xenobiotics are simply not soluble enough in cellular or body fluids to be efficiently removed. Therefore, once the potential toxins enter the cytoplasm, biotransformation is required to eliminate or inactivate them and to make them more hydrophilic (Figure 1). The first step in this process is often an oxidative modification (phase I), in which the chemicals are converted into more hydrophilic metabolites, which are then excreted. This oxidation is primarily carried out by flavoprotein monooxygenase (FMO) and cytochrome P450 enzymes (CYP), particularly from the CYP1, CYP2, CYP3 and CYP4 families. After oxidation, reductive or conjugative modifications (phase II) are carried out by enzymes such as glutathione S-transferases (GSTs), sulphotransferases (SULTs), UDP-glucuronosyltransferases (UGTs), N-acetyltransferases (NATs), aldoketo-keto reductases (AKRs), epoxide hydrolases (EPHXs) and NAD(P)H-quinone oxidoreductases (NQOs). These enzymes enable primary or secondary conjugation reactions or reduce and hydrolyse toxins (Goldstone et al., 2006).

Considering the context described, the central theme of this dissertation, and the fact the central paradigm in toxicology traditionally encompasses (1) source of contamination, (2) absorption, distribution, metabolism and elimination (ADME) of chemicals, and (3) effects of contaminants (Stegeman et al. 2010), it is important to explain in more detail a relatively new “chemical defensome” paradigm (Goldstone, 2006), and more specifically the role of membrane transporters in the ADME processes. In general, chemical defensome concept extends the traditional ADME paradigm by emphasizing coordinated action among sensors, metabolic enzymes, and transporters

Ocjena rada u tijeku

to protect cells against chemical treats. Defensome genes and proteins include transcription factors that sense toxicant or cellular damage, membrane transport proteins that mediate uptake or efflux of xenobiotics and their metabolites across the cell membrane, enzymes that are involved in the metabolism of xenobiotics in the cytosol, and antioxidant enzymes that protect the cell against reactive oxygen species (ROS) and other radicals (Stegeman et al. 2010). Antioxidant defense mechanisms are a crucial component of the protective systems of organisms that live in an aerobic environment. Reactive oxygen species (ROS), which can be produced by toxins, UV radiation or regular metabolic activities, can damage DNA, lipids and proteins, which can lead to various diseases and toxic effects. The most important antioxidant enzymes involved in the neutralisation of ROS include superoxide dismutases (SODs), catalases (CATs) and peroxidases such as glutathione peroxidases (GPXs) and thioredoxins (TXNs) (Goldstone et al., 2006).

Importantly, a large portion of the defensome includes the phase 0 polyspecific uptake transporters that mediate entrance of compounds into the cell, and the phase III efflux transporters (Figure 1) from the ATP-binding Cassette superfamily (ABC) and Multidrug and Toxic compound Extrusion (MATE) family that mediate efflux of compounds and their metabolites out of the cell. As crucial parts of ADME processes, membrane transporters are recognized as key determinants of toxicological response to various xenobiotics (Klaassen and Lu, 2008). It has traditionally been considered that compounds (especially lipophilic) enter the cell by passive diffusion. In the past decades, however, uptake transporters have been characterized and recognized as key players in mediating the entrance of metabolites and foreign compounds into the cell by the means of facilitated diffusion. Together with the efflux transporters from the ABC and MATE families, uptake transporters from the Organic anion transporting polypeptide (OATP/Oatp) family (gene name SLC21, synonym SLCO) and SLC22/Slc22 family determine cellular concentrations and pharmacological or toxic effects of xenobiotics (Klaassen and Lu, 2008; Zair et al.; 2008; Koepsell, 2013).

Ocjena rada
u tijeku

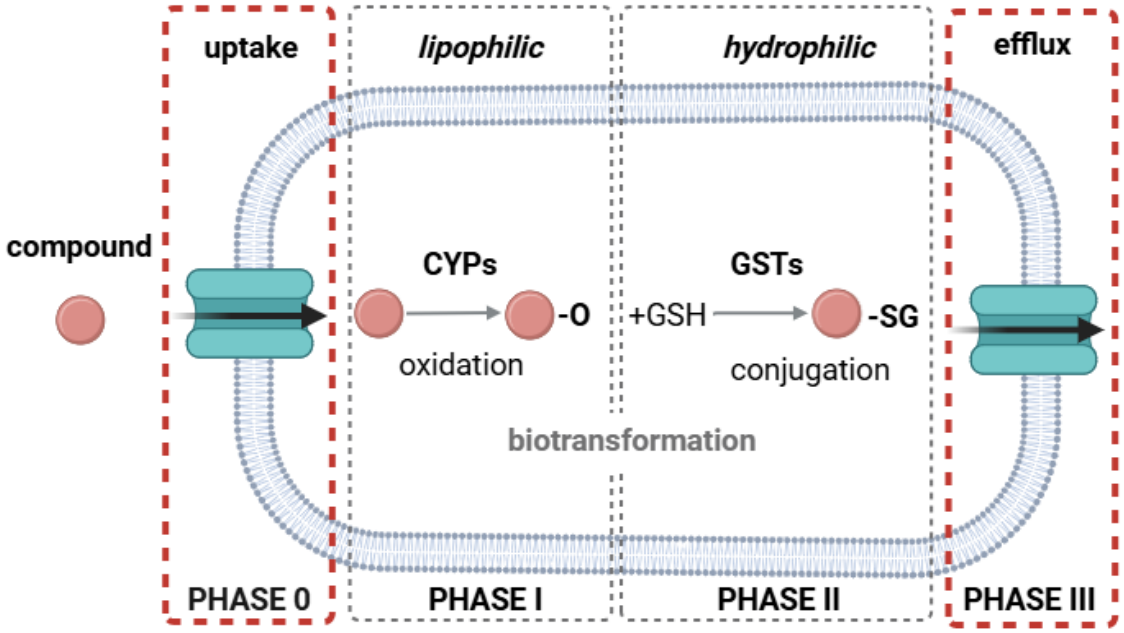

Figure 1. Schematic representation of the four phases of ADME at the cellular level. Membrane transporters are part of phase 0 (uptake transporters) and phase III (efflux transporters). After a (endogenous or exogenous) compound has entered the cell, it is biotransformed with phase I and II enzymes so that it can be efficiently removed from the cell.

1.2. Membrane transporters and ADME at the level of organisms and specific organs

Membrane transporters have a wide, but specific tissue distributions. There are two major superfamilies of transporters: the solute carrier (SLC) and ATP-binding cassette (ABC) transporters (Dean et al., 2001). SLC family comprises more than 400 membrane-bound proteins (Talevi & Bellera, 2022) and mainly includes organic anion-transporting polypeptides (OATPs/SLCOs), organic anion transporters (OATs/SLC22As), organic cation transporter (OCTs/SLC22As), organic cation and carnitine transporters (OCTNs/SLC22As), peptide transporters (PEPTs/SLC15As), and multidrug and toxin extrusions (MATEs/SLC47As). Generally, OCTs transport organic cations, OATPs transport large and fairly hydrophobic organic anions, OATs transport the smaller and more hydrophilic organic anions, PEPTs are responsible for the uptake of di-/tripeptides and peptide-like drugs, and MATEs are responsible for efflux of organic cations.

Ocjena u tijeku

Consequently, knowledge and awareness within the biomedical field and pharmaceutical industry related to the impact of membrane transporters on ADME, multiple endogenous and xenobiotic processes and drug safety, is growing rapidly (Keogh, 2012). There is interplay between efflux and uptake transporters which results with their different distribution in the cell, tissue or organs. Many drugs are substrates and/or inhibitors of multiple transporters, and the following scenarios contribute to this interaction: (i) same location on the cell surface, different function, (ii) opposite location on the cell surface, complementary function, and (iii) complex distribution in different tissues and cell layers (Keogh, 2012). That fine and complex regulation of expression and localization of membrane transporters enables cells to maintain and regulate internal traffic and availability of all substances needed for growth and differentiation, but also to get rid of toxic compounds and thus to maintain homeostasis.

1.2.1. Membrane transporters in the intestine

As already emphasized, the primary purpose of cellular detoxification is to remove endogenous and/or exogenous molecules from the organism by processes that typically converts lipophilic chemicals into hydrophilic products to facilitate their excretion (Almazroo et al., 2017; Benedetti et al., 2009; Ionescu & Caira, 2005). However, it is important to point out that drug-metabolizing enzymes in some cases convert substances into their pharmacologically active form. E.g., prodrugs (pharmacologically inactive) are synthesised to overcome absorption/bioavailability issues and are converted into an active drug after absorption into the body (Almazroo et al., 2017).

At the organism level, the principle site for the absorption of orally administered drugs nutrients and toxins is gastrointestinal tract. This process depends not only on transcellular and paracellular diffusion through intestinal wall (Turner, 2009), but also on uptake transporters expressed at the brush-border membrane of enterocytes (Kullak-Ublick et al., 2004) and efflux transporters which can reduce oral bioavailability of drugs (Zaïr et al., 2008). Except xenobiotic compounds, transporters are engaged for the uptake or efflux processes of endogenous compounds (e.g., bile acids, sterols) and nutrients. After uptake from gut lumen into the enterocytes, compounds are translocated by the efflux protein pumps across the basolateral membrane into the portal blood circulation, then to the liver, and finally into the systemic circulation.

Ocjena rada u tijeku

The enterocyte apical (luminal) membrane hosts numerous uptake transporters. From the (eco)toxicological standpoint, the most relevant among them are some members of the SLC (Solute Carrier) superfamily: organic anion transporting polypeptide 2B1 (OATP2B1), organic cation transporter 1 (OCT1) and 3 (OCT3), as well as efflux transporters. The most relevant among efflux transporters appear to be the ABCB1 (P-glycoprotein, MDR1), ABCC2 (MRP2) and breast cancer resistance protein (BCRP). On the basolateral membrane, except some bidirectional transporters (Figure 2) critical transporters are multidrug resistant protein 1 (MRP1) and 3 (MRP3) (Drozdzik et al., 2020). Therefore, uptake of endo- and xenobiotics into enterocytes is mostly mediated by members of the SLC superfamily (OATP, PEPT1 (SLC15), ASBT (SLC10) and MCT1 (SLC16)), and efflux of original substances or their metabolites is mediated by members of the ABC superfamily (MRP2, BCRP and P-gp) (Xue et al., 2019) (Figure 2). This complex interplay between drug-metabolizing enzymes and transporters, both of them expressed in the gut, alters overall systemic availability of numerous drugs (Almazroo et al., 2017).

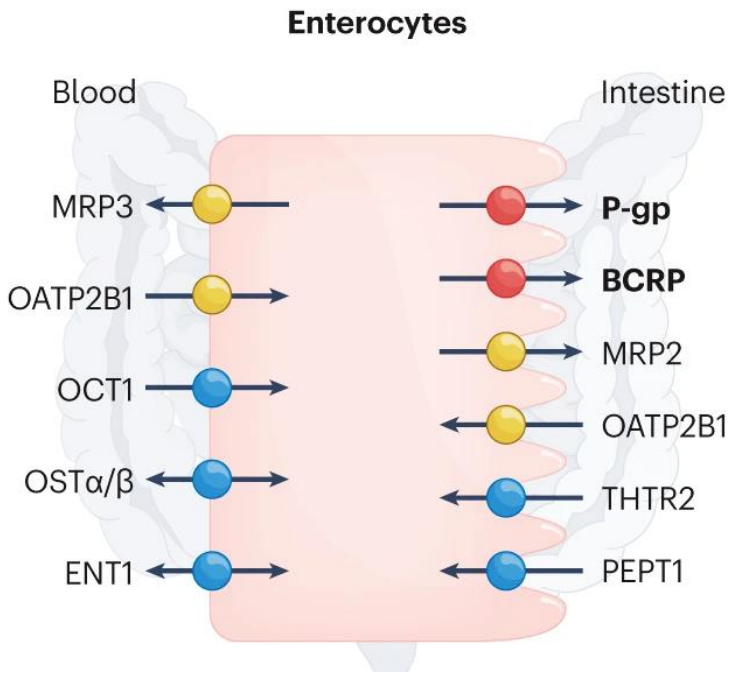

Figure 2. Membrane transporters in the plasma membrane of enterocytes. Figure adapted from Galetin et al., 2024.

Ociarada.u

The expression, function and localization of intestinal transporters are controlled and regulated by multiple regulatory mechanisms at both transcriptional and post-transcriptional levels. At the transcriptional level, nuclear receptors, important mediators, directly regulate the expression of transporter genes. Post-transcriptional regulation, on the other hand, occurs independently of the mRNA level and influences protein synthesis, cellular localization and functional activity. In addition, physiological and pathophysiological conditions can dynamically modulate the expression and activity of transporters, which emphasizes the complexity of these regulatory networks (Xue et al., 2019). Among patophysiological conditions, research on polymorphisms within the SLC transporter family has mainly focused on the OATP transporters. For example, the OATP2B1 variant S486F (identified in ~31 % of Japanese individuals) reduces transport capacity by over 50 % (Nozawa et al., 2002). Similarly, genetic variations in OATP1A2, such as the A516C and A404T variants, significantly impair the uptake of substrates such as estrone-3-sulphate and delta opioid receptor agonists *in vitro* (W. Lee et al., 2005). However, as mentioned above, the low intestinal expression of OATP1A2 probably has limited clinical impact on the absorption kinetics of substrates that rely on this transporter (Xue et al., 2019).

To summarize, oral absorption of drugs is determined by intestinal ABC transporters providing efflux activity and the uptake transporters that facilitate absorption of drugs (Estudante et al., 2013; König et al., 2013; Kramer, 2011). Interestingly, intestinal transporters are not uniformly distributed; each segment of the gastrointestinal tract has a distinct set of transporters, influencing drug absorption depending on where it is administered (Drozdzik et al., 2014, 2020).

1.2.2. Membrane transporters in the liver

Following absorption in the intestine, xenobiotics and nutrients reach the liver, a primary organ for drug metabolism and detoxification processes. Numerous studies have shown that the liver is responsible for more than 70 % of the metabolism and excretion of human drugs in the clinic (Patel et al., 2016), and as the main site of drug metabolism, parenchymal liver cells (hepatocytes) account for almost 80 % of the total liver volume and 60 % of the total number of liver cells from (Kmieć, 2001; Pan, 2019). After entering the bloodstream, the compounds are transported via the portal vein to the liver, where they are first metabolized. Hepatic excretion of drugs/xenobiotics, mediated by the membrane transporters expressed at the sinusoidal (basolateral) membrane of liver

Ocjena rada u tijeku

hepatocytes (Figure 3), is primarily linked to metabolism mediated by phase I and phase II enzyme reactions (Zuber et al., 2002). The most common phase I drug-metabolizing enzymes are represented by CYP450 superfamily, the major group of enzymes that chemically modify drugs and xenobiotics (Benedetti et al., 2009). They catalyze several reactions, including oxidation (which is the primary reaction), sulphoxidation, aromatic hydroxylation, aliphatic hydroxylation, N-dealkylation, O-dealkylation, and deamination (Ionescu & Caira, 2005). The expression and activity of CYP450 enzymes can be modified and reguleted by several factors. Elevated mRNA levels increase protein synthesis, which leads to increased enzymatic activity. Induction of CYP450 enzymes accelerates the clearance of certain drugs, reducing their systemic exposure and therapeutic efficacy. Conversely, CYP450 inducers may reduce the likelihood of hepatotoxicity associated with certain drugs by promoting their metabolic degradation (Parikh & Levitsky, 2013). Furthermore, inhibition of CYP450 enzymes by endogenous compounds (e.g., hormones) or exogenous substances (e.g., drugs, food components) reduces their metabolic capacity and thus impairs drug clearance. This reduced enzyme activity prolongs the presence of the drug in the systemic circulation and leads to increased blood concentrations of CYP450 substrates. Such accumulation increases the risk of dose-dependent adverse effects, including toxicity (Parikh & Levitsky, 2013; Tischer & Fontana, 2014). Another path of phase I drug metabolism is reduction which is coupled with secondary enzymatic system, either NADH cytochrome-b5 reductase system or NADPH cytochrome-c reductase (Almazroo et al., 2017). The most common phase II drug-metabolizing enzymes are UDP-glucuronosyltransferases (UGTs), sulfotransferases (SULTs), N-acetyltransferases (NATs), glutathione S-transferases (GSTs), thiopurine S-methyltransferases (TPMTs), and catechol O-methyltransferases (COMTs). In results, in contrast to original lipophilic drugs and xenobiotics, their more polar metabolites are excreted by efflux transporters (Chan et al., 2004).

Ocjena rada u tijeku

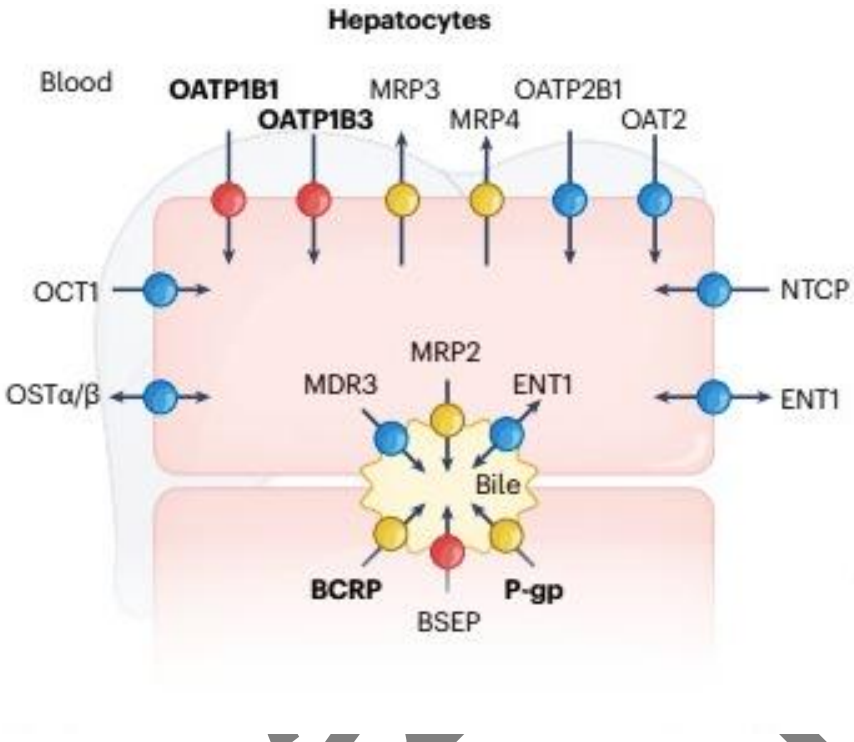

Figure 3. Membrane transporters in the plasma membrane of hepatocytes. Figure adapted from Galetin et al., 2024.

1.2.3. Membrane transporters in kidneys

Except hepatic metabolism and excretion, renal excretion is the major route of elimination. Again, various membrane transporters play an important role at both basolateral and apical membranes (Zaïr et al., 2008).

Kidneys play an important role in clearing toxins but contribute to a lesser extent in terms of overall drug metabolism. Nephrons are the main functional unit of kidney and drugs are normally filtered based on glomerular filtration, secreted at the proximal tubules, and reabsorbed by the tubules. In addition, kidneys do contribute to the metabolism of some endogenous compounds and xenobiotics. Phase III transporters play a critical role in actively secreting drug molecules against their electrochemical gradients and collaborate to facilitate the active excretion of a wide range of compounds from the bloodstream into urine (Yang & Han, 2019). Several key renal transporters that significantly influence drug-drug interactions and renal clearance, impacting both therapeutic

Ocjena u tijeku

outcomes and adverse effects include organic anion transporters (OAT1 and OAT3), organic cation transporter 2 (OCT2), multidrug and toxin extrusions (MATE1 and MATE2/K), P-glycoprotein (P-gp), and breast cancer resistance protein (BCRP) (Figure 4). Renal transporters also known to be involved in disposition, or toxicity of drugs or endogenous compounds are monocarboxylate transporters (MCTs) which are responsible for the reabsorption of γ-hydroxybutyric acid (GHB), urate transporter 1 (URAT1) which is involved in the excretion of uric acid and is a target for drugs to treat gout, and OAT2 which was recently found as a major transporter mediating the active renal secretion of creatinine (Deeks, 2017; M. E. Morris & Felmlee, 2008; Shen et al., 2017).

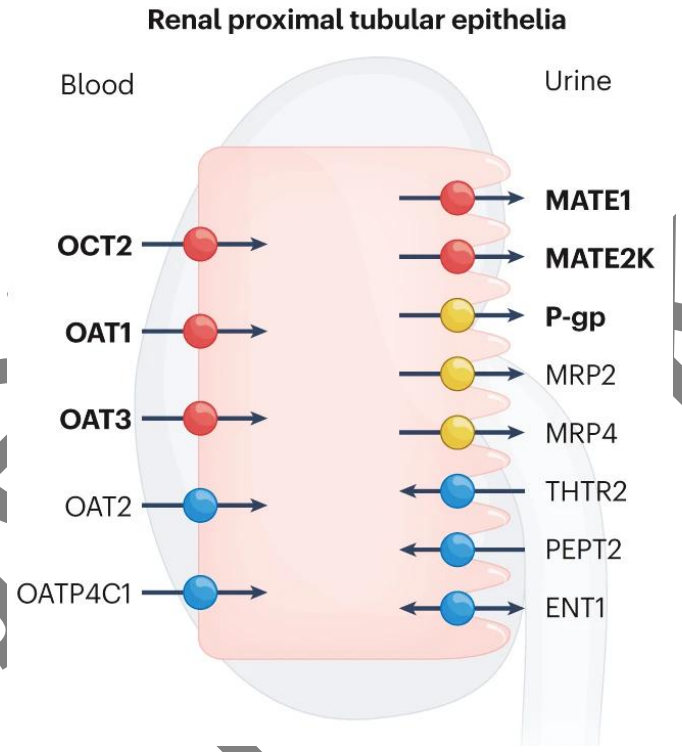

Figure 4. Membrane transporters in the renal proximal tubular epithelia. Figure adapted from Galetin et al., 2024

1.2.4. Membrane transporters in the blood brain barrier

After renal excretion, another critical barrier influencing drug disposition and therapeutic efficacy is the blood-brain barrier. The blood-brain barrier (BBB) is a highly selective physical and

biochemical barrier that separates the blood from the brain and the parenchyma of the spinal cord. In addition to its primary function of protecting the brain from physiological fluctuations in plasma concentrations of various solutes, the BBB also facilitates the exchange of essential nutrients, metabolic end-products, signaling molecules and ions between the blood and the interstitial fluid of the brain (Redzic, 2011) (L. Liu & Liu, 2019). Efflux transporters at the blood-brain barrier (BBB) include P-glycoprotein (P-gp), breast cancer resistance protein (BCRP), and multidrug-associated resistance proteins (MRPs), which function to remove drugs from the central nervous system (CNS) (Figure 5) (Sanchez-Covarrubias et al., 2014; Strazielle & Ghersi-Egea, 2013). In contrast, influx transporters such as organic anion-transporting polypeptides (OATPs), organic anion transporters (OATs), organic cation transporters (OCTs), and peptide transporters (PEPTs) facilitate drug entry into the CNS (Figure 5) (Sanchez-Covarrubias et al., 2014).

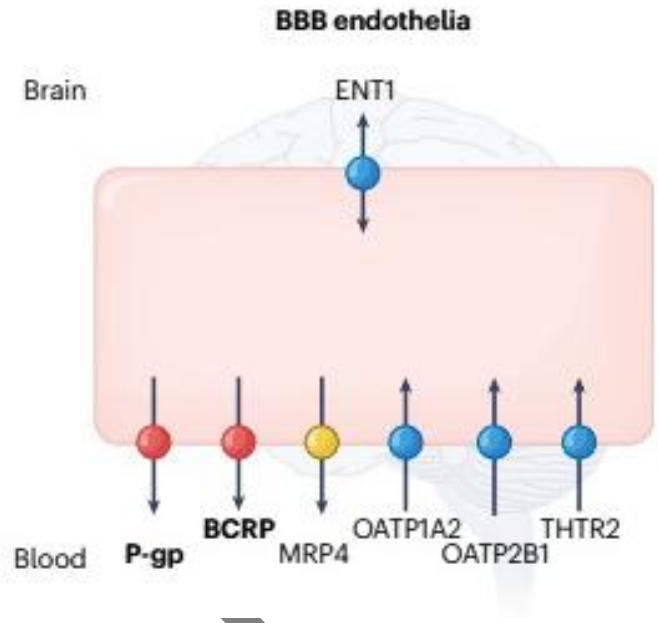

Figure 5. Membrane transporters in the blood-brain barrier (BBB) endothelia. Figure is adapted from Galetin et al., 2024

1.2.5. Membrane transporters in skin and gills – important barriers in fish

Gills are a key interface between fish and their environment, and it has been shown that in larvae or adult fish, primary routes of xenobiotic entry, except the gut, are skin and gills. Gills provide excellent conditions for efficient gas and solute exchange, and many functions of mammalian

kidneys are in fish carried out by gills (Evans et al., 2005; Rombough, 2007). Apart from the contribution of membrane transporters in maintaining critical physiological functions of fish gills such as ion exchange and pH regulation in the branchial tissue, membrane transporters also have important homeostatic function, although their presence and function in gills is not fully understood. As for the fish skin, dermal uptake may contribute up to 50% of the total uptake of compounds that are hydrophobic (Sukardi et al., 2011). E.g., it has been shown that exposing zebrafish to compounds in water relies on aqueous solubility and it is only efficient for hydrophilic drugs (Guarin et al., 2021).

Furthermore, apart from a relatively well described presence and role of ABC and SLC transporters in trafficking of physiological and xenobiotic compounds and their metabolites in liver and kidney, there is also evidence showing the presence of functional ABC transporters in fish gills. E.g., among ABC transporters, the most prominently expressed in gills of rainbow trout (*Oncorhynchus mykiss*) was shown to be Abcb5 (Kropf et al., 2020) and less expressed, but probably important in transfer of metabolites and located on the apical and/or basolateral side of gills, is the Abcg2 transporter. In the same study authors hypothesized that apically located ABC transporters in gills probably have roles in toxicological defense: (i) through direct efflux at the surface and thus preventing chemicals from entering the body, (ii) by excretion of xenobiotics and their metabolites. In contrast to apical extrusion of compounds entering the gills from water, basolateral localization of ABC transporters is probably due to their function in the transport of substrates from the gills into the blood and together with biotransformation enzymes successfully eliminate metabolites and conjugates out of the cells. Accordingly, the presence and activity of Cyp1a (phase I) and Gstp (phase II) enzymes has been shown in fish gills (Kropf et al., 2020). In addition, among analyzed SLC transporters in zebrafish gills, there was a pronounced dominance of *Slc21* over *Slc22* genes, even though they were overall lower expressed in comparison to other tissues. Oatp2b1 was found to be highly expressed, followed by moderate expression of Oatp1d1 and Oatp3a1, Oatp3a, Oatp2a1 and Oct2 in both genders. In males, Oatp1f2, Oct1 and Oct6 showed moderate expression, contrary to low expression in females (Popovic et al., 2010).

To summarize, although further research is clearly needed, recent evidence implies that the first uptake and biotransformation of xenobiotics in fish actually take place in gills which further

Ocjena rada u tijeku

protects other organs from potentially harmful effects of environmental xenobiotics (Barron et al., 1989; Bartram et al., 2012).

Considering membrane transporters in the skin, some studies aimed at identifying and determining the expression pattern of the SLC transporters in human skin showed interindividual variability in their expression levels, which might be one of the determinants of developing drug-induced skin diseases. Therefore, accumulation of drugs and metabolites in the dermal cells can be a determinant of the onset of drug-induced skin toxicity. However, comparatively little is known about the expression pattern of human drug transporters in the skin. Previously reported expressions of ABC transporters in the human skin revealed that a wide variety of ABC family transporters were highly or moderately expressed (Takenaka et al., 2013). In contrast, another study revealed that expression of SLC family transporters in human skin was restricted, while being highly expressed in the liver, while the expression level of SLCO2B1 in the skin was approximately the same as in the liver. Label-free techniques facilitate the quantification of several proteins, including enzymes present in human skin, and this information is crucial for comprehending skin physiology and function. Recently, a label-free measurement of enzymes in human skin has been published for the first time (Couto et al., 2021). In this study the authors employed this methodology to compare proteins present in human skin with those in three-dimensional models that replicate human skin and ABC transporters (ABCA8 and ABCB11), along with eight SLC transporters (SLC12A2, SLC25A3, SLC25A5, SLC25A6, SLC29A1, SLC44A1, SLC44A2, SLC4A1) have been reported.

In zebrafish, mRNA expression of zebrafish *abcb5* was found in epidermal cells of the embryo (Luckenbach et al., 2014), which is consistent with epidermal *ABCB5* expression in mammals, where this protein was hypothesised to regulate membrane potential and cell fusion of skin progenitor cells (Frank et al., 2003). Presence and activity of ABC drug transporters in the teleost epidermis was confirmed using a rainbow trout skin primary culture system (Shúilleabháin et al., 2005).

1.3. SLC family of membrane transporters

There are two major reasons why SLC transporters are so important and widely studied in the context of human health: (i) their inactivity directly cause disease, as mutations have been linked to various diseases due to resulting imbalance in the uptake, disposal or absorption of metabolites

Ocjena rada U tijeku

and ions resulting with different phenotypes and diseases; and (ii) they do not transport only endogenous compounds and their metabolites, but also drugs and thus indirectly affect disease outcome through pharmacokinetics and drug-drug interactions (El-Gebali et al., 2013; Lin et al., 2015; M. D. Pizzagalli et al., 2021).

SLC superfamily includes over 400 transport proteins, ubiquitously distributed in different cells in both prokaryotes and eukaryotes, that are involved in a transport of a wide variety of substances across cell membranes (Bai et al., 2017; Povey et al., 2001). Based on the sequence homology and function, human SLCs are classified into 66 families (Ferrada & Superti-Furga, 2022; Perland & Fredriksson, 2017; Saier et al., 2021). Most SLC transporters act as influx transporters that facilitate the movement of solutes from the extracellular environment into the cells. This process can occur by passive diffusion or passive facilitative transport along a concentration gradient, and by cotransport or counter-transport, where the movement of a solute against its concentration gradient is driven by the gradient of another solute, so called secondary active transport (Colas et al., 2016; X. Liu, 2019; M. D. Pizzagalli et al., 2021). Facilitative transport is a system that in which one molecule is transported in thermodynamically favorable direction (Stein & Litman, 2015). In secondary active system, transporters couple the passage of two or more substrates, free energy is provided by a transport of one substrate down its electrochemical gradient and used to drive the transport of the other substrate/s, e.g., transport is proportional to the electrochemical gradient of the coupled ion. What makes research on transporters challenging is that SLC transporters and ABC transporters often have overlapping substrate specificities and share their tissue distribution. This synergistic coordination with each other, as well as with phase I and II biotransformation enzymes, enables them to transport a wide range of substrates, providing a more efficient elimination of end- and xenobiotics in the indicated tissues.

Although structures are still unknown for many transport proteins (most of the available structures are from the prokaryotic species), some of the SLC transporters with known structures share a distinct feature and a pseudosymmetry across the transmembrane (TM) domains (Bai et al., 2017). Based on that fact, two of the most common structural folds among SLC proteins are the major facilitator superfamily (MFS) and leucine transporter (LeuT)-like fold (Bai et al., 2017; Shi, 2013). The differences are (i) the MFS fold consists of two pseudo-repeats of six TM helices connected by a cytoplasmic loop and the LeuT-like fold consist of two five-TM helices and each of them

Ocjena rada u tijeku

contains a bundle and a scaffold domain; and (ii) MFS fold proteins utilize a rocker and switch mechanism, and LeuT fold proteins utilize a rocking bundle approach (Garibsingh & Schlessinger, 2019; Shi, 2013). In the rocker-switch mechanism, there is a centrally localized substrate binding site between the two transmembrane domains which is only available on one side of the membrane at a time. During the intermediate steps of the transport, substrate is occluded from access to the outer and inner membrane space and finally two transmembrane domains shift around the substrate binding site, exposing it to the other side of the membrane and releasing the substrate (Drew & Boudker, 2016). Problem with the research on the structure and function of SLCs, and membrane transporters in general, is that they are not soluble (they are embedded in the membranes) and it is very difficult to purify them (Hediger et al., 2013). Consequently, computer modeling has been often used instead, which relies on the structures of SLC homologues in other species with crystallized structures identified (Schwede et al., 2009). However, one of the major limitations in homology modeling which is frequently based on using bacterial transporters to elucidate the structure and function of human ones, is that crystalized bacterial proteins can lack long cytoplasmic tails which play important roles in activity and specificity of the transporter (Mikros & Diallinas, 2019).

1.3.1. The SLCO (formerly SLC21) subfamily of proteins

In this study we have specifically focused on the transporter(s) of organic anions which belong to the SLCO subfamily of proteins and have been implied as (eco)toxicologically relevant in fish species.

Organic anion transporting polypeptides (OATPs) are membrane proteins that mediate the uptake of a wide range of substrates across the plasma membrane and are expressed in various cells and tissues, where they mediate the uptake of structurally unrelated organic anions, cations and even neutral compounds into the cytoplasm. OATPs are classified into six subfamilies, OATP1 to OATP6. In humans, there are 12 OATPs encoded by 11 solute carrier of organic anion transporting polypeptide (SLCO) genes: OATP1A2, OATP1B1, OATP1B3, the splice variant OATP1B3–1B7, OATP1C1, OATP2A1, OATP2B1, OATP3A1, OATP4A1, OATP4C1, OATP5A1 and OATP6A1, of which OATP1B1 and OATP1B3 are the best characterized (Hagenbuch et al.,

Ocjena rada u tijeku

2025). No OATP homologs were found in the prokaryotes and plants, what suggests that OATPs have evolved with the animals and furthermore, they have been identified and partially characterized in essentially every animal species (Hagenbuch et al., 2025).

In the next sections we will focus on the OATP1 subfamily that has been most extensively studied because of the link to human diseases and cancer treatment. In result, knock-out animal models were so far only generated for the members of this subfamily (Hagenbuch and Stieger, 2013).

Polymorphic variants of these transporters can impair their function, leading to reduced drug clearance and increasing the likelihood of adverse drug effects, particularly rhabdomyolysis caused by statins. For example, a single nucleotide polymorphism in the SLCO1B1 gene encoding OATP1B1 protein decreases its ability to transport simvastatin acid from portal circulation into the liver. As a consequence, increased plasma concentrations of simvastatin acid enhances risk of simvastatin induced myopathy (Kalliokoski & Niemi, 2009) In addition, the simultaneous administration of multiple drugs that rely on OATPs for transport (OATP substrates) can lead to clinically significant and potentially harmful drug-drug interactions (Ciută et al., 2023).

1.3.1.1. Cellular and tissue distribution of OATPs

The liver facilitates vital biotransformation processes due to its strategic location between the gut and the systemic circulation and has a central role in protecting the body from toxic compounds by metabolism and excretion (Patel et al., 2016; Schulze et al., 2019). OATPs are expressed at the basolateral membrane, facing the perisinusoidal space (or the space of Disse) and the portal blood plasma, from where they mediate the uptake of a multitude of endogenous and exogenous compounds into the cytoplasm of hepatocytes (Alam et al., 2018; Ciută et al., 2023; Hagenbuch & Stieger, 2013; Roth et al., 2012).

OATP1A2 has the strongest expression in the brain, followed by the lungs, liver, kidneys, and testes (Kullak-Ublick et al., 2004). At the protein level, OATP1A2 has been detected in brain capillaries, the apical membrane of the distal nephron, in cholangiocytes (Gao et al., 2000, 2005) the basolateral membrane of the pars plana in the ciliary body (Gao et al., 2005), in the retina, and

Ocjena rada u tijeku

in neurons (Gao et al., 2015). In addition, twelve protein isoforms have been identified, encoded by 30 different transcripts. However, none of these variants appear to be functionally active.

OATP1B1 and OATP1B3 are primarily classified as “liver-specific” transporters. However, OATP1B1 mRNA has been also found in the placenta (H. Wang et al., 2012), in the hormone-independent breast cancer cell line MDAMB-231 (Banerjee et al., 2012), and in several human cancers (Pressler et al., 2011). At the protein level, OATP1B1 is predominantly localized to the sinusoidal or basolateral membrane of human hepatocytes.

As previously noted, OATP1B3 is another so-called liver-specific OATP. There are two isoforms of this protein. Isoform 1 has 702 aminoacids and is known as the liver-type (Lt)-OATP1B3. Isoform 2, referred to as cancer-type (Ct)-OATP1B3, is a 674-amino acid splice variant. This variant is commonly found in various cancer cell lines and human cancers (Thakkar et al., 2013). While Lt-OATP1B3 functions as a broad-specificity transporter for both endogenous and xenobiotic compounds, Ct-OATP1B3 is primarily localised intracellularly in a lysosomal fraction and has a much-reduced function (Haberkorn et al., 2022; Thakkar et al., 2013).

OATP1B3e1B7 (SLCO1B3eSLCO1B7) is a splice variant of the SLCO1B1 and SLCO1B7 genes and encodes a protein of 687 amino acids. It is mainly expressed intracellularly in the liver and the small intestine, where it might mediate the transport of drugs into and out of the smooth endoplasmic reticulum, facilitating their conjugation (Hagenbuch et al., 2025).

OATP1C1(SLCO1C1) is the third member of the OATP1 family, isolated from a human brain cDNA library (F. Pizzagalli et al., 2002). Four isoforms have been reported, encoding for proteins with 612 to 730 amino acids, respectively. However, only isoform 2, encoding a 712-amino acid protein, has been shown to be functional. It is mainly expressed in the brain, the testes, and the heart. Functionally, it is a high-affinity thyroid hormone transporter with a narrow substrate specificity (F. Pizzagalli et al., 2002).

1.3.1.2. Mechanism of transport

Although it is known today how important OATPs are for the cellular and organism homeostasis, comparativelly little is known about their mechanism of transport. It is known that they are sodium independent transporters and they work as exchangers, which means imported substrate is

Ocjena rada u tijeku

exchanged against another anion (Hagenbuch et al., 2025). The first identified counterion was bicarbonate (Satlin et al., 1997) where rapid intracellular acidification acompanying thaurocholate uptake was observed. Examples of other counterions reported to be involved in OATP transport are: glutathione (GSH), in research where *Xenopus laevis* oocytes expressing rOATP1A1 showed enchanced uptake of thaurocholate and leukotriene C4 after injecting GSH into cells (L. Li et al., 1998) and study on rOATP1A4 again expressed in *X. laevis* revealed GSH, S-methylglutathione, S-sulfobromophthalein-glutathione, S-dinitrophenyl glutathione, and ophthalmic acid as counterions which stimulated uptake of thaurocholate (L. Li et al., 2000).

Next factor that influences transport for several OATP proteins is pH, e.g., it was demonstrated that uptake mediated by OATP2B1increases by lowering extracellular pH (Kobayashi et al., 2003; Nozawa et al., 2004). Until now research showed that all human OATPs were stimulated by acidic extracellular environment, except OATP1C1 (Leuthold et al., 2009). Additionaly, the level of pH stimulation was depending on the investigated substrate, e.g., transport of prostaglandin E_2 or bromosulfophtalein by OATP2B1 was not stimulated when extracellular pH was lowered, but the transport of thyroxine or pemetrexed was (Visentin et al., 2012).

1.3.1.3. Substrate specificity of OATPs

OATP1A2, ubiquitously expressed, transports essential physiological compounds, including steroid and thyroid hormones, bilirubin, bile salts, and eicosanoids. Except for its role in hormone and bile salt homeostasis, OATP1A2 also transports various pharmaceuticals. Its broad distribution suggests an important role on the tissue-specific disposition, pharmacokinetics, and toxicity of xenobiotics (Badagnani et al., 2006). In contrast to the ubiquitously expressed OATP1A2, OATP1B1 and OATP1B3 are primarily liver-specific transporters, expressed on the sinusoidal membrane of hepatocytes (Kalliokoski & Niemi, 2009) with a largely overlapping substrate range encompassing steroid conjugates, bile salts, and bilirubin. Despite this overlap, their affinities for specific substrates can vary significantly (Hagenbuch & Gui, 2008). OATP1B1 and OATP1B3 have been widely studies for their critical role in the transport and clearance of various drugs, including lipid-lowering agents and chemotherapeutics, leading to their biliary excretion. Unlike most OATPs, OATP1C1 exhibits a narrow substrate range, primarily transporting thyroid

Ocjena rada u tijeku

hormones: thyroxine (T4), triiodothyronine (T3), reverse triiodothyronine (rT3), and their sulfated conjugates. Predominantly expressed at the blood-brain barrier (BBB), OATP1C1 is not known to transport xenobiotics (Roth et al., 2012).

Consequently, members of the OATP superfamily are recognized as important drug transporters, and numerous reports have compiled comprehensive lists of their drug substrates (Hagenbuch and Gui, 2008; Fahrmayr et al., 2010; Niemi et al., 2011; Emami Riedmaier et al., 2012; Grandvuinet et al., 2012; Nakanishi and Tamai, 2012; Obaidat et al., 2012; Roth et al., 2012; Tamai, 2012; Chu et al., 2013; Hagenbuch and Stieger, 2013; Kovacsics et al., 2017; Oswald, 2019; Kinzi et al, 2021; Nies et al., 2022). Besides these reviews, the DRUGBANK Online (https://go.drugbank.com) is a good source of substrates and inhibitors of OATPs and other transporters, and access is free for most academic researchers.

1.3.1.4. Structure vs. transport mechanisms of OATPs

We have already mentioned fold and transmembrane topology of members of the MFS, characterized by 12 transmembrane helices, cytoplasmic (intracellular) amino and carboxy terminals, and a pseudosymmetry of the N-terminal and C-terminal bundle of 6 transmembrane domain (TM) helices. OATPs share those features and additionally, contain long extracellular loops (ECLs) and a Kazal-like domain in ECL5. The function of Kazal-like domain has remained unclear. Furthermore, OATP transporters have a signature motif located at the external half of TM6 and encompassing part of the ECL3. This motif contains the sequence D-x-RW-(I/V)-GAWW-x-G-(F/L)-L, x denotes any amino acid residue (Hagenbuch et al., 2025) (Figure 6).

Ocjena rada u tijeku

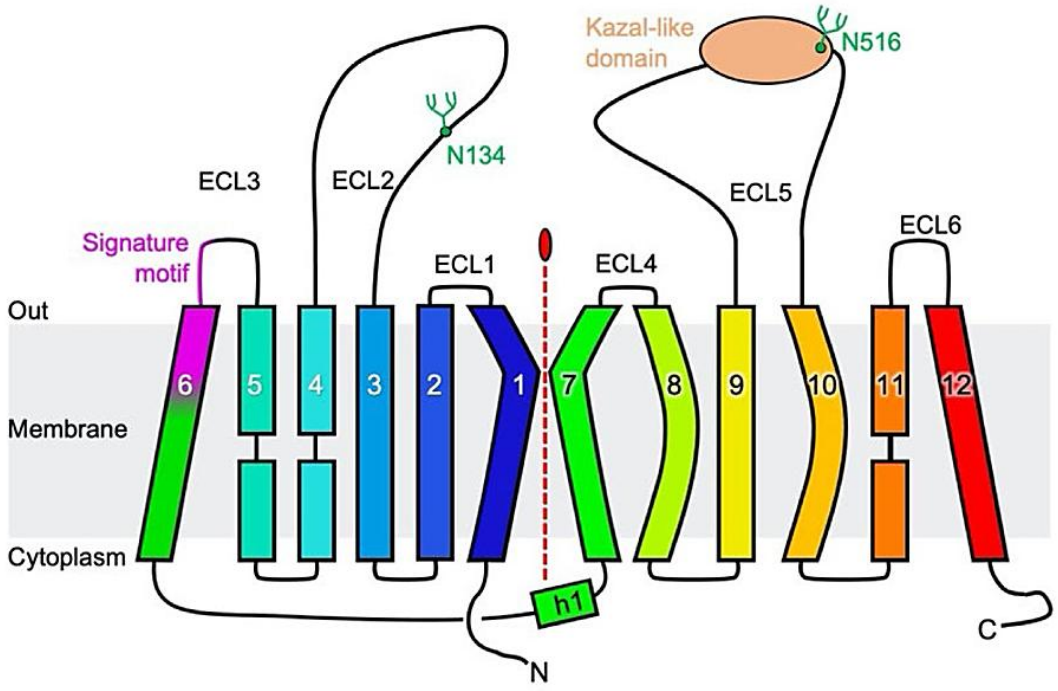

Figure 6. OATP1B protein topology with transmembrane (TM) helices and extracellular loops (ECLs) numbered. The TM helices are numbered and arranged to highlight the pseudo-2-fold rotation symmetry (indicated by red dashed line and ellipse). The colors are aranged from blue (N-terminus) to red (C-terminus). Extracellular loops (ECLs) are numbered and N-glycosylation sites (N134, N516) are indicated. Figure from Hagenbuch et al., 2025.

While the role of liver OATPs in endogenous substrate transport and drug disposition is well established, their mechanism of transport has remained unclear. But some progress has been made recently. Recent research of two groups presented cryoelectron microscopy (cryoEM) structures of human OATP1B1 and OATP1B3 proteins (Ciută et al., 2023; Shan et al., 2023). Shan et al. reported structures of OATP1B1 determined without protein binders but in two conformations and bound to distinct compounds. Ciută et al. (2023) reported structures with synthetic Fab fragments of E1Sbound OATP1B1 and another of OATP1B3 without bound drug but, interestingly, with evidence of bound bicarbonate. At least three states of OATP transport were suggested. State I, represented by the E1S-bound OATP1B1 structure, shows an inward-facing conformation and a polyspecific binding pocket containing a substrate ready for release into the cytosol. In state II, which is observed in our bicarbonate-bound OATP1B3 structure, the substrate binding pocket is narrowed due to a conformational change in TM7 and TM8. This narrowing is allosterically linked

Ocjena u tijeku

to bicarbonate binding near the OATP signature motif, effectively blocking substrate re-entry. Probably state II transitions to an outwardly open conformation (state III), which can successfully trap a new substrate from the extracellular environment. So called, rocker-switch alternating access mechanism. For cycle to be fully completed, the release of bicarbonate should be involved, binding of the substrate and return to the inward open state I (Ciută et al., 2023) (Figure 7).

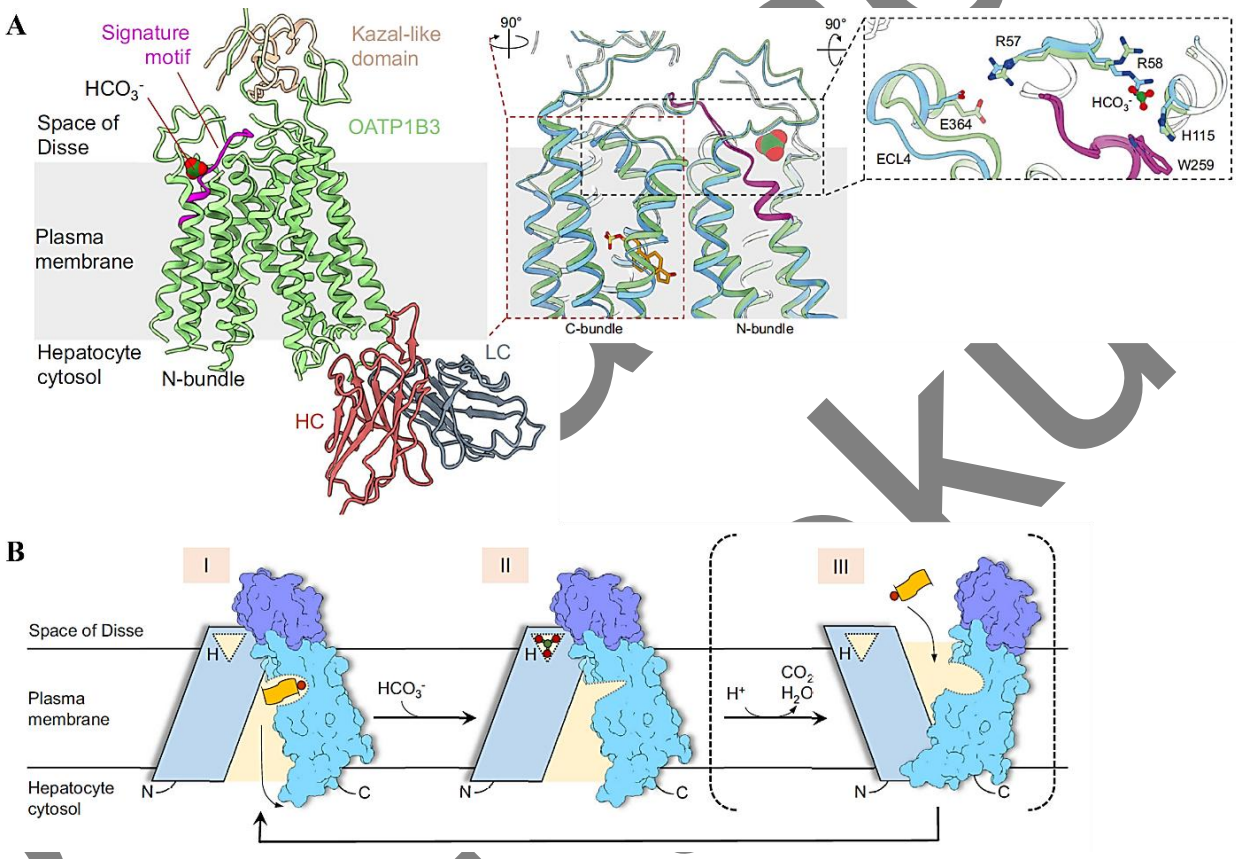

Figure 7. Ribbon representation of the bicarbonate and E1S- bound to OATP1B3. A) In the centre view, the structure is parallel to the membrane. Dotted frames indicate the enlarged areas. The red arrow indicates the shift in TM8. (right) Close-up of the interface between the N- and C-terminal bundles showing a shift in ECL4. B) Proposed structure-based mechanism of organic anion substrate transport mediated by pH-sensitive OATP proteins. The anionic part of the drug substrate (orange rectangle) is coloured red. H stands for an important histidine residue, which is responsible for mediating protonation (adapted from Ciuta et al., 2023).

1.4. Zebrafish as a model organism for studying membrane transportes

Having established the crucial physiological and pharmacological relevance of OATPs, in next chapters we present an overview of recent knowledge related to zebrafish as an advantageous model organism for exploring transporter function and toxicological implications, both in the context of biomedical and envirnmental research. Zng formatebrafish (*Danio rerio*), a tropical freshwater teleost from Cyprinidae family, is well established vertebrate model with cell development, molecular mechanism and organ physiology similar to those in humans. It has been used to study chemical toxicity, vertebrate development, genetics, physiology, behaviour, cancer, neurodegenerative, cardiovascular and metabolic diseases (Grunwald & Eisen, 2002; Y. Liu, 2023).

What makes zebrafish a great model organism is the high level of genome similarity shared between zebrafish and humans. To be more precise, ~70% of human genes have at least one obvious zebrafish ortholog, compared to 80% of human genes with mouse orthologs (Howe et al., 2013; Postlethwait et al., 1998). That fact has greatly facilitated the use of zebrafish for understanding human genetic diseases and relationships between genotype and phenotype of various human diseases (Choi et al., 2021). There are also numerous other advantages and strengths of using the zebrafish as a model organism. Compared to mammals, maintaining zebrafish is less expensive. In addition, external fertilization and the development of hundreds of embryos in a single clutch allow easy observation and manipulation of embryonic development. Adult zebrafish reach sexual maturity within three to five months, and their small size, both as embryos and as adults, enables a cost-effective research and reduces the quantities of expensive substances or new drugs required for studies (Spitsbergen & Kent, 2003). Optical clarity or transparency of the developing embryo allows live imaging at the organism level as well as the individual cell fates throughout organogenesis (Lieschke & Currie, 2007; Shin & Fishman, 2002). Additionally, the use of transgenic animals that can be easily generated under the control of various selected gene promoters, and improvement of the Tol2-based transgenic system in zebrafish in a spatiotemporal manner by coupling with regulatory elements such as GAL4/UAS or Cre/LoxP (Halpern et al., 2008; Langenau et al., 2005) allow live imaging of cells and tracking of cellular dynamics *in vivo.* These advantages make it easier to study and explain molecular mechanisms of development of various organs (Choi et al., 2021).

Ocjena rada u tijeku

Furthermore, recent advances in genome editing techniques have greatly facilitated targeted genetic modification. Techniques such as Zinc Finger Nucleases (ZFNs), Transcription Activator-Like Effector Nucleases (TALENs), morpholino oligonucleotide-mediated silencing and Clustered Regularly Interspaced Short Palindromic Repeats (CRISPR)/CRISPR-associated protein 9 (Cas9) have allowed researchers to study molecular pathways and phenotypic outcomes, enhancing research in the zebrafish model. Of all the techniques mentioned, the CRISPR/Cas9 approach is characterized by its simplicity and versatility, enabling multiplex gene(s) editing and precise genome modifications (Hwang et al., 2013; P. Liu et al., 2019; Varshney et al., 2015).

The zebrafish chorion can be thought of as a sieve, but not as a wall, or more precisely as a permeability barrier for chemicals under certain conditions (Nishimura et al., 2016). It has pores about 0.5 µm in diameter and 2 µm apart (K. J. Lee et al., 2007; Rawson et al., 2000), but penetration of chemicals through the chorion depends on different factors including compound's physicochemical properties (Kim & Tanguay, 2014; Wiegand et al., 2000), charge in the aquatic test medium (Cameron & Hunter, 1984), and electrostatic attraction between chemicals and the chorion (Burnison et al., 2006). It is assumed that dechorionisation facilitates the penetration of chemicals and increases the sensitivity of the embryo to the tested compounds. It has been shown that the sensitivity to detect teratogens was higher in dechorionised embryos than in embryos with intact chorion (Panzica-Kelly et al., 2015). One should also be aware that the specificity in detecting non-teratogens was lower in dechorionised embryos compared to chorion-intact embryos. Therefore, dechorionisation, especially at very early stages (e.g., blastula stage) without damaging the embryos, is a major challenge (Panzica-Kelly et al., 2015; Truong et al., 2014).

Furthermore, the space between the embryo and the chorion in the teleost egg is filled with an extraembryonic fluid, which is inherited from the mother and is known as perivitelline fluid (PVF). The embryo is immersed in the PVF and thus partially isolated from the external environment. The exact composition of the PVF in vertebrates is still unknown. It protects the embryo from dehydration, helps the embryo to maintain a safe osmotic balance and provides mechanical protection. There is an evidence for an immune defensive role of the PVF and through proteomic profiling, it was revealed that the composition of the PVF was complex and underwent dynamic changes during development (De la Paz et al., 2020).

Ocjena rada u tijeku

Figure 8. **An example of a male zebrafish (A) and a female zebrafish (B).** Figure adapted from (Avdesh et al., 2012). Males have a characteristic torpedo-like shape and a golden colour between the stripes. Females are easily recognised by their larger, light silver belly.

Interestingly, no clear sex-determining chromosome was found in zebrafish (von Hofsten & Olsson, 2005). Initially, all animals have undifferentiated ovary-like gonads, and in males all oocytes disappear and males undergo testicular differentiation, which is usually completed by the third month of development (Devlin & Nagahama, 2002; Maack & Segner, 2003). The timing of gonadal development varies and depends on the husbandry conditions or the type of strain studied (Maack & Segner, 2003). In addition to genetics, it has also been observed that the sex ratio often varies and depends on rearing density, hypoxia or food availability (Lawrence et al., 2007; Shang et al., 2006), environmental changes that involve hormones (Hill & Janz, 2003; Westerfield, 1995) and temperature (Uchida et al., 2004). Females have a larger, light silver belly, their blue stripes alternate with silver stripes, and their dorsal fin has a stronger yellow hue. Males usually have no protruding belly and have a torpedo-like shape. They also have a golden-reddish hue between the blue stripes, especially on the anal and caudal fins (Figure 8) (Nasiadka & Clark, 2012).

Osijek rijeka Utijeku

Apart from olfactory perceptions, which play a role in triggering reproduction, other factors such as visual stimuli and behaviour are probably involved in the selection of mating partners. Previous studies have shown that zebrafish females favour larger males (Pyron, 2003) and strategically distribute their eggs differentially toward larger males (Skinner & Watt, 2007). Another interesting factor is pigmentation. Some studies suggest that phenotypic traits such as carotenoid colouration of males, longitudinal stripes of melanophores and symmetry of caudal fin patterns may influence mate choice (Pritchard, 2001). The importance of visual factors was also investigated using the preferences of wild-type and colour mutant zebrafish. This showed that zebrafish are able to visually distinguish differences in pigmentation patterns and that their preferences for certain phenotypes are based on experiences during development (Engeszer et al., 2004).

1.4.1. Embryogenesis and organogenesis

The stages of early development and the period after hatching of zebrafish embryos are described in the greatest detail in Kimmel et al. (1995). As mentioned above, one of the major advantages of the zebrafish as a model organism is the transparency of the embryos, which facilitates the observation and monitoring of embryonic development and associated changes.

The following text is a brief overview of zebrafish embryonic development. At 24 hpf, the basic body plan of the embryo begins to take shape. Anatomically, the embryo already contains the notochord, the somites, the otoliths, the developing eyes, the brain and the pericardial cavity (Figure 9). The embryo also begins to show its first movements, such as the curling of the tail, which can serve as an important parameter in assessing the effects of certain chemical exposures (von Hellfeld et al., 2020).

At 2 dpf the embryos begin to hatch, although most still remain in the chorion. At this stage, craniofacial development can be assessed, including possible disruption of cartilage structures. In addition, observations of blood flow and the unlooped heart region, can reveal cardiac and circulatory malformations. At this stage, the eyes and ears are fully developed, distinct regions of the brain are visible, and the spine becomes apparent above the notochord (Figure 10). The caudal

Ocjena rada u tijeku

fin and pectoral fin buds also begin to form, although they are not shown in the (Figure 10) (von Hellfeld et al., 2020).

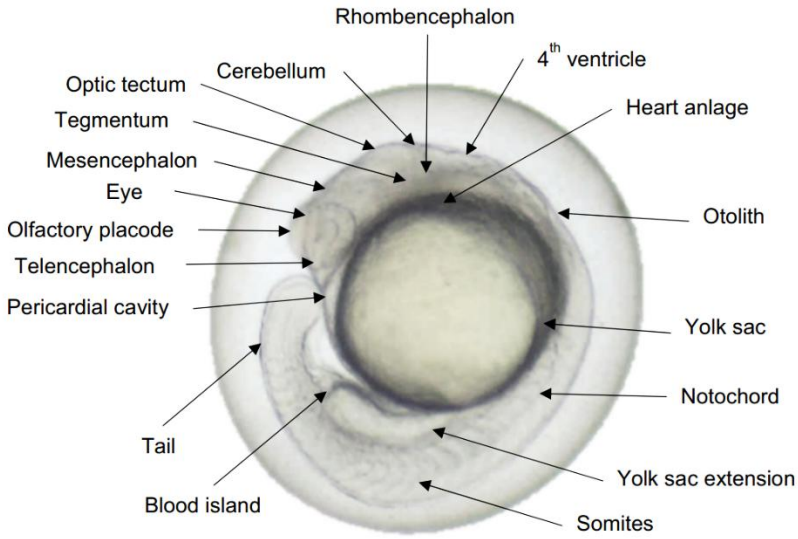

Figure 9. Morphology of normal zebrafish embryo at 1 dpf. Figure adapted from von Hellfeld et al., 2020.

By 3 dpf, the overall anatomy of the embryos is largely developed (Figure 10). As most embryos have hatched at this stage, it is possible to assess the curvature of the spine and recognise phenotypic anomalies such as lordosis, kyphosis and scoliosis. In addition, fin development continues and behavioural changes, especially in relation to active swimming, can be quantitatively analysed (von Hellfeld et al., 2020).

In embryos at the age of 4 dpf, the volume of the yolk sac is significantly reduced due to resorption. The intestinal tract is fully formed and the swim bladder is also developed (Figure 11) (von Hellfeld et al., 2020).

At 5 dpf, the yolk sac is completely absorbed (Figure 11). The facial features are flattened, which enables efficient prey capture, and active feeding typically begins between 128 and 144 hpf (von Hellfeld et al., 2020).

Ocjena u tijeku

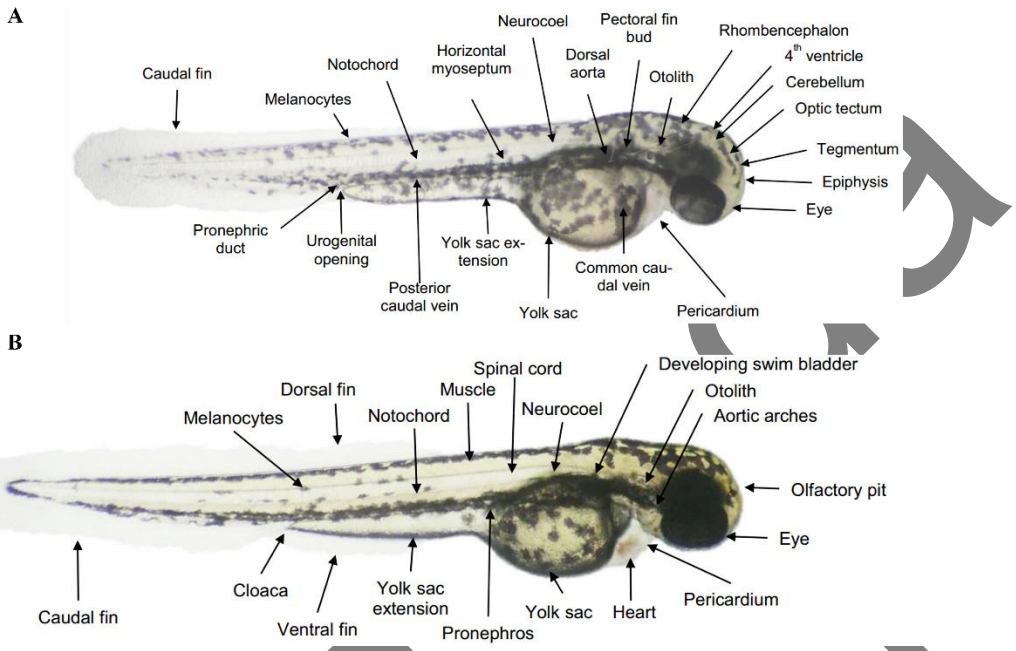

Figure 10. Morphology of normal zebrafish embryos at 2 dpf (A) and 3 dpf (B). Figure adapted from von Hellfeld et al., 2020.

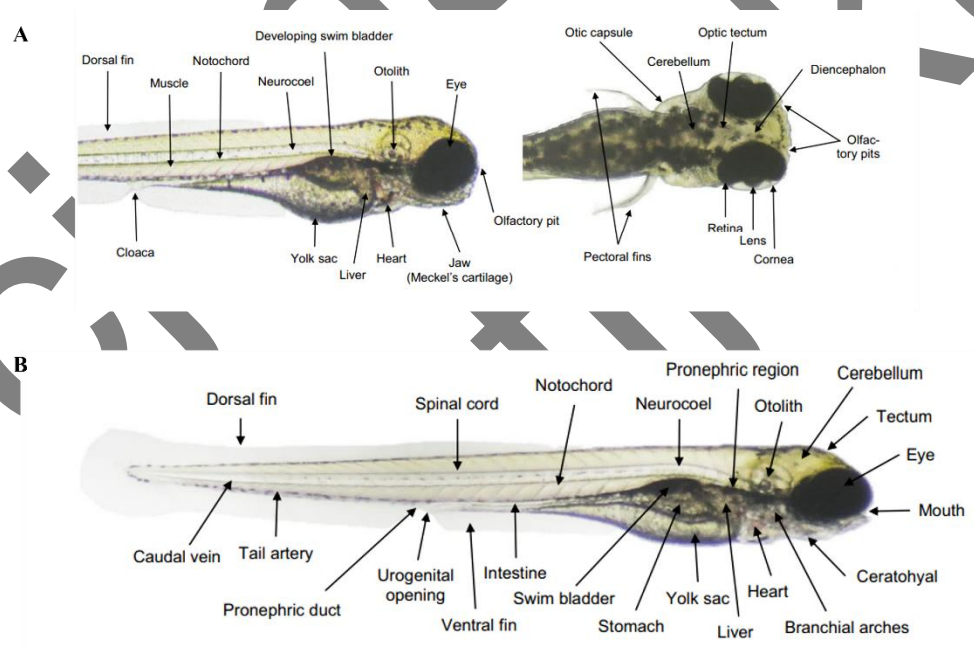

Figure 11. Morphology of normal zebrafish embryo at 4 dpf (A) and 5 dpf (B). Figure adapted from von Hellfeld et al., 2020.

Original

Regardless of species, the major constituents in yolk are proteins and lipids. There is evidence that yolk and yolk sac are metabolically active. For instance, yolk concentrations of several lipid species, cholesterol and sphingomyelins actually increase during embryonic development which is the sign of metabolic function in the yolk (Fraher et al., 2016). Secondly, studies investigating RNA transcripts in oocytes and recently fertilized zebrafish zygotes, showed that maternal transfer of RNA transcripts have a parent-of-origin signature and regulate developmental processes and contribute to metabolic processes in the oocyte, zygote and embryo (Abrams & Mullins, 2009; Rauwerda et al., 2016). The zebrafish model provides researchers a number of tools and strategies to better study and understand embryonic nutrition, and how it is affected by toxicant exposures because the yolk can selectively aggregate lipophilic xenobiotics from the surrounding aquatic environment (Sant & Timme-Laragy, 2018). Uptake of different compounds into the yolk across the yolk sac epithelium, which contains several active receptors for receptor-mediated endocytosis or pinocytosis, but also the arrangement and function of membrane transporters on the epithelium of the yolk sac and their impairment due to toxicological perturbations, still needs to be investigated (Sant & Timme-Laragy, 2018).

The increasing input of anthropogenic substances into the environment has necessitated reliable and accurate acute toxicity assessments. Most legislation to identify environmental hazards and assess the risks associated with chemicals, pharmaceuticals, biocides, additives and effluents relies on vertebrate models, including rats and fish. The Fish Embryo Acute Toxicity (FET) test using zebrafish (*Danio rerio*) embryos, as described in the OECD Test Guideline (TG 236), serves as an alternative to conventional acute fish toxicity tests, including the OECD Acute Fish Toxicity Test (TG 203). The original FET test was designed to utilise only four core morphological endpoints – coagulation of the embryo, lack of somite development, lack of heartbeat and non-detachment of the tail – to achieve a sensitivity comparable to the acute fish test. A comprehensive database of common and specific morphological changes observed in zebrafish embryos following exposure to various chemicals has been built (Belanger et al., 2013; Scholz et al., 2014), along with recommendations, standardised nomenclature and a comprehensive database documenting these morphological changes in zebrafish embryos. Typical morphological changes and need for standardized nomenclature were also formalized by von Hellfeld et al. (2020). In addition to the endpoints described in OECD TG 236, all additional observations documented as lethal or sublethal endpoints were: reduced heart beat or reduced blood circulation, suppressed or absent

Ocjena rada u tijeku

pigmentation, delayed or altered development, altered locomotion, spinal deformities and the formation of various oedemas together with the accumulation of blood cells in pericardial and yolk oedemas, craniofacial malformations, impaired yolk absorption, and changes in zebrafish embryonic behaviour. In summary, morphological findings can provide important clues to possible deleterious mechanisms, although further molecular studies are still required to clarify the underlying mechanisms (von Hellfeld et al., 2020).

1.4.2. Zebrafish membrane transporters

There is a growing number of studies which emphasise the diversity of membrane transporters in zebrafish as an established model organism, and their similarity to transporters in other vertebrates. However, drug transporters in zebrafish are still poorly characterised. A thorough characterisation of the similarities and differences between zebrafish and human transporters is essential to enable translational studies on transporter activity and bioavailability of drugs in zebrafish.

The first insight into the zebrafish Slc22 membrane transporters was done in our group (Mihaljevic et al., 2016). Orthological relationships with related transporters in other vertebrate species were found by phylogenetic and syntenic studies of fish Slc22. The expression pattern of *oct1* is comparable to that of *OCT1* and *OCT2* in humans, with very high expression in the kidney, followed by high expression in the liver and moderate expression in the brain. This suggests that Oct1 in zebrafish may have similar functions to OCT1 and 2 in humans (Koepsell, 2011). In contrast, the moderate expression of *oct2* in all tissues examined, apart from the kidney and testis, suggests a more specialised physiological function and a possible role in the clearance of endogenous cations and drugs by the kidneys. Therefore, human *OCT2*, which is mainly expressed in the kidney, has a different expression pattern than zebrafish *oct2* (Ciarimboli et al., 2010; Koepsell et al., 2003). Furthermore, since zebrafish lack an orthologue for *OCT3*, it is plausible that their *oct1* and *oct2* transporters take over the function of *OCT3*, especially given the large substrate overlap between OCT1, 2 and 3 in mammals (Koepsell et al., 2003; Nies et al., 2009).

Seven genes for organic anion transporters were found in zebrafish. The extensive conservation of OAT1 and OAT3 function in vertebrate physiology is evidenced by the one-to-one orthology of

Ocjena rada u tijeku

oat1 and *oat3* to *OAT1* and *OAT3* in humans (Mihaljevic et al., 2016). However, there are some differences in the tissue expression data between the human orthologues and zebrafish, particularly in the case of *oat1*. The female brain and testis are the sites where oat1 is most highly expressed in zebrafish. Compared to *oat1*, tissue expression of *oat3* is more widespread in zebrafish, with the kidney, especially in females, showing the highest expression, followed by the testis, large intestine and brain with moderate expression. As *oat3* is highly expressed in the kidney in zebrafish, it may play a similar role in the transport and elimination of xenobiotics as its human orthologue, *OAT3*. Five members of the *oat2 (a–e)* subfamily were found in zebrafish. Interestingly, all fish species analysed showed one-to-many orthologues with human genes, whereas the *OAT2/oat2* genes of higher tetrapods showed one-to-one orthologies. This could be due to further duplications of single genes or gene clusters, an additional whole genome duplication (WGD) in salmonids (such as rainbow trout) and an independent WGD in teleost fish (Berthelot et al., 2014; Howe et al., 2013). The fact that all other tetrapods studied have only one *OAT2/Oat2* ortholog raises the possibility that the second round of genome duplication triggered the diversity of Oat2 genes.

Zebrafish (*Danio rerio*) have 52 ABC transporter genes, with orthologs for 77% of the 48 human ABC transporters (Annilo et al., 2006). Zebrafish have no direct ortholog of *ABCB1* but instead have two genes, *abcb4* and *abcb5*, which have a similar function. A marked expression in both male and female gonads of *abcc1* mRNA was showed and *abcc5* mRNA was highly expressed in testis (Long, Li, & Cui, 2011; Long, Li, Li, et al., 2011). More about ABC transporters in zebrafish can be found in recent review on progress in characterizing ABC multidrug transporters in zebrafish (Thomas et al., 2024).

1.5. Zebrafish Oatp subfamily of proteins

Highly diverse Oatp family includes over 300 Oatps annotated in different animals (Hagenbuch & Meier, 2004). Apart from 14 distinct members in zebrafish (Popovic et al., 2010, 2013), Oatp1 has been identified in little skate (Cai et al., 2002), rainbow trout (Steiner et al., 2014) and in fathead minnows (Muzzio et al., 2014). They are all expressed predominantly in liver and kidneys, but also in gills and brain and transport variety of substrates, both endogenous and exogenous

Ocjena rada u tijeku

(Willi & Fent, 2018). By phylogenetic and tissue analysis done in our laboratory (Popovic et al., 2010), several Oatp1 members have been identified: Oatp1d1 (only reported in zebrafish), Oatp1e1, Oatp1c1 and Oatp1f2 and importantly, analyses indicated that Oatp1 family in zebrafish is clearly different from Oatp1 family in other vertebrates. The main difference is that within the zebrafish genome, orthologs of Oatp1a and 1b cannot be found, and phylogenetically closest are Oatp1d1 and 1e1.

The diversification of the OATP1/Oatp1 family took place after jawed fish appeared, after the second round of the whole genome duplication event (Figure 12). The Oatp1d subfamily originated in teleosts and is not found in tetrapods, while the OATP1A/Oatp1a and OATP1B/Oatp1b subfamilies arose at the base of the tetrapod lineage (Froschauer et al., 2006). The only family found in all vertebrates from cartilaginous fish to humans is OATP1C/Oatp1c which might represent the sequence most similar to the common ancestor of the OATP1/Oatp1 family (F. Pizzagalli et al., 2002).

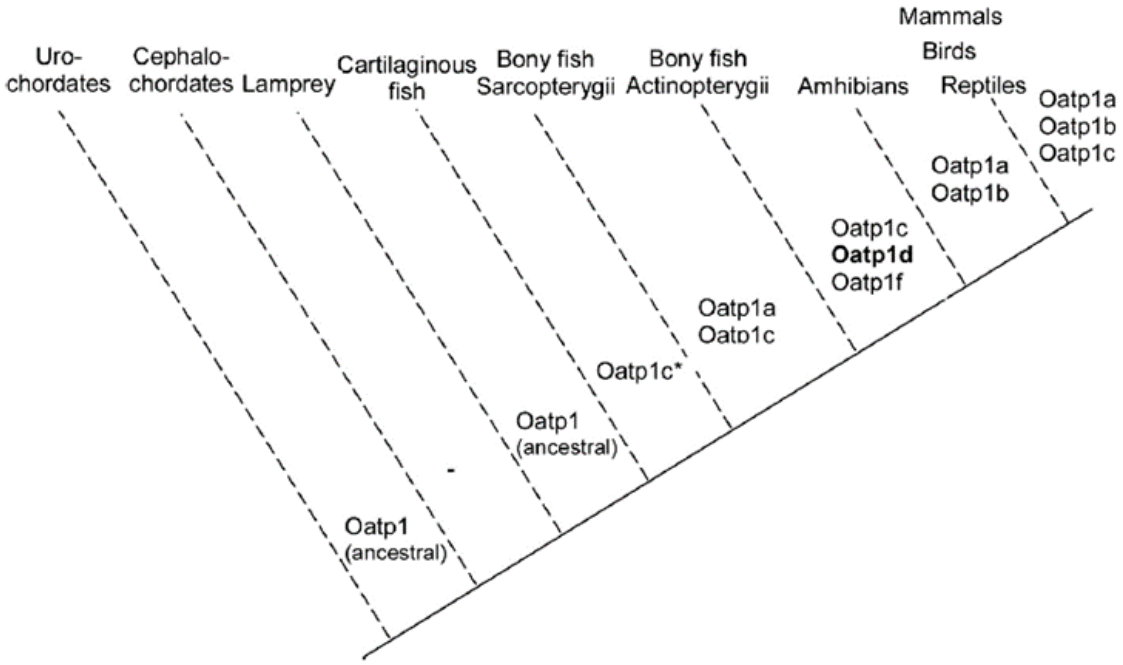

Figure 12. Schematic representation of evolution of the Oatp1 family in chordates. Diversification of the OATP1/Oatp1 family occurred after the after the split of jawless and jawed fish which followed the second round of the whole genome duplication event, but before the split of cartilaginous and bony fish (Popovic et al., 2013).

1.5.1. Zebrafish Oatp1d1

This study is specifically focused on *in vivo* characterization of the organic anion transporting polypeptide 1d1 (Oatp1d1) using zebrafish model, and in the following sections we will explain why particularly this transporter is interesting in terms of its ecotoxicological relevance. Briefly, there are two major reasons. First, previous genome and phylogenetic analysis of SLCO/Slco genes in vertebrates revealed the presence of an Oatp subfamily that is fish-specific, named Oatp1d, that includes two genes: the ubiquitously expressed Oatp1d1 and negligibly expressed Oatp1d2. And secondly, our initial *in vitro* studies showed that this fish specific transmembrane protein plays an important role in the transport of various endogenous substances and exogenous compounds across cellular membranes in zebrafish.

1.5.1.1. Cellular and tissue distribution

Oatp1d1 is ubiquitously expressed in all tissues, with the highest expression in the liver, brain and testes. Following these, notable expressions were also observed in the intestine, kidney, gills, and skeletal muscles. There are sex differences, and they are most pronounced in testes, as *oatp1d1* expression is 50 times higher than in ovaries. In zebrafish liver, *oatp1d1* expression is 10 times higher in males and again, it is 2.5-fold higher in the male kidney. Other tissues investigated did not show differences between genders (Popovic et al., 2013).

1.5.1.2. Mechanism of transport

As already mentioned, the transport mechanism of OATPs/Oatps is not yet fully understood. *In vitro* studies have shown that the transport activity of Oatp1d1 is influenced by changes in pH, both extracellular (pHo) and intracellular (pHi), which affect proton flux and are closely linked to bicarbonate concentration (HCO_3^-). In short, when the extracellular pH is low (pHo 5.5), i.e. there is an excess of H^+- ions, HCO_3^- combines with H^+ to form H_2O and CO_2. Conversely, the opposite effect occurs when the intracellular pH is lower than the extracellular pH, due to intracellular

Ocjena rada u tijeku

acidification or extracellular alkalization (pHo 8.0). Experimental results have shown an increased transport rate after extracellular acidification (pHo 5.5).

The proposed mechanism suggests that when the proton gradient is inward, the HCO_3 gradient is outward and stimulates the transport activity of Oatp1d1. If, on the other hand, the proton gradient is directed outwards, the transport activity is reduced. This indicates a bicarbonate antiport mechanism similar to that of mammalian OATPs/Oatps (Popovic et al., 2013). Regarding the role of protonation, the pH dependence of protein activity is thought to be related to protonation of histidine residues, as is the case in mammalian transporters where His102 has been identified as a candidate residue. In our laboratory, mutagenesis studies have demonstrated that protonation of His79 in intracellular loop 1 (IL1) is critical for the function of Oatp1d1. His79 has been shown to be partially responsible for the reduction in transport activity following intracellular acidification and is conserved within the vertebrate OATP1/Oatp1 family (Popovic et al., 2013).

Based on Michaelis-Menten kinetic parameters, Oatp1d1 likely possesses a single binding site for both model substrates, estrone-3-sulphate (E3S) and lucifer yellow (LY), similar to OATP1A2. In contrast, OATP1B1 and OATP1B3 probably have two different binding sites for E3S (Hirano et al., 2006; Noé et al., 2007; Roth et al., 2011; Tamai et al., 2000).

1.5.1.3. Structure and function of zebrafish Oatp1d1

Predicted membrane topology showed that Oatp1d1 probably has 12 TMDs as hypothesized for the majority of mammalian Oatps. Furthermore, conserved motifs were identified in all zebrafish Oatp members: superfamily signature motif, large extracellular loop 5 between TMD9 and TMD10 that contains 10 conserved cysteine residues and Kazal SCL21 domain. Kazal SLC21 domain is 49 amino acids long ($CX_3CXCX_6PVC\ X_6YXSXCXAGC\ X_{11}Y\ X_2CXCV$) and contains eight conserved cysteine residues from ECL5. Next, the N-glycosylation pattern which is involved in posttranslational processing of mammalian OATPs/Oatps (P. Wang et al., 2008) is conserved within the OATP1/Oatp1 family and, with the four N-linked glycosylation sites involved (Asn-122, -133, -499 and -512), is important for membrane localization, when all of them were mutated the Oatp1d1 protein was inactive and remained in cytosol (Popovic et al., 2013). Next, the evolutionarily conserved in all OATP1/Oatp1 family members from fish to mammals, except OATP1C/Oatp1c subfamily. CRAC motif ((L/V)*X*1–5Y*X*1–5(R/K)) is important for the

Ocjena rada u tijeku

membrane localization of Oatp1d1, mutation in CRAC motif (Y184A) impaired zebrafish Oatp1d1 membrane targeting. Since the CRAC motif is known to be present in many proteins that interact with cholesterol, it is assumed to play a similar role in the Oatp1d1 protein as well.

Interestingly, results showed that Oatp1d1 is present in the plasma membrane as a dimer and possibly as a higher order oligomer, with highly conserved glycophorin motifs in TMD5 (residues 208–212) and TMD8 (residues 385–390) involved in oligomer formation. Change in these motifs impaired Oatp1d1 activity because of the inability to localize in the plasma membrane and additionally, after they were mutated, there was the absence of oligomeric form in the total cell lysates (Popovic et al., 2013). Monomers are linked into dimers via disulfide bonds and dimers organize into the oligomers independently of disulfide bonds and dimerization, through disulfide bounds, has also been shown for OATP2B1 (Hänggi et al., 2006).

1.5.1.4.Substrate specificity

Oatp1d1 in teleosts is functionally similar to OATP1A/Oatp1a and OATP1B/Oatp1b members in mammals (Popovic et al., 2013). More specifically, comparison of substrate and inhibitor preferences of Oatp1d1 with mammalian OATP1/Oatp1 transporters clearly indicates that zebrafish Oatp1d1 is more similar to OATP1A2, OATP1B1, and OATP1B3 then to OATP1C. Due to Oatp1d1 high expression in liver, previous work in our lab proposed its role in the uptake and elimination of excess steroid hormone metabolites through bile, similar to the role of OATP1A2, OATP1B1 and OATP1B3.

Transport activity measurements were done on transiently or stably transfected HEK293 cells overexpressing Oatp1d1 and compounds were classified as interactors if inhibition of LY uptake was >50%. Further, to determine the type of interaction and classify compounds as substrates or inhibitors, kinetic parameters of LY uptake in the presence or absence of interacting compound were compared.

1.5.1.4.1. Oatp1d1 transport of endogenous compounds

Oatp1d1 is high affinity transporter of conjugated steroid hormones estrone-3-sulfate (E3S), estradiol-17β-glucuronide (E17ß-glucuronide) and dehydroepiandrosterone sulfate (DHEAS), but

Ocjena rada u tijeku

non-conjugated steroids like estradiol, progesterone, androstenedione, dihydrotestosterone and testosterone inhibit its function. Similar to OATP1A2, Oatp1d1 transports cortisol (Hagenbuch & Gui, 2008; Popovic et al., 2013). Nevertheless, differences are present in terms of its substrate selectivity and affinity in comparison with OATP1A2, OATP1B1, andOATP1B3. For example, Oatp1d1 does not transport bilirubin, T3, T4, bile salts, and ouabain (Popovic et al., 2013). In mammals, transport of thyroids is primarily done by OATP1C1 and OATP1A2 in the brain, whereas OATP1B1 is crucial for their elimination through liver (Fujiwara et al., 2001; van der Deure et al., 2010). Similar to the function of the OATP6/Oatp6 family in mammalian testes (Klaassen & Lu, 2008), the high expression of *oatp1d1* in zebrafish testes suggests (Popovic et al., 2013) a possible role in the uptake of DHEAS as a precursor for androgen and estrogen synthesis in gonads. In addition, high expression of Oatp1d1 in the brain and its uptake of DHEAS may be very important in the brain due to function of DHEAS as a neurosteroid and high expression of Oatp1d1, similar to OATP1A2 (Popovic et al., 2013). Inhibition of Oatp1d1 by unconjugated steroids could reduce the uptake of conjugated steroid hormones in the target tissues and thus influence the hormone balance in plasma in a way that Oatp1d1 could play a role in the negative feedback regulation of steroid hormone synthesis (James, 2011; Popovic et al., 2013). Another study (Willi & Fent, 2018) showed that many progestins and glucocorticoids show strong interaction with Oatp1d1, either as substrate or inhibitors and the interaction activity showed a positive correlation with the lipophilicity of the steroids. Authors reported that IC_{50} values were lowest for P4, followed by the following order of increasing values: 17α-hydroxyprogesterone > clobetasol propionate > spironolactone > 21α-hydroxyprogesterone > fludrocortisone acetate and additional glucocorticoids.

1.5.1.4.2. Oatp1d1 transport of xenobiotics

Apart from physiological substrates, it has been shown that the uptake of microcystins (MCs), known as cyanobacetrial secondary metabolites, is mostly mediated by OATPs/Oatps (Fischer et al., 2010). Caynotoxins represent a serious risk to fish, other aquatic organisms and human health during so-called harmful algal blooms (HABs) and consequent release into the aquatic environment. Microcystins, most dominant type of cyanotoxins and highly toxic compounds often associated with hepatotoxicity, nephropathy, neurotoxicity (Chen et al., 2009). Rate of MC uptake significantly varies for different congeners and zebrafish Oatp1d1 acts as a ubiquitously expressed, multi-specific transporters of various MC congeners, while for example, members of the Oatp1f

Ocjena rada u tijeku

subfamily are expressed exclusively in the kidney and transport only specific MC congeners (Steiner et al., 2016). Marić et al (2021) showed that the strongest interactors were also the most lipophilic congeners -LW and -LF, followed by congeners -LA, -LR and -YR, in correlation with their log POW. Only truly hydrophilic congener, MC-RR, with log POW value of -0.2, was not significantly transported by Oatp1d1, in the same study.

Another *in vitro* study in our group (Popovic et al., 2014) showed that PFOS, nonylphenol, gemfibrozil, diclofenac, EE2 and caffeine are high affinity substrates of zebrafish Oatp1d1 and PFOA and synthetic estrogens, E2 and E1 are strong Oatp1d1 inhibitors. Both groups of compounds could disrupt normal transport function of Oatp1d1 and interfere with transport of physiological substrates (DHEAS, E3S and E17ß-glucuronide) (Popovic et al., 2014).

Importantly, considering data obtained so far on the interaction with environmental substances, for the purpose of this study we selected diclofenac and PFOS as highly relevant environmental pollutants that have been extensively studied in relation to the function of Oatp1d1. Therefore, in the following paragraphs we will describe in more detail data related to environmental relevance, toxicity and interaction of selected model contaminants with zebrafish Oatp1d1 transporter.

Diclofenac

Diclofenac is a widely used non-steroidal anti-inflammatory drug (NSAID). In addition to its role as a pharmaceutical agent, diclofenac has also attracted attention as an environmental pollutant due to its widespread use and incomplete removal during wastewater treatment (Zhang et al., 2020). The fate of diclofenac in the aquatic environment involves various processes, including biodegradation, photolysis and sorption to sediment particles (Diniz et al., 2015; Escapa et al., 2018). However, these processes do not always result in the complete removal of diclofenac, contributing to its persistence and potential accumulation in the aquatic environment. Furthermore, diclofenac and its metabolites can be classified as pseudo-persistent compounds, as the greatest ecological risk is due to its continuous input into the environment (Kallio et al., 2010; Mehinto et al., 2010). Another interesting example is the known toxicity of diclofenac to *Gyps* vultures. The authors point out that diclofenac is probably toxic to all eight vulture species within the *Gyps* genus and that three endemic vulture species are threatened with extinction following a dramatic decline in South Asia due to exposure to diclofenac used as a veterinary drug in the carcasses they

Ocjena rada u tijeku

scavenge. Although environmental concentrations of diclofenac detected in municipal wastewater effluent, surface water, groundwater and drinking water, could not cause lethal effects on organisms at concentrations in the order of ng/L to µg/L (10^{-6} to 10^{-3} µM) (Benotti et al., 2009; Sacher et al., 2001; Tauxe-Wuersch et al., 2005), chronic toxicity is possible. Cytological alterations were observed in the liver, kidney and gills of rainbow trout (*Oncorhynchus mykiss*) exposure to 3.38×10^{-3} µM diclofenac, in brown trout (*Salmo trutta*) exposed to 1.69×10^{-3} µM and the lowest observed effective concentration (LOEC) for renal lesions was 1.69×10^{-2} µM (Hoeger et al., 2005; Schwaiger et al., 2004; Triebskorn et al., 2004).

The primary mode of action of diclofenac is inhibition of cyclooxygenase (COX) enzymes, leading to dysregulation of prostaglandin synthesis and signaling. This disruption impairs critical processes such as angiogenesis, cell proliferation and tissue differentiation, which are essential for normal embryonic development (Praskova et al., 2014). Exposure to diclofenac during early development has been shown to disrupt normal embryogenesis in zebrafish, leading to a spectrum of developmental abnormalities. Craniofacial defects, cardiac malformations, spinal deformities and reduced body size are among the developmental abnormalities observed as a result of diclofenac exposure. These effects are dose-dependent, with higher concentrations of diclofenac having more pronounced negative effects on zebrafish embryos (Chabchoubi et al., 2023; J.-B. Chen et al., 2014)). Metabolism of diclofenac in zebrafish involves conversion to reactive metabolites, including 4'-hydroxydiclofenac and 5'-hydroxydiclofenac, which are mediated by cytochrome P450 enzymes. These metabolites contribute to oxidative stress and cellular damage, which exacerbates the toxic effects of diclofenac on zebrafish embryos (Nawaji et al., 2020). In addition, diclofenac exposure activates apoptotic signaling pathways and disrupts mitochondrial function. These molecular changes contribute to the observed developmental defects, including organ-specific damage and morphological abnormalities (Jung et al., 2020).

PFOS

Per- and polyfluoroalkyl substances (PFAS) are a diverse group of man-made chemicals that have been widely used in various industrial applications and consumer products since the 1940s. These substances are characterized by their strong carbon-fluorine bonds, which give them remarkable resistance to water, oil and heat. This resistance has made PFAS invaluable in numerous areas, such as non-stick cookware, water-repellent clothing, stain-resistant fabrics and carpets, food

Ocjena rada u tijeku

packaging, firefighting foams, and personal care products such as shampoos and dental floss (Buck et al., 2011). However, the same chemical stability that makes PFAS so useful also leads to environmental persistence and widespread contamination, raising significant ecological and health concerns (Lau et al., 2007).

PFAS are not easily degradable and can persist in the environment for long periods of time (Prevedouros et al., 2006). They have been detected in various environmental media, including surface waters (rivers, lakes and oceans), groundwater and drinking water supplies, soils and sediments and even atmospheric dust (Post et al., 2012). Environmental concentrations of PFAS can vary widely, typically ranging from parts per trillion (ppt) to parts per billion (ppb), depending on proximity to sources such as industrial sites, firefighting training areas, and wastewater treatment plants (Y.-Q. Wang et al., 2022). The persistence and bioaccumulative nature of PFAS results in their accumulation in the tissues of aquatic organisms, leading to higher concentrations in predators at the top of the food chain. This bioaccumulation poses a risk not only to wildlife, but also to humans who consume contaminated food (Consoer et al., 2016). PFAS exposure can result in various toxic effects on aquatic organisms, including developmental and reproductive toxicity, endocrine disruption, immune system effects and behavioral changes (Ankley et al., 2021; Houde et al., 2006). These toxic effects can lead to reduced hatching rates, abnormal development, reproductive failures, altered growth, metabolism and increased susceptibility to diseases. Additionally, PFAS exposure can result in behavioral changes, such as altered feeding and avoidance of predators, which can impact survival and reproduction (Lou et al., 2013).

Perfluorooctane sulfonate (PFOS) is a specific type of PFAS that has been widely used due to its hydrophobic and lipophobic properties. PFOS has been widely produced and utilized in various industrial and consumer products, including stain and water repellents for textiles, upholstery, carpets and leather products; firefighting foams used in aqueous film-forming foams (AFFF) for fire suppression, particularly at airports and military bases; coating and etching processes in the metal plating industry; electronics manufacturing processes such as photolithography; pesticides and insecticides; and paper and packaging materials to resist grease and moisture (Sato et al., 2009).

PFOS poses significant risks to aquatic organisms due to its persistence, bioaccumulative nature, and toxicity. PFOS readily bioaccumulates in aquatic organisms, leading to higher concentrations

Ocjena rada u tijeku

in top predators (Conder et al., 2008). Exposure to PFOS has been associated with various adverse effects on aquatic organisms, including developmental and reproductive toxicity, endocrine disruption, liver toxicity, immune system effects and behavioral changes (Ankley et al., 2021). These toxic effects can result in developmental abnormalities, reduced hatching success, impaired reproductive function, liver damage, altered lipid metabolism, increased susceptibility to infections and diseases, and changes in food intake, predator avoidance and mating behavior (Houde et al., 2006). The effects of PFOS on lipid metabolism, particularly in zebrafish embryos, involve several pathways and cellular processes. PFOS can interact with peroxisome proliferator-activated receptors (PPARs), particularly PPARα, resulting in altered expression of genes involved in fatty acid oxidation, lipid transport and lipid synthesis (Rosenmai et al., 2016). PFOS exposure induces oxidative stress through the generation of reactive oxygen species (ROS), which can damage cellular components, including lipids, leading to lipid peroxidation(Lau et al., 2007). PFOS-induced mitochondrial dysfunction can impair lipid metabolism, resulting in energy deficits and lipid accumulation (Domingo & Nadal, 2019) Additionally, PFOS can induce endoplasmic reticulum (ER) stress and impair protein folding and lipid homeostasis (Ankley et al., 2021). PFOS can disrupt the normal function of lipoproteins and enzymes involved in lipid transport and storage, leading to abnormal lipid accumulation or depletion in tissues (Houde et al., 2011). Furthermore, PFOS exposure can lead to changes in the expression of key genes involved in lipid metabolism and hormonal disruption, affecting lipid metabolic processes (Rosenmai et al., 2016).

Studies have shown that PFOS exposure leads to increased lipid accumulation in zebrafish embryos due to impaired lipid catabolism and enhanced lipid synthesis (Domingo & Nadal, 2019). PFOS exposure can change the composition of lipids in zebrafish embryos, including increased triglyceride and cholesterol levels (Lau et al., 2007). PFOS has been shown to upregulate genes involved in lipid synthesis and downregulate genes involved in lipid oxidation (Ankley et al., 2021).

PFOS interacts with various organic anion transporters (OATs) and organic anion transporting polypeptides (OATPs). Research has shown that PFOS can be transported by several OATs, including hOAT4 (Nakagawa et al., 2009) and OATPs such as OATP1A2, OATP1B1 and OATP1B3, which are expressed in different tissues including the liver, kidney and intestine. Studies have shown that hOAT4 is involved in the renal clearance of PFOS and facilitates its

Ocjena rada u tijeku

excretion from the body (Nakagawa et al., 2009). Similarly, OATPs in the liver and intestine contribute to the disposition of PFOS by mediating its uptake into hepatocytes and enterocytes (O. Kimura et al., 2020). This transport activity affects the bioavailability and toxicity of PFOS, influencing its accumulation in tissues and its potential health effects (Zhao et al., 2016, p. 201). An important aspect of PFOS interaction with these transporters is its impact on reproductive toxicity, particularly through OATP3a1 in Sertoli cells, which may lead to adverse effects on male reproductive health (T. Li et al., 2023).

The toxicokinetic of PFOS in zebrafish is determined influenced by its interaction with various transporters, including Oatps and Oats. These interactions can lead to significant changes in the bioconcentration and tissue distribution of PFOS in zebrafish (Consoer et al., 2016). Zebrafish Oats, including Oat1 and Oat3, play an important role in modulating the transport activity of PFOS. Specifically, zebrafish Oat1 and Oat3 exhibit interactions with environmental contaminants, including PFOS, affecting their bioavailability and toxicity in zebrafish (Dragojević et al., 2020). Oatp1d1 has a high affinity towards PFOS. This interaction highlights the role of OATP1d1 in mediating the uptake and potential toxic effects of PFOS in zebrafish (Popovic et al., 2014). Additionally, the functional conservation of OATPs/Oatps in vertebrates suggests that zebrafish Oatp1d1 might serve as a functional ortholog to human OATP2B1, showing strong interactions with PFOS and impacting its toxicity (Dragojević et al., 2021). The expression of downstream pathways, including those involving Oatps, was significantly altered in zebrafish embryos, indicating the crucial role of these transporters in mediating the effects of PFOS (Jantzen et al., 2016).

1.6. Aim of research and key research objectives

Considering that our previous *in vitro* studies strongly indicate that Oatp1d1 is a potentially important fish transporter in the context of environmental toxicology, and that the physiological consequences of impaired Oatp1d1 activity are still unknown, we have generated a CRISPR/Cas9 mutant zebrafish line lacking a functional Oatp1d1 protein. This mutant line will serve as a key model for *in vivo* research presented in this thesis.

Ocjena rada u tijeku

The main aim of the research presented is the detailed *in vivo* characterization of the Oatp1d1 transporter in zebrafish as a model organism, in order to better understand its physiological and ecotoxicological relevance. To fulfill this general goal, we have set four specific research objectives:

1) Characterization of the phenotype of the Oatp1d1 mutant line;
2) Development of Oatp1d1 antibodies to characterize the Oatp1d1 mutant line and the distribution, expression and localization of Oatp1d1 in zebrafish embryos and tissues;
3) Analysis of the changes in gene expression of *oatp1d1* and other organic anion transporter genes caused by Oatp1d1 mutation;
4) Analysis of the changes caused by exposure of mutant and wild-type zebrafish embryos and larvae to selected environmental contaminants.

1.7. Key research hypotheses

Due to the overlapping substrate specificity and the similar localization pattern of the zebrafish organic anion transporters, we hypothesize that the mutation of the *oatp1d1* gene and the resulting loss of function of the Oap1d1 transporter will not cause deformities and mortality in embryonic development and that the fish will develop normally.

At the gene expression level, we expect to observe changes in the expression of other organic anion transporter genes with overlapping substrate preferences, due to possible mechanisms of gene compensation.

We expect differences in the form of both higher and/or lower sensitivity between the Oatp1d1 mutants and the wild type zebrafish in response to exposure to toxic Oatp1d1 model environmental contaminants, possibly depending on the nature of metabolism of different substrates and the formation of toxic metabolites.

2. Materials and Methods

Ocjena rada u tijeku

2.1. Materials

2.1.1. Biological models

Competent DH5α E. coli cells (Life Technologies, CA, USA) were used for cloning. These cells were grown on agar plates (Sigma-Aldrich, Taufkirchen, Germany) and in liquid Luria-Bertani medium (Becton, Dickinson and Company, Sparks, USA) supplemented with 100 µg/ml ampicillin (Sigma-Aldrich, Taufkirchen, Germany). Human embryonic kidney cells (HEK293T) (ATCC, CRL-1573) were used for immunocytochemistry and protein localization analyses.

Zebrafish (*Danio rerio*), AB strain, were purchased from the European Zebrafish Resource Centre (EZRC, Karlsruhe, Germany). All handling and experiments were conducted in accordance with the EU Guide for the Care and Use of Laboratory Animals, Council Directive (86/609/EEC), and the Croatian Constitutional Act on the Protection of Animals (NN 135/06 and 37/13) under the project license HR-POK-023.

2.1.2. Non-biological materials

Chemicals, enzymes, molecular biology kits, and oligonucleotides used in this study were as follows: standard chemicals (Table 1), enzymes (Table 2), commercial kits (Table 3), oligonucleotides (Table 4). Oligonucleotides with modifications, used for morpholino oligonucleotide mediated zebrafish embryos silencing (Table 5). Antibodies used in the western blot and immunocytochemistry and immunohistochemistry analysis are listed in (Table 6). All equipment used in this study is listed in (Table 7).

Table 1. Standard chemicals used in the study.

CHEMICAL	SOURCE	CAT. NO.
Agarose	Sigma-Aldrich, Germany	A9535
BSA (bovine serum albumin)	Carl Roth, Germany	8076.4
DMEM	Capricorn Scientific, Germany	DMEM-HPA
DNase/RNase-free water	Invitrogen, USA	10977035
Ethanol	Kemika, Croatia	505655

Ocjena rada u tijeku

FBS (fetal bovine serum)	Capricorn Scientific, Germany	FBS-GI-12A
GeneRuler DNA ladder mix	Thermo Fisher Scientific, USA	SM1551
Methanol	Kemika, Croatia	P140500
PFA	Sigma-Aldrich, Germany	30525-89-4
Xylol	Kemika, Croatia	
PTU (phenylthiourea)	Sigma	103-85-5
propanole	Kemika, Croatia	
Saharoza	Kemika, Croatia	57-50-1
SDS	Roth	0183.1
Triton X-100 (T-X-100)	Merck	9036-19-5
Tricaine methane-sulfonate (MS-222)	Sigma Aldrich	E10521
Dicolofenac sodium salt	Sigma Aldrich	15307-79-6
perfluorooctanoic acid (PFOA)	Sigma Aldrich	171468
perfluorooctanesulfonic acid (PFOS), K salt	Sigma Aldrich	33829-100MG
T3	Sigma Aldrich	T6397
T4	Sigma Aldrich	T2376
17β-E2	Sigma Aldrich	E8875
TCDC	Sigma Aldrich	T6260
Lucifer Yellow	Sigma Aldrich	L0144
Calcein	Sigma Aldrich	C0875
DCFH-DA	Sigma Aldrich	D6883
Acridine orange	AlfaAesar	L13159

Ocjena rada u tijeku

Table 2. List of buffers and media used in the study.

NAME	COMPOSITION	pH
Citrate buffer (CT3)	w/v (acidium citricum) = 0.21%	3.0
Citrate buffer (CT6)	CT3 : CT8 = 1 : 1	6.0
Citrate buffer (CT8)	w/v (sodium citrate x 2 H2O = 0.294%	8.0
PBSt	10x PBS : 0.1% Tween-20 = 100 : 1	
High salt PBS	w/v (NaCl) = 1.8%	
PBS		
PBS + NaN3	v/v (NaN3) = 0.1%	
E3 medium	(NaCl) = 250 mM, c (KCl) = 8.5 mM, c (CaCl2) = 16.5 mM, c (MgSO4) = 16.5 mM	7.8
OCT medium	w/v (polivinil alkohol) = 10.24%, w/v (polietilen glikol) = 4.26%	
Vectashield medium		
LB (Lysogeny Broth)		
TAE buffer	c (Tris) = 40 mM, c (EDTA) = 1 mM	8.0
TBSt	c (Tris) = 20 mM, c (NaCl) = 150 mM, w/v (Tween-20) = 0.1%,	7.6

Table 3. List of enzymes used in this study.

ENZYME	SOURCE	CAT.NO
BamHI, restriction enzyme	New England Biolabs, USA	R0136S
GoTaq qPCR mix	PROMEGA, USA	A6001
NotI, restriction enzyme	New England Biolabs, USA	R0189S
Phusion polymerase	New England Biolabs, USA	M0530L
Power SYBR Green PCR Master mix	Applied Biosystems, USA	4367659
Reverse transcriptase	New England Biolabs, USA	4374966
XbalI, restriction enzyme	New England Biolabs, USA	R0145S
XholI, restriction enzyme	New England Biolabs, USA	R0146S

Ocjena rada u tijeku

Table 4. List of commercial kits used in this study.

MOLECULAR BIOLOGY KIT	SOURCE	CAT NO
CloneJET PCR Cloning Kit	Thermo Fisher Scientific, USA	K1232
In-fusion cloning kit	Takara, Japan	638947
Monarch DNA Gel Extraction Kit	New England Biolabs, USA	19783
Monarch Genomic DNA Purification Kit	New England Biolabs, USA	T3010S
Monarch PCR & DNA Cleanup Kit	New England Biolabs, USA	T3010S
Monarch RNA Cleanup Kit	New England Biolabs, USA	T2040L
Monarch Total RNA Miniprep kit	New England Biolabs, USA	T2010S-50
Power SYBR Green PCR Master Mix	Thermo Fisher Scientific, USA	4367659
ProtoScript II First Strand cDNA Synthesis kit	New England Biolabs, USA	E6560l
Zyppy Plasmid Miniprep Kit	Zymo research, USA	D4036

Table 5. List of oligonucleotides used in this study. All oligonucleotides were purchased from Macrogen EU.

OLIGONUCLEOTIDE NAME	SEQUENCE	PURPOSE
DrOatp1d1-qPCR-F	acgccctgtacagctcatcct	qRT-PCR
DrOatp1d1-qPCR-R	actggtcctttagcgcttgct	qRT-PCR
DrOatp2b1-qPCR-F	acgcagactgggtttgactgt	qRT-PCR
DrOatp2b1-qPCR-R	gcagccaataaaaagaagtggaa	qRT-PCR
DrOatp5a2-qPCR-F	cctgggcggcatcaatatc	qRT-PCR
DrOatp5a2-qPCR-R	gatccggcagccacaattc	qRT-PCR
DrOatp1f2-qPCR-F	acagctgccacccacactaat	qRT-PCR
DrOatp1f2-qPCR-R	ggcatccagaaaaaggctgtt	qRT-PCR
DrOat1-qPCR-F	TGCTGTTCTGATCTTGGACGA	qRT-PCR

Ocjena rada u tijeku

DrOat1-qPCR-R	TGCTATTAAACCAGCGATGAC	qRT-PCR
DrOat3-qPCR-F	GGGTCAGCATTTACCTCATCCA	qRT-PCR
DrOat3-qPCR-R	GATGGCCGTCGTCCTAACAT	qRT-PCR
DrOat2a-qPCR-F	TCGCCATTGCAAGAACCTTAT	qRT-PCR
DrOat2a-qPCR-R	AAGGTGCGATGCTTAACATCTG	qRT-PCR
DrOat2c-qPCR-F	GATTGTAAGTGTTCCAGCACAAGAA	qRT-PCR
DrOat2c-qPCR-R	TGAGCTGCTGGACGAGTTTATC	qRT-PCR
DrOat2d-qPCR-F	ACAGTATGGCATGGGCTGTT	qRT-PCR
DrOat2d-qPCR-R	AAGGTGAAGTGACAGCCACT	qRT-PCR
DrOat2e-qPCR-F	GGTGTTATGATCAGTTTGGATT	qRT-PCR
DrOat2e-qPCR-R	TTGGAGCAGTTACTGTGAGG	qRT-PCR
DrOct1-qPCR-F	GTTATGTCCCGTACGTTTTAC	qRT-PCR
DrOct1-qPCR-R	TGAATGTGGGCAGAGTCATG	qRT-PCR
Cyp1a-qPCR-F	TGGGCAGCGGAAACCCTG	qRT-PCR
Cyp1a-qPCR-R	CAGGAACTTCTTCATCGTCG	qRT-PCR
Cyp3a-qPCR-F	TTCCTGCAGCTGATGGTTG	qRT-PCR
Cyp3a-qPCR-R	GGTTGCCAGATTGTAGAAGA	qRT-PCR
Gstt1-F	ATCTCATGGCTCAAAGGTCT	qRT-PCR
Gstt1-R	AAGACATGTTGAGATCCTCCA	qRT-PCR
Gstp1-2-F	CTACAACCTGTTCGATCTCCT	qRT-PCR
Gstp1-2-R	GGGCAGAGATCTTGTCCAC	qRT-PCR
DrAbcg2a-qPCR-F	GTATACAGCCACCGCCATGACT	qRT-PCR
DrAbcg2a-qPCR-R	AAGACAAAGCTGATGGTCATGAAG	qRT-PCR
Oatp1d1_ex9_check_F	GATGATCACGTTCAAGCCGA	qRT-PCR
Oatp1d1_ex9_check_R	TGAACAGAAAGCCAGAACCG	qRT-PCR
p53_F	GGGCAATCAGCGAGCAAA	qRT-PCR
p53_R	ACTGACCTTCCTGAGTCTCCA	qRT-PCR
hhex_F	GGTAAGCCTCTGCTGTGGTC	qRT-PCR
hhex_R	TCTTCTCCAGCTCGATGGTT	qRT-PCR
pax8_F	GAAGATCGCGGAGTACAAGC	qRT-PCR
pax8_R	CTGCACTTTAGTACGGATGA	qRT-PCR

Oglena rada u tileku

casp3a_F	CTGCACTTTAGTACGGATGA	qRT-PCR
casp3a_R	ATCCTTTCACGACCATCT	qRT-PCR
casp8_F	GGGCAAAGCTGGGAAGATC	qRT-PCR
casp8_R	CTTCTTCTAGAGGAAGTCTGC	qRT-PCR
casp9_F	CTGAGGCAAGCCATAATCG	qRT-PCR
casp9_R	AGAGGACATGGGAATAGCGT	qRT-PCR
DrSlco1d1_ex2_F	ACGGAGAAGAAGAAGGAGCC	splice morpholino efficiency
DrSlco1d1_ex2_R	CCTTGGAAGAAATGCGGCAT	splice morpholino efficiency
Oatp1d1_rescue_F	AGAGGATCTGCTCGAGATGAGTACGGAGAAGAAGAAGGAGC	InFusion cloning
Oatp1d1_rescue_F	TCACTATAGTTCTAGATCAGATGGTGGTCTCCTGG	InFusion cloning
1d1_rescue_verif_F	CTTGGGCGACCTCACCAT	rescue construct
1d1_rescue_verif_R	GCACATGGCAGCCAAAAAC	rescue construct
DrAtp50_qPCR_ex6_ex7_F2	CTTGCAGAGCTGAAAGTGGC	Housekeeping gene, qRT-PCR
DrAtp50_qPCR_ex6_ex7_R2	ACCACCAAGGATTGAGGCAT	Housekeeping gene, qRT-PCR

Table 6. List of modified oligonucleotides used in this study.

NAME	SEQUENCE	MODIFICATION	PURPOSE	SOURCE
*oatp1d1*MO-ATG	TTCTTCTTCTCCGTACTCATGGTG	Morpholino oligonucleotide	5′ UTR blocking zebrafish oatp1d1	Genetools LLC, USA
*oatp1d1*MO-splice	TGTGATTTCGACTCTCACCGATTTC	Morpholino oligonucleotide	ex2-in2 splice blocking, zebrafish oatp1d1	Genetools LLC, USA

Ocjena rada u tijeku

Table 7. List of antibodies used for imunocitochemistry and immunohistochemistry.

ANTIBODY	HOST	PRODUCER
Anti-Oatp1d1 (epitope 644-660) polyclonal primary	rabbit	Genosphere biotechnologies, Germany
Anti-Oatp1d1 (epitope 674-689) polyclonal primary	rabbit	Genosphere biotechnologies, Germany
GAR-CY3 (goat anti-rabbit IgG conjugated with Cy3) secondary	goat	Jackson ImmunoResearch Laboratories

Table 8. List of equipment used in this study.

EQUIPMENT	PRODUCER	PURPOSE
PCR, T100 Thermal Cycler	Bio-Rad Laboratories, USA	PCRs, incubations
BInocular lupa	Motic, China	Embryos
Fluorescent loupe	Zeiss Discovery V8	Fluorescence detection
Centrifuge Mikro 120	Hettich, Germany	Sample preparation
Centrifuge Universal 32R	Hettich, Germany	Sample preparation
Fluorescent Microscope	Motic AE31E	Embryos, tissues visualization
Fluorescent Microscope	Axio Imager.Z2, Carl Zeiss, Oberkochen, Germany	Embryos visualization
Ultra Turrax T25	IKA, Germany	Homogenization
Real-Time PCR System	Applied Biosystems, USA	qPCR analysis
ChemiDoc™ XRS+ System	Bio-Rad Laboratories, USA	signal detection on agarose gels
BioSpec nano micro-volume spectrophotometer	Shimadzu, Kyoto, Japan	RNA concentration
Infinite 200	Tecan, Switzerland	Multimode microplate reader
FemtoJet® 4x, Microinjector	Eppendorf, USA	Microinjections
Cryomicrotome Leica CM 1850	Leica Instruments, Nussloch, Germany	cryosections
DanioVision observation chamber	Noldus Information and Technology, Wageningen, the Netherlands	Behaviour experiments
Electrophoresis chamber Biometra Compact XS/S	Analytic Jena	Running RT-PCR and PCR products
Opton II RS microscope	Opton Feintechnik, Oberkochen, Germany	Fluorescence microscopy

Osiena rada u fiziku

Rocking Platform	Labnet, USA	Shaking of samples

2.2. Methods

2.2.1. Animals and sample collection

Wild-type (WT) zebrafish, ABO strain (European Zebrafish Resource Centre, Karlsruhe, Germany), were maintained under standard conditions, with a 14-hour light/10-hour dark cycle and a water temperature of 27–28 °C. The fish were fed with a standard food of the appropriate size (Gemma Micro, Skretting, Norway). Embryos were obtained by morning spawning from 1 to 1.5 year old zebrafish, transferred to a petri dish containing E3 medium (5 mM NaCl, 0.17 mM KCl, 0.33 mM CaCl2, 0.33 mM MgSO4) and reared in an incubator at 28 °C with the same light/dark period as the adults. Embryo development was observed under a dissecting microscope (Motic AE31E, Motic, Barcelona, Spain) and embryos were staged as previously described (Kimmel et al., 1995).

2.2.2. Generation of the *oatp1d1* mutant zebrafish line

Short guide (sg)RNA (5′GGACTCGCATTTGTAAGGCA3′) targeting exon four was selected using the CRISPR scan algorithm (Kielkopf et al., 2020) and generated as previously described (Modzelewski et al., 2018) (Figure 13). A mixture of 600 ng/µL of Cas9 protein (NEB: M0386) and sgRNA complex was prepared at a 1:1 ratio and 1 nL of the mixture was injected into zebrafish embryos at the one-cell stage. When the injected fish (F0) reached adulthood at about three months of age, they were crossed with WT fish and their progeny were analyzed by high-resolution melting analysis (HRMA). Embryos positive for mutations were subsequently sequenced and several mutations were detected in the germline of the F0 fish. Female and male F0 fish that carried the same mutation (deletion of 5 nucleotides (GTGCC) at position 9115-9119) on the genomic DNA in the germline, resulting in a premature stop codon mutation at 140 amino acids, were selected as

Ocjena rada u tijeku

founders (Figure 13). The founders were then crossed with the aim of producing homozygous mutant embryos. As the offspring grew, their fins were clipped to isolate the genetic material of each fish for genotyping (IACUC standard procedure, 2022). Female and male fish with homozygous mutation (premature stop codon at 140 amino acids) were selected for further crosses to generate F2 generations of fish lacking the functional Oatp1d1 protein. Genotyping by sequencing confirmed that all F2 fish were homozygous mutants with 1 or 2 mutations.

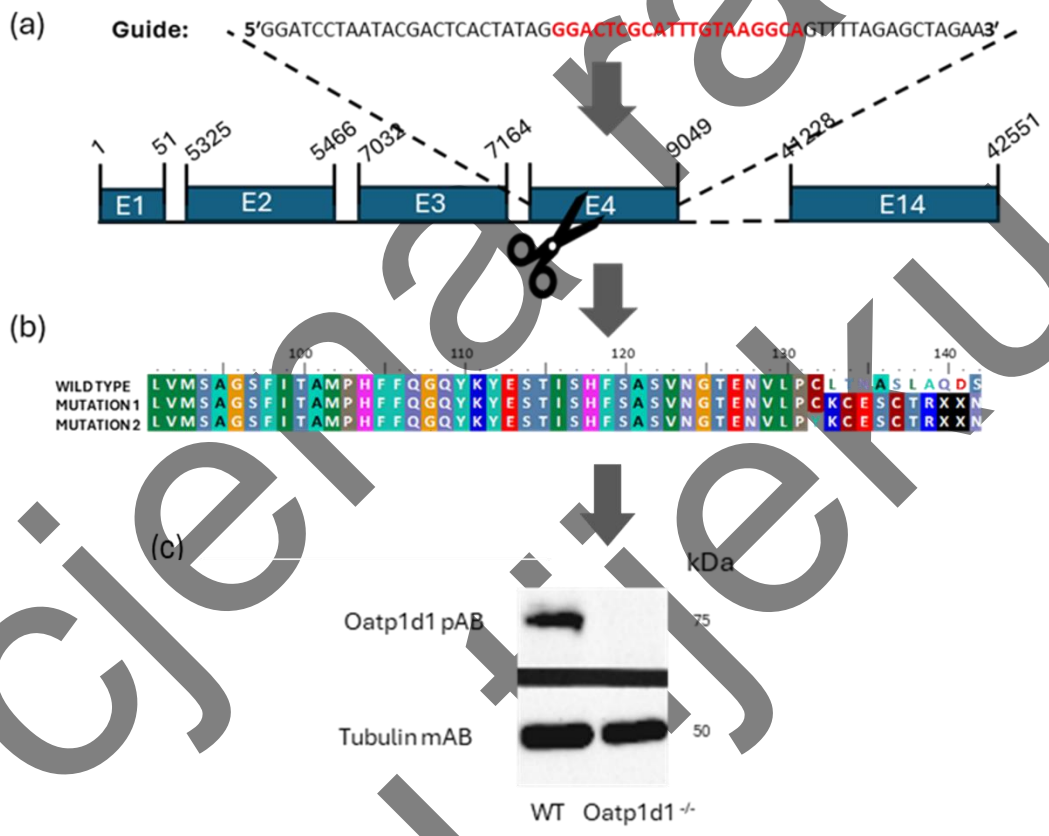

Figure 13. Development and confirmation of Oatp1d1 knockout mutants. **(a)** Schematic representation of CRISPR/Cas9 guide design and targeting of exon 4 of the *oatp1d1* gene; **(b)** Sequences of WT Oatp1d1 protein and mutants with frameshift causing the stop codon at 140 amino acid; **(c)** western blot results of adult liver lacking the specific Oatp1d1 signal.

2.2.3. Immunocitochemistry

Ocjena rada u tijeku

A stable HEK293T-drOatp1d1 cell line was used for subcellular localisation of the Oatp1d1 protein by immunofluorescence. The cells were maintained in Dulbecco's modified Eagle medium (DMEM) with 10 % fetal bovine serum (FBS) and stored in a cell incubator at a constant temperature of 37 °C and a humidified atmosphere with 5 % CO_2.

For immunocitochemistry, the cells were seeded in a 24-well microplate at a density of 5x10^5 cells/mL on round glass coverslips and incubated in a cell incubator for 24 or 48 hours until 80 % confluence was reached. The next step was fixation in 4 % paraformaldehyde (PFA) for 25 minutes. They were then washed three times in a 100 mM glycine/PBS solution, permeabilised by incubation in methanol for 15 minutes and washed again three times in PBS. For antigen retrieval, SDS heated in a warm bath was used, with an incubation time of 5 minutes. Blocking was performed in a 5% solution of milk powder in TTBS with an incubation time of 30 minutes. The coverslips were then placed on slides and incubated for one hour in a humid chamber at 37 °C with a primary Oatp1d1 antibody diluted 1:100 in PBS. The cells were then washed three times in PBS and incubated for one hour in a humid chamber at 37 °C with the secondary antibody GAR-CY3 diluted 1:400. Finally, the samples were washed again three times in PBS. The cell nuclei were visualised by incubation with the fluorescent intercalator DAPI (300 nM DAPI/PBS) for 45 minutes at room temperature. After the last wash in PBS, the coverslips with the cells were mounted on slides in Vectashield Antifade Mounting Medium (Vector Laboratories Ltd, CA, USA) fluorescence preservation medium and stored at +4 °C until fluorescence detection with an inverted fluorescence microscope (Motic AE31E).

2.2.4. Preparation of zebrafish embryo cryosections

WT and Oatp1d1 mutant zebrafish embryos at 5 dpf were fixed using a modified protocol as described by (Ferguson & Shive, 2019). Fixation was performed in 4% PFA for 1 hour at RT with constant shaking. After fixation, the embryos were transferred to phosphate-buffered saline with Tween® 20 (PBSt) and subjected to two wash cycles of 5 minutes each. The embryos were then incubated in a 30 % sucrose solution until sedimentation was observed at the bottom of the tube, which usually occurred within one hour. The sucrose solution was then replaced with a 2.5 % bovine gelatine and 25 % sucrose solution in which the embryos were incubated overnight with constant shaking. For cryopreservation, half the volume of the gelatine/sucrose solution was

Ocjena rada u tijeku

replaced with Optimal Cutting Temperature (OCT) medium, followed by incubation at RT with constant agitation until the embryos had sunk to the bottom of the 2 mL tube. This procedure was repeated again after half of the solution had been replaced a second time with OCT medium to ensure complete infiltration. The fixed embryos were aligned laterally in the plastic cryomolds using fine needles and a magnifying lens for precision. The cryomolds were first filled half full with OCT medium and then stored at -20 °C. The cryopreservation process was completed by filling the cryomolds halfway with OCT medium. The samples frozen in OCT medium were removed from the cryomolds, mounted on cutting holders and further embedded in OCT medium before being placed in a cryomicrotome (Leica CM 1850, Leica Instruments, Nussloch, Germany) set to a cutting thickness of 8 µm and a temperature of -20 °C. In order to obtain cross-sections of all body parts, each embedded sample was cut in three series of nine sections each. The first series mainly included the head region of the embryos, the second series contained internal organs such as the beginning of the digestive system and the kidneys, while the third series mainly showed the liver and tail region of the embryos. The samples were carefully sectioned and transferred to Superfrost®Plus slides (Fisher Scientific, Massachusetts, USA), air-dried at RT for 2-3 minutes and stored at 4 °C until use.

2.2.5. Preparation of zebrafish liver tissue cryosections

Adult WT and Oatp1d1 mutant zebrafish were euthanised with Tricaine MS-222. After cessation of vital signs, such as eye movement, balance and heartbeat, the abdominal organs were exposed and isolated by a longitudinal surgical incision along the ventral side of the zebrafish body. The cryosections were prepared as previously described by (Karaica et al., 2023). Isolated abdominal organs (liver and gastrointestinal tract together) were immersed in 1 mL of 4 % PFA for 24 h at 4 °C and then rinsed twice with 1 mL of 1x PBSt at RT for 5 min. The samples were then incubated sequentially in 1 mL of 30 % sucrose in PBS + 0.02 % NaN_3 for 1 h and in 1 mL of a mixture of 2.5 % bovine golden gelatin and 25 % sucrose supplemented with 0.02 % NaN_3 for 1 h at RT. Half the volume of the gelatin-sucrose mixture was then replaced with OCT medium and incubated for 30 min at RT. This step was then repeated twice before the samples were carefully transferred with forceps to a cryomold half-filled with OCT medium and placed in the desired orientation. The cryomolds were transferred to the cryomicrotome at a set temperature of –20 °C. The frozen

Ocjena rada u tijeku

samples were then placed on the cryomicrotome sample holder, sectioned to 10 µm thickness and transferred to Superfrost®Plus slides, air-dried for 2-3 min at RT and stored at 4 °C until use.

2.2.6. Antigen Retrieval

The preparation of samples for immunohistochemical analysis involves the fixation and immobilisation of antigens while preserving the cellular and subcellular architecture. Reagents that create bonds between proteins, e.g. aldehydes that form methylene bridges between amino acid side chains, are primarily used for this purpose. However, such intra- and intermolecular bonds alter the secondary, tertiary and quaternary structure of proteins and thus reduce the availability of epitopes for the antibody. Therefore, prior to incubation with the primary antibody, the sample must be exposed to conditions that break these bonds and restore the epitope, e.g. by heating or treatment with enzymes. The optimal method for epitope retrieval depends on the epitope itself, the primary antibody, the type of tissue and the fixation method.

All protocol steps are listed in Table 9. The protocols can be categorised into four groups: DCT (deparaffinisation and citrate buffer), CT (citrate buffer), SDS and phalloidin. DCT protocols are the longest, as they involve deparaffinisation processes by incubating the samples in a series of alcohols. After these steps, the samples are heated in citrate buffer with a pH of 3, 6 or 8 for both the DCT and CT protocols. SDS +/- protocols are based on (non-)incubation of the sample in the detergent SDS and subsequent washing in a high salt phosphate buffer. The phalloidin protocol is the shortest and simplest protocol, named after the original protein for which this protocol was used.

Table 9 Antigen Retrieval – eight conditions were used to optimise the protocol for the best signal in embryo and adult sections.

DCT	CT	SDS -/+
XYLOL - 30´	Fridge at +4°C	Fridge at +4°C
PROPANOL - 5´		
ETHANOL 98% - 5´		
ETHANOL 75% - 5´		
ETHANOL 60% - 5´		
reDistilled H2O - 5´		

Ocjena rada u tijeku

Rinse in 1x PBS - 15´	Rinse in 1x PBS - 15´	
Microwave heating (800W) 4x5´ in a suitable citrate buffer (pH 3, 6 or 8) – check the level of the buffer at the end of each 5´ interval	Microwave heating (800W) 4x5´ in a suitable citrate buffer (pH 3, 6 or 8) – check the level of the buffer at the end of each 5´ interval	
20´ passive cooling at room temperature (RT)	20´ passive cooling at room temperature (RT)	
3x5´ Rinse in 1x PBS	3x5´ Rinse in 1x PBS	
0,5% T-X-100 in PBS - 15´	0,5% T-X-100 in PBS - 15´	
2% T-X-100 in PBS - 30´	2% T-X-100 in PBS - 30´	10´ in 1xPBS for SDS+/-
		Cover the SDS+ slides with few drops of 1% SDS and leave for 5´; Leave SDS- slides in 1xPBS
		After 5´ SDS + / - slides place in 1xPBS 4x5´
2x5´ Rinse in 1x PBS	2x5´ Rinse in 1x PBS	
Incubation in humidity chamber at RT in 1% BSA (bovine serum albumin) - 30´	Incubation in humidity chamber at RT in 1% BSA (bovine serum albumin) - 30´	Incubation in humidity chamber at RT in 1% BSA (bovine serum albumin) - 30´
PRIMARY ANTIBODY – INCUBATION in humidity chamber at +4°C – 12-24h	PRIMARY ANTIBODY – INCUBATION in humidity chamber at +4°C – 12-24h	PRIMARY ANTIBODY – INCUBATION in humidity chamber at +4°C – 12-24h
Rinse primary antibody in 0,1% T-X-100 in PBS - 10´	Rinse primary antibody in 0,1% T-X-100 in PBS - 10´	Rinse 2x in High-Salt PBS for 5´
Rinse 2x in PBS for 5´	Rinse 2x in PBS for 5´	Rinse 2x in PBS for 5´
SECONDARY ANTIBODY – INCUBATION in humidity chamber at RT – 1-2h	SECONDARY ANTIBODY – INCUBATION in humidity chamber at RT – 1-2h	SECONDARY ANTIBODY – INCUBATION in humidity chamber at RT – 1-2h
Rinse secondary antibody in 0,1% T-X-100 in PBS - 10´	Rinse secondary antibody in 0,1% T-X-100 in PBS - 10´	Rinse 2x in High-Salt PBS for 5´
Rinse 2x in PBS for 5´	Rinse 2x in PBS for 5´	Rinse 2x in PBS for 5´
Apply fluorescence preserving medium (10µl VECTASHIELD 1:2) and cover with a cover glass (seal the edges with nail polish to prevent evaporation of the medium)	Apply fluorescence preserving medium (10µl VECTASHIELD 1:2) and cover with a cover glass (seal the edges with nail polish to prevent evaporation of the medium)	Apply fluorescence preserving medium (10µl VECTASHIELD 1:2) and cover with a cover glass (seal the edges with nail polish to prevent evaporation of the medium)

Ocjena rada u tijeku

2.2.7. Immunofluorescence staining of zebrafish liver cryosections

To test the specific binding of a non-commercial affinity-purified rabbit polyclonal antibody against the C-terminal peptide of the zebrafish Oatp1d1 protein (zfOatp1d1 antibody, hapten sequence: 674-689 amino acids; Genosphere Biotechnologies, France) (Table 7), zebrafish embryos and adult liver cryosections prepared from WT and Oatp1d1 mutant zebrafish were used. Nine antigen retrieval techniques were first applied to WT zebrafish liver cryosections to determine the optimal binding conditions for the antibody tested (Karaica et al., 2023). An optimal condition using citrate buffer at pH 6 and Triton-X-100 detergent was identified and subsequently used in zebrafish embryo and liver cryosections, respectively. In brief, zebrafish cryosections were first hydrated in 1x PBS for 10 min, incubated in CT buffer, pH 6 or 0.1% Triton-X-100 detergent for 10 min, rinsed in 1x PBS for 10 min and incubated in 1% BSA (bovine serum albumin) in a humid chamber at RT in the dark for 30 min. The samples were then incubated with the zfOatp1d1 antibody (1:500 dilution; 0.46 mg/ml stock concentration) overnight in a humid chamber at 4 °C, rinsed 2x for 5 min in 1x PBS and then incubated with Cy3-labelled secondary goat anti-rabbit IgG antibody (GAR-CY3; 1:800, 1.5 mg/mL stock concentration) for 1 h in a humid chamber at RT. Finally, the samples were rinsed in 1x PBS for 10 min and covered with 10 µL Vectashield with coverslip and sealed with nail polish for long-term storage at 4 °C.

2.2.8. Fluorescence microscopy

The Opton II RS microscope (Opton Feintechnik, Oberkochen, Germany) with computer-controlled spot RT slider digital camera and Diagnostic Instruments Software v3.4 (Stearling Heights, MI, USA) was used for microscopic image acquisition. Images were acquired under 250x magnification while image processing was performed using FIJI/Image J 2.0.0. (Rueden et al., 2017; Schneider et al., 2012). The final images were created using the FIJI/Image J 2.0.0. ScientiFig plugin (Aigouy & Mirouse, 2013).

2.2.9. Prediction of the Oatp1d1 protein structure by the AlphaFold 3 algorithm

Ocjena rada u tijeku

With the development of AlphaFold (Jumper et al., 2021) enormous progress has been made in the prediction of protein structures. We used AlphaFold 3 to predict the structure of the monomeric Oatp1d1. The accuracy of the predicted 3D protein structure was determined using AlphaFold's internal confidence scoring system pLDDT (Predicted local distance difference test), a per-atom confidence estimate on a scale of 0to 100, with a higher value indicating higher confidence, PAE (predicted aligned error) - an estimate of the error in the relative position and orientation between two tokens in the predicted structure, and pTM (predicted template modelling) and iPTM (interface predicted template modelling) scores, which measure the accuracy of the entire structure - a pTM score above 0.5 means that the predicted overall fold of the complex could be similar to the actual structure. ipTM measures the accuracy of the predicted relative positions of the subunits within the complex. Values above 0.8 represent confident high quality predictions, while values below 0.6 indicate a failed prediction. ipTM values between 0.6 and 0.8 are a grey area where predictions can be correct or incorrect. For a detailed description (Abramson et al., 2024).

The positioning of the 3D structure of a membrane protein in the membrane (lipid bilayer) involves the calculation of the interactions and free energies of the protein in the membrane and the prediction of the membrane deformations caused by the protein, taking into account the hydrophobic thicknesses of the artificial lipid bilayers (Lomize et al., 2011). The whole procedure was optimised on a representative set of membrane proteins from the OPM database (Lomize et al., 2012), whose 3D structure was determined. We used the PPM 3.0 method, which is implemented on the web server (https://opm.phar.umich.edu/ppm_server3). Other tools were also used to position the membrane protein in the membrane, such as DeepTMHMM-1.0 (https://services.healthtech.dtu.dk/services/DeepTMHMM-1.0/), TOPCONS (https://topcons.cbr.su.se/) and TMDET (https://academic.oup.com/bioinformatics/article/21/7/1276/268950). All further details on protein topology prediction, prediction accuracy and homology analyses of the zebrafish Oatp1d1 protein can be found in the supplementary material. It is assumed that most membrane transporters are not located to the AlphaFold model, the prediction of multi-chain protein complexes remains a challenge in many cases (R. Evans et al., 2022). We used AlphaFold Multimer model on ColabFold v1.5.5 (https://colab.research.google.com/github/sokrypton/ColabFold/blob/main/AlphaFold2.ipynb), which was specifically trained for multimeric inputs (Mirdita et al., 2022) to obtain structures of

Ocjena rada u tijeku

Oatp1d1 dimer and trimer. We analysed the AlphaFold multimer structures based on a combination of the previously mentioned metrics, including pTM, ipTM, pLDDT and PAE.

2.2.10. Molecular docking

The docking study was performed using the 3D structure of the Oatp1d1 protein predicted by AlphaFold 3. Only protein atoms were used for the docking calculations. The hydrogen atoms were added using the MolProbity program (Williams et al., 2018). We selected several substrates and inhibitors that were identified *in vitro*. Three substrates for zebrafish Oatp1d1 were used for the docking study: diclofenac, PFOS and lucifer yellow and inhibitors: PFOA, 17β, chlorpyrifos-methyl and clofibrate. Their 3D structures were created *in silico* using the Maestro program (Schrödinger, 2021). Docking preparation was performed with AutoDock Tools 4 (G. M. Morris et al., 2009) using default settings. Docking calculations were performed for each protein and compound. In the first set of docking calculations, the grid size was set to the maximum (126 Å x 126 Å x 126 Å) and the entire protein was included ("blind docking") (Table S2). The other docking calculations were performed with a smaller grid (22 Å x 22 Å x 22 Å) (Table S2) which covers the transport cavity. Docking studies were performed using AutoDock Vina 1.1.2 (Trott & Olson, 2009) with search exhaustiveness set to 32. The results were analysed using AutoDock Vina, Maestro and VMD (Humphrey et al., 1996).

2.2.11. Gene silencing with morpholino oligonucleotides

Morpholino oligonucleotides are stable, uncharged, water-soluble, chemically modified oligonucleotides that bind to the complementary RNA sequence of the target gene and thereby inhibit the translation of mRNA, the splicing of pre-mRNA and the maturation of miRNA (Moulton, 2017; Nasevicius & Ekker, 2000). They are composed of standard nucleic acid bases (A, C, G and T), but have a different backbone in which the ribose/deoxyribose rings have been replaced by morpholino rings and the standard phosphodiester bonds have been replaced by phosphorodiamidate bonds (Summerton & Weller, 1997) making them resistant to degradation by nucleases (Eimon, 2014; Hudziak et al., 1996). Two morpholino oligonucleotides, one targeting the 5'-UTR region of the zebrafish *oatp1d1* gene and the other targeting the exon 2 intron 2

Ocjena rada u tijeku

boundary, were designed to block zebrafish *oatp1d1* translation and transcription, respectively, and ordered from Genetools (USA). One nanolitre of the microinjection mixture containing 75 and 100 µM of each MO, 0.3 M KCl and 0.015% phenol red was injected into each embryo at the one to four cell-stage. One-, three- and five-day-old morphants were collected as follows: (i) 10 embryos for qPCR analysis to check the efficacy of the MO-ATG and (ii) 10 embryos for RT-PCR analysis to check the efficacy of the splice blocking morpholino. A morpholino oligo directed against a splice junction is expected to produce either a complete or partial deletion of a single exon or a complete or partial insertion of a single intron. The mRNA product generated by a MO-splice was analysed by RT-PCR, and a single set of primers targeting sequences outside (5' and 3') the predicted deletion or insertion was designed (Table 5). Total RNA was extracted using the TRIZOL method and transcribed into cDNA according to the previously described protocol. The efficiency of the splice-blocking morpholino was checked by RT-PCR on ng cDNA with primer pairs annealing upstream and downstream of the morpholino target. Amplicons of WT and the *oatp1d1* morphants were separated by 1% agarose gel electrophoresis. The silencing efficiency was quantified using ImageJ (fig) and the morphants were used together with WT and Oatp1d1 mutants in further exposure experiments with diclofenac and PFOS.

2.2.12. RNA Rescue experiments/Transient overexpression in zebrafish embryos

To verify the specificity of the phenotype caused by the mutation, we performed rescue experiments in which we injected mRNA encoding full-length *oatp1d1* coding sequence into one to four cell stage embryos. Because the MO-ATG targets the endogenous 5′UTR of *oatp1d1*, it cannot bind to the mRNA rescue construct, which has a different upstream sequence derived from the plasmid from which it was in vitro transcribed. The coding sequence of Oatp1d1 (ENSDARG00000104108.3) was amplified using Infusion primers (Table 5) on cDNA derived from adult liver tissue or 5 dpf WT embryos. The PCR product was then cloned into the pCS2+6xMyc vector between the XhoI and XbaI restriction sites using the Infusion kit (Takara Bio USA, Inc.) The plasmids were linearised using the NotI restriction enzyme and *in vitro* transcribed using the HiScribe SP6 RNA kit (NEB, #E2070) in conjunction with the ARCA kit (NEB, #S1411) to cap the resulting RNAs, which were then purified using the Monarch RNA cleanup kit (NEB, #T2040) for subsequent injections. For injection experiments, 1 nL of a solution of mRNA (250 ng/ul) in 300 µM KCl was injected between the 1- and 4-cell stages.

Ocjena rada u tijeku

2.2.13. RNA isolation and gene expression analysis in embryos and adult tissues

First, we analysed the expression of *oatp1d1* in mutants, both in embryos and adult tissues, compared to WT embryos and adult animals. To characterise the phenotype of the mutants and to investigate possible compensatory mechanisms, we analysed the expression of different genes both under normal conditions and after exposure to specific compounds. Zebrafish were anaesthetised with 0.02% tricaine MS-222 and tissues (liver, kidney, intestine, brain, testis, gills, eyes, skin, muscle and heart) from at least three individual fish were stored in RNA later at -20 °C for RNA isolation. Two to three independent pools were collected. Embryos (three or more independent pools, 10 – 20 embryos per pool) were collected at different developmental stages (1 – 7 dpf), frozen dry and stored at -80 °C until RNA extraction. Tissues were homogenised using an Ultra Turrax T25 homogeniser (IKA, Germany) at medium intensity (13500 rpm) for 10 s (sometimes two cycles of 10 s per sample, depending on the tissue) and embryos were homogenised using a pestle homogenizer. RNA was isolated using the Trizol reagent according to the manufacturer's instructions (Sigma-Aldrich, Taufkirchen, Germany), checked for quality by gel electrophoresis (expected two bands) and quantified using the BioSpec nano microvolume spectrophotometer (Shimadzu, Kyoto, Japan). Reverse transcription (1 µg total RNA or 500 ng if lower RNA concentrations were obtained) was performed with the ProtoScript II First Strand cDNA Synthesis Kit (NEB, E6560L), resulting in cDNA concentrations of 50 and 25 ng/µL, respectively, and with the High-Capacity cDNA Reverse Transcription Kit with RNase Inhibitor (Applied Biosystems, Foster City, CA, USA), resulting in a cDNA concentration of 100 ng/µL. One- and three-day-old morphants (10 embryos per sample, three individual replicates) were collected to determine the gene expression of *oatp1d1* after gene silencing (ATG morpholino for qPCR and splice morpholino samples for RT-PCR). Embryos were collected at 8 hpf and 1, 2, 3 and 7 dpf for RT-PCR to determine the expression of the injected mRNA (oatp1d1 mRNA for the rescue experiment). Specific qRT-PCR primers for Slc21 and Slc22 transporters were previously described in (Mihaljevic et al., 2016; Popovic et al., 2013) for oxidative stress, apoptosis and thyroid development (reference) and purchased from Macrogen. The primer efficiencies for the oxidative stress and thyroid development primers were determined. Primer sequences, optimal concentrations and primer efficiencies of the target gene sequences are given in the table. qRT-PCR was performed using the GoTAQ qPCR mix (Promega, A6001). Elongation factor (*EF1α*)

Ocjena rada u tijeku

was chosen as the housekeeping gene for the tissues as its expression is similar in all tissues analysed, and the *ATP50* gene (*atp5po*, ATP synthase peripheral stalk subunit OSCP, Gene ID: 335191) was chosen as the housekeeping gene for the embryos as its expression is similar at all stages of embryo development. The qRT-PCR reaction mixture was prepared to a final volume of 10 µL with 10 ng of cDNA per reaction, and relative quantification was performed as previously described (Lončar et al., 2010) except that data were presented as mean normalized expression (MNE) multiplied by a factor of 10^6. Arbitrary thresholds for expression of transcripts in qRT-PCR data were defined as follows: genes were considered minimally expressed if the MNE was <999 ×10^7, low if the MNE was 1000 - 4,999, mild if the MNE was 5,000 - 8,999, moderate if the MNE was 9000 - 19999, moderately high if the MNE was 20000 - 29999, high if the MNE was 30000 - 49999, and very high if it was above 50000. Data were analysed using ABI PRISM Sequence Detection Software 1.4 (Applied Biosystems, Foster City, CA, USA) and GraphPad Prism Software version 9.0. Equation used to determine the MNE values:

$$MNE = E\,(HKG)\;Ct\,(HKG) \,/\, E\,(gene)\;Ct\,(gene) \times 10^6$$

where MNE stands for mean normalized expression; E (HKG) is housekeeping gene efficiency; E (gene) is target gene efficiency; Ct (HKG) is mean Ct value for the housekeeping gene and Ct (gene) is mean Ct value of the target gene. Data are presented as gene of interest expression relative to the housekeeping gene expression multiplied by the factor of 10^6.

2.2.14. Phenotype characterization of Oatp1d1 mutants

Embryonic development of the mutants was observed from the one-cell stage until five days after fertilisation (5 dpf). Compared to WT embryos, we observed if the development of mutants and morphants is delayed, whether there are malformations in the development of organs, resorption of the yolk sac and pigmentation of embryos. Embryos, larvae and adult fish were anaesthetised in ice-cold water due to the influence of Tricaine methane-sulfonate (MS-222) on the melanophores and photographed with a 13-megapixel Samsung camera with an aperture of f/1.9 attached to the ocular of the Motic SMZ-171 binoculars. After observing the pigment changes in the Oatp1d1 embryos as well as in the adults, we took the embryo matrix (6 hpf to 2 mpf) and measured the fluorescence with Tecan on excitation/emission 360/420 nm. The embryos (5 to 10 of them depending on stage, in case of older larvae even less) were incubated in methanol for 45

Ocjena rada u tijeku

minutes, vortexed 3 x 30 seconds and centrifuged at 10 000 g for 10 minutes. The supernatant was separated and 150 or 200 uL were taken from each sample for fluorescence measurement. For the adult fish, the most important factors were the reproduction, swimming, behaviour and size of the fish. We also wanted to check whether the pigmentation pattern was altered by the surface of the tank in which the fish were kept. We reared new mutants in modules with dark and light surfaces and their offspring were used for fluorescence measurements. To test whether the pigmentation phenotype can be rescued, mutant males and females were outcrossed to obtain heterozygous embryos and their pigmentation patterns and maternal effects were studied.

2.2.15. Exposure experiments

Due to bioethical considerations and technical complexity, exposure experiments were performed on zebrafish embryos up to 5 dpf. Since most membrane transporters, including Oatp1d1, show the highest expression at 72-96 hpf (hours post fertilization), it may be necessary to also perform experiments with older (juvenile) stages. WT and Oatp1d1 mutant embryos were exposed to selected compounds previously identified (*in vitro*) as strong Oatp1d1 interactors. After the initial tests with a wide range of concentrations of the selected compounds, the concentrations causing sublethal toxic effects were determined and the differences in the response of WTs and mutants were analysed in further replicates. The experiments were performed in 24-well microplates containing 1 mL of E3 medium with specific concentrations of compounds and 10 embryos per well. During the exposure, we observed: a) phenotypic changes during early embryonic development as a result of exposure of embryos to Oatp1d1 protein substrates and b) differences in the sensitivity of mutant embryos compared to WT embryos to the toxic compound present. Due to the possible degradation of the compounds after dissolving them in the exposure medium, we microinjected LY, model fluorescent substrate of Oatp1d1, into the yolk sac of the embryo. Some of the embryos were manually dechorionated using tweezers prior to exposure because chorion is not equally permeable for different compounds.

Phenotype analyses were performed on mutants to determine phenotype changes caused by the mutation itself, but also in parallel on mutant and WT embryos due to changes caused by exposure to substrates and/or inhibitors of the Oatp1d1 protein previously identified *in vitro*. All phenotypic changes were observed under a magnifying glass and a fluorescence microscope was used due to

Ocjena rada
u tijeku

exposure to fluorescent substrates. Methods such as TBARS (for oxidative stress), staining with fluorescent dyes DCFH-DA for ROS detection and acridine orange for apoptosis detection, were used to quantify the observed changes on a biochemical/molecular level.

2.2.15.1. Diclofenac exposure experiments with zebrafish embryos

To investigate the effects of diclofenac (CAS: 15307-81-0, monopotassium salt) on embryonic development, we performed exposure experiments with diclofenac concentrations ranging from 5 to 40 µM. Diclofenac stock solutions (100 mM) were prepared in dimethyl sulfoxide (DMSO) and working solutions were prepared in E3 medium (DMSO <0.05%). Negative controls were prepared with E3 medium and DMSO. Sets of ten embryos were distributed in 24-well plates containing 1 mL of E3 medium per well. Exposure to diclofenac began on 1 dpf and continued for up to 4 dpf or three days post-exposure (dpe). During this time, lethality and developmental abnormalities caused by diclofenac were recorded.

2.2.15.2. PFOS exposure experiments with zebrafish embryos

To investigate the effects of PFOS (CAS: 1763-23-1, Heptadecafluorooctanesulfonic Acid Potassium Salt) on embryonic development, we performed exposure experiments with PFOS concentrations ranging from 5 to 30 µM. PFOS stock solutions (100 mM) were prepared in DMSO and working solutions in E3 medium (DMSO <0.05%). Negative controls were prepared with E3 medium and DMSO. Sets of ten embryos (1 dpf) were distributed in 24-well plates containing 1 mL of exposure medium per well. Exposure lasted up to 5 dpf or 3-4 days post-exposure (dpe). During this time, mortality, developmental abnormalities such as brain necrosis, inflation of swim bladder and scoliosis caused by PFOS were recorded.

2.2.16. Phalloidin staining

Embryos previously exposed to diclofenac (10 of them exposed to diclofenac in duplicates and randomly selected 7 to 10 of them for staining) were anesthesized in Tricaine (MS-222), fixed in 4% PFA over night at RT on shaker. PFA was rinsed off next day 3 x 5 min with PBDT (1x PBS, 0.1% Tween 20, pH 7.4 + 1% DMSO) at RT on a shaker. Samples were incubated with fluorescein-phalloidin (green) diluted 1:100 in 1% NGS (Normal Goat Serum) / PBDT over night at 4 °C and

Ocjena rada u tijeku

on shaker. Next day samples were rinsed/washed 6 x 30 min with PBDT at RT on a shaker and stored in PBDT + 0.02 % Azide (N_aN_3) at 4°C. Finally, stained embryos were chosen under the binocular and tissues (heads and tails) were prepared with needles and forceps. Tissues were mounted in 10 µL of Vectashield Antifade Mounting Medium (Vector Laboratories Ltd, CA, USA) within a Vaseline ring. Samples were visualised under a fluorescence microscope (Axio Imager.Z2, Carl Zeiss, Oberkochen, Germany).

2.2.17. Acridine orange staining (apoptosis assay)

Apoptotic cells in zebrafish embryos were visualised using acridine orange (AO), a nucleic acid selective metachromatic dye that emits green fluorescence when intercalated with DNA. It is often used to detect apoptosis in zebrafish because it can permeate apoptotic cells and bind to DNA, whereas normal cells are nonpermeable to acridine orange (Asharani et al., 2008). After exposure to 15 µM PFOS, at 120 hpf (5 dpf) zebrafish embryos were selected and stained with AO (5 µg/mL) for 20 min in the dark according to the protocol (Hema et al., 2023). Stained embryos were washed 3x 5 min in E3, anesthetised in 0.02 % Tricaine (MS-222) and dead/apoptotic cells were visualized under a fluorescence microscope using a green fluorescence filter (excitation – 480 nm, emission – 535 nm).

2.2.18. Lipid peroxidation assay (TBARS)

Lipid peroxidation, an indicator of excessive ROS formation, generates the highly reactive by-product malondialdehyde, which was determined using the thiobarbituric acid reactive substances (TBARS) assay (Adeyemi et al., 2015). It was performed according to the protocol (Muthulakshmi et al., 2018), with slight modifications. In brief, about 10 embryos previously exposed to diclofenac were sonicated for about 10 s in 100 µL of RIPA buffer (0.1 % SDS). The samples were then placed on ice for 30 min and centrifuged at 10,000 g for 5 min. The homogenate was mixed with 100 µL of 5% trichloroacetic acid (TCA) and then incubated on ice for 15 min. The sample was then mixed with 100 µl of 0.67 % thiobarbituric acid and centrifuged at 2200 g for 10 min at 4 ºC. After centrifugation, the supernatant (200 µL) was boiled for 10 min, cooled to room temperature and centrifuged at 13 000 g for 5 min. The absorbance was then measured at 535 nm in a microplate

Ocjena rada u tijeku

reader (Tecan) and protein quantification was performed using the Bradford assay (Kielkopf et al., 2020).

2.2.19. ROS (Reactive Oxygen Species) assay

PFOS-induced ROS formation was visualised with cell-permeable 2′,7′-dichlorodihydrofluorescein diacetate (H2DCFDA). This is a non-fluorescent fluorescein derivative that is cell-permeable and is commonly used as a reagent to study the production of reactive oxygen species in living cells. More specifically, DCFH-DA is taken up by the cells where cellular esterases cleave off the acetyl groups, forming DCFH. This DCFH is then oxidised by ROS and converted to DCF, which emits green fluorescence at an excitation wavelength of 485 nm and an emission wavelength of 530 nm (H. Kim & Xue, 2020). Zebrafish embryos (WT and MO-splice) exposed to 20, 15 and 2 µM PFOS (96 hours of exposure), were randomly selected from duplicates of ten embryos per well, washed with PBS and incubated in 10 µM DCFH-DA for 20 min in the dark. After incubation, embryos were washed 3x with E3 and 1x with PBS to remove excess dye, anaesthetised with 0.02 % Tricaine (MS-222) and observed under a fluorescence microscope using green fluorescence filter (excitation – 480 nm, emission – 535 nm). The experiments were repeated three times, and seven to ten embryos were used for imaging. The fluorescence signal was quantified using ImageJ software and the statistical analyses were performed using GraphPad Prism 9.0.0 software.

2.2.20. Locomotor activity assessment upon exposure to PFOS

One of the approaches to determine phenotypic changes and to compare behavioural differences between WT and Oatp1d1 mutant embryos was the quantification of swimming behaviour. Since we observed behavioural changes after PFOS exposure, the WT embryos appeared to be more active, especially during the first days of exposure, while the Oatp1d1 mutants showed a lower response to mechanical stimuli (e.g. plate movements), we decided to quantify this behaviour.

We chose a sublethal concentration of PFOS (10 µM) that does not cause any visible phenotypic changes at the time of measurement. Embryos were exposed from 24 hpf until the 5 dpf, when swimming behaviour was recorded. Due to the long exposure time (4 days), embryos (10 per condition) were kept in 24-well plates and then transferred individually to 96-well plates on the

Ocjena rada u tijeku

day of measurement. After 72-96 hours of exposure, a locomotor behavior test was performed with both PFOS-treated and untreated groups and with both WT and Oatp1d1 mutant embryos. The experiment was repeated twice, with approximately 10 embryos per condition. Locomotor activity was measured using the DanioVision system (Noldus Information Technology, Netherlands) as described (Crnčević et al., 2025). The measurements were performed over a period of 20 minutes and consisted of alternating light and dark phases, 5 minutes of darkness followed by 10 minutes of light. The temperature during the measurements was kept at 27.5 °C. A smoothing profile with a minimum distance threshold of 0.2 cm was applied to reduce background noise. After tracking, embryos were examined under an inverted microscope and malformed or dead embryos were excluded from the analysis. Further data analysis and statistical evaluation was performed using GraphPad Prism 9.0.0 software.

2.2.21. Statistical Analysis

Quantification of morpholino oligonucleotide-mediated silencing efficiency and fluorescence signalling in zebrafish embryos matrix was performed using ImageJ. software and Microsoft Excel (Microsoft Office 2013). GraphPad Prism 9.0.0 Software was used for graphical visualisation and statistical analysis. The normality of the data was tested using the Shapiro-Wilk test (alpha = 0.05) when the number of replicates was at least three. When comparing two groups (WT and Oatp1d1 mutants), a multiple unpaired t-test with False Discovery Rate (FDR) correction for multiple comparisons (significance threshold Q = 1%) was performed as a parametric test for data that passed normality. A non-parametric Mann-Whitney test was used if the data did not have a Gaussian (normal) distribution or the number of replicates was less than three. Significance was declared when $p \leq 0.05$ for the differences between two independent variables and when FDR was used when q values were below the specified threshold (indicated as “discovery"). One-way analysis of variance (ANOVA) and Tukey's post hc test were used to assess the significance of differences between the behaviour of WT and mutant embryos.

3. RESULTS

3.1. Characterisation of Oatp1d1 zebrafish mutant line

Ocjena rada
u tijeku

Using the CRISPR/Cas9 system, zebrafish strain with deficient Oatp1d1 protein was created. We confirmed the successful creation of mutation in F2 generation by sequencing, which showed deletion of 5 nucleotides (GTGCC) at a position 9115-9119 of genomic DNA, which resulted in frameshift mutation and premature stop codon mutation at 140 amino acid position (Figure 13).

To confirm the absence of the Oatp1d1 protein in the mutant embryos and adults two customized Oatp1d1 antibodies were designed: ab1_1d1 (CSHREKKQALKDQLKAPE) and ab2_1d1 (CSSAIVKCENPDQETTI). Due to the transmembrane nature of transporter localization, the epitopes of Oatp1d1 are largely obscured by the plasma membrane. Therefore, the antibodies were designed to target the more open intracellular C-terminus of the protein at amino acids 644 – 660 and 674 – 689, respectively. Using a custom designed zebrafish Oatp1d1 antibody we confirmed the absence of Oatp1d1 protein in the liver of both, zebrafish males and females. Specificity of custom Oatp1d1 antibody was tested on HEK293 cell line stably overexpressing zebrafish Oatp1d1 in the plasma membrane (FlpIn293/Oatp1d1 cells). Antibody was further used for immunohistochemistry analyses of protein localization and lack of the same in mutants. Further characterization also included gene expression analyses and comparison of mutants and wild types (both embryos and adults) and subsequently phenotype characterization of Oatp1d1 mutants

3.1.1. Lack of protein expression and localisation in Oatp1d1 mutants

Initial verification of specificity of the developed antibodies was conducted on HEK293 cell line stably overexpressing zebrafish Oatp1d1 in the plasma membrane (FlpIn293/Oatp1d1 cells). Immunocytochemistry revealed the localisation of Oatp1d1 in plasma membrane, staining the membrane in red with both developed antibodies (Figure 14a).

Furthermore, Oatp1d1 protein expression was confirmed in the tested cells and liver of adult zebrafish using western blot analysis with both antibodies, showing the band of the expected size at 75 kDa (Vujica et al., 2024). As a negative control for testing custom antibodies specificities, mock-transfected cells and Oatp1d1 mutant fish were used, which showed no signal in the plasma membranes and lacked the expected band in western blot analysis (Figure 14a).

Ocjena rada u tijeku

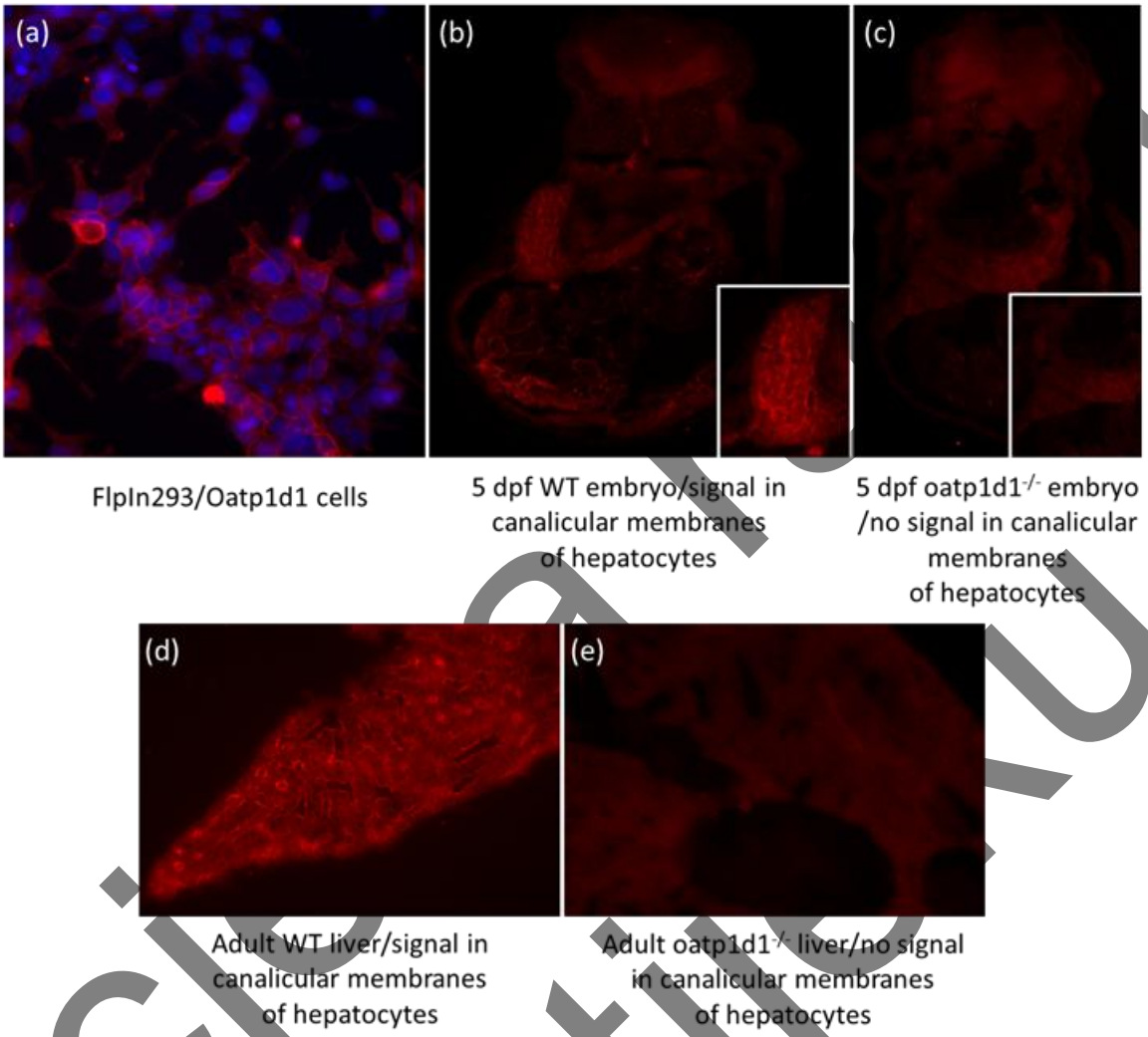

Figure 14. Immunohistological localisation of Oatp1d1 in Flpin293/Oatp1d1 stable cell line, zebrafish embryo and adults (Cy3 red signal). (a) Membrane localisation of Oatp1d1 in Flpin293/Oatp1d1 cells; **(b)** Localisation of a specific Oatp1d1 signal in canalicular membranes of hepatocytes in 5 dpf WT embryo; **(c)** Lack of Oatp1d1 specific signal in 5dpf Oatp1d1 mutant embryo; **(d)** Specific Oatp1d1 signal in canalicular membranes of liver hepatocytes of adult WT zebrafish; **(e)** Lack of Oatp1d1 specific signal in liver of Oatp1d1 mutants.

Immunohistochemistry on 5 dpf embryos showed the localisation of Oatp1d1 in the canalicular membranes of hepatocytes, whereas the specific signal was absent in Oatp1d1 mutant embryos (Figure 14b and c). The same localisation of Oatp1d1 in the canalicular membranes of hepatocytes

was confirmed in the adult liver as well and lack of the localisation in adult mutant liver (Figure 14d and e). In the membranes of glomerular podocytes the signal was also absent in the mutant fish and used as a negative control (Figure S6).

3.1.2. Expression profiles of *oatp1d1* in WT and Oatp1d1 mutant embryos

To determine the effects of the Oatp1d1 mutation, we first analyzed the changes in transcript expression, primarily of the target gene itself, during embryonic development from 6 hpf to 5 dpf and compared mutant and WT embryos. The results show that *oatp1d1* expression is dynamically regulated during zebrafish development, peaking in early gastrulation and during late embryonic and larval stages. The expression of *oatp1d1* in WT embryos increased during embryonic development from 3 dpf and reached a maximum at 5 dpf, while the expression of *oatp1d1* in the mutant embryos remained at a lower level during the first five days of development, confirming that we actually observed differences at the transcriptional level in addition to differences at the protein level (Figure 15). There are statistically significant differences at 1 dpf, 3 dpf and 4 dpf. Although multiple unpaired t-test revealed no statistically significant difference between WT and mutant embryos at 5 dpf, there is a notable difference in expression (Figure 15).

At 7 dpf, we observed an increase in expression in the mutants, which would be worth investigating further as it is unclear whether this represents an alternative transcript variant that is non-functional and possibly a compensatory response of the organism to the mutation (Figure 15).

Ocjena rada u tijeku

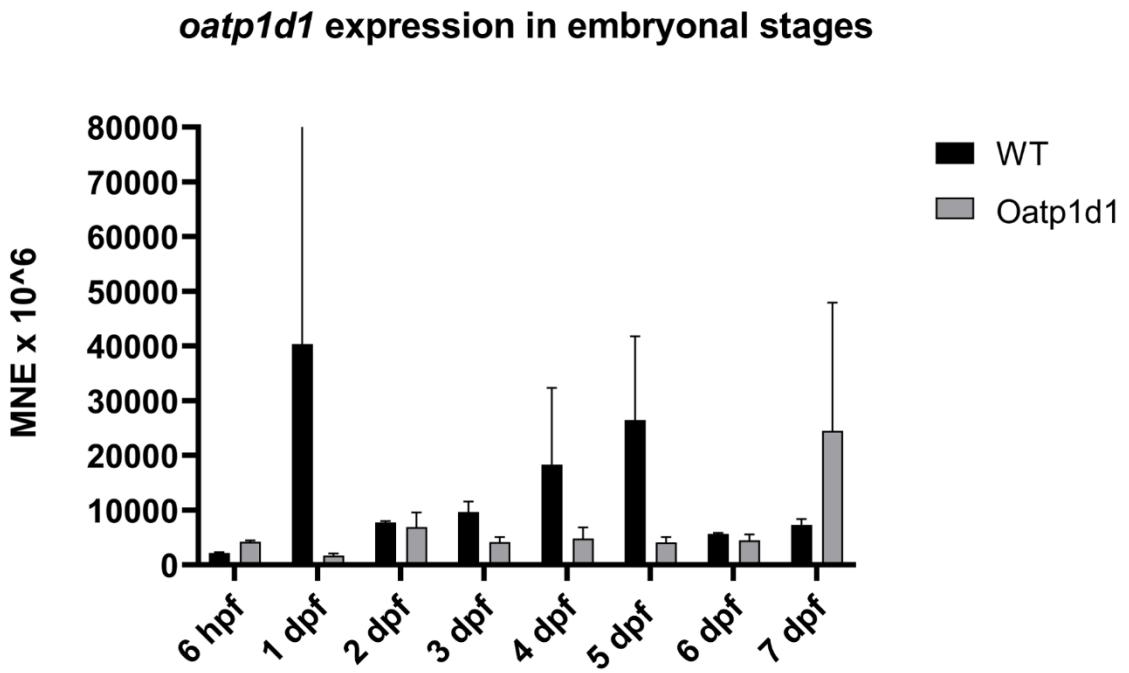

Figure 15. Expression patterns of *oatp1d1* in WT and Oatp1d1 mutant embryos during embryonic development. Statistically significant differences are labelled * ($p \leq 0.05$), ** ($p < 0.01$), *** ($p < 0.001$), **** ($p < 0.0001$). Data represent MNE (mean normalised expression) ± SD (n = 4 - 5 biological replicates) normalised to the housekeeping gene *ATP50*. The statistical tests used are the Shapiro-Wilk test for normality of distribution and the multiple unpaired t-test with false discovery rate (FDR) correction for multiple comparisons to determine the significance of differences in stages between WT and Oatp1d1 embryos. The individual p and q values are listed in Supplement material (Table S3). Statistical analyses and graphical representations were performed using GraphPad Prism 9.0.0 software.

3.1.3. Gene expressions of other transporters (*slc21* and *slc22* family) in Oatp1d1 mutant embryos

To identify the effects of the *oatp1d1* mutation, we next examined the changes in transcript expression of the other transporters of the *slc21* family and the organic anion transporters of the *slc22* family. Expression of the *oatp2b1* gene showed a slightly different pattern than that of the *oatp1d1* gene, with higher expression in the mutant embryos at 1 dpf. However, the expression pattern shifts after 2 dpf, with higher expression of *oatp2b1* in WT embryos than in mutant

Ocjenski u tijeku

embryos (Figure 16). Other *slc21* genes showed variable expression patterns between WT and mutants, but with lower expression compared to *oatp1d1* and *oatp2b1* (Figure 7).

Organic anion transporters from the *slc22* family also showed altered expression patterns in mutant embryos. Differences in expression between WT and mutants were observed for *oat1* only after 4 dpf, where the mutants showed a 3-fold upregulation, while the expression pattern changed the next day, after 5 dpf, and a 1.9-fold downregulation of *oat1* was observed (Figure 16). The expression of *oat2a* was downregulated in the mutant embryos throughout almost the entire embryonic development, starting at 2 dpf (Figure 16). *Oat2d* showed a peak in expression at 1 and 2 dpf with a clear 4- to 7-fold upregulation in the mutants, followed by lower expression at later stages (Figure 16). *Oat2e* oscillated between upregulation and downregulation in the mutants throughout development, with a 2-fold upregulation at 1 hpf and a 3.4-fold upregulation at 4 hpf, while it showed a 2- to 3-fold downregulation in the mutants at the remaining stages (Figure 16). *Oat3* was upregulated 3-fold in the mutants at 1 and 4 dpf, while expression levels were similar at 5 dpf (Figure 16).

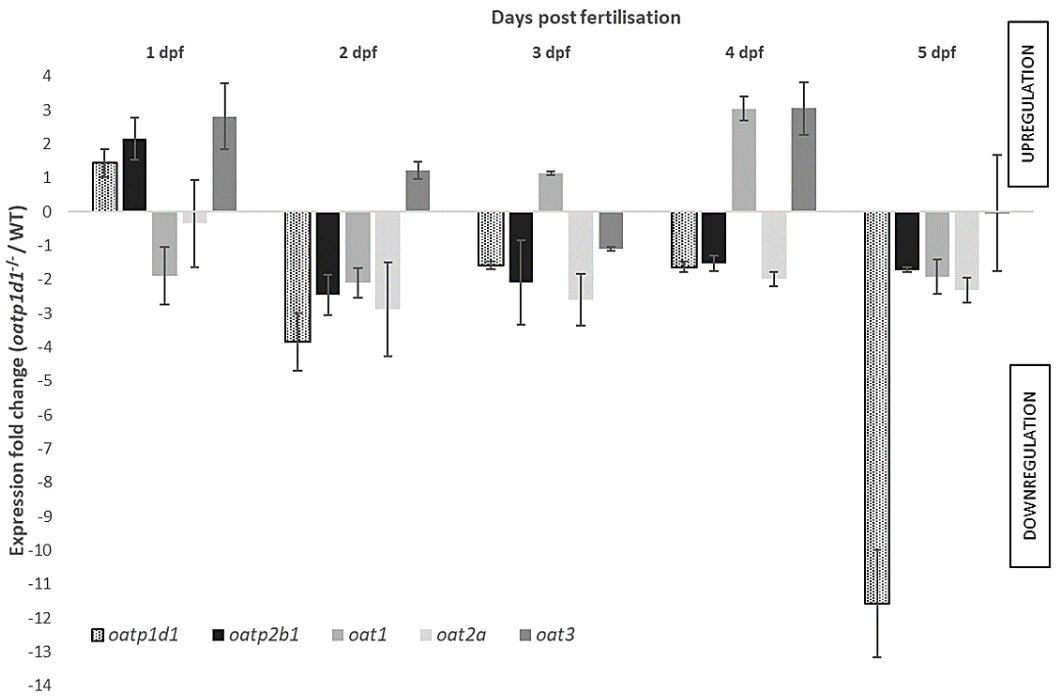

Ciena rada eku

Figure 16. Expression fold change (mutants/WT) of genes encoding for zebrafish organic anion transporters (oa*tp1d1, oatp2b1, oat1, oat2a* and *oat3*) during the first five days of embryonic development. Upregulation in the mutant transcript expression is presented as a positive fold-change and the downregulation as a negative fold-change (-1/fold). Results of two to three independent determinations for each developmental stage (pools of 10 embryos) are presented. Data represent MNE (mean normalized expression) ± SE normalized to the *ATP50*.

3.1.4. Comparative analysis of *oatp1d1* gene expression in tissues of WT and Oatp1d1 mutant adult fish

In adult fish, the results obtained are consistent with previous findings (Popovic et al., 2013) for the following tissues: liver, kidney, intestine, gills, brain, gonads and skeletal muscle, while expression in the skin, eyes and heart had not been studied at that time (Figure 17). The relationships between male and female expression levels in WT tissues remain the same as reported in Popovic et al. (2013) with the only difference that the overall expression levels are slightly higher in our case, probably due to improved and optimized RNA extraction methods.

The highest expression of *oatp1d1* is observed in the liver, brain and intestine (Figure 17). The difference between WT males and females in the expression of *oatp1d1* is most pronounced in the liver, where expression is five times higher in males than in females. In the gills, expression is about two times higher in males. Conversely, females show 2.5 times higher expression in the skin and 3 times higher expression in the skeletal muscles than males. In kidney, intestine, brain, gonads and eyes, the expression of *oatp1d1* is similarly high in both sexes (Figure 17).

Ocjena rada u tijeku

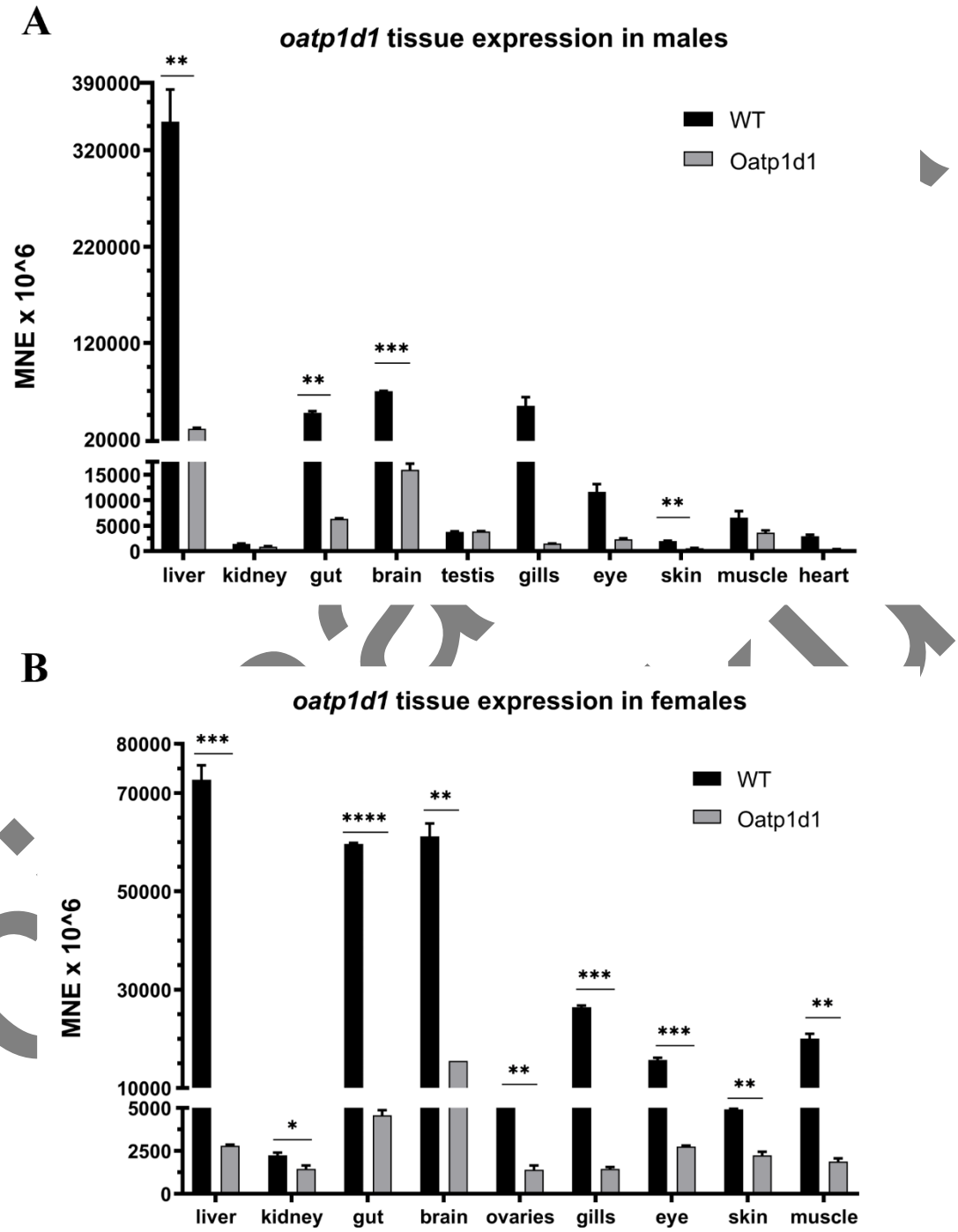

Figure 17. Tissue expression pattern of *oatp1d1* in WT and Oatp1d1 fish. A) tissue samples from males; B) tissue samples from females. Statistically significant differences are marked with * ($p \leq 0.05$), ** ($p < 0.01$), *** ($p < 0.001$), **** ($p < 0.0001$). Data represent MNE (mean normalized expression) ± SD (n = 2) normalized to the housekeeping gene elongation factor *(EF1α)*. The individual p and q values are listed in Supplement material (Tables S4 and S5). Statistical test used is multiple unpaired t-test obtained in GraphPad Prism software version 9.0.0.

In mutants, the expression of *oatp1d1* is generally strongly reduced. Statistically significant differences in the expression of *oatp1d1* between mutant and WT tissues in males were found in the liver ($p < 0.01$), where expression is 11-fold lower in mutants, in the intestine ($p < 0.01$) with a 7-fold lower expression, in the brain ($p < 0.001$) with a 4-fold lower expression and in the skin ($p < 0.01$) with a 3-fold lower expression (Figure 17). In the gills of mutant males, the expression of *oatp1d1* is also much lower than in WT males, although statistical analysis revealed no significant difference. The kidney, testis, muscle and heart also generally show low expression levels in the tissues of WT males, so they are not as relevant for comparison with the mutants, which nevertheless still show lower expression levels (Figure 17).

In females, the overall expression of *oatp1d1* is significantly reduced in the mutants in every tissue analyzed (Figure 17). The greatest differences between WT and mutant female tissues were observed in the liver, where expression was reduced 26-fold in the mutants, 18-fold in the gills, 13-fold in the intestine and 10-fold in the muscles (Figure 17).

3.1.5. Tissue expression profile of *oatp2b1* (*Slc21*) in WT and Oatp1d1 mutant adult fish

As previously reported (Popovic et al., 2010), the highest expression of *oatp2b1* in WTs is found in the gills, but also in skin, with no significant differences between the sexes. When comparing WTs and mutants, the expression in the liver of males 2-fold higher than in mutants and in females almost 3-fold higher in the liver of mutants. In the brain of males, expression is 1.9-fold higher in mutants, whereas it is downregulated in the brain of females and 2-fold lower in mutants. In the skin of females 1.3-fold higher in mutants than in WTs (Figure 18).

Ocjena rada u tijeku

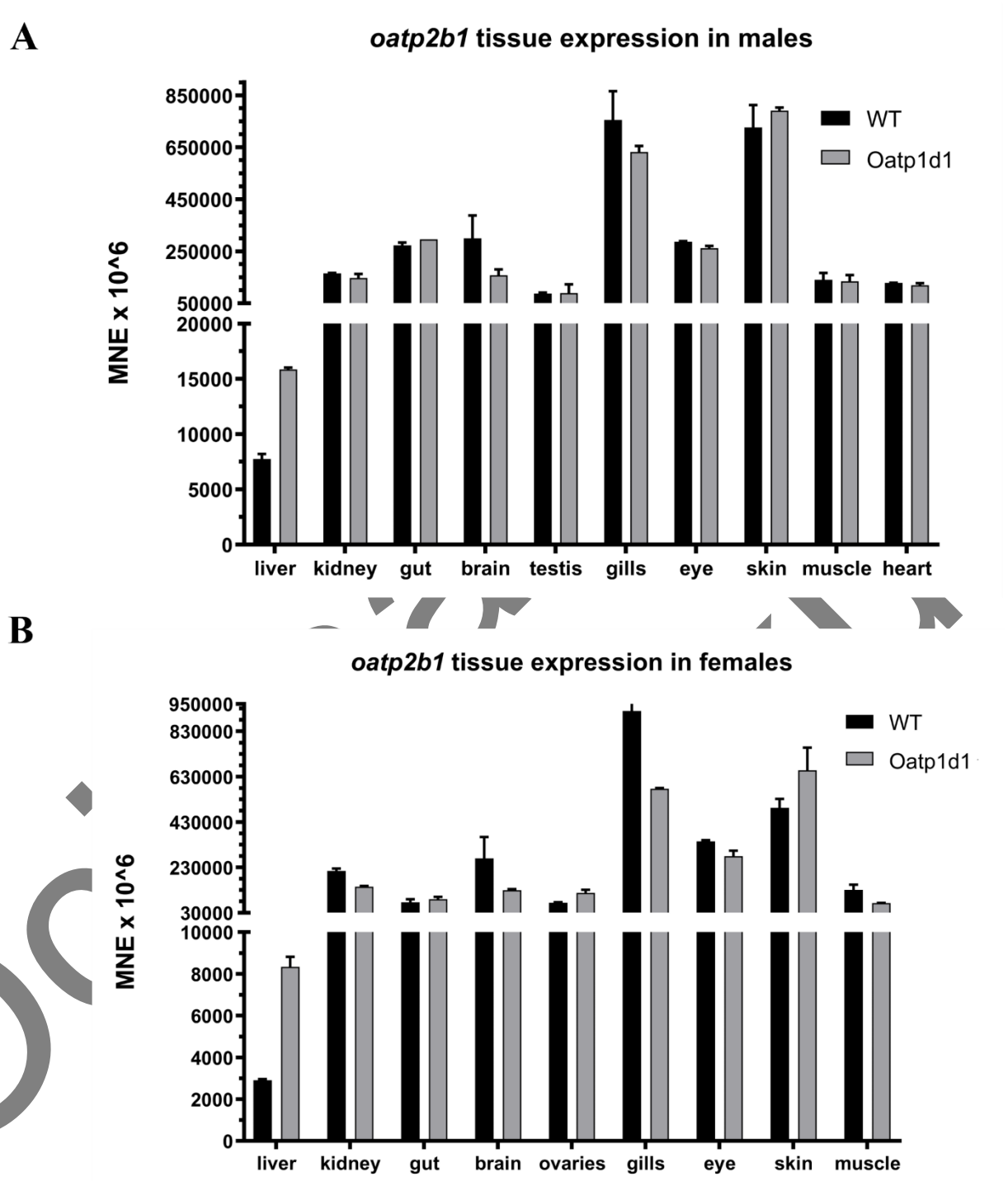

Figure 18. Tissue expression pattern of *oatp2b1* in WT and Oatp1d1 fish. A) tissue samples from males; B) tissue samples from females. Data represent MNE (mean normalized expression) ± SD (n = 2) normalized to the housekeeping gene elongation factor *(EF1α).* Statistical test used is multiple unpaired t-test obtained in GraphPad Prism software version 9.0.0 and there were no statistically significant differences between WT and mutant tissues.

Although no significant changes in *oatb2b1* expression were observed between WT and mutant tissues, the results suggest a moderate up- and down-regulation, possibly reflecting compensatory regulation or disruption of the common transport pathways of *oatp1d1* and *oatp2b1*.

3.1.6. Tissue expression profile of *oat2a* (*Slc22*) in WT and Oatp1d1 mutant adult fish

In the case of *oat2a*, the highest expression was observed in WTs in skin, eye and brain, both in males and females with similar levels in the mentioned tissues, thus no sex differences. In males, minimal changes were observed between WTs and mutants, which are not significant (Figure 19).

In females, mutants show increased expression of *oat2a* in the skin and eye, especially in the skin, where expression is two-fold higher than in WT females (Figure 19). This may indicate a compensatory upregulation of *oat2a* in the absence of functional Oatp1d1. Statistical data for skin and muscle in female tissues showed uncorrected p-values below 0.05, these differences remained statistically insignificant after applying the FDR (False Discovery Rate) correction for multiple comparisons (q-values = 0.045). Therefore, no tissue showed a statistically significant difference at the conventional $q < 0.05$ threshold. These results suggest potential tissue-specific trends that merit further investigation with larger sample sizes.

Ocjena rada u tijeku

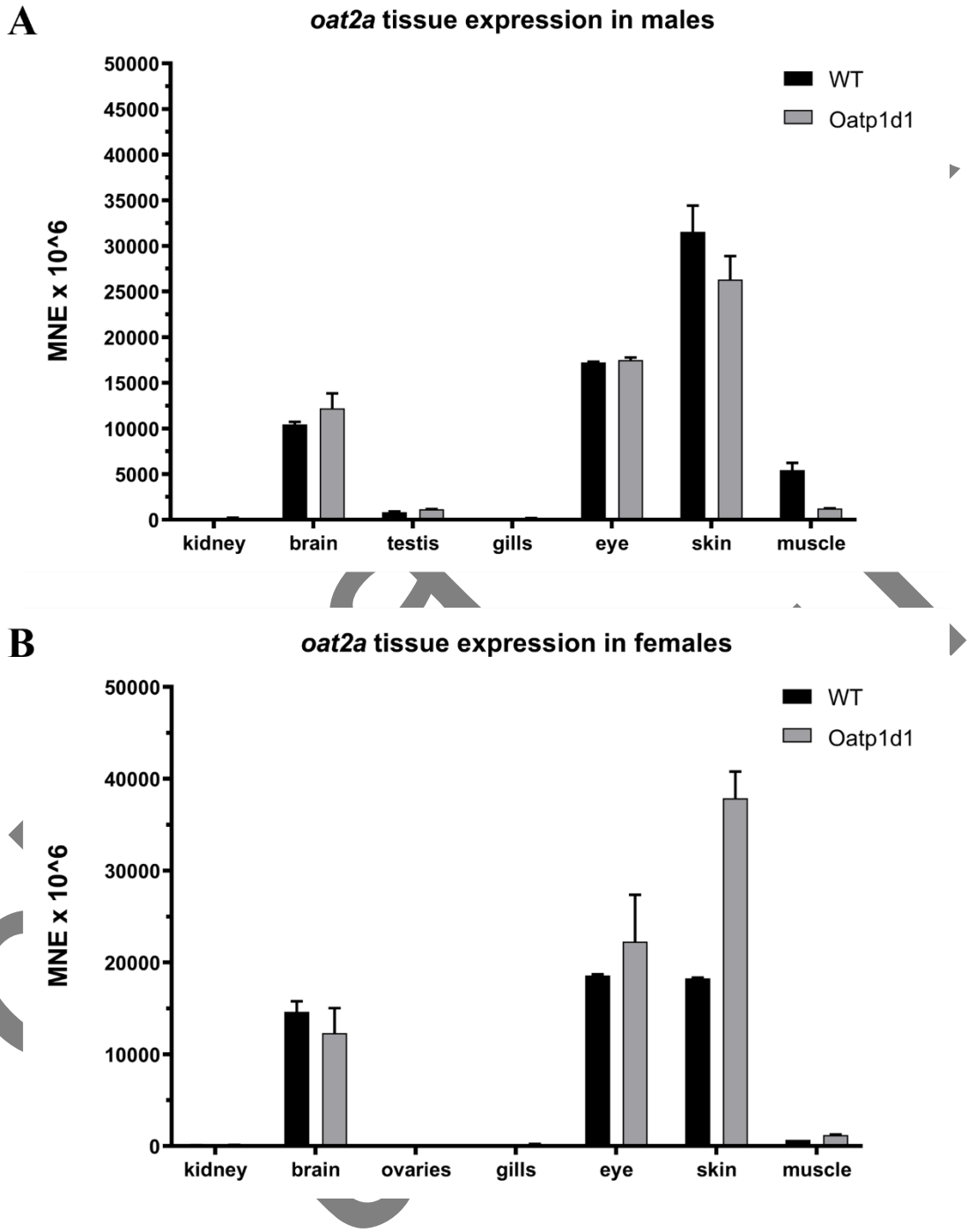

Figure 19. Tissue expression pattern of *oat2a* in WT and Oatp1d1 fish. A) tissue samples from males; B) tissue samples from females. Data represent MNE (mean normalized expression) ± SD (n = 2) normalized to the housekeeping gene elongation factor *(EF1α).* Statistical test used is multiple unpaired t-test obtained in GraphPad Prism software version 9.0.0 and there were no statistically significant differences between WT and mutant tissues.

3.2. Phenotype characterization of Oatp1d1 mutants

To characterize the phenotype of the mutant embryos, their development was observed from 1 hpf to 5 dpf. The embryos are expected to survive because Oatp1d1 is not an essential protein, as there are probably other similar proteins that can take over its role. Each generation of mutants produced embryos that had particles between the chorion and the embryo itself (Figure 20). These particles, which we have not yet been able to characterize, disappeared with the development of the embryos by about 1 dpf, as they were either absorbed or degraded. In the progeny of Oatp1d1 males crossed with WT females, the particles were not present, whereas crossing mutant females with WT males again resulted in embryos with these particles. This indicates that the particles are a result of the maternal transfer that takes place in the ovaries of the mutants.

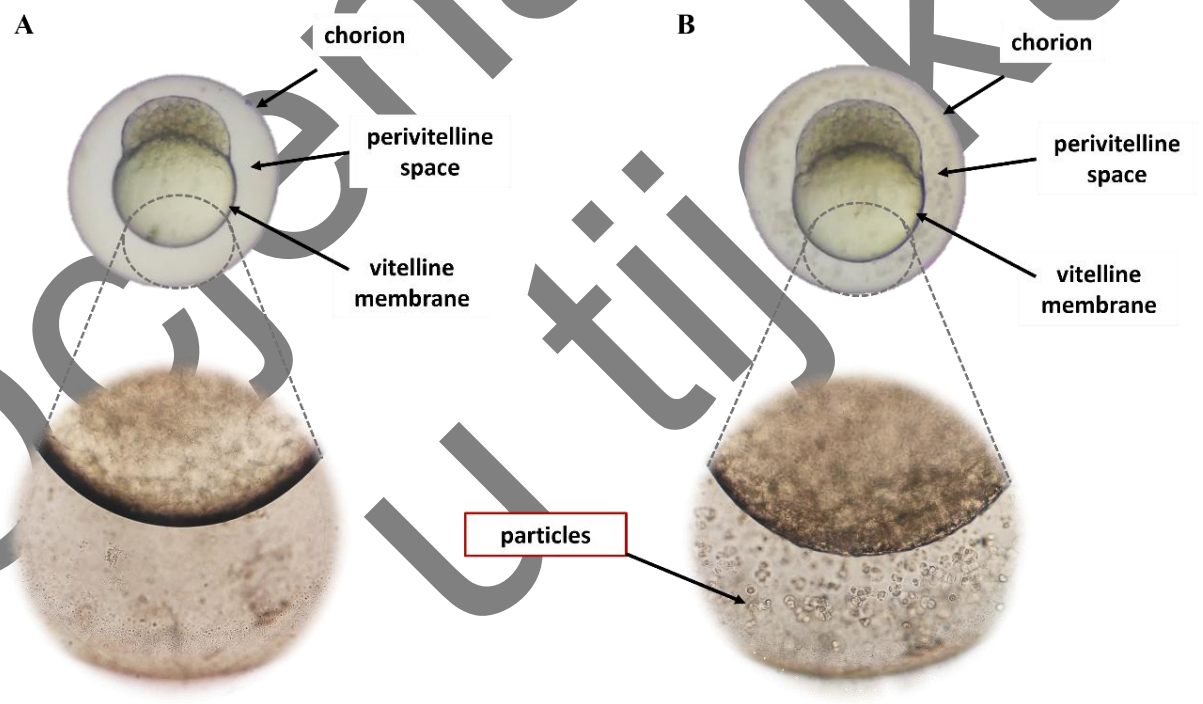

Figure 20. Oatp1d1 mutation causes changes in early embryonic development. Particles observed in the perivitelline fluid (PVF) in a 2-3 hpf old Oatp1d1 mutant embryo (A). WT embryo (2-3 hpf old) embryo without particles in the PVF (B). Arrows show parts of an early developing zebrafish embryo, chorion, perivitelline space and vitelline membrane.

Ogled rada u tijeku

Next, we observed changes in pigments in Oatp1d1 embryos. The absence of yellow pigments, pteridines and probably also carotenoids during later larval development became visible under the magnifying glass and also when exposing larvae and embryos to methylene blue (methylthionium chloride) (Figures 21 and 22B), a redox dye that specifically labels xanthophores and pterinosomes. Since it is already known that xantophores autofluorescence upon excitation with UV light, the anesthetized embryos were imaged with a fluorescence microscope and a clear difference in the fluorescence of pteridines was observed between WT embryos and the absence of fluorescence in Oatp1d1 embryos (Figure 22A). We developed an assay to track the fluorescence of the yellow pigment cells using a spectrophotometer, and at each stage, after about 20 hpf, when the pigment cells begin to differentiate, we observed significantly lower fluorescence in the mutant embryo samples compared to the WT samples at each developmental stage (p values in (Figure 22C; Table S6). After crossing male or female mutants with WT fish, the pigments returned to the WT pattern and the phenotype disappeared. This was confirmed by both methylene blue (data not shown) and fluorescence measurements (Figure 23A and B). This confirms that the lack of yellow pigments is related to the mutation of the Oatp1d1 protein or to compensatory mechanisms resulting from this mutation and that is not related to maternal transmission.

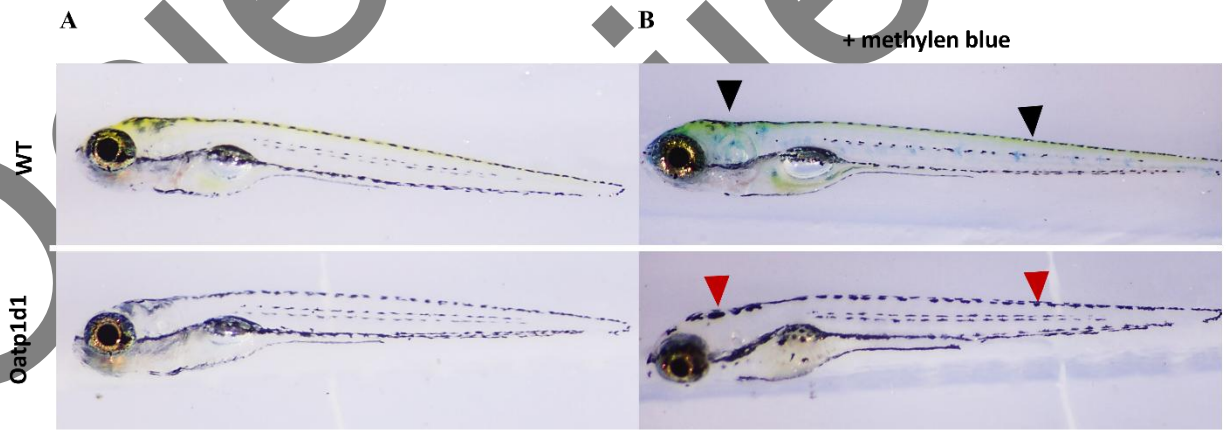

Figure 21. Zebrafish larvae at 18 dpf with and without methylene blue staining the xanthophores. A) WT larvae (top) and Oatp1d1 mutant larvae (bottom) without methylene blue, visible yellow color the head and dorsal part of the WT larvae. B) Wild-type larvae (top) have a green-blue staining in the xanthophores stained with methylene blue (black triangle); Oatp1d1

Oriena rada Siekų

mutant larvae (bottom) without methylene blue staining, as no xanthophores are present (red triangles).

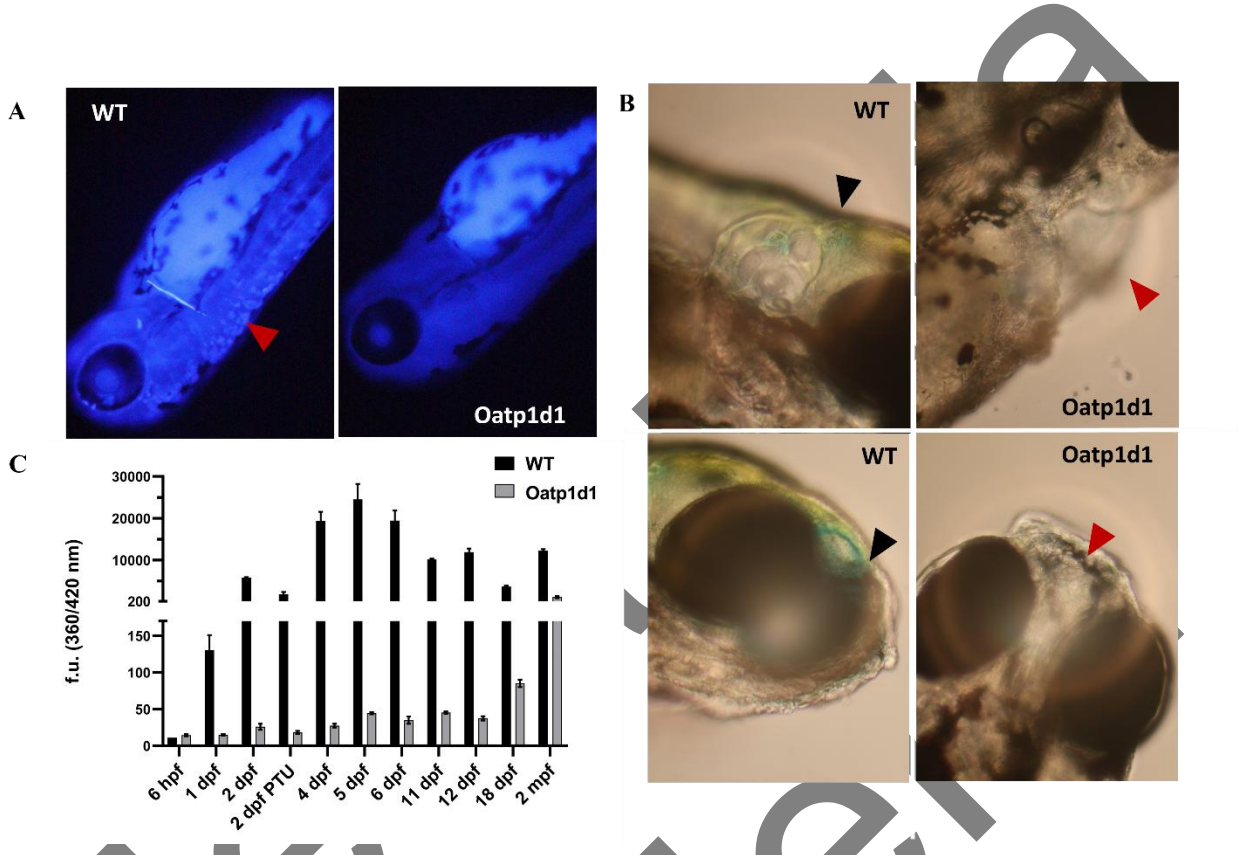

Figure 22. Oatp1d1 mutant embryos show a lack of yellow pigments. Autofluorescence of xanthophores in embryos (A), imaged with a fluorescence microscope under a UV filter (red triangle shows blue dots). Embryos treated with methylene blue (B) imaged under a light microscope. The black triangle indicates the xanthophores stained with methylene blue in WT embryos, which is probably localised in the pterinosomes of the xanthophores, the red triangle indicates the absence of methylene blue staining and thus the absence of pterinosomes or xanthophores or the transport of methylene blue into pigment cells. Stained xanthophores can be seen on the top of the head, around the olfactory pit (B bottom) and in the ear region (B top). C) Measurements of the fluorescence signal of the matrix of zebrafish embryos at wavelengths 360/420. At each stage, the fluorescence of the matrix of Oatp1d1 embryos differed significantly from the fluorescence of the matrix of WT embryos. Details in Supplement (Table S6).

Ocjena utjecaja

Adult fish of the Oatp1d1 mutant line showed normal behavior and swimming behavior and developed and spawned normally. The phenotypic change observed was indeed the opposite pigmentation pattern compared to the embryos. As previously mentioned, the embryos and larvae of the mutants lacked the yellow pigment cells, the xanthophores, while the adult fish showed a higher number of xanthophores and probably also melanophores (not quantified). The fish appeared much darker than adult WT fish (Figure 24A and B**)**, making them easy to distinguish. Figure 22C shows that the fluorescence of Oatp1d1 larvae increases around two months after fertilization and approaches the values measured in WT larvae. It is likely that a change in pigmentation occurs during the transition from the larval to the adult stage, which has already been demonstrated (Saunders et al., 2019), and that a disruption of the pigmentation pattern occurs again during this transition.

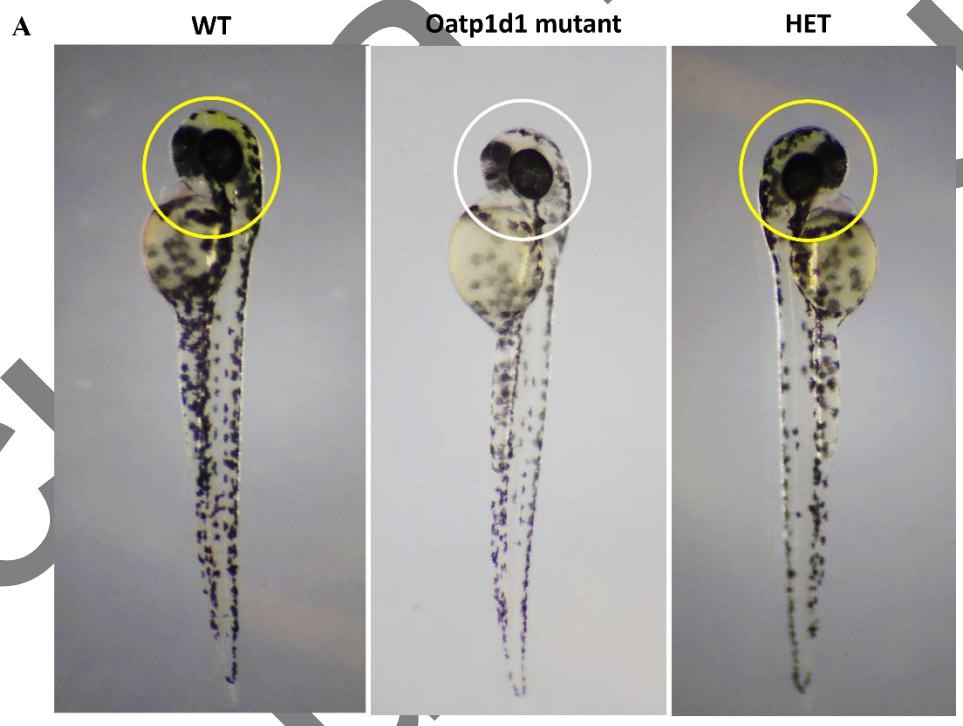

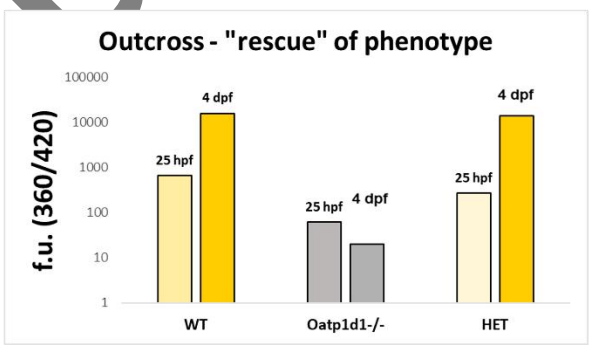

Ociena rada

Figure 23. Crossing Oatp1d1 males and females with WT females and males to obtain heterozygous embryos and rescue the pigment phenotype. A) Heterozygous embryos (2 dpf) have yellow pigments in the head, like the WT embryos. B) The measurement of the fluorescence signal (excitation/emission 360/420) shows the rescue of the fluorescence signal of the pteridines in heterozygous embryos.

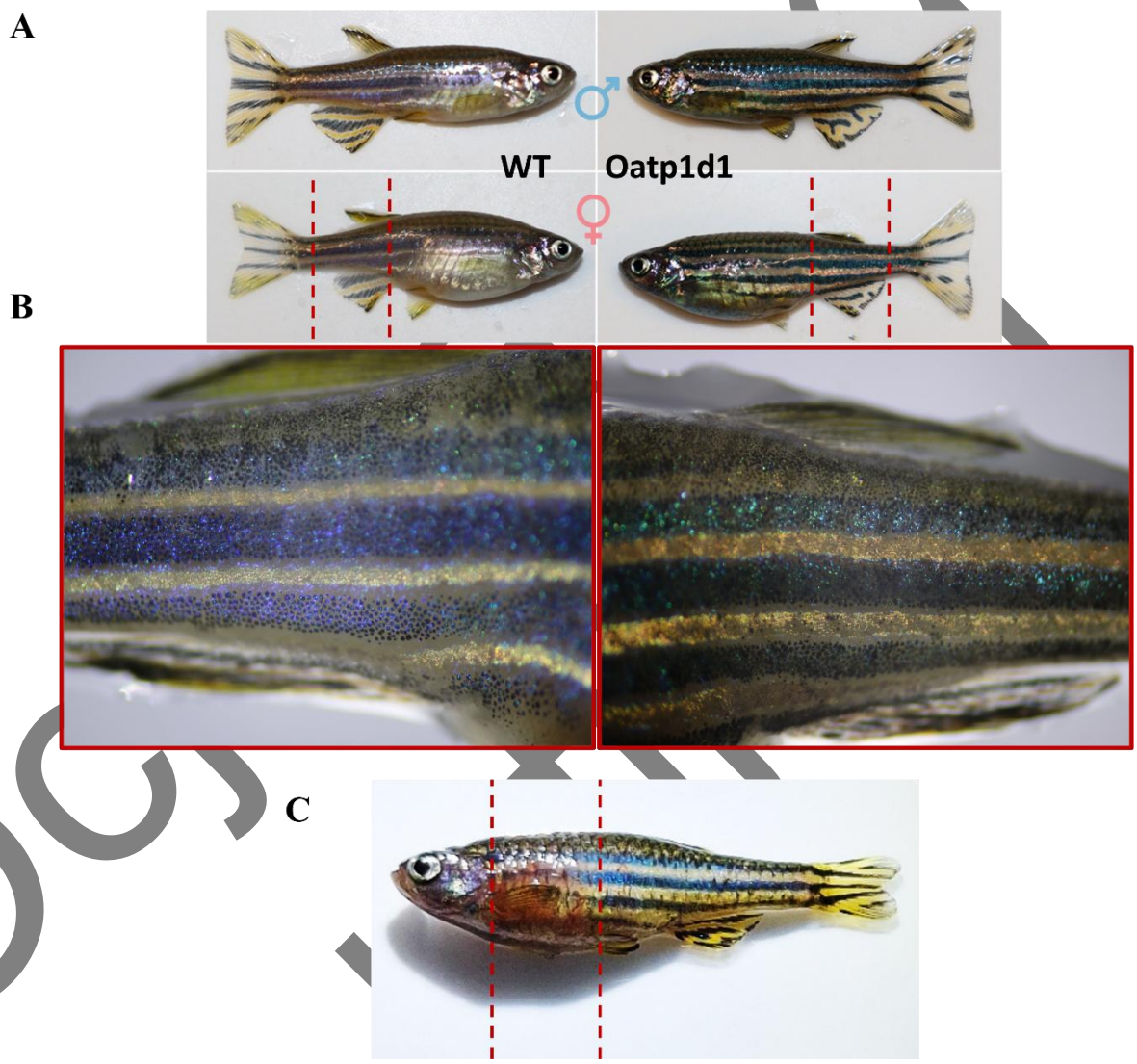

Figure 24. Oatp1d1 mutation alters pigment pattern in adult fish. A) WT male, Oatp1d1 male, WT female, and Oatp1d1 female. The images reveal noticeable differences between males and females. Males have a more spindle-shaped body, while females have a rounder abdomen, especially when ready for spawning. A clear difference in pigmentation is also observed, as Oatp1d1 adults appear darker and have more xanthophores (enlarged photos B). C) Red spots on the skin of the Oatp1d1 mutant fish.

In addition to the altered pigmentation in adult mutants, red spots were observed on the skin of the Oatp1d1 mutant fish (Figure 24C), appearing in the head and abdominal area at around 9 months of age. They occasionally disappear and then reappear. This coincides with poorer spawning performance, as evidenced by a higher number of unfertilized embryos, and the fish stop spawning after about a year and a half.

3.2.1. T3 and T4 alter pigmentation patterns in WT embryos, recapitulating Oatp1d1 mutant phenotype

Since thyroid hormones T3 and T4 have been shown to affect pigment development in both the adult and larval stages (Saunders et al., 2019), we wanted to determine whether they also affect pigmentation during embryonic development, particularly with regard to the disrupted pigmentation pattern observed in Oatp1d1 mutant embryos. Embryos at 24 hours hpf were exposed to 10 µM T4 and 1 µM T3. In three independent experiments, embryos were treated in duplicate wells (n = 10 per well) and both hormones produced the same effects. As early as 48 hpf, a reduction in yellow pigmentation was observed in the treated embryos, resulting in a phenotype similar to that of the Oatp1d1 mutants. In both the WT and mutant groups, melanophores appeared shrinked and clustered into punctate patterns in response to T4 and T3 exposure (Figure 25A and 26). Measurement of the fluorescence signal of T4 exposed WT embryos at 2 dpf confirmed lower signal in T4 exposed embryos (Figure 25B).

Ocjena rada u tijeku

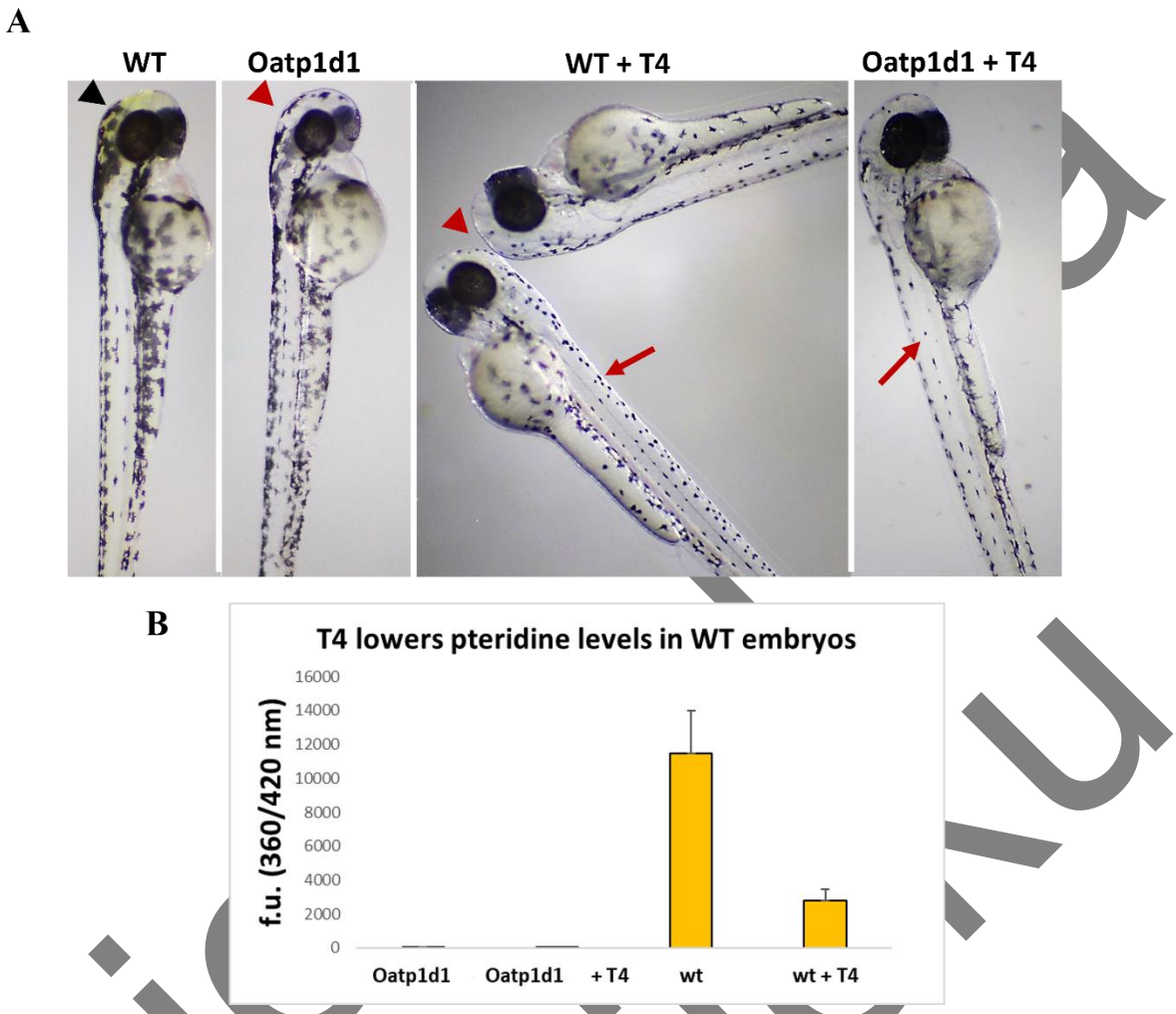

Figure 25. Exposure with thyroid hormone (T4) induces a pigment phenotype similar to that of Oatp1d1 mutant embryos. Wild-type (WT) and Oatp1d1 mutant embryos were exposed to 10 µM T4 24 hours post fertilisation (hpf) and imaged at 48 hpf. A distinguishing feature between untreated WT and Oatp1d1 embryos is the absence of yellow pigmentation in the dorsal head region of the mutants (A). After T4 exposure, both WT and mutant embryos showed reduced and contracted melanophores, indicated by red arrows, an effect consistent with hormone treatment. In addition, WT embryos exposed to T4 showed a loss of yellow pigmentation (red triangle) resembling the phenotype observed in untreated mutants. These results suggest that elevated thyroid hormone levels in WT embryos can induce similar pigmentation changes as in Oatp1d1 mutants. B) The measurement of the fluorescence signal (excitation/emission 360/420) shows the reduced fluorescence signal of the pteridines in T4 exposed WT embryos.

Oslo University

It is hypothesized that thyroid hormones inhibit the Oatp1d1 protein in WT embryos, leading to a mutation-like phenotype. The exact role of Oatp1d1 in the pteridine biosynthetic pathway and how thyroid hormones contribute to its regulation remains to be investigated.

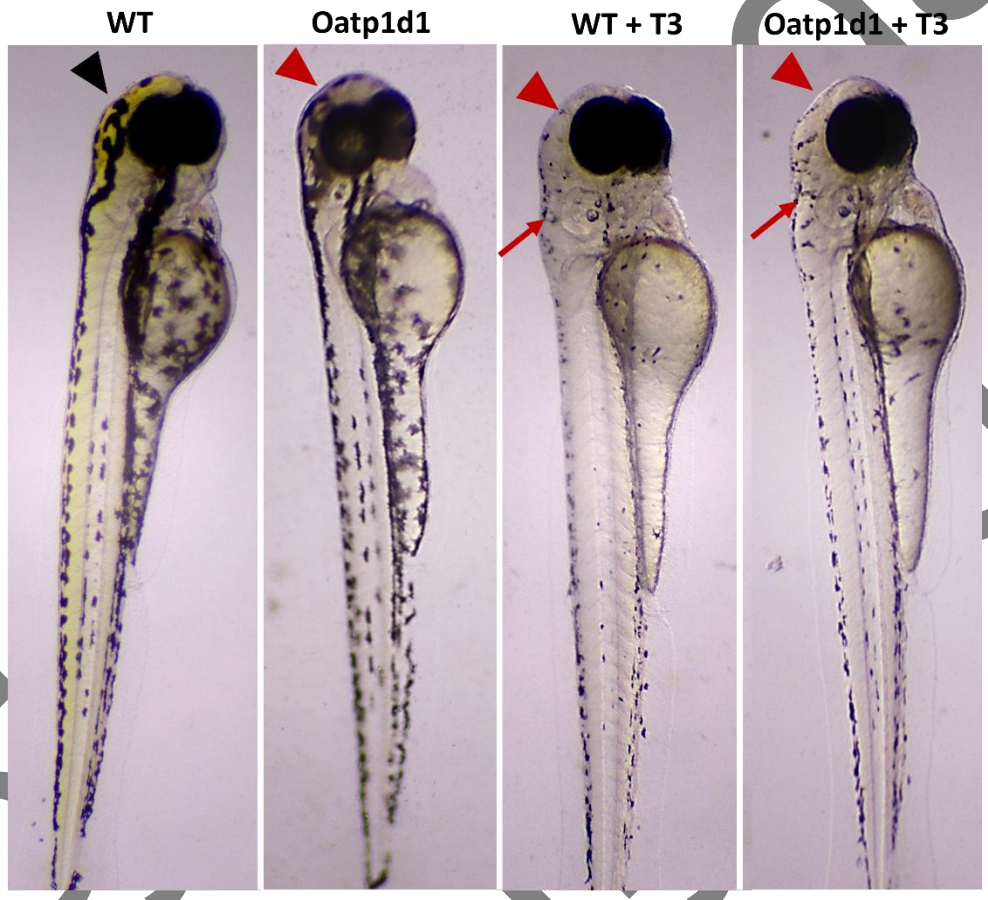

Figure 26. Thyroid hormone (T3) treatment induces a pigment phenotype resembling that of Oatp1d1 mutant embryos. Wild-type (WT) and Oatp1d1 mutant embryos were treated with 1 µM triiodothyronine (T3) 24 hours post fertilisation (hpf) and imaged at 48 hpf. As with previous observations, a clear phenotypic difference between untreated WT and Oatp1d1 embryos is the absence of yellow pigmentation in the dorsal head region of the mutants (A). After T3 exposure, both WT and mutant embryos showed contracted and aggregated melanophores marked by red arrows, a typical response to thyroid hormones. In addition, WT embryos treated with T3 showed a loss of yellow pigmentation (red triangle), consistent with the appearance of untreated Oatp1d1 mutants. These results indicate that elevated T3 levels in WT embryos may recapitulate the pigmentation defects observed in Oatp1d1 mutants.

Ocular

3.2.2. Exposure to fluorescent substrates reveals differential gut uptake in WT and Oatp1d1 mutant embryos

Embryos (5 dpf) were exposed to 50 µM lucifer yellow, a model substrate of the Oatp1d1 protein (Popovic et al., 2013), to assess possible differences in accumulation, either in signal intensity or localisation, between WT and Oatp1d1 embryos due to the absence of the protein. The accumulation of lucifer yellow appears as a fluorescent signal in the gut of WT embryos, while the same localisation of lucifer yellow is seen in Oatp1d1 embryos, but with a stronger signal, which was confirmed with quantification of the fluorescent signal (Figure 27A and B).

Ocjena rada u tijeku

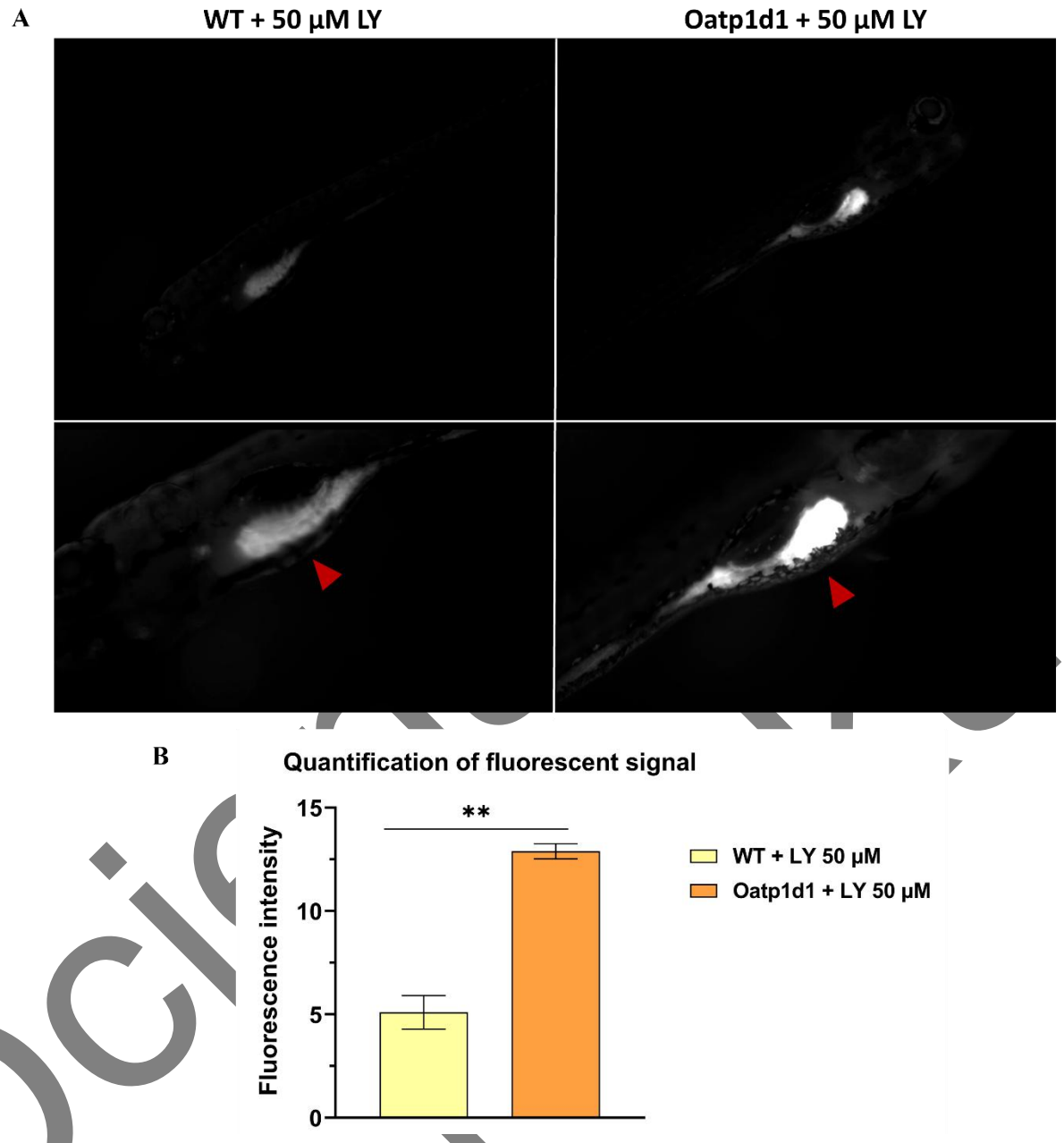

Figure 27. Oatp1d1 embryos show a stronger accumulation of lucifer yellow compared to WT embryos. A substrate of the Oatp1d1 protein, lucifer yellow, shows a more intense signal in the intestine of Oatp1d1 embryos. Embryos (5 dpf) were exposed for three hours, and imaged under a stereomicroscope with a GFP filter. The red triangles indicate the intestine of the embryo. The experiments were repeated three times with 7 to 10 embryos per exposure. B) Quantification of the fluorescence signal in GraphPad Prism 9.0.0. The data Represent mean fluorescence intensity ± SD. 0.0064

When lucifer yellow was microinjected into the yolk and observed over the next two hours, the fluorescence initially spread throughout the yolk within the first hour, possibly reaching the pronephros (Figure 28). Compared to the starting point (0 hps), a weak fluorescent signal was also visible in the rest of the embryo's body, which is probably due to the circulation of lucifer yellow throughout the organism. After two hours, the signal in the yolk weakened, suggesting that lucifer yellow was excreted from the embryo. The yolk itself exhibits autofluorescence at similar wavelengths to lucifer yellow, so it is preferable to perform the exposure on older embryos when there is less yolk. Due to the absence of pteridines in Oatp1d1 mutants, we were unable to measure fluorescence with a spectrophotometer to confirm our microscopic observations. It is planned to perform microinjections in older embryos when most of the yolk has been absorbed and to compare WT and mutant embryos to determine whether LY is equally transported from the injection site to the rest of the embryo. This microinjection experiment thus served as a process optimization for future experiments.

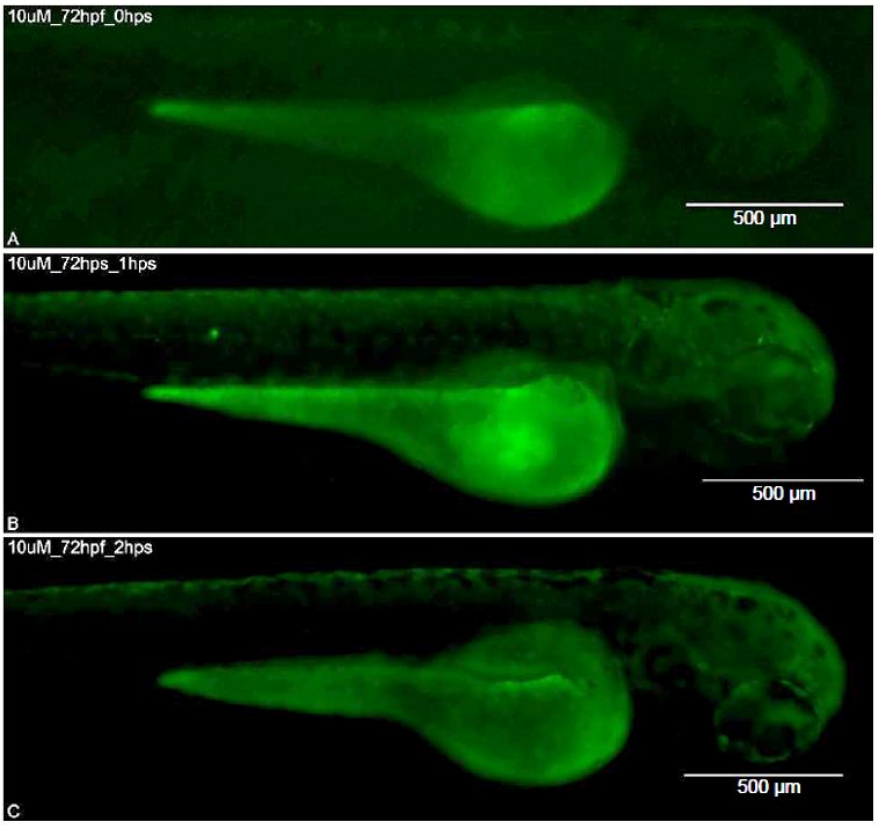

Figure 28. Accumulation of the fluorescent dye LY in zebrafish embryos after microinjection. The fluorescent signal is initially localised in the yolk sac 1 hour post exposure

(hpe) (A). At 2 hpe (B), the signal begins to spread dorsally throughout the embryo, probably due to uptake from the yolk sac and subsequent distribution via the bloodstream. At 3 hpe (C) the fluorescence intensity in the yolk sac is reduced, indicating a redistribution of the dye.

As with exposure to lucifer yellow, the same result was obtained with calcein. Embryos 5 dpf were exposed for 90 minutes, washed with E3 medium and visualised under a fluorescence microscope. Again, Oatp1d1 embryos showed a stronger signal in the intestine, indicating a reduced metabolism of calcein and its less efficient excretion from the embryos (Figure 29).

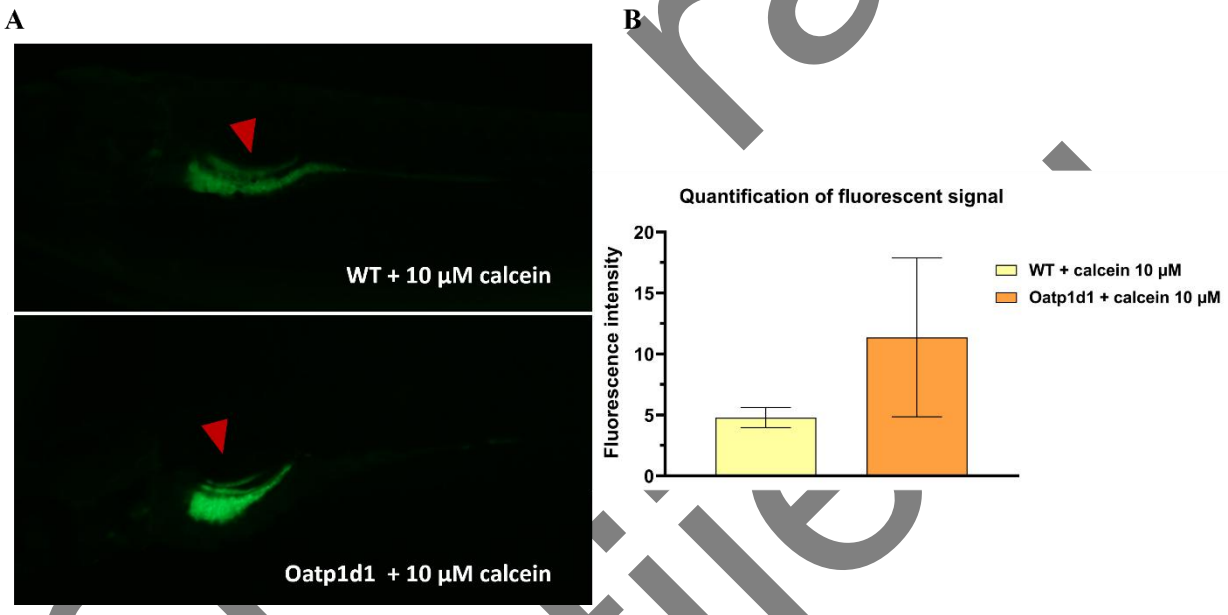

Figure 29. Oatp1d1 embryos (B) show a higher accumulation of calcein, a substrate of the Oatp1d1 protein, compared to WT embryos (A). Five-day-old embryos were exposed for 90 minutes, washed with E3 medium, anaesthetised with MS-222 and imaged under a stereomicroscope with a GFP filter. The red triangles indicate the intestine of the embryos. The experiments were repeated three times with 7 to 10 embryos per exposure. B) Quantification of the fluorescent signal in GraphPad Prism 9.0.0. The data represent the mean fluorescence intensity ± SD.

3.2.3. WT embryos exhibit greater sensitivity to diclofenac compared to Oatp1d1 mutants

Ocjena rada

Exposure of embryos to increasing concentrations of diclofenac resulted in lethal effects at higher concentrations, with some characteristic sublethal effects at lower concentration ranges. The typical duration of the experiment was up to 3 dpf, with the first sublethal effects, such as haemorrhage and oedema around the heart, occurring on the second day (the first day of exposure), depending on the diclofenac concentration. After two days of exposure or at 3 dpf, the effects were more pronounced, with muscle degradation observed in WT embryos at 20 µM and higher concentrations. At the highest concentrations, many WT embryos remained in the chorion and were developmentally delayed, eventually leading to death. In addition, significant oedema around the heart was observed on the third day at a concentration of 20 µM, together with deformation of the atrium and ventricle and a slowed heart rate in WT embryos. In the mutants, effects such as greater oedema around the heart and body curvature only occurred at concentrations of 30 µM and higher, while at 10, 15 and 20 µM concentrations of diclofenac there were no effects. Mutant embryos showed different phenotypes in terms of higher resistance to diclofenac exposure and delayed onset of sublethal effects, as summarised in (Figure 31). Mortality rates (LC_{50}) differed between WT and mutant embryos with a calculated LC_{50} of 35.91 for WT and 23.48 µM for Oatp1d1 mutants, respectively (Figure 30). The mortality rates of the unexposed and the DMSO-exposed negative control groups were below 5 % (Figure S1). Exposure of WT embryos to diclofenac concentrations as low as 20 µM resulted in delayed development and other abnormalities that manifested as muscle degradation in the form of spinal curvature deformities, pericardial oedema, and blood pooling in the heart region, and were lethal at higher concentrations (Figure 31).

Ocjena rada u tijeku

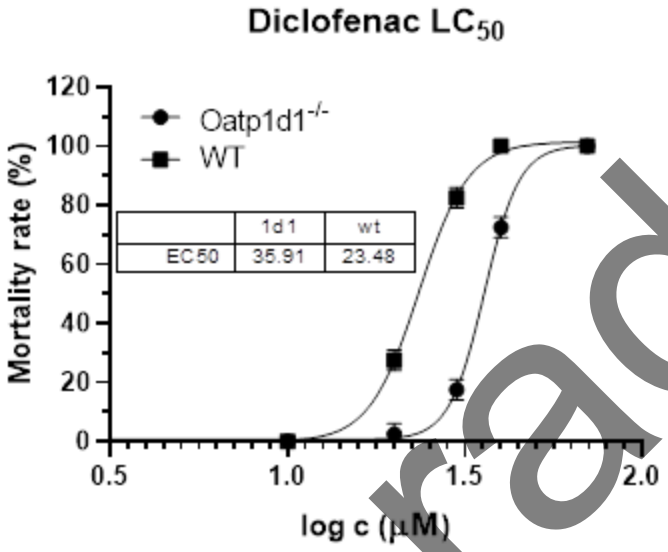

Figure 30. Dose–response curves used for the LC_{50} calculations for zebrafish WT and Oatp1d1 mutant embryos exposed to diclofenac for 72 h. Data represent results from three independent experiments done in triplicates. Error bars indicate standard deviations (SD). The dose–response curves were generated using GraphPad Prism 9.0.0 software.

Ocjena rada u tijeku

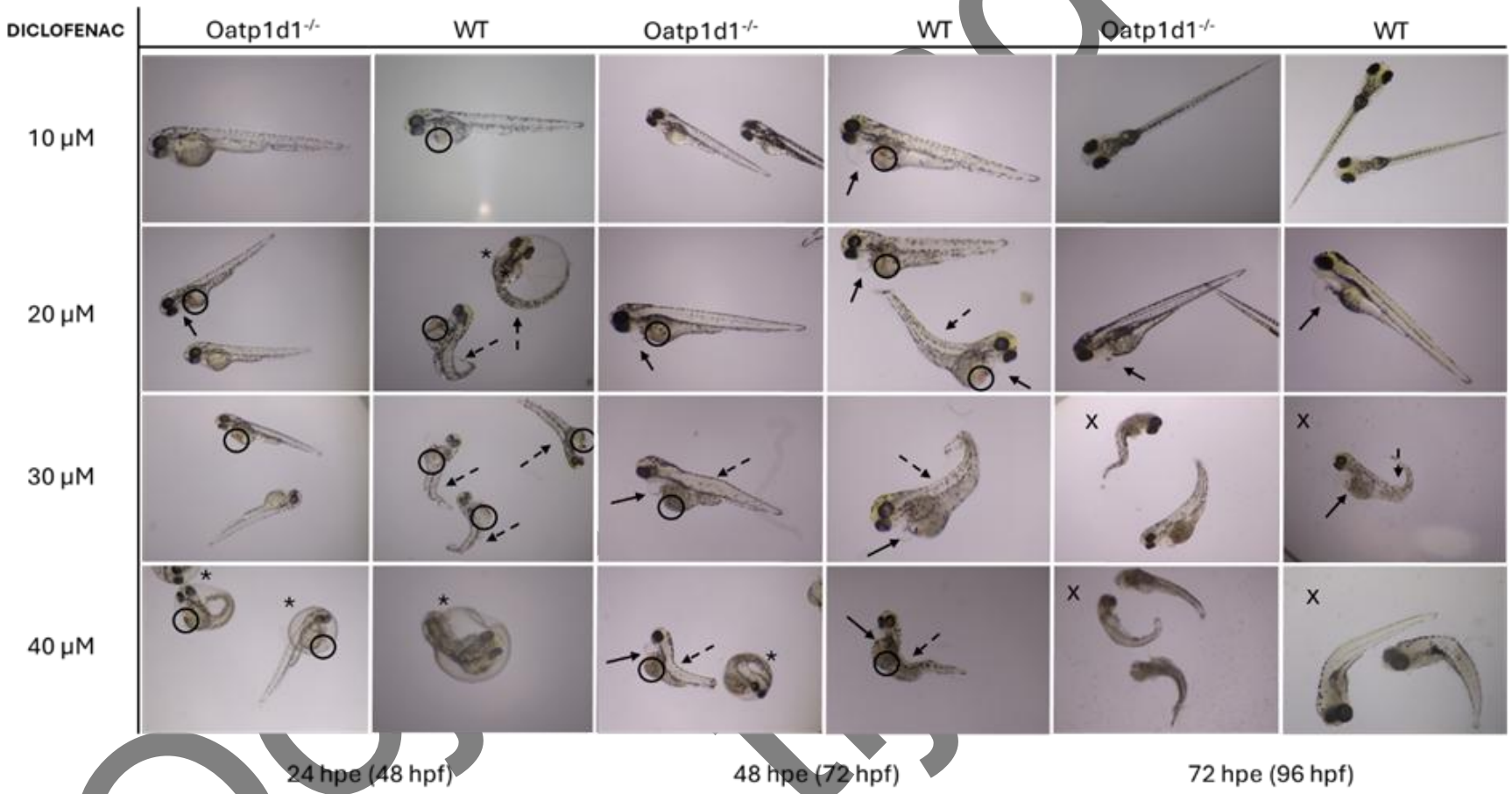

Figure 31. Effects of diclofenac exposure on embryonal development of WT and Oatp1d1 mutant embryos over the exposure period of 72 hours. Reported developmental abnormalities caused by diclofenac exposure are yolk sac edema (arrow), blood accumulation (circled), spine curvature (dashed arrow), delayed hatching (asterisk), necrosis and death (x).

Obsolete

3.2.3.1. Effect of diclofenac on gene expression in WT and Oatp1d1 mutant embryos

Exposure of both WT and mutant embryos to sublethal concentrations of diclofenac resulted in significant changes in the gene expression of organic anion transporters. In particular, exposure of 3 dpf embryos to 15 μM diclofenac led to pronounced changes in the expression of monitored genes. For *oatp1d1*, downregulation of 1.5-fold was observed in unexposed embryos, while exposure to diclofenac increased downregulation to 3-fold, indicating that *oatp1d1* expression decreased 2-fold in the mutants (Figure 32). Conversely, both *oat1* and *oat3* showed a similar expression pattern when exposed to diclofenac, with downregulation in unexposed embryos shifting to upregulation when exposed to the drug. For *oat2a* and *oatp2b1*, a different pattern of expression change was observed, while downregulation in the mutants was present regardless of diclofenac exposure, it decreased significantly upon exposure to the drug (Figure 32).

Ocjena rada u tijeku

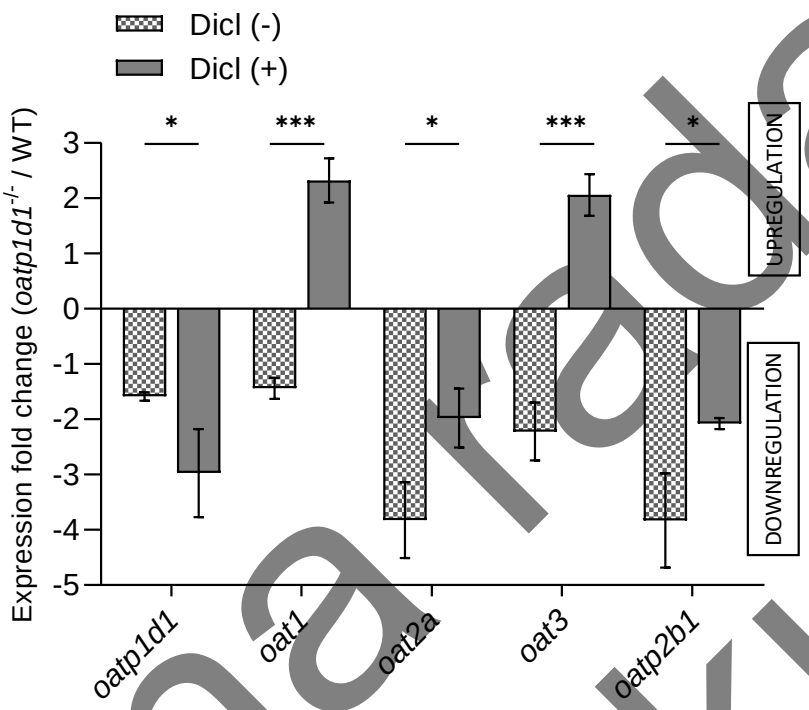

Figure 32. Transcript expression fold changes of observed genes (*oatp1d1*, *oat1*, *oat2a*, *oat3* and *oatp2b1*) in WT and Oatp1d1 mutant embryos (3 dpf) when exposed to diclofenac (25 µM). Data are presented as MNE expression fold (oatp1d1$^{-/-}$/WT) of two independent experiments ± standard deviations (SD). Upregulation in the mutant transcript expression is presented as positive fold change and downregulation as negative fold change (-1/fold). Statistically significant changes as a result from unpaired Student's t-test are shown as *p < 0.05, **p < 0.01, ***p < 0.001.

3.2.3.2. Gene silencing with morpholinos

After both morpholinos, the splice and the ATG variants, were injected into embryos at the 1-4 cell stage at concentrations of 300, 150 and 50 µM (data not shown), the two highest concentrations were discarded due to toxic effects and embryo degradation. The concentrations chosen for further experiments were 100 and 75 µM for both morpholinos, as they showed no lethal effects and the embryos were developing normally. At the same time, the efficacy and specificity of the morpholinos were investigated. For the MO-ATG, due to technical difficulties with membrane

Ocjena rada u tijeku

transporters and their detection in embryos with Western blot method, a qRT-PCR was performed instead to verify at least a reduction in *oatp1d1* expression. However, this does not provide a complete verification of the MO-ATG as it stops translation, so even if mRNA is still detected, this does not mean that the protein is present and functional. Nevertheless, some reduction in expression was observed. In the case of the MO-splice, embryos were taken at 1, 3 and 5 dpf, as we wanted to know how long the morpholino would be active. After RT-PCR, we expected the most common consequence of defective splicing due to the action of morpholino, exon skipping. However, we observed a less frequent occurrence: cryptic intron retention (Figure 33A). After sequencing, it was clear that the extra band at around 2000 bp actually contained part of an intron 2 which leads to frameshift and premature stop codon and these transcripts are potentially eliminated by nonsense-mediated decay (Bill et al., 2009). The efficiency of the splicing morpholino depended on the concentration of morpholino (Figure 33D) on the first and third day of embryo age, while it appears to decrease notably on the fifth day (Figure 33D) regardless of morpholino concentration. Schematic representation of MO-splice is in (Figure 33B) and embryos injected with both MO-ATG (75 µM) and MO-splice (75 and 100 µM) morpholinos developed normally (Figure 33E).

Ocjena rada u tijeku

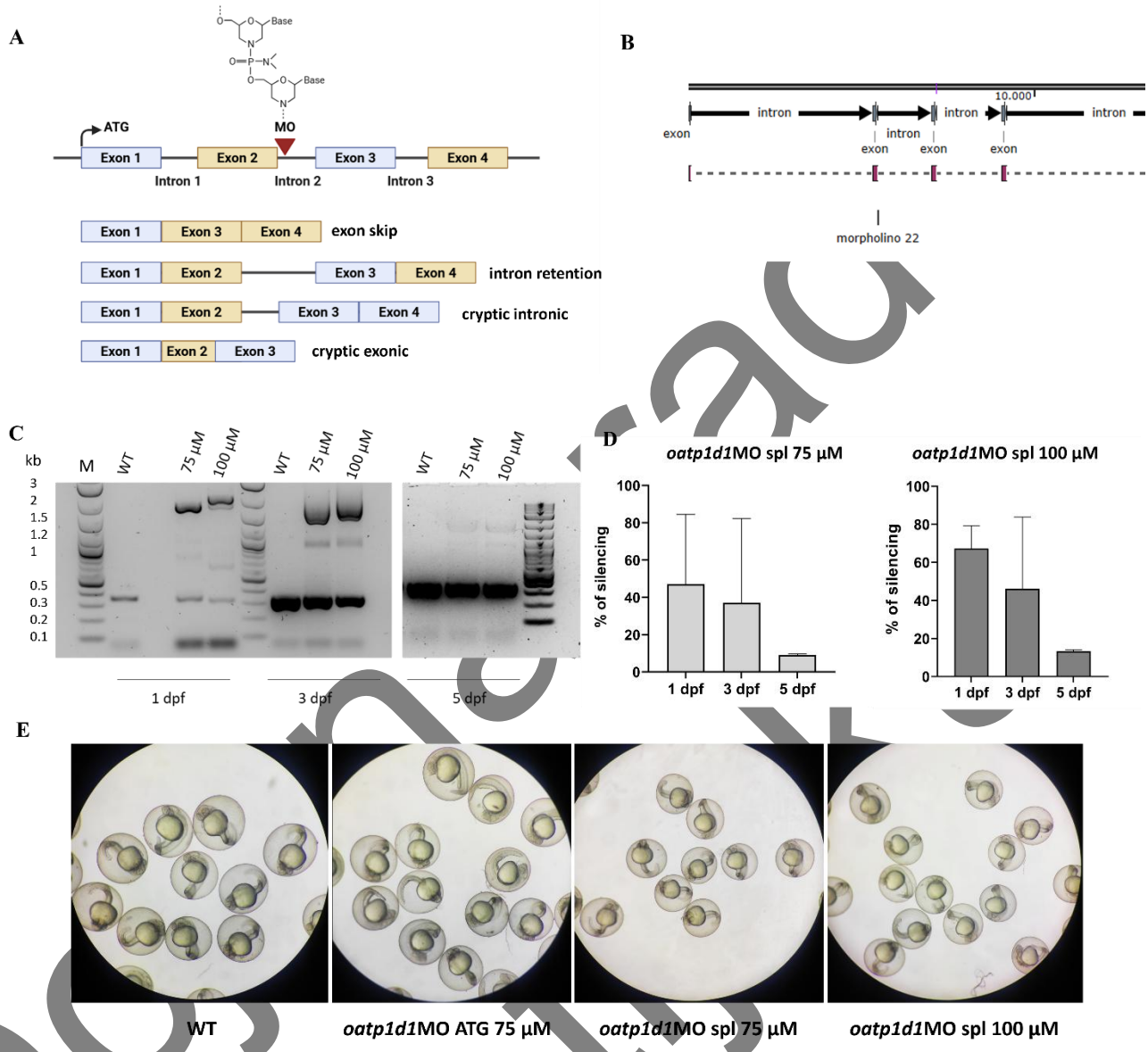

Figure 33. Splice morpholino optimization for *oatp1d1* gene silencing. A) possible outcomes of gene silencing using MO-splice targeting exon 2 – intron 2 boundary B) Enlarged image from SnapGene showing the coding sequence (CDS) of *oatp1d1* and the MO-splice binding site. C) RT-PCR testing of 75 µM and 100 µM splice morpholino on cDNA samples from embryos at day 1, 3 and 5 (dpf) using specially designed primers targeting the start of the *oatp1d1* sequence and exon 3. The expected wild-type (WT) band is 326 bp (51 bp of exon 1, 142 bp of exon 2 and 133 bp of exon 3). Additional bands observed at approximately 2000 bp represent cryptic intronic sequences due to the morpholino effect and retention of intron 2 (1565 bp). D) Quantification of gel bands corresponding to the WT band expressed as percentage of silencing efficiency. E) Injected embryos at 24 hpf appeared morphologically normal and developed correctly at the morpholino concentrations tested. E) Injected embryos developed normally.

Original Article

No pigment changes were observed with the morpholino injected embryos, which we had expected. However, another possibility is that the absence of pteridines or some precursors for their formation is actually a consequence of compensatory mechanisms after the mutation and not of the mutation itself. Morpholinos do not trigger compensatory mechanisms (Rossi et al., 2015a). Therefore, we would not expect to observe the same phenotype in WT embryos after injection. For this reason, we continued to use morpholino-injected embryos in exposure/toxicity experiments with diclofenac and PFOS to see if we obtain the same or similar phenotype in WT embryos as in Oatp1d1 mutants.

The next step was to verify both morpholinos. From embryos injected with MO-ATG at 24 and 48 hpf, RNA was isolated, converted to cDNA and qRT-PCR was performed to verify the reduction in *oatp1d1* gene expression. The graph shows the results of three independent replicates (three different injections) of 7-10 embryos each.

Ocjena rada u tijeku

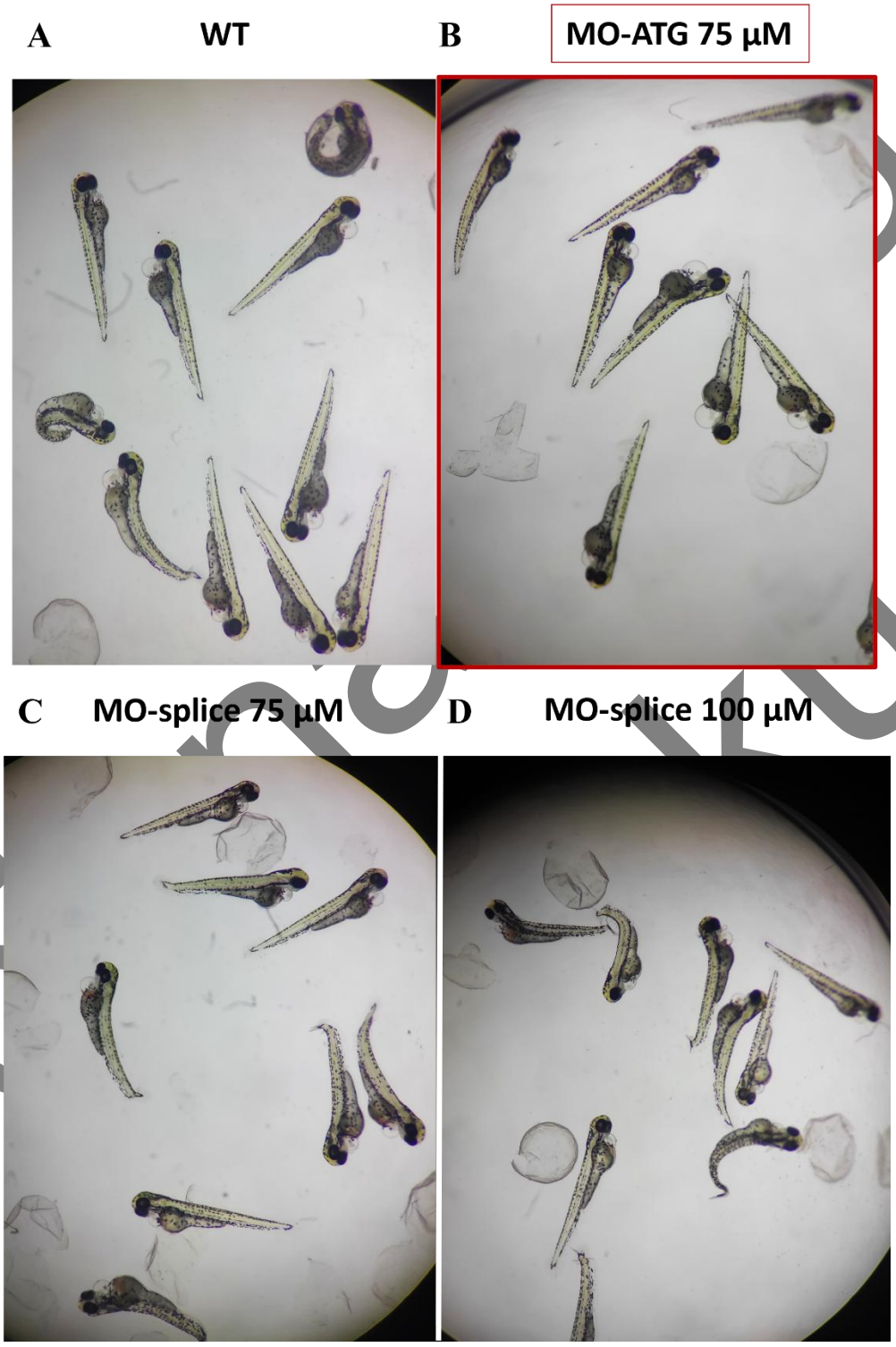

Figure 34. Testing MO-ATG 75 µM (B) and MO-splice 75 µM (C) and 150 µM (D) after exposure to 20 µM diclofenac. A) WT embryos exposed to diclofenac. It can be observed that the B) embryos look better than the others; they were not curved by diclofenac, although major oedema around the heart and muscle degradation were rarely observed. Thus, they show the

expected effect of knockdown the *oatp1d1* gene. For further experiments with diclofenac, MO-ATG 75 µM was used.

After determining the efficacy of morpholinos and the concentrations that are not toxic to embryos, 75 µM and 100 µM were selected for exposure experiments with diclofenac (Figure 35B).

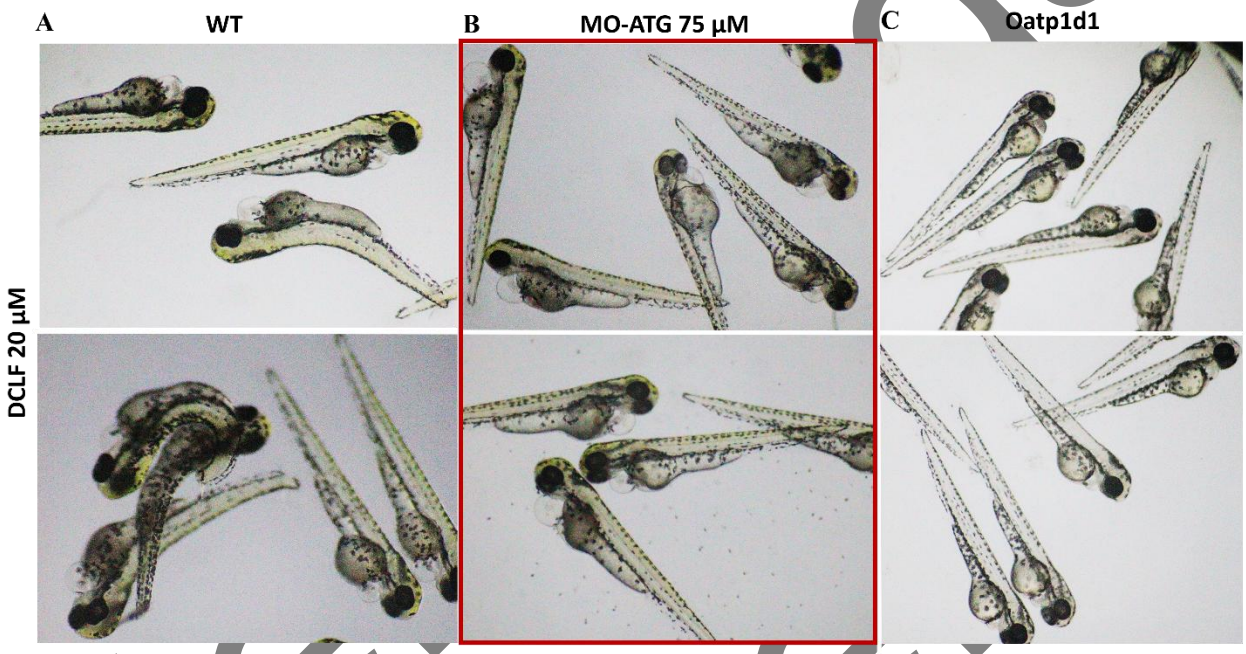

Figure 35. Silencing of *oatp1d1* gene reduces sensitivity of WT embryos to diclofenac. WT embryos, *oatp1d1* morphants injected with 75 µM MO-ATG and Oatp1d1 mutants exposed to 20 µM diclofenac. Compared to WT embryos, the MO-ATG embryos showed milder phenotypic effects after diclofenac exposure. Although pericardial oedema was present, the morphants exhibited less or no body curvature and muscle degradation was less pronounced than in WT embryos. The results from embryos injected with 100 µM MO1-ATG (data not shown), because of higher morpholino concentration induced non-specific body curvature, which could lead to misinterpretation as a false negative effect.

Ocieutiena

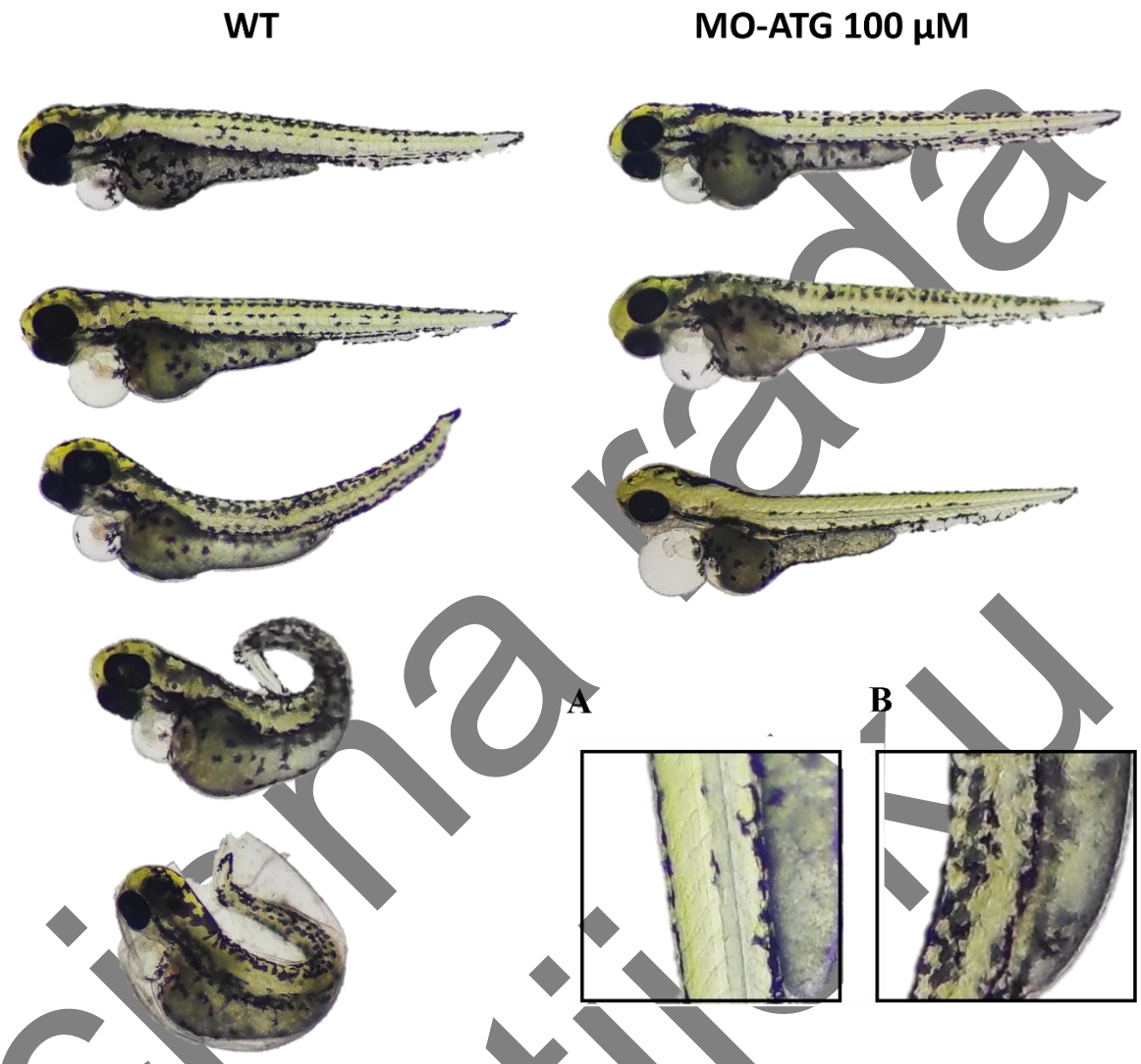

Figure 36. Representative images of WT and MO1-injected embryos exposed to 20 µM diclofenac. Different levels of effects were observed in WT embryos at this diclofenac concentration on the second day of exposure (3 days post-fertilization, dpf). MO1-ATG injected embryos progressed to stage 3. No body curvature or muscle degradation was observed, or these effects were only mildly expressed, and no embryos remained curled within the chorion. **A)** MO-ATG embryo showing no signs of muscle degradation following diclofenac exposure; muscle segmentation is clearly visible. **B)** WT embryo displaying pronounced muscle degradation after diclofenac treatment.

Ocjena rada u tijeku

In the next phase of our study, we aimed to examine muscle degradation and the differences between WT embryos, MO-injected embryos and Oatp1d1 mutants in more detail and therefore chose a method for labelling/staining actin filaments in embryos. The image shows the tail region of embryos exposed to 20 µM diclofenac and incubated with phalloidin FITC staining. In WT embryos (Figures 37 and 38), diclofenac exposure resulted in muscle degradation and disorganization of myofibrils. In contrast, Oatp1d1 mutant embryos exposed to diclofenac (Figure 37), showed well-organised actin fillaments. In the case of MO-ATG, a phenotype intermediate between WT and mutants is observed; the actin filaments are not fully organized, but they are also not degraded as in WT-exposed embryos. Dechorionisation of the embryos had no effect on the results obtained (Figure 38).

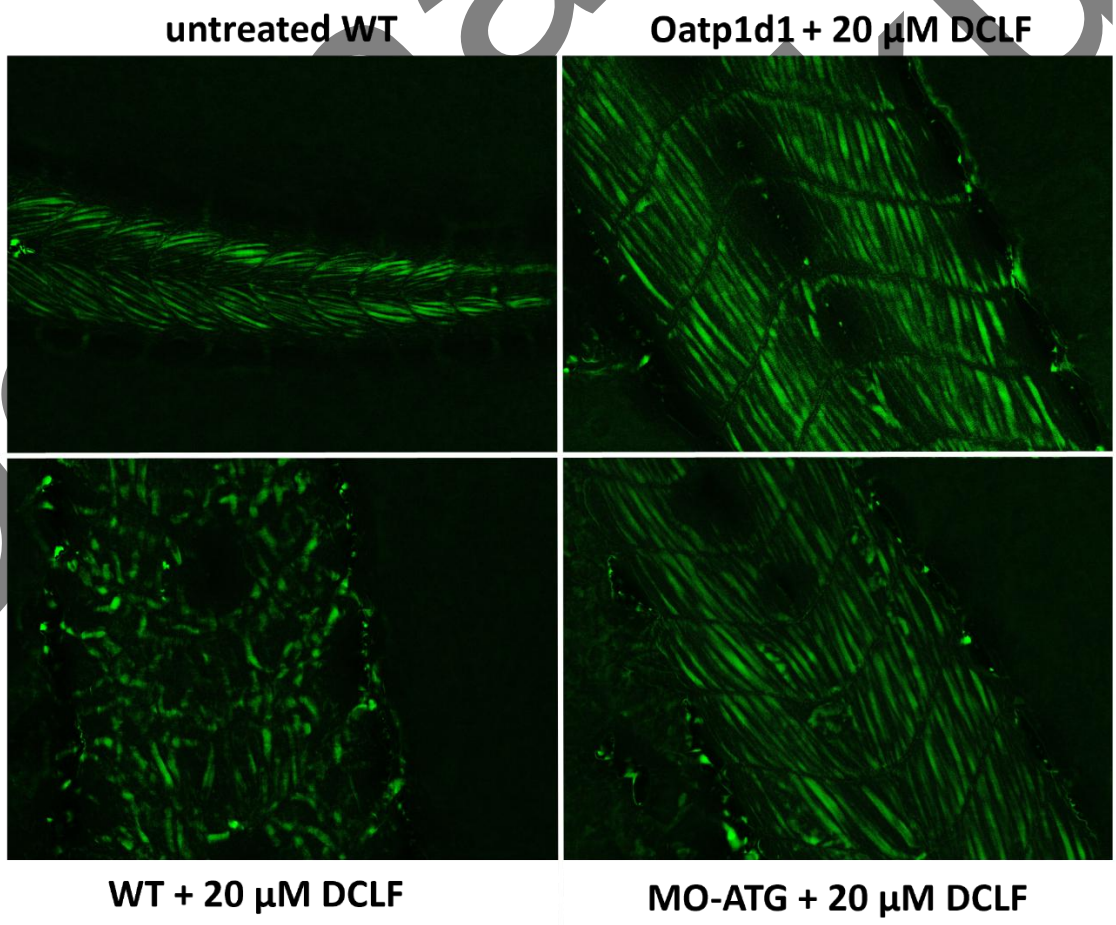

Figure 37. Phalloidin staining reveals muscle degradation following diclofenac exposure. The effect of diclofenac in 3 dpf embryos can be observed as muscle degradation and disorganisation of myofibrils, in contrast to Oatp1d1 embryos with 20 µM diclofenac. In the case of *oatp1d1* morpholino knockdown (MO-ATG), a phenotype intermediate between WT and mutants is observed. Embryos were stained with phalloidin FITC (1:100) to visualise muscle fibres (actin filaments) and visualized under a fluorescence microscope (Axio Imager.Z2, Carl Zeiss, Oberkochen, Germany).

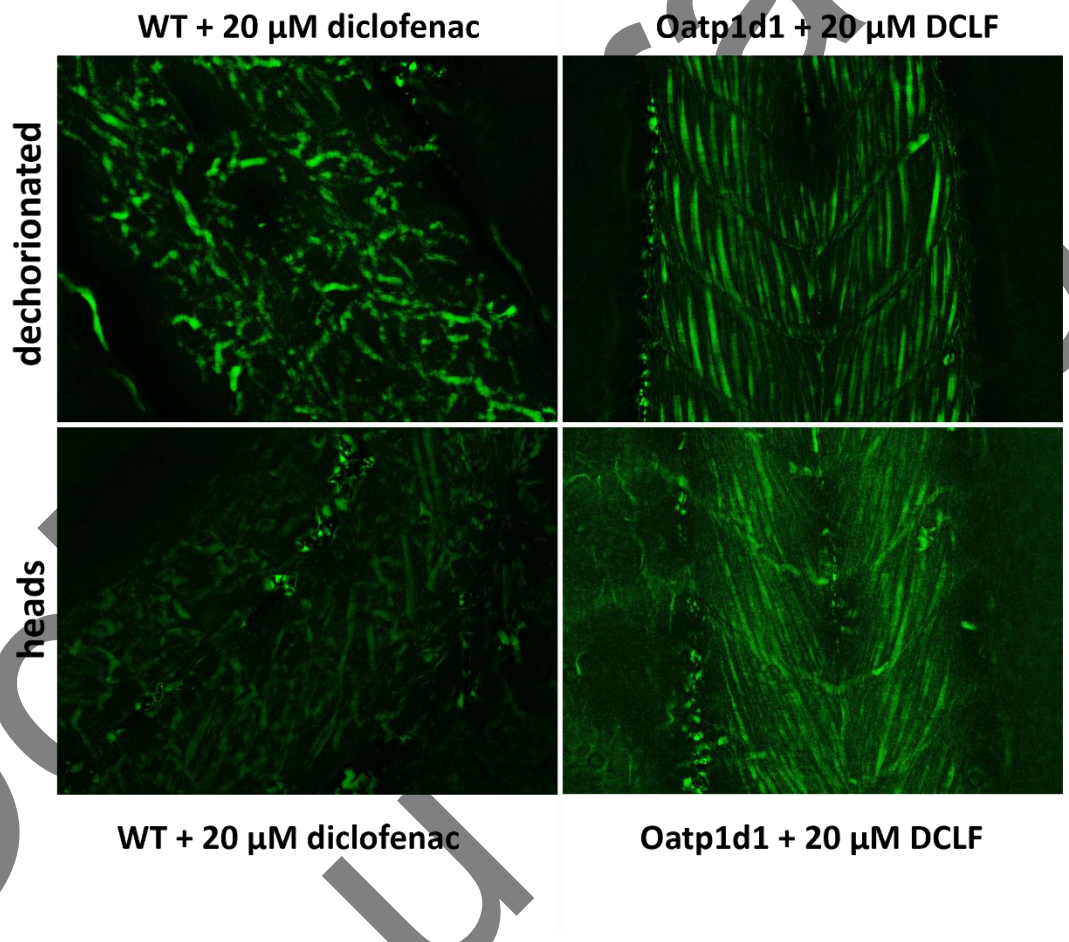

Figure 38. Visualisation of diclofenac-induced muscle damage using phalloidin staining. The effect of diclofenac in 3 dpf old zebrafish embryos can be observed as muscle degradation and disorganisation of myofibrils, in contrast to Oatp1d1 embryos with 20 µM diclofenac. Dechorionisation has no influence on the observed effects when the embryos are exposed without dechorionisation. The dorsal head regions show the same effects as the tails of the embryos. The embryos were stained with phalloidin FITC (1:100) to visualise muscle fibres (actin filaments) and viewed under a fluorescence microscope (Axio Imager.Z2, Carl Zeiss, Oberkochen, Germany).

Unpublished

3.2.4. PFOS exposure experiments – Oatp1d1 embryos exhibit greater sensitivity to compared to WT embryos

Exposure of WT and mutant embryos to PFOS resulted in changes in normal embryonic development. Increasing concentrations of PFOS resulted in lethal effects at later stages and higher concentrations, with some characteristic sublethal effects at lower concentration ranges. Mortality rates (LC_{50}) differed between WT and mutant embryos with a calculated LC_{50} of 23.57 for WT and 16.71 µM for Oatp1d1 mutants (Figure 38).

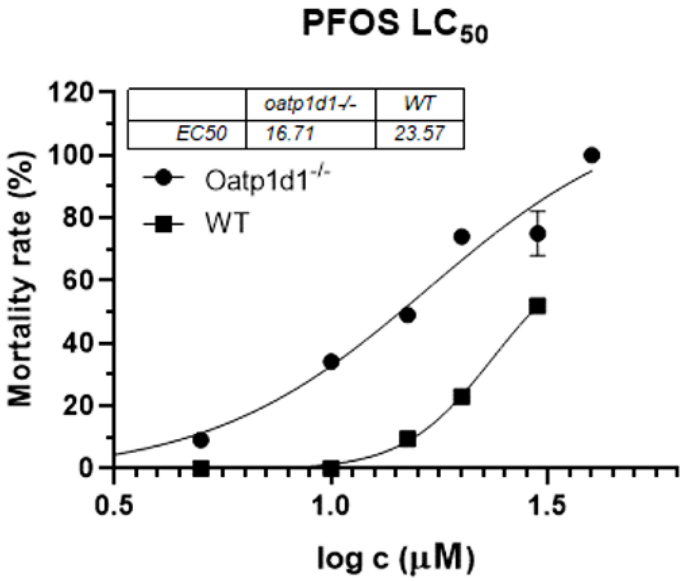

Figure 38. Dose–response curves used to calculate the LC50 of zebrafish WT and oatp1d1 mutant embryos exposed to increasing concentrations of PFOS for 96 hours. The data are results of a typical experiment performed in triplicate. The error bars indicate the standard deviations (SD). The dose–response curves were generated using GraphPad Prism 9.0.0 software.

.

Oci uu rada .u

The most prominent effects of PFOS exposure and differences between *oatp1d1* mutants were visible from 4 dpf and later. PFOS impaired the normal development of the swim bladder and resulted in a non-existent or very small and rounded swim bladder, causing the embryos to lie on their side, be less active (Figures 39 and 40) and eventually lead to body curvature (Figure 41 A and B). Oatp1d1 mutants showed all the effects of PFOS exposure before the WT embryos, with a shift of about 12-24 hours. The percentage of embryos with deformed swim bladders was higher in Oatp1d1 mutant embryos and increased with higher concentrations of PFOS (Figure 40B). This effect also contributed to the lower activities of PFOS exposed mutant embryos. They would not respond to mechanical or light stimuli. While WT embryos were even hyperactive at 3-4 dpf, they also became slower afterwards, depending on the PFOS concentration. In addition, the exposed mutant embryos developed necrosis in the head (visible as a grey "surface") and in the intestinal area (Figures 39 and 40A).

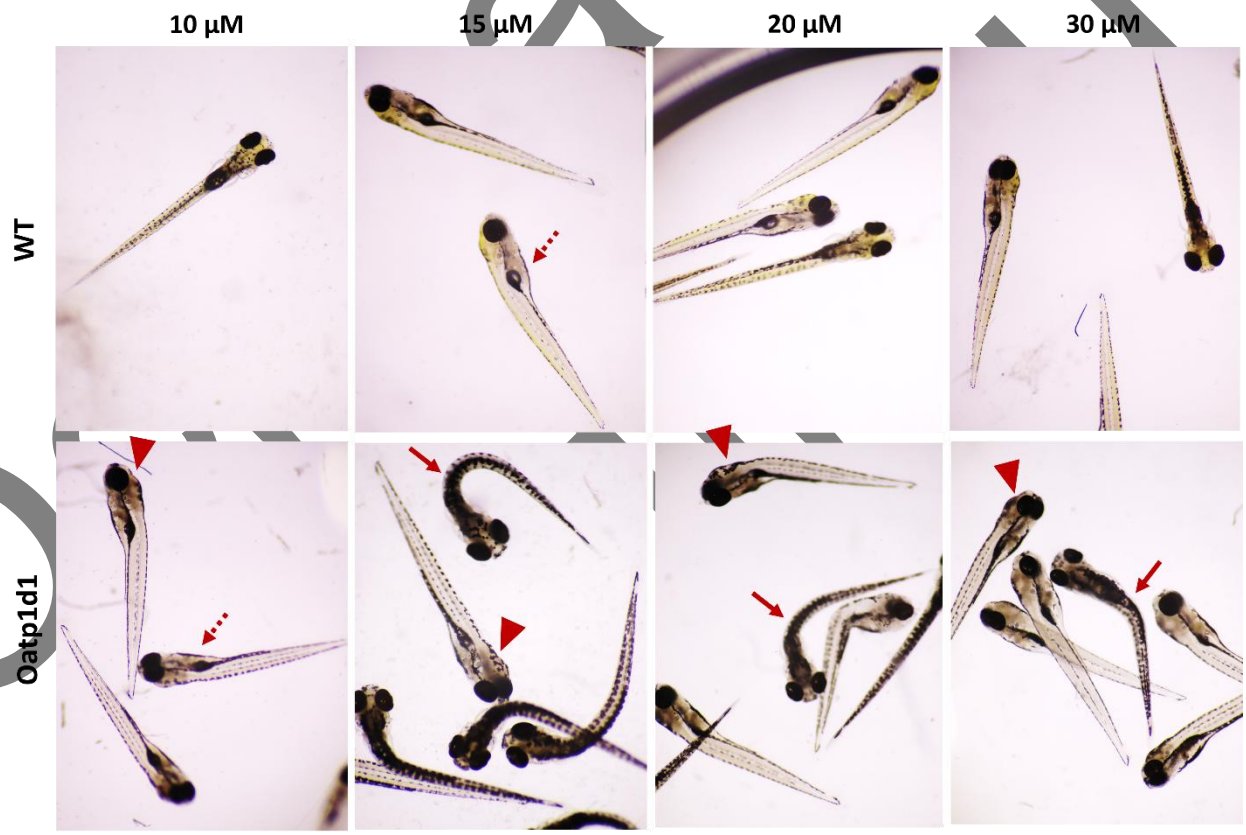

Figure 39. A range of PFOS concentrations, 10, 15, 20, 30 µM, showed effects on the mutants at different concentrations, starting at 10 µM, at which the mutants lie on their side and brain necrosis is visible. At higher concentrations, intestinal necrosis, deformed swim bladders

and scoliosis were observed in the mutants at 4-5 dpf or 3-4 dpe, in addition to brain necrosis. WT embryos showed all these effects later, at 5-6 dpf or around 5 dpe, and at concentrations of 20 µM and higher

Representative images highlighting impaired swim bladder development in Oatp1d1 mutants and its absence accompanied by visible head necrosis. (Figure 40A).

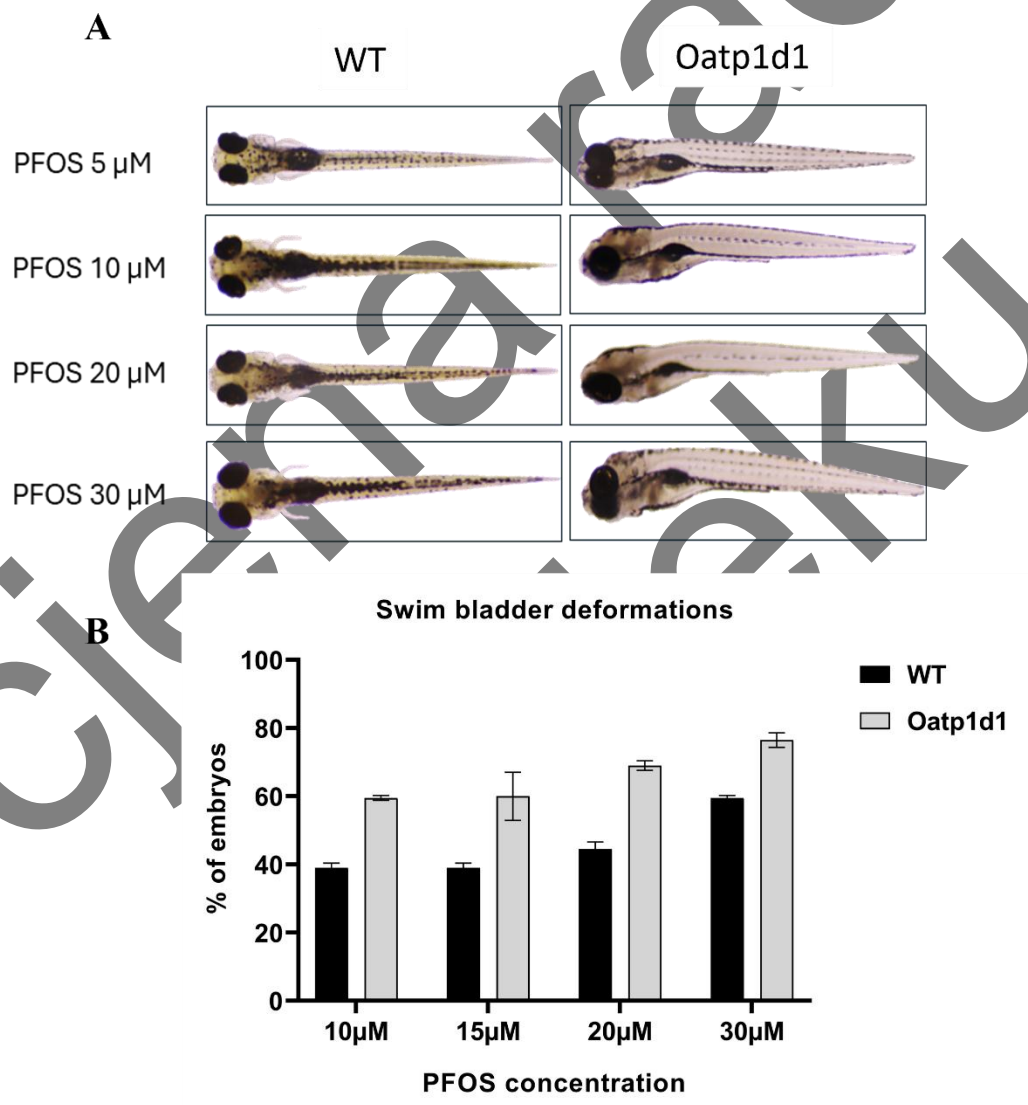

Figure 40. Effects of PFOS exposure on the development of Oatp1d1 mutant embryos (4 dpf). The onset of necrosis in the head and gut is visible (A), together with deformations of the swim bladder that cause the mutant embryos to lie on their side and be less active. (B) Quantification of swim bladder deformations at different PFOS concentrations. At each concentration, a higher

Ocjena rada sku

number of Oatp1d1 mutant embryos exhibited a deformed swim bladder. Data were obtained from at least three independent experiments.

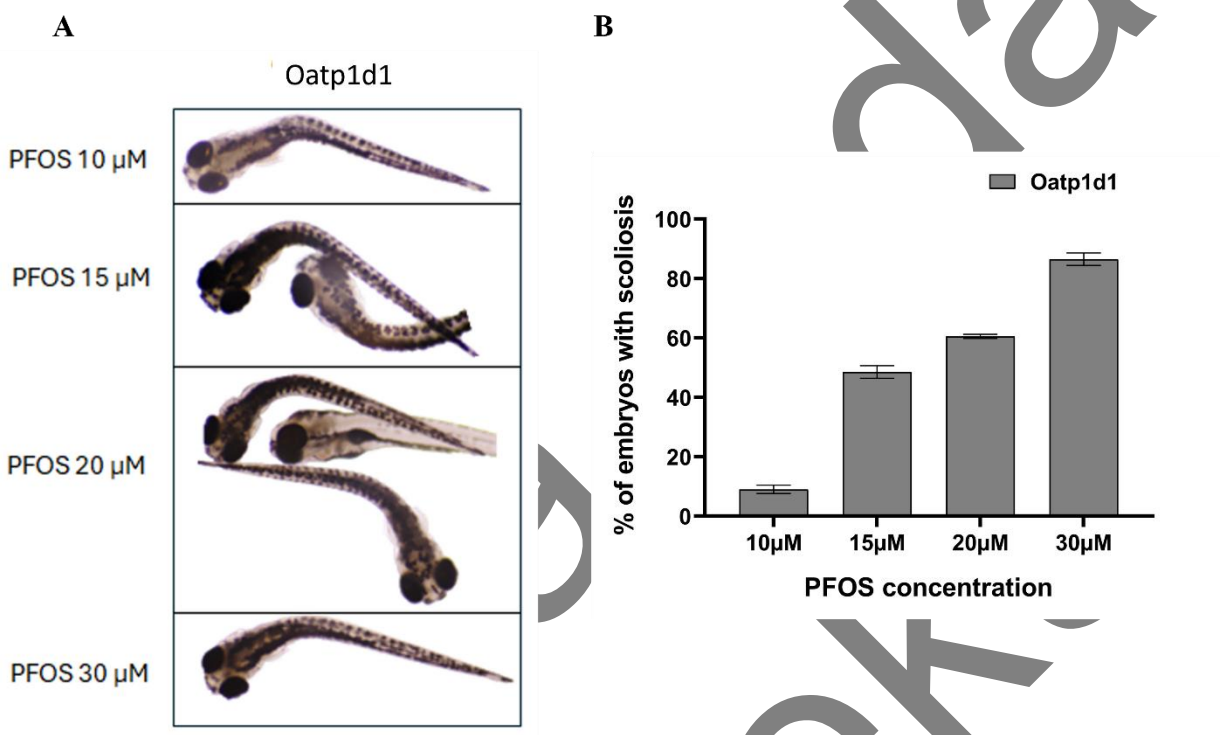

Figure 41. The occurrence of scoliosis in Oatp1d1 mutant embryos as an effect of PFOS treatment. (A) Images showing the scoliosis effect in mutant embryos at 4 – 5 dpf and different PFOS concentrations. (B) Dose response of the occurrence of the scoliosis in PFOS-treated Oatp1d1 mutant embryos. Data were obtained from at least three independent experiments.

In addition to the developmental changes and differences observed, we measured the behavior of the exposed embryos using the EthoVision software package. Importantly, we decided not to monitor behavior of embryos at points and concentrations when the macroscopic effects of PFOS were already visible, but when the Oatp1d1 embryos were slower, as it was critical that the embryos showed no degradation, necrosis or scoliosis, otherwise the results would not be valid. During each experiment, we observed the embryos and their responses to stimuli, and depending on the concentration (earlier at higher concentration), around the fourth day of exposure, we

Ocjena u tijeku

monitored the behavior and responses of embryos to day-night changes. The results obtained are shown in (Figure 42).

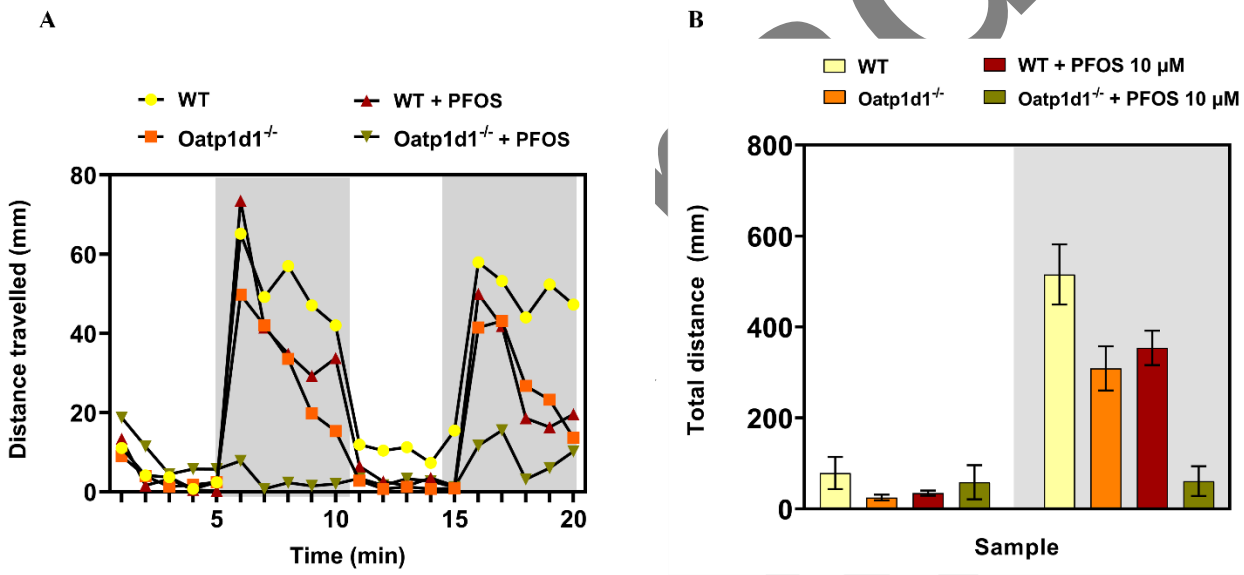

Figure 42. Changes in the locomotor activity of Oatp1d1 mutant embryos (5 dpf) exposed to PFOS at a concentration of 10 µM (4 dpe). Control larvae were exposed to E3 medium only. A) Mean distance travelled (mm) per minute by each experimental group during the 20- minute measurement, white boxes indicate dark phases and white boxes indicate light phases during the measurement. B) Total distance travelled (mm), again under dark and light conditions. The data are shown as mean ± SE. Statistically significant differences are marked with asterisks, and analysis was performed in GraphPad Prism Software 9.0 using ANOVA. Details of the statistical analyses are given in Table S7.

3.2.4.1. PFOS exposure alters transporter gene expression

PFOS exposure caused changes in the transcript expression of numerous genes involved in biotransformation processes. *Oatp1d1* showed a 1.5-fold upregulation in 5 dpf WT embryos after exposure to 15 µM PFOS for 1 h, while the mutant embryos showed no change (Figure 43B). Prolonged exposure to 5 µM PFOS caused no changes in the transcript expression of *oatp1d1* in both WT and mutant embryos (Figure 43A). However, after 4 dpf, wt embryos showed a down-regulation of 0.19-fold after exposure to 30 µM PFOS for three days (Figure 44A). On the other hand, a lower PFOS concentration (15 µM) led to a 2.16- and 3.23-fold upregulation of *oatp2b1* at 4 dpf and 3 days of exposure in both WT and mutant embryos (Figure 44B).

Oapt2b1 showed a 1.5-fold upregulation in 5 dpf WT embryos after exposure to 15 µM PFOS for 1 h, and a 1.14-fold upregulation in mutant embryos (Figure 43B). Prolonged exposure to 5 µM PFOS caused minor changes in *oatp2b1* transcript expression in both WT and mutant embryos by 1.12- and 1.2-fold, respectively (Figure 43A). WT embryos (4 dpf) showed a 0.77-fold down-regulation after three days of exposure to 15 µM PFOS, while mutant embryos showed a 1.73-fold up-regulation (Figure 44B).

Both *oat1* and *oat3* genes showed generally low expression under all conditions, with weak modulations of transcript expression upon exposure to different PFOS concentrations (Figures 43 and 44).

Abcg2a showed 1.5-fold upregulation in 5 dpf WT embryos after exposure to 15 µM PFOS for 1 h and a 1.14-fold upregulation in mutant embryos (Figure 43B). Prolonged exposure to 5 µM PFOS caused no changes in the transcript expression of *abcg2a* in both WT and mutant embryos

Ocjena rada u tijeku

(Figure 43A). However, at 4 dpf WT embryos showed high downregulation of 0.26-fold in wt and 0.46-fold in mutant embryos after three days of exposure to 30 µM PFOS (Figure 44A).

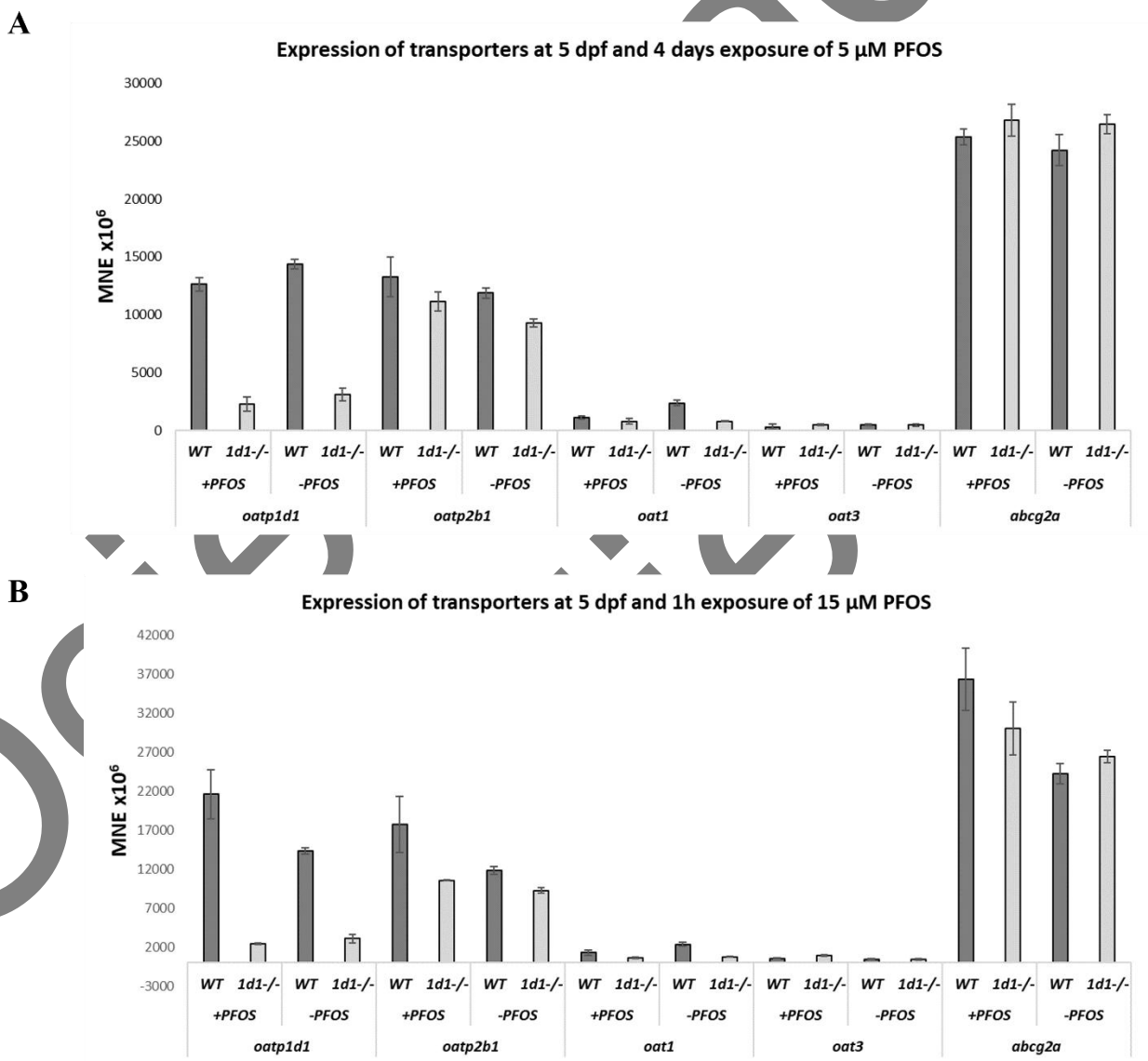

Figure 43. Transcriptional patterns of *oatp1d1*, *oatp2b1*, *oat1*, *oat3* and *abcg2a* in WT and Oatp1d1 mutant embryos A) at 5 dpf with and without four-day exposure to 5 µM PFOS; B) at 5 dpf and with and without one hour exposure to 15 µM PFOS. Results from pools of 10

embryos per sample are shown. Data represent MNE (mean normalised expression) ± SD, normalised to the housekeeping gene *ATP50*. Results from pools of 10 embryos per sample are shown. Data represent MNE (mean normalised expression) ± SD, normalised to the house gene *ATP50*.

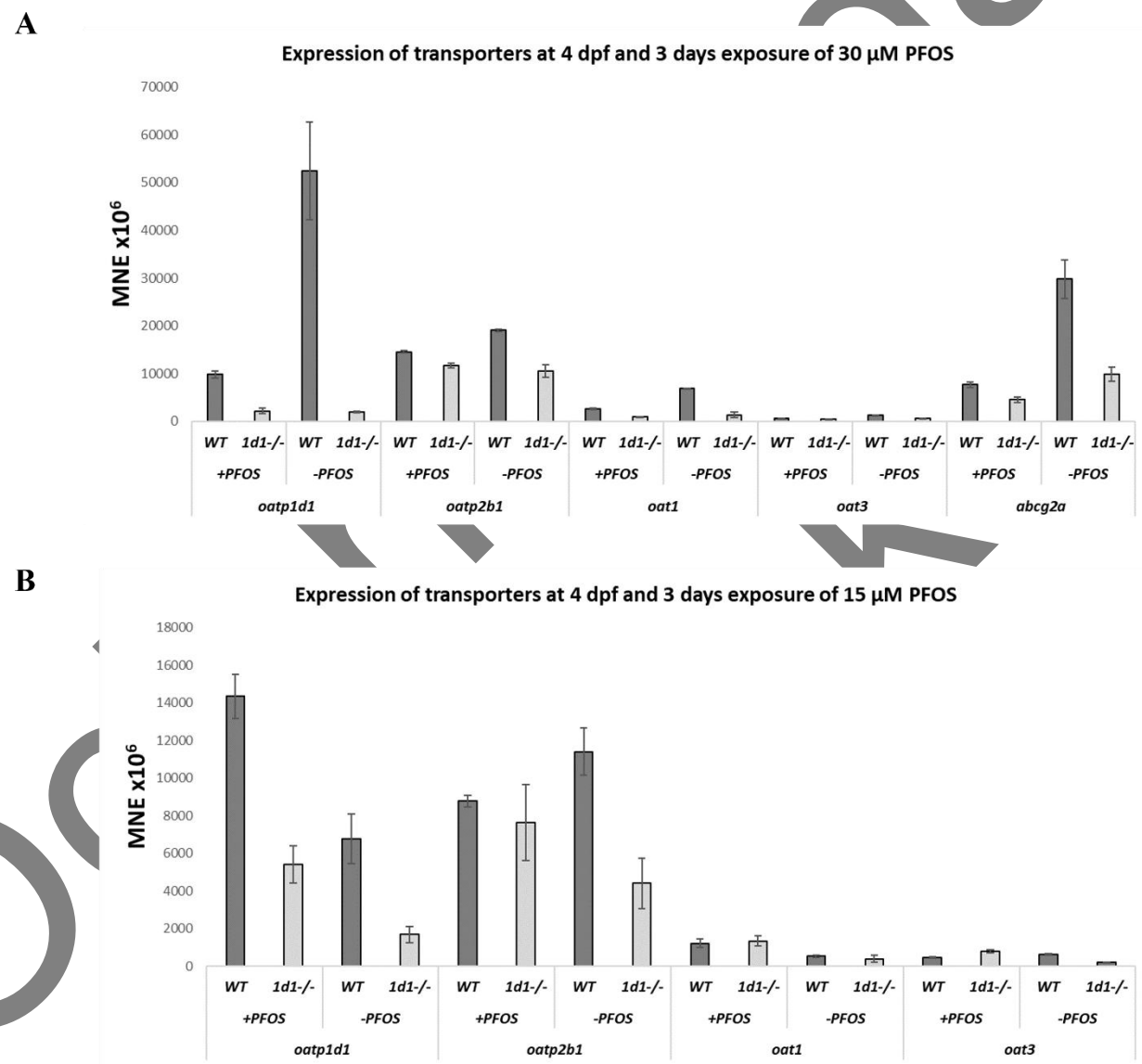

Figure 44. Transcriptional patterns of *oatp1d1*, *oatp2b1*, *oat1*, *oat3* and *abcg2a* in WT and Oatp1d1 mutant embryos at 4 dpf with and without three-day exposure to 30 µM PFOS. Results from pools of 10 embryos per sample are shown. Data represent MNE (mean normalised expression) ± SD, normalised to the house gene *ATP50*. **B) Transcription patterns of *oatp1d1*, *oatp2b1*, *oat1*, *oat3* in WT and Oatp1d1 mutant embryos at 4 dpf with and without three-day**

exposure to 15 µM PFOS. Results from pools of 10 embryos per sample are shown. Data represent MNE (mean normalised expression) ± SD, normalised to the house gene *ATP50*.

3.2.4.2. PFOS exposure alters transcriptional modulation of phase I and phase II enzymes

The *cyp1a* gene showed generally low expression under all conditions, with weak modulations of transcript expression upon exposure to different PFOS concentrations (Figure 45). *Cyp3a* showed a 2.16-fold upregulation in 5 dpf WT embryos after exposure to 15 µM PFOS for 1 h Figure 45, whereas mutant embryos showed a higher upregulation of 4.78-fold (Figure 45). Prolonged exposure to 5 µM PFOS caused 0.75-fold downregulation of *cyp3a* transcript in WT embryos, and 3.12-fold upregulation in mutant embryos (Figure 45B). However, at 4 dpf, WT embryos showed high downregulation of 0.03-fold upon exposure to 30 µM PFOS for three days, and lower downregulation of 0.72 in mutant embryos (Figure 46).

Ocjena rada u tijeku

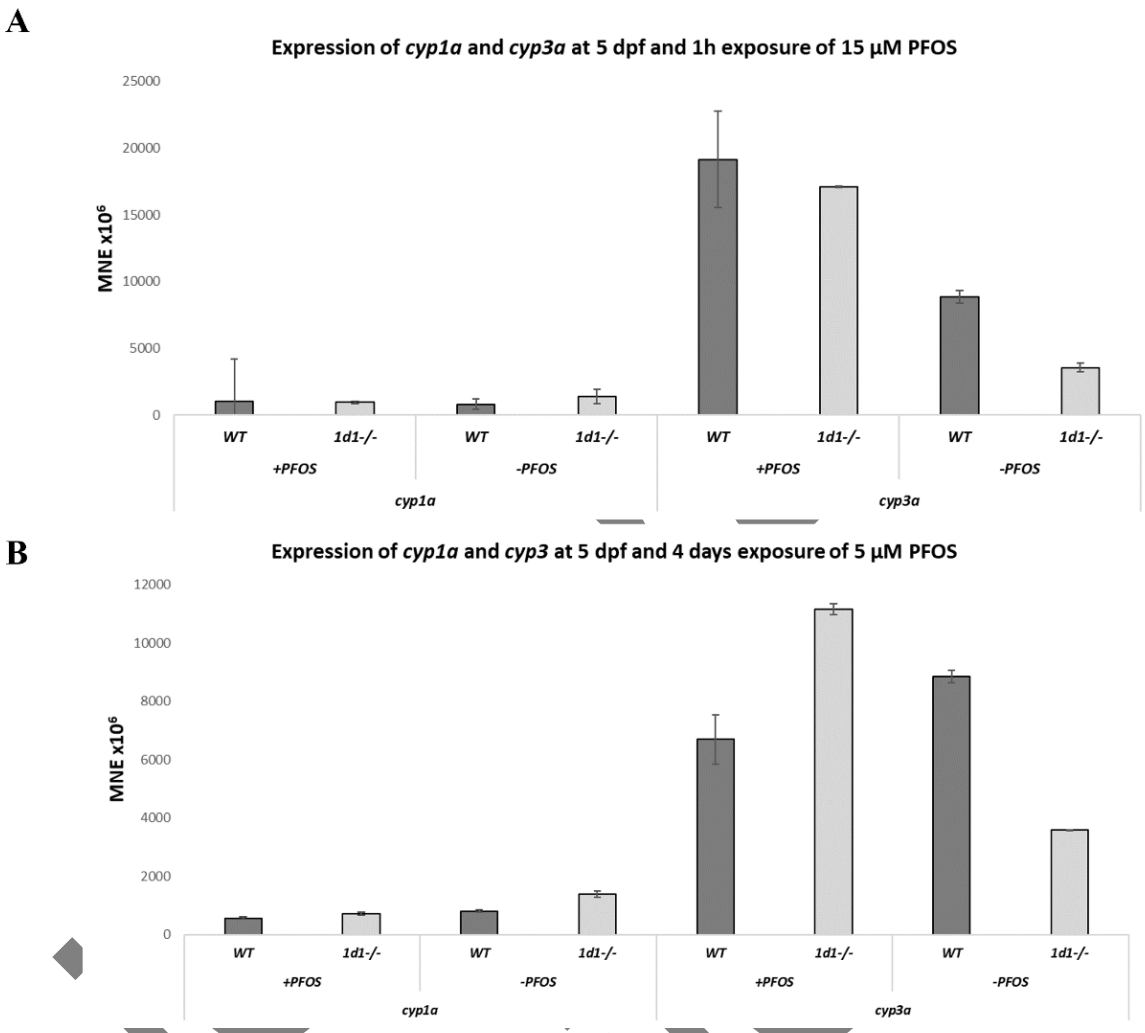

Figure 45. Transcription patterns of cyp1a and cyp3a in WT and oatp1d1 mutant embryos A) at 5 dpf with and without one hour exposure to 15 µM PFOS; B) at 5 dpf with and without four-day exposure to 5 µM PFOS. The results of pools of 10 embryos per sample are shown. The data represent MNE (mean normalised expression) ± SD, normalised to the house gene *ATP50*.

Ogs utg

A

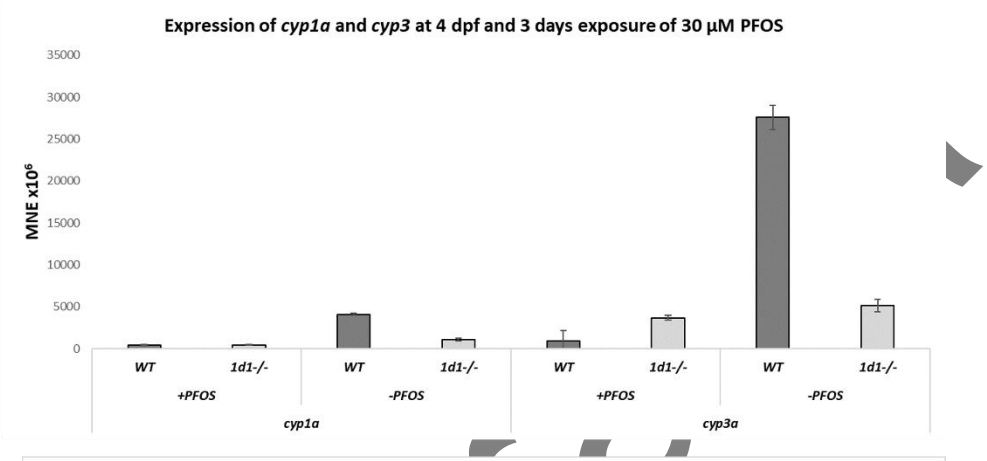

B

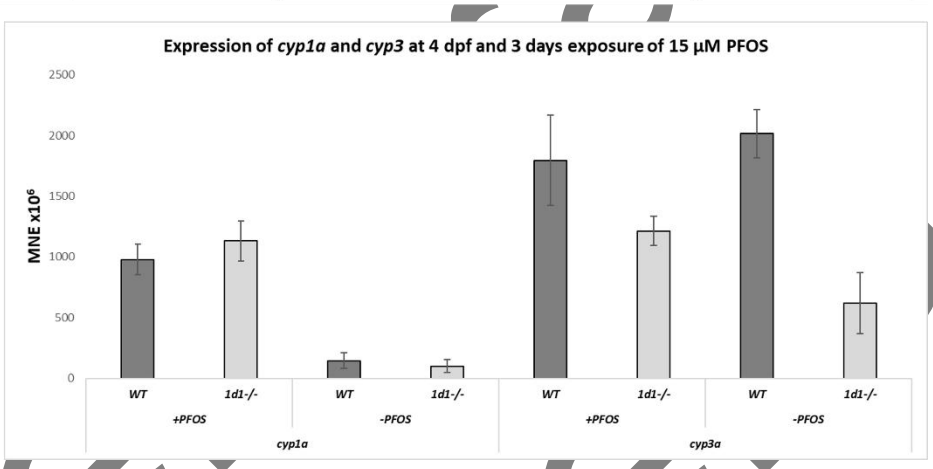

Figure 46. Transcription patterns of cyp1a and cyp3a in WT and Oatp1d1 mutant embryos A) at 4 dpf with and without three-day exposure to 30 µM PFOS; B) at 4 dpf with and without three-day exposure to 15 µM PFOS. The results of pools of 10 embryos per sample are shown. The data represent MNE (mean normalised expression) ± SD, normalised to the house gene *ATP50*.

The *gstr1* gene showed generally low expression under all conditions, with weak modulations of transcript expression upon exposure to different PFOS concentrations (Figure 47). *Gstp1-2* genes showed a 0.78-fold and 0.72-fold downregulation in WT and mutant embryos, respectively, after exposure to 15 µM PFOS for 1 hour (Fig. S4). Prolonged exposure to 5 µM PFOS caused a 0.84-fold down-regulation of the *gstp1-2* transcript in WT embryos and a 0.77-fold down-regulation in mutant embryos (Figure 47). WT embryos with 4 dpf showed a 0.81-fold down-regulation after three days of exposure to 5 µM PFOS and no modulation of transcript expression in mutant embryos (Figure 47).

Ogiev Utiev

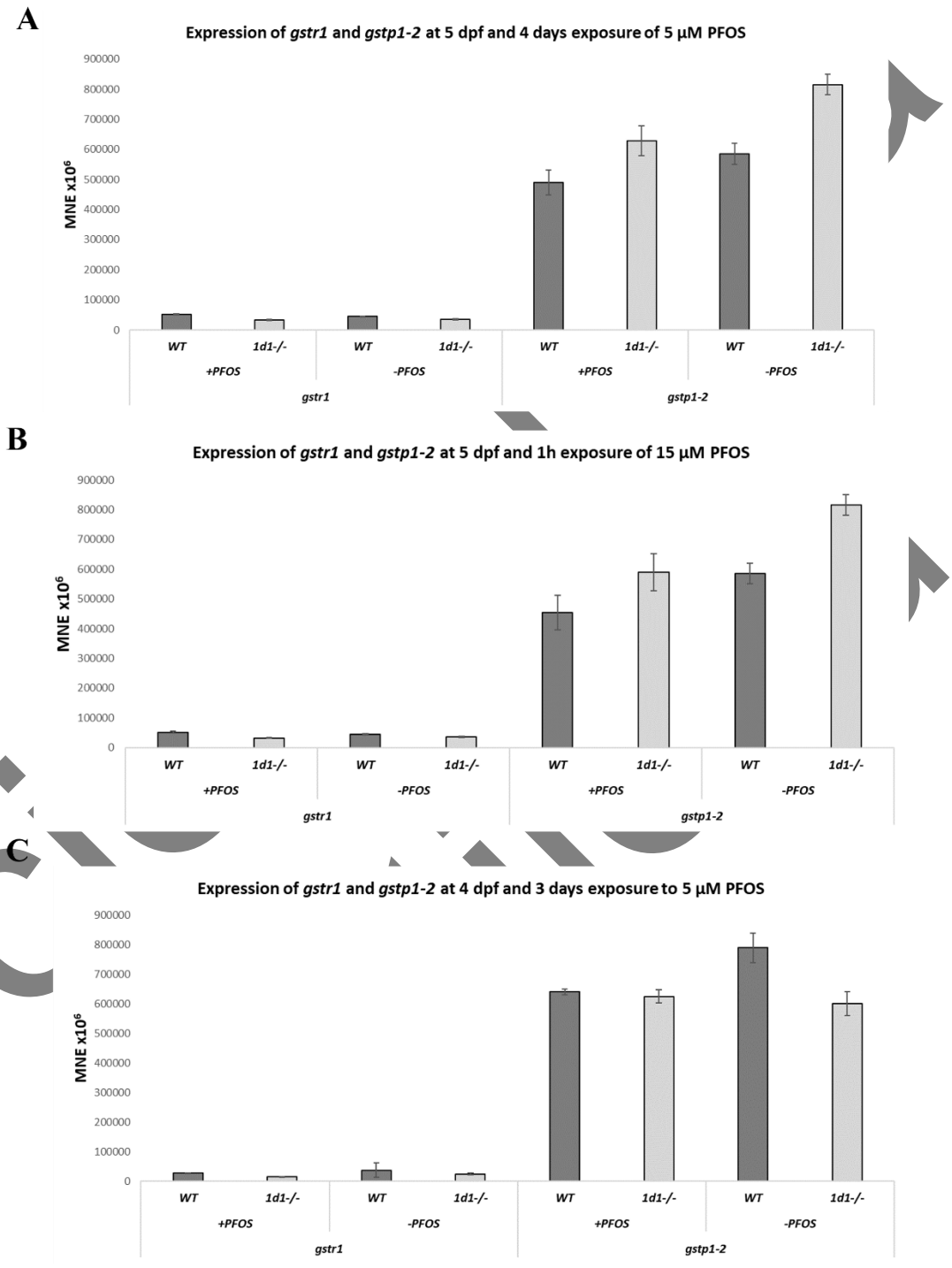

Figure 47. Transcript expression patterns of *gstr1* and *gstp1-2* in WT and Oatp1d1 mutant embryos. A) at 5 dpf with and without 4 days of exposure to 5 µM PFOS; B) at 5 dpf with and without 1 h of exposure to 15 µM PFOS; C) at 4 dpf with and without 3 days of exposure to 5 µM

PFOS. Results of pools of 10 embryos per sample are presented. Data represents MNE (mean normalized expression) ± SD normalized to the housekeeping gene *ATP50*.

3.2.4.3. Modulating PFOS uptake into WT embryos with different inhibitors of Oatp1d1 protein

Next, we aimed to test whether inhibition of the Oatp1d1 protein in WT embryos exposed to PFOS could result in the same or similar toxic effects as those observed in the mutants. The selected compounds were all non-competitive inhibitors of the Oatp1d1 protein that had previously been tested *in vitro*. The compounds tested as non-competitive inhibitors were TCDC, PFOA, and 17β-E2. We chose the PFOS concentration of 15 µM as a sublethal concentration with low effects (prolonged exposure could cause curvature). In the case of PFOA, we can see an additive toxic effect, where mutants with PFOS showed an exacerbated phenotype while WT embryos did not change (Figure 49). TCDC and LY together with PFOS did not induce any changes in either Oatp1d1 mutants or WT embryos (Figure 49). 17β-E2 is indeed a candidate as a non-competitive inhibitor. In four independent experiments, we consistently obtained the same results: WT embryos adopted an earlier mutant phenotype, lay on their side, had a deformed swim bladder and showed spinal curvature at higher concentrations of 17β-E2 (Figure 48). None of the described effects of the combination of 17β-E2 and PFOS were visible when the embryos were only exposed to 17β-E2 (Figure 48). We were not able to achieve the desired effects with the other inhibitors (Figure 49), at least not in the concentrations used.

Ocjena rada u tijeku

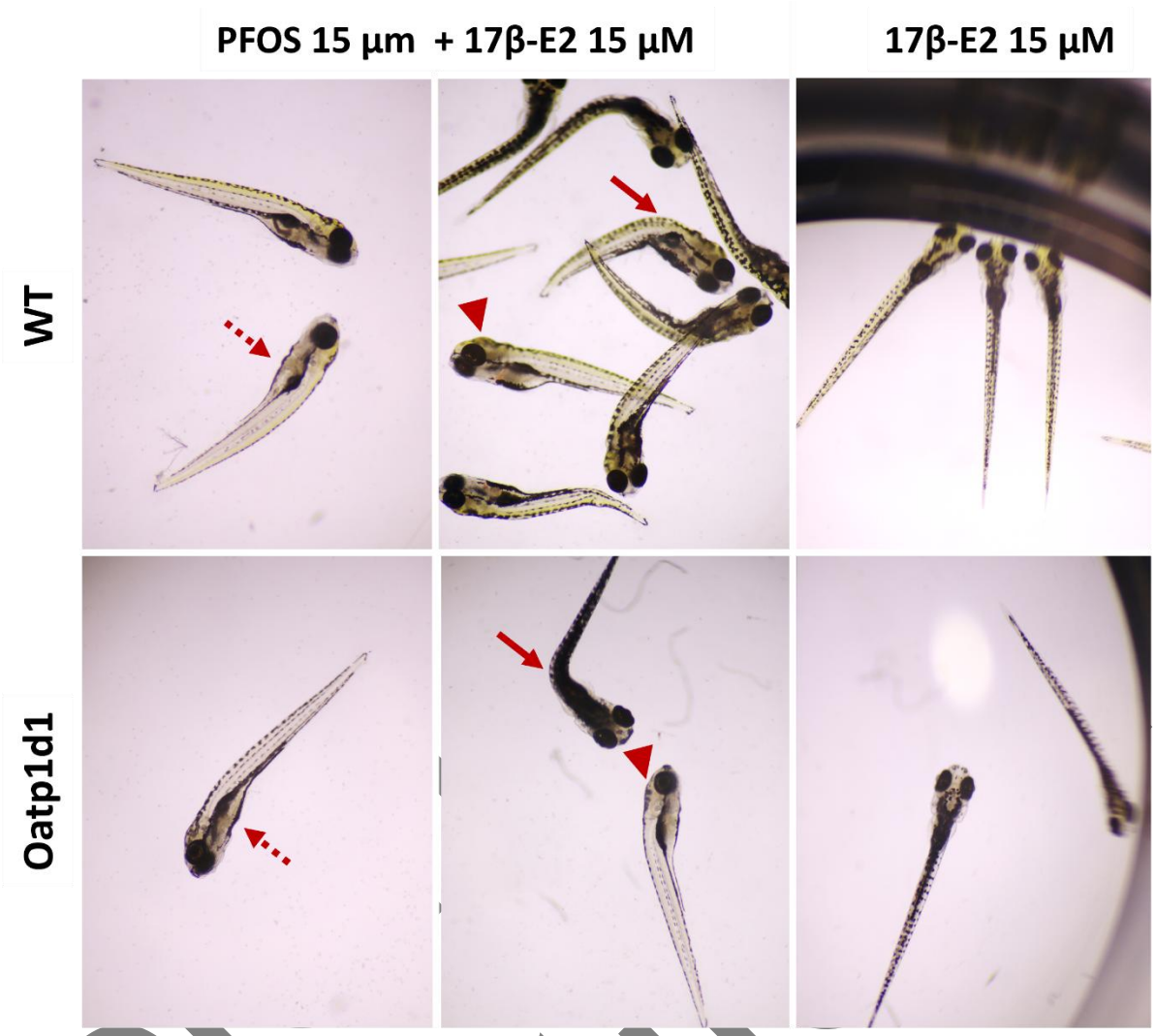

Figure 48. 17β inhibits the Oatp1d1 transport of PFOS in WT embryos. Embryos exposed to 17β-E2 15 µM and PFOS 15 µM at 24 hpf and to 17β-E2 and PFOS separately as control (images for PFOS are not shown as the effect was the same as previously shown). It can be observed that the WT embryos resemble the phenotype of the mutants, with brain necrosis (red triangle), lying on their side, necrotic appearance of the digestive system and lack or rounded swim bladder (red dashed arrow) and also body curvature and scoliosis (red arrow). When exposed to 17β-E2 only, neither WT nor mutant embryos show any phenotype.

Oslo Universitet

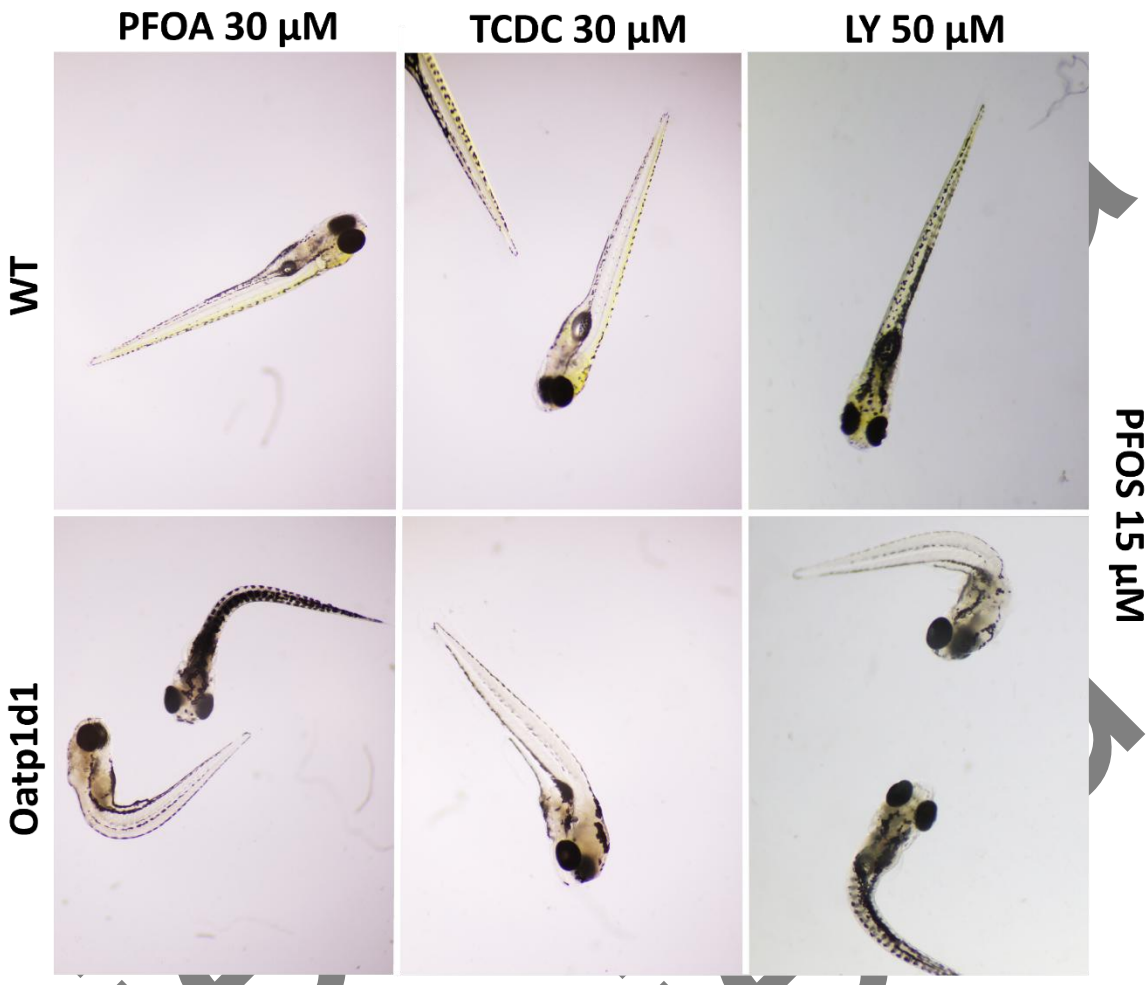

Figure 49. PFOA, TCDC and lucifer yellow do not inhibit the Oatp1d1 transport of PFOS in WT embryos at the concentrations used. Embryos were exposed at 24 hpf with PFOA 30 µM and PFOS 15 µM, TCDC 30 µM and PFOS 15 µM, LY 50 µM and PFOS 15 µM. The addition of these noncompetitive inhibitors does not change the phenotype of the WT embryos; they remain more resistant than Oatp1d1 embryos.

3.2.4.4. Oxidative stress after PFOS exposure

As the data from the TBARS assay were not reproducible (Figure S9), we continued with DCFH-DA, as the oxidation of DCFH-DA to 2',7'-dichlorofluorescein (DCF) is commonly used to detect all ROS, including hydroxyl radicals (- OH) and nitrogen dioxide (- NO_2). In zebrafish embryos/larvae, PFOS exposure has been reported to cause oxidative damage and significantly induce protein expression of peroxiredoxin 2, which is thought to be involved in cellular defense

against oxidative stress (X. Shi et al., 2009; X. Shi & Zhou, 2010). In our case, a PFOS exposure of 15 µM caused a higher level of oxidative stress, which can be seen as DCFH-DA fluorescence in the head and the rest of the body (Figure 50A), which is not the case in WT embryos (Figure 50A). Quantification of the fluorescence signal revealed a significantly higher level of oxidative stress in Oatp1d1 mutants (Figure 50B).

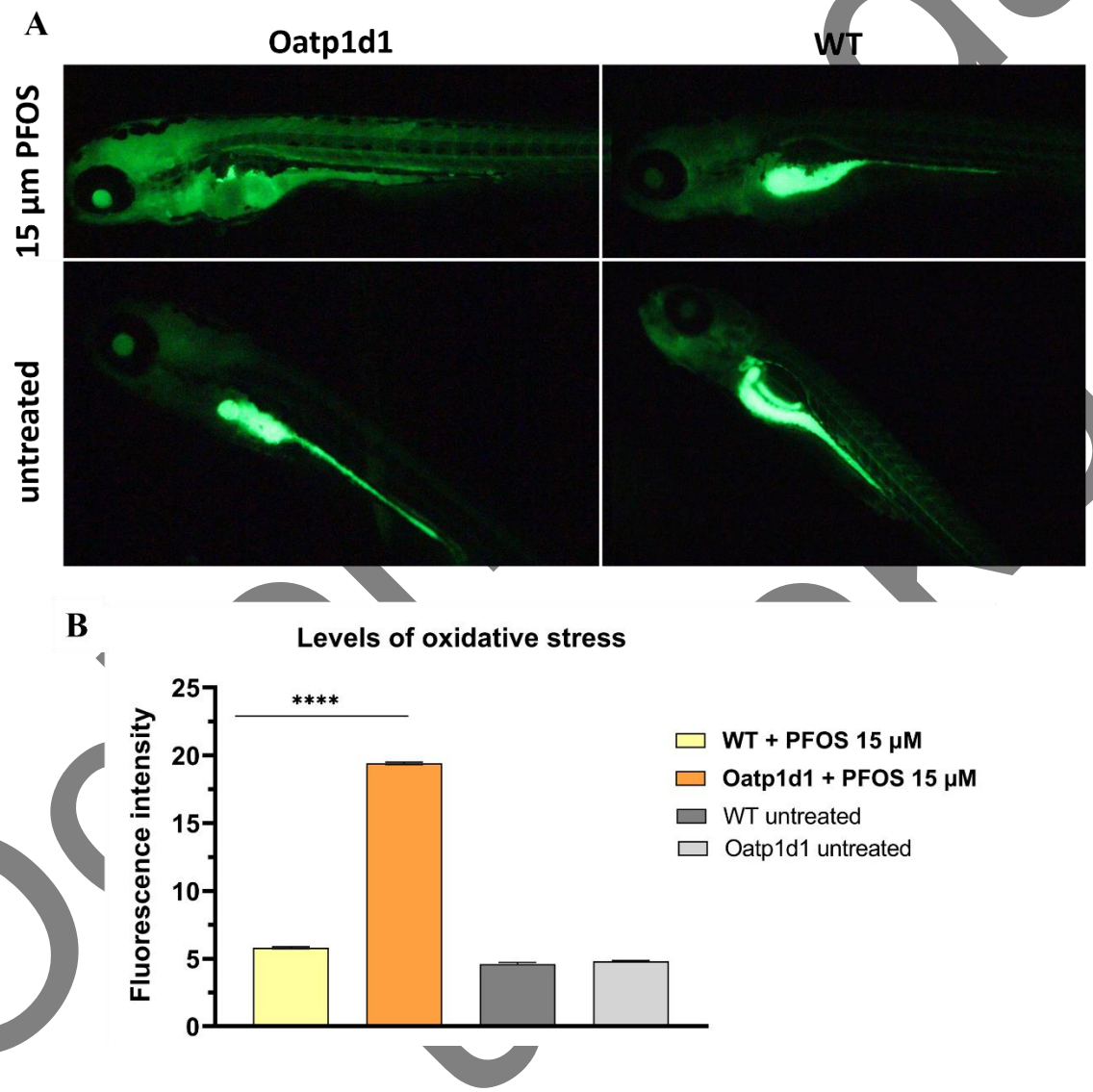

Figure 50. PFOS induced oxidative stress (ROS production) is more pronounced in Oatp1d1 mutants. Representative images, A) WT and Oatp1d1 mutant embryos (10 embryos per condition, in duplicate, in three independent experiments) were exposed to 15 µM PFOS followed by staining with 10 µM DCFH-DA to detect ROS. The strongest fluorescent signal indicative of ROS production was observed in the head region, around the heart and along the dorsal axis in the Oatp1d1 mutant embryos. In contrast, untreated embryos showed a signal mainly localised in the intestinal region; B) The intensity of the fluorescence signal was quantified using ImageJ software.

Statistically significant differences determined with a multiple unpaired t-test using GraphPad Prism software version 9.0.0 are labelled **** ($p < 0.0001$; $p=0.000038$).

3.2.4.5. Apoptosis after PFOS exposure

We used acridine orange (AO), a fluorescent DNA intercalating dye, to assess apoptosis in zebrafish to determine whether exposure to PFOS affects cell death in specific cells or tissues and whether there are differences between Oatp1d1 mutants and WT embryos. The Figure 51 shows a difference in fluorescence between Oatp1d1- and WT-exposed embryos. At the same PFOS concentration (15 µM), Oatp1d1 mutant embryos show a stronger signal and more punctate staining of cells undergoing apoptosis. In addition, the yolk is more degraded and less absorbed in Oatp1d1 embryos. In unexposed embryos (both WT and Oatp1d1 mutants) incubated with AO alone, the yolk is not degraded and is better absorbed, and AO is localized in the nasal epithelium. In the enlarged figure (Figure 51B) examples of these effects are further emphasized. More specifically, there is more punctate staining, i.e. apoptotic cells, in Oatp1d1 embryos exposed to PFOS. Enlarged images of the head (Figure 51C) confirm a stronger signal in the Oatp1d1 mutants, with fluorescence distributed over the entire head, brain and visible dots, while in WT embryos only a few dots in the dorsal part of the head fluoresce, almost as in unexposed embryos. Together with the nasal epithelium, neuromasts (more intensely coloured and larger dots) are also observed in non-exposed embryos. The graph (Figure 51D) shows the quantification of the AO fluorescence signal and confirms that Oatp1d1 embryos exposed to 15 µM PFOS show higher apoptosis after four days of exposure and at 5 dpf

Ocjena rada u tijeku

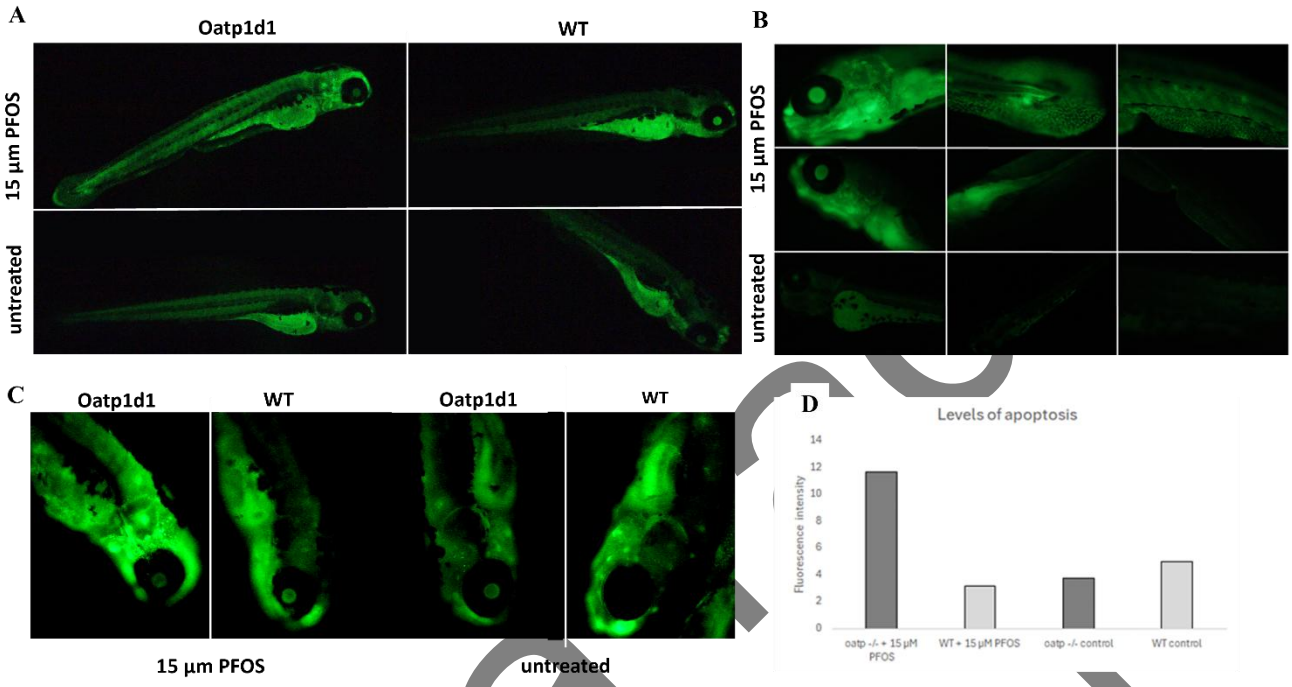

Figure 51. PFOS induces apoptosis in embryos, as visualised by acridine orange staining, with a more pronounced effect in Oatp1d1 mutant embryos. Representative images of embryos (10 per condition, treated in duplicates and repeated three times) exposed to 15 µM PFOS followed by staining with 10 µM acridine orange: A) Whole-embryo images show punctate fluorescent signals throughout the bodies of the Oatp1d1 mutant embryos, especially in the head, dorsal region, and tail, indicating apoptotic cells as a result of PFOS exposure: B) Enlarged images highlight specific embryonic regions: the left panel shows the head, the middle panel shows the tail tip, and the right panel displays the mid-body region (from the cloaca to the posterior tail). The punctate green fluorescence corresponds to the acridine orange staining of apoptotic cells; C) A comparison of the embryonic heads reveals a stronger apoptotic signal in Oatp1d1 mutants than in WT embryos. In untreated embryos, punctate signals can be observed below the eye and near the mouth, corresponding to neuromasts rather than apoptotic cells. The fluorescence at the top of the head corresponds to the nasal epithelium; D) Quantification of fluorescence intensity in embryos was performed using ImageJ software. The graph represents levels of apoptosis.

3.2.4.6. Gene silencing with morpholinos and oxidative stress

The strongest DCF fluorescence signal, indicating increased reactive oxygen species (ROS), was observed in the head and body (excluding the intestine) of Oatp1d1 mutant embryos, followed by morpholino-injected embryos (Figure 52A**)**. WT embryos showed the lowest levels of oxidative

Ocena autoreferatu

stress. A slightly increased signal was observed at 2 µM PFOS, although the reason for this remains unclear. Unexposed embryos exhibited DCF accumulation only in the intestinal region (Figure 52A**)**. Quantification of fluorescent signal confirmed observed effects (Figure 52B).

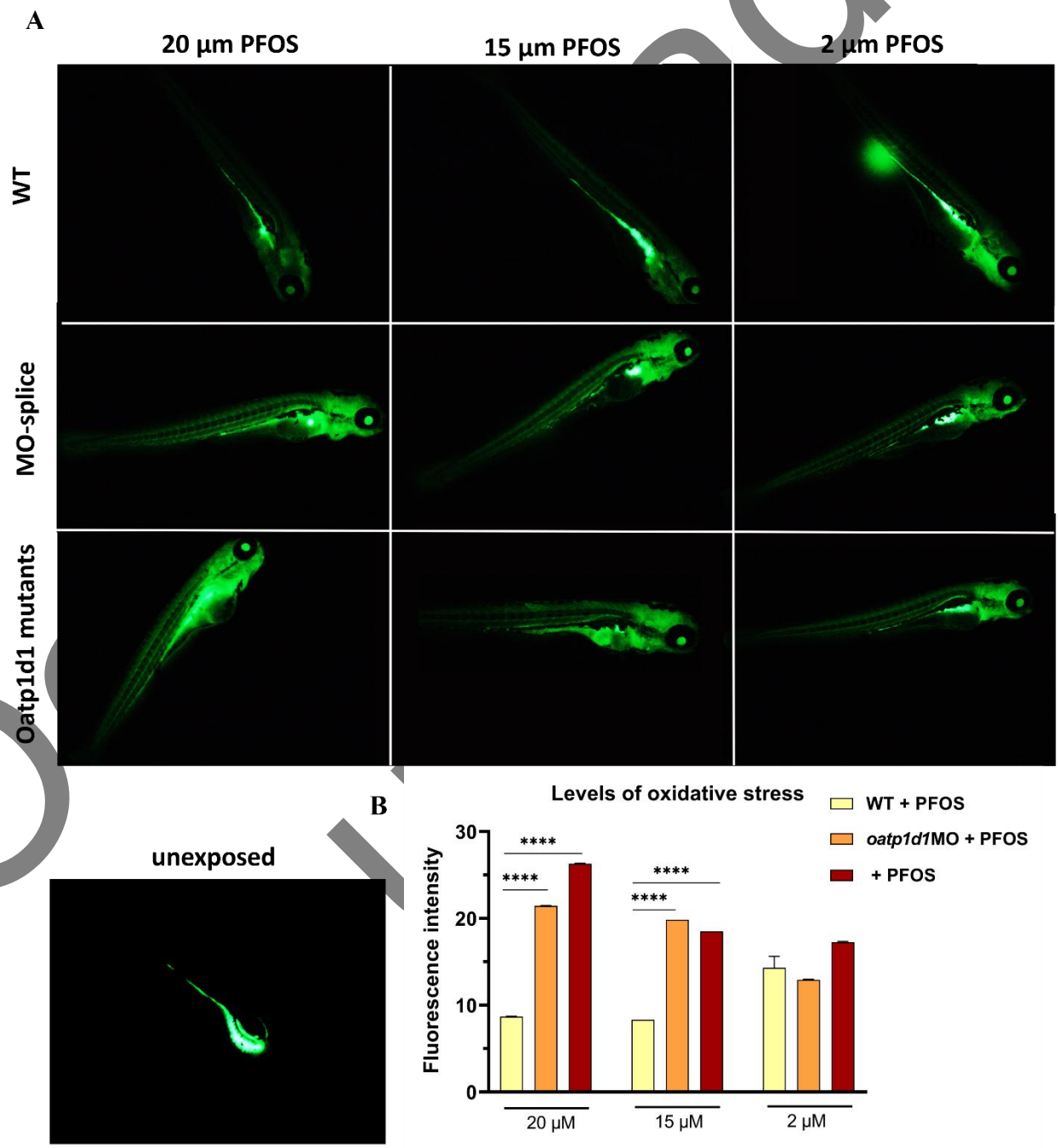

Uncorrected Proof

Figure 52. Oatp1d1 morpholino-injected embryos exhibit increased susceptibility to oxidative stress compared to WT embryos. Representative images: A) WT, MO-splice, and Oatp1d1 mutant embryos (10 embryos per condition, treated in duplicates and repeated 2–3 times) were exposed to various concentrations of PFOS (20, 15, and 2 µM), followed by incubation with 10 µM DCFH-DA. The embryos were imaged under identical magnification and exposure settings. B) Fluorescence intensity was quantified using ImageJ software. The graph represents levels of oxidative stress at different PFOS concentrations. Statistically significant differences are marked with **** ($p < 0.0001$). Statistical test used is unpaired t-test obtained in GraphPad Prism software version 9.0.0.

3.2.5. Rescue experiment using *oatp1d1* mRNA construct

To confirm that the mutant phenotype results from the loss of transport function of the Oatp1d1 protein, we constructed a rescue mRNA encoding the full-length *oatp1d1* coding sequence and microinjected it into zebrafish embryos at the one- to four-cell stage. The first step was to verify the rescue construct in embryos using specially designed primers (Table 5) that specifically target the construct. As shown in (Figure 53A), clear bands are visible in 2 dpf embryos, but only in injected samples, with a stronger signal observed in WT embryos. No bands were detected in non-injected embryos. When primers targeting both the endogenous and construct-derived oatp1d1 mRNA were used (Figure 53B), stronger bands were detected in embryos injected with the RNA construct, indicating increased transcript levels. However, after 3 dpf, the band intensity decreased sharply. Several bands were observed in embryos at 7 dpf, which is probably due to non-specific amplification.

Although we expected the rescue of yellow pigmentation in the mutants, this was not observed. Considering that expression of the *oat2a* gene was downregulated in the mutants, it is possible that another gene, such as *oat2a,* should be targeted for effective rescue of the phenotype of the mutants.

Although the expression of the oatp1d1 transporter naturally increases after 3 dpf and the stability of the rescue construct is likely limited (as indicated by the results), we proceeded with the diclofenac exposure experiments as the phenotypic effects and responses to exposure in embryos after 3 dpf are evident. In the case of PFOS exposure, we performed the rescue experiments even though the phenotype changes occur even later and rescue was unlikely.

Ocjena rada u tijeku

The first indication of a potential rescue phenotype appeared during the early stages of diclofenac exposure, where haemorrhages were observed in Oatp1d1 mRNA-injected embryos (Figure 53C, red arrows) a feature that was not present in non-injected Oatp1d1 mutants at a concentration of 20 µM.

Ocjena rada u tijeku

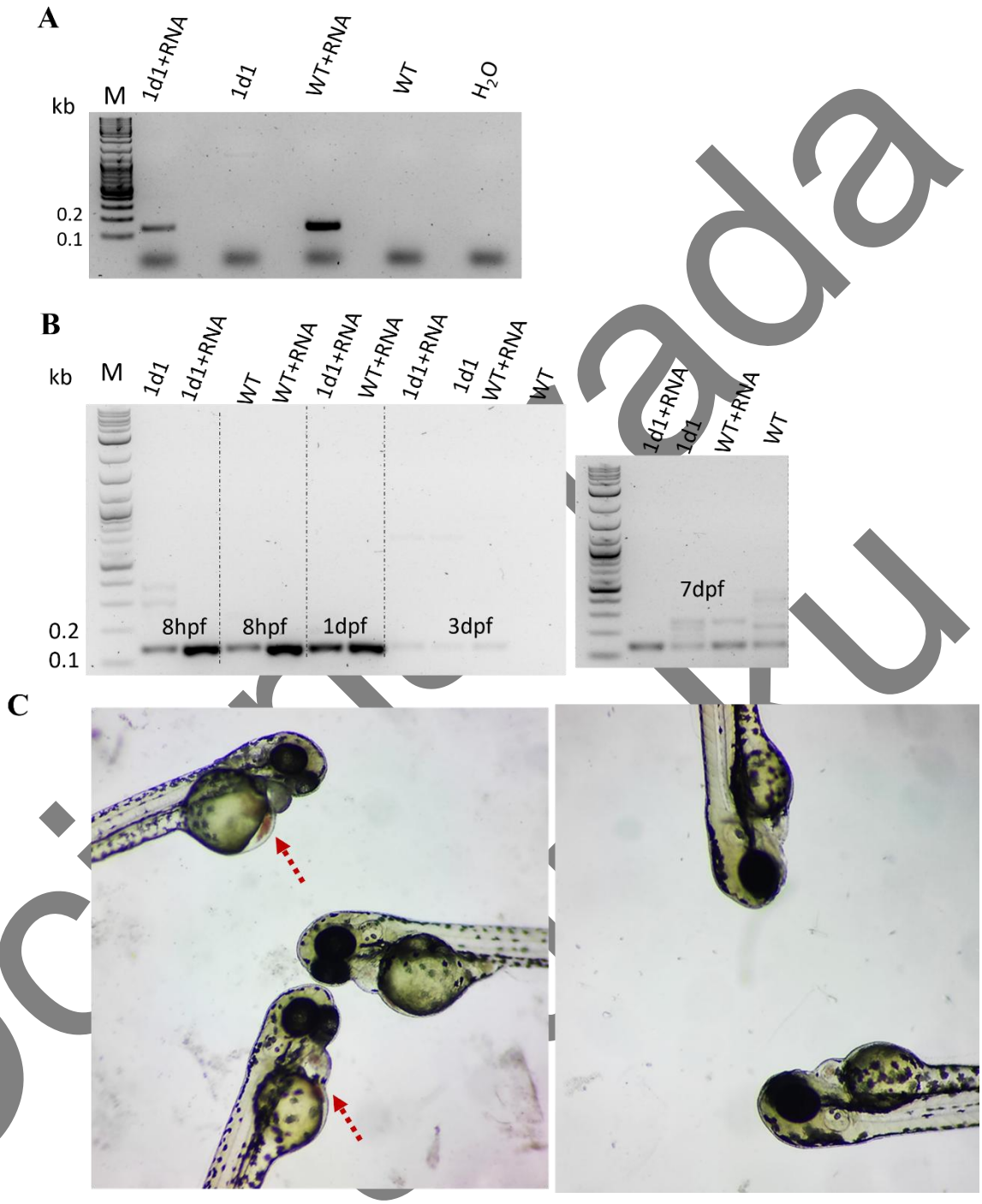

Figure 53. Rescue construct verification and exposure of injected embryos to 20 µM diclofenac. A) Primers that specifically target only the rescue mRNA coding for oatp1d1 show bands on the gel only in samples injected into embryos. The intensity of the PCR band is stronger in WT embryos, and non-injected embryos show no band. B) Primers that detect both endogenous and injected mRNA show bands with higher intensity in injected samples. Already at 3 dpf the singal fades and at 7 dpf there are some unspecific bands. C) Preliminary experiment with Oatp1d1

Oriģinālā

injected embryos exposed to diclofenac. The red arrows indicate haemorrhages in the injected embryos, while no effects are observed in the Oatp1d1 mutants, as expected.

A possible sign of partial rescue was also observed in experiments with diclofenac exposure (Figure 54), where injected embryos showed slight body curvature, haemorrhage and generally poorer condition compared to Oatp1d1 mutants. However, these results were not reproducible across all replicates, so we cannot say with certainty that a rescue of the mutant phenotype has occurred. One possible explanation is that the mechanism behind the increased resistance observed in Oatp1d1 mutants remains unclear. If this resistance is the result of compensatory mechanisms and not direct loss of Oatp1d1 function, then injection of oatp1d1 mRNA may not be sufficient to restore the phenotype, similar to what we have observed in attempts to rescue pigmentation.

Ocjena rada u tijeku

Figure 54. Rescue experiments with mRNA encoding full-length oatp1d1 and subsequent exposure to PFOS and diclofenac. A) No rescue of the mutant phenotype was observed after exposure to PFOS. The injected embryos resembled the wild-type (WT) phenotype, indicating that oatp1d1 mRNA has no effect on reversing the PFOS-induced changes. B) In contrast, a partial rescue phenotype was observed after diclofenac exposure. The injected embryos exhibited haemorrhage, pericardial oedema and a slight body curvature, features observed in WT embryos exposed to diclofenac. These experiments were repeated three times in the case of PFOS and five times in the case of diclofenac, and partial rescue was observed in two independent replicates in the case of diclofenac.

Ocjena rukopisa

3.2.6. Prediction of Oatp1d1 protein structure using AlphaFold 3 algorithm

In order to better explain interaction of PFOS and diclofenac with Oatp1d1 protein, we used AlphaFold 3 to predict the 3D structure of the protein (Figure 53A) and docking calculations to verify the binding of selected model substrates and inhibitors, similarly as done previously by Vujica et al (2023). Using the PPM 3.0 method 12 TM segments were identified. The total number of TM segments, their sequence positions (Table S1) and 2D topologies (Fig. S2) predicted by PPM 3.0 from the predicted 3D structure of Oatp1d1 were consistent with those predicted by the TOPCONS consensus method and other single methods used (Figures S3 and S4) (Bernsel et al., 2009). Both the N-and C-termini of the Oatp1d1 protein are predicted to be located in the cellular (cytoplasmic) space (Figure 55B). Finally, the 3D topology and the mutual positions of the TM segments (helices) are confirmed by the ΔG_{assoc} (free association energies) of the TM segments (Figure S5) and the most likely association pathway (Table S5) determined using the TMPfold server (A. L. Lomize et al., 2020).

Ocjena rada u tijeku

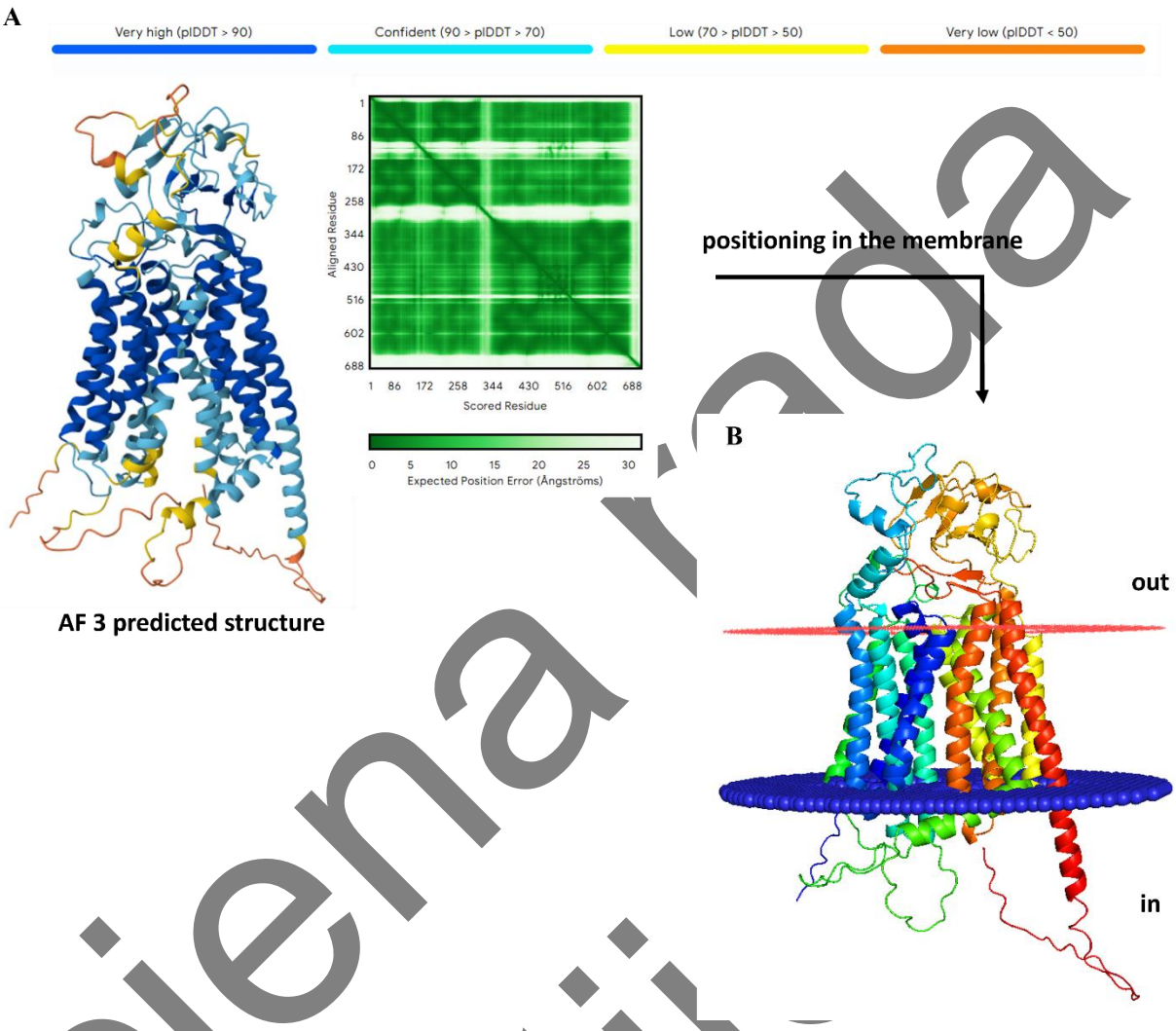

Figure 55. Predicted 3D structure of zebrafish Oatp1d1 and positioning in the membrane A) Structure determined with the AlphaFold 3 algorithm. B) The obtained structure positioned in the membrane using the PPM 3.0 method. The chains are coloured from N- to C- terminus (blue to red), both intracellular. *Out* stands for extracellular space, *in* for the intracellular space.

3.2.7. Molecular docking of Oatp1d1 substrates and inhibitors

Based on the 3D structure positioned in the cell membrane, a molecular docking analysis of selected Oatp1d1 substrates and inhibitors was performed. We selected diclofenac and PFOS to verify their binding as substrates based on *in vitro* results (Popovic et al., 2013, 2014) and lucifer yellow as Oatp1d1 model florescence substrate, which has already been used in molecular docking in Oatp1d1 (Marić et al., 2021). We also wanted to see where the inhibitors would bind, at a site

Ocjena rada u tijeku

other than the active site or not. We chose 17β-E2, PFOA, chlorpyrifos-methyl and clofibrate, again based on the previously mentioned *in vitro* results from our group. All substrates bound to the same active site (Figure 56A), with PFOS showing the highest affinity for the Oatp1d1 protein, followed by lucifer yellow and diclofenac. All binding affinities are listed in (Table S). Interestingly, noncompetitive inhibitors, 17β-E2, PFOA and chlorpyrifos-methyl all bind to the active site, but also near the signature motif, whereas the uncompetitive inhibitor clofibrate binds to different sites than the noncompetitive inhibitors listed. The binding of 17β-E2 is shown in Figure 56B, all other inhibitors and the binding affinities are listed in (Figure 57) Table S.

Ocjena rada u tijeku

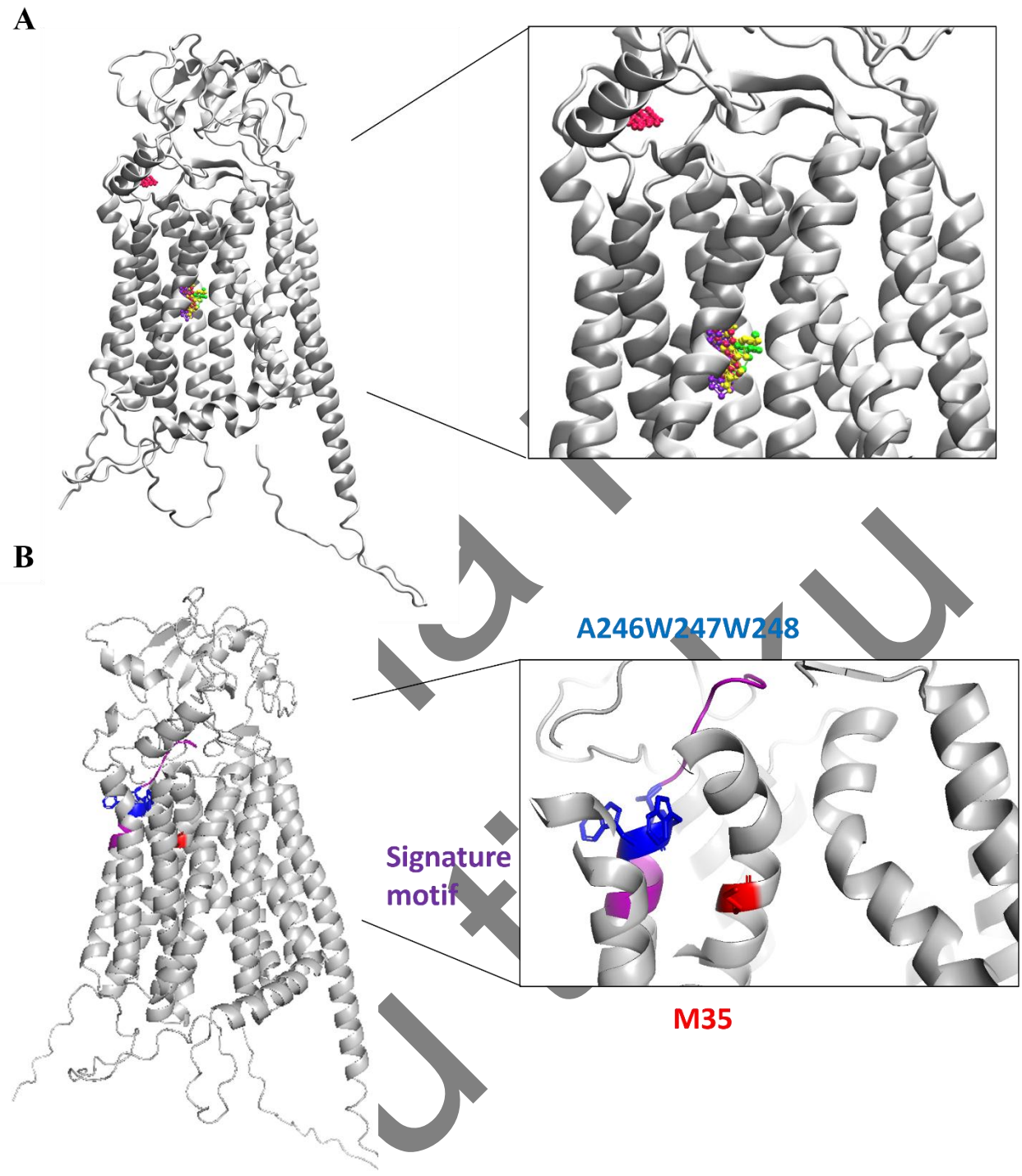

Figure 56. Molecular docking of selected substrates and an inhibitor with the Oatp1d1 protein. A) AlphaFold3 (AF3) structure of Oatp1d1. The 17β-E2 is shown in red and binds both to the primary active site and to a site distant from the active site. Other substrates, diclofenac (green), lucifer yellow (yellow) and PFOS (purple), bind to the same active site, which is consistent

with in vitro data (Popovic et al., 2013) indicating that Oatp1d1 has a single active site. The binding energies are listed in the Supplement (Table). B) The signature motif of the OATP transporter family is highlighted in purple. Within this motif, the AWW amino acid sequence is responsible for the binding of bicarbonate ions, which is essential for substrate transport into the intracellular space, according to the literature. In addition, residue M35, already reported by Marić et al., 2021, corresponds to M37 in the current sequence version and represents the site where lucifer yellow binds in the active site. The difference in the numbering of the residues probably reflects an update of the sequence.

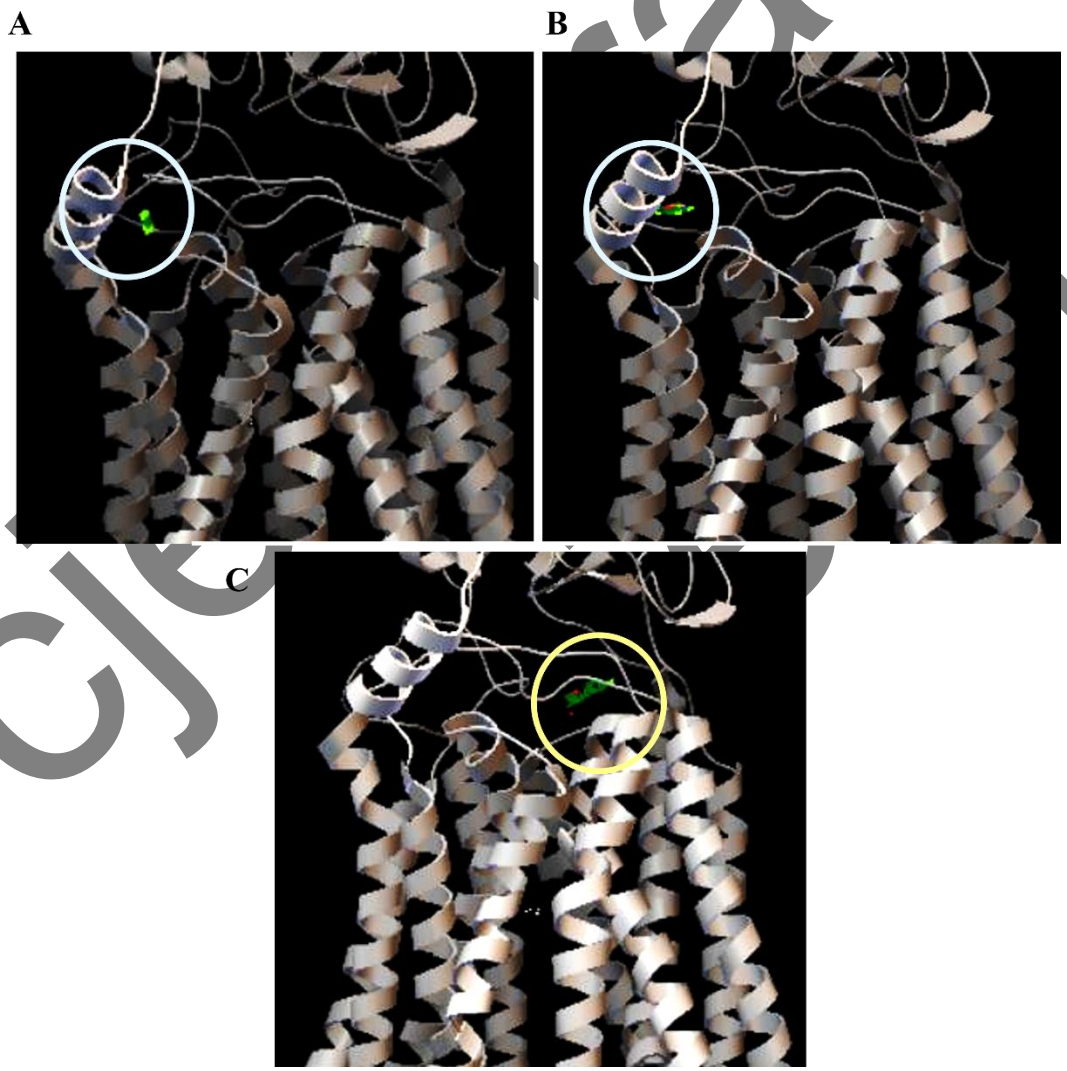

Figure 57. Molecular docking of selected inhibitors to the Oatp1d1 protein. Non-competitive inhibitors of the Oatp1d1 protein (A) PFOA and (B) chlorpyrifos-methyl near the signature motif (see Figure 56B). The uncompetitive inhibitor of the Oatp1d1 protein, (C) clofibrate, binds

Ocjenski rad

to different sites than the non-competitive inhibitors (17β-E2, PFOA and chlorpyrifos-methyl). The binding energies are listed in the Supplement (Table).

4. DISCUSSION

This study represents the first *in vivo* characterization of an uptake transporter in zebrafish by using a functional knockout model. We focused specifically on the organic anion transporting polypeptide 1d1 (Oatp1d1), as data of ours and other research groups have shown that this fish-specific transmembrane protein plays an important role in the transport of various endogenous substances and exogenous compounds across cellular membranes. Therefore, our primary goal was to obtain findings that would serve as a basis for further *in vivo* research aimed at better understanding of the physiological and protective role of Oatp1d1 and its possible correlation with human OATP proteins.

As pointed out, Oatp1d1 in teleosts is functionally similar to OATP1A/Oatp1a and OATP1B/Oatp1b members in mammals (Popovic et al., 2013). It has been shown previously that zebrafish Oatp1d1 probably does have a significant role in the uptake and elimination of important physiological substrates like steroid hormone metabolites, similar to the role of human OATP1A2, OATP1B1 and OATP1B3. It transports cortisol, is a high affinity transporter of conjugated steroid hormones estrone-3-sulfate (E3S), estradiol-17β-glucuronide (E17ß-glucuronide) and dehydroepiandrosterone sulfate (DHEAS), but non-conjugated steroids like estradiol, progesterone, androstenedione, dihydrotestosterone and testosterone inhibit its function (Hagenbuch & Gui, 2008; Popovic et al., 2013).

Apart from physiological substrates, Oatp1d1 does transport and interact with xenobiotics. It has been shown that the uptake of microcystins (MCs), cyanobacetrial secondary metabolites, is mostly mediated by OATPs/Oatps (Fischer et al., 2010). Microcystins, most dominant type of cyanotoxins are highly toxic compounds often associated with hepatotoxicity, nephropathy and

Ocjena rada u tijeku

neurotoxicity (Chen et al., 2009). Rate of MC uptake significantly varies for different congeners and zebrafish Oatp1d1 acts as a ubiquitously expressed, multi-specific transporters of various MC congeners, while members of e.g., the Oatp1f subfamily are expressed exclusively in the kidney and transport only specific MC congeners (Steiner et al., 2016). Marić et al (2021) showed that the strongest interactors were also the most lipophilic congeners MC-LW and -LF, followed by congeners -LA, -LR and -YR, in correlation with their log POW. Besides MCs, results of another *in vitro* study performed by our group (Popovic et al., 2014), showed that prominent environmental contaminants such as PFOS, nonylphenol, gemfibrozil, diclofenac, EE2 and caffeine are high affinity substrates of zebrafish Oatp1d1. On the contrary, PFOA and synthetic estrogens E2 and E1 are strong Oatp1d1 inhibitors. Both groups of compounds could disrupt normal transport function of Oatp1d1 and interfere with transport of physiological substrates (DHEAS, E3S and E17ß-glucuronide) (Popovic et al., 2014).

Consequently, to address potential (eco)toxicological role of zebrafish Oatp1d1 *in vivo*, we first generated Oatp1d1 mutants using CRISPR-Cas9 methodology. This gene editing method enables precise gene excision, in our case a partial deletion (5 nucleotides (GTGCC) at a position 9115-9119 of genomic DNA) in exon four and the associated loss of a certain number of amino acids, resulting in a premature stop codon. The main goal of the subsequent process was to develop fish carrying mutations on both alleles (homozygous mutants) by crossing heterozygous individuals, followed by identification of homozygous mutants and continued breeding from the F3 generation onwards for detailed phenotypic characterization. There are two reasons why we expected that the Oatp1d1 mutation would not be lethal: (1) because Oatp1d1 most likely does not play a critical role in early zebrafish development, at least not when there is no additional pressure from external contaminants; and (2) because there are several other transporters that may potentially compensate for the loss of Oatp1d1 (developmental redundancy in transport mechanisms) or due to compensatory mechanisms by similar transporters (Rossi et al., 2015a, 2015b). However, our assumption was that despite the compensatory mechanism(s), or even because of them, some phenotypic changes would occur during embryonic development. After confirming the presence and non-lethal effect of the *oatp1d1* mutation, we first validated the loss of the Oatp1d1 at the protein level by immunohistochemistry with specific antibodies against Oatp1d1, followed by Western blot analysis. In addition, gene expression was analyzed by qPCR in different embryonic stages and in adult tissues.

Ocjena rada u tijeku

After the successful creation and verification of the mutated line, our main goal was to characterize phenotype of the mutants and to investigate the possible consequences of the loss of function of the Oatp1d1 transporter and potential adaptation of the zebrafish by changes in expression of other transport proteins with overlapping substrate preferences. When observing the phenotype of exposed embryos, we included different endpoints to assess the effects of test compounds previously shown to be strong Oatp1d1 interactors in zebrafish. Each endpoint required methodological optimization in terms of exposure duration and compound concentration, as comparisons at the molecular level differ from macroscopic observations.

4.1. Oatp1d1 mutants lack functional protein and have lower *oatp1d1* transcriptional levels

We designed novel, custom-made Oatp1d1 antibodies and showed that Oatp1d1 localizes to the canalicular membranes of embryonic and adult hepatocytes. As expected, in mutant embryos and adults we observed an absence of the signal, confirming that they lack Oatp1d1 protein (Figure 14). Interestingly, the expression and localization of Oatp1d1 was also confirmed in the adult kidney in the membranes of glomerular podocytes (supplement), which is a novel finding as *oatp1d1* previously showed low expression at the transcript level in the kidney compared to expression in other tissues (Popovic et al., 2013). In summary, considering data on determining Oatp1d1 expression (Figure 15) and localization at the protein level, the obtained expression levels of *oatp1d1* gene were consistent with the data previously obtained at the transcriptional level (Popovic et al., 2013).

4.2. Molecular docking

Based on our molecular docking results and analysis of the reported structures of the OATP proteins and comparison with the obtained Oatp1d1 structure, we have confirmed that all substrates (LY, diclofenac and PFOS) bind to the same active site, so we have additionally confirmed in silico that they are transported by Oatp1d1. Futhermore, 17β-E2, PFOA and chlorpyrifos-methyl bind just above (or near) the signature motif of the OATP protein (Figure 56). It is hypothesised that by binding there, they block the binding of the HCO_3^-, which normally binds allosterically and causes a conformational narrowing of the active site, facilitating substrate release

Ocjena rada u tijeku

into the intracellular space. Since these compounds have been shown to be non-competitive inhibitors by Michaelis-Menten parameters, they bind to both the free protein and the protein-substrate complex. We can therefore assume that we still observe their affinity and binding to the active site of the protein. However, probably the more relevant interaction appears to be further away from the active, allosterically affecting the active site where the substrate is already bound, as we have described. In this way, the substrate remains "trapped" inside the protein and is not released into the cell. This observation is consistent with the kinetic parameters that characterise non-competitive inhibitors, where their presence reduces V_{max} without affecting K_m. On the other hand, non-competitive inhibitors such as clofibrate can only bind to the enzyme-substrate complex at a specific binding site. Their interaction with the protein leads to a reduction in both V_{max} and K_m. With clofibrate, we observed a binding mode to the Oatp1d1 protein that was completely different from that of all other inhibitors used in the docking study, which was perhaps to be expected as it is the only non-competitive inhibitor tested (Figure 57). Clofibrate is thought to block the entry of the substrate itself by binding to a different site away from the active site. This probably explains the observed reduction in both V_{max} and K_m.

4.3. The Oatp1d1 mutation alters the mutant phenotype

The first observation we made was the presence of particles in the perivitelline space between the chorion and the embryo (Figure 20). This phenotype was not detected in the WT siblings, suggesting a potential link between the loss of Oatp1d1 function and the accumulation of these particles. Furthermore, the particles in the Oatp1d1 mutant embryos either disintegrate over time or are absorbed by the embryos, as very few are left after 24 hpf. Importantly, since crossing of Oatp1d1 males with WT females results in "normal" embryos without these particles, the presence of these particles most probably depends exclusively on mutant mothers. Early developmental stages are predominantly regulated by maternal gene products, however, maternally controlled processes in vertebrates remain insufficiently characterized (Abrams & Mullins, 2009). It is known that perivitelline fluid (PVF) in zebrafish is formed during oocyte activation. The cortical response involves the rapid exocytosis of cortical granules located at the periphery of the oocyte. These granules release various macromolecules such as glycoproteins, mucopolysaccharides and lectins into the space between the vitelline membrane and the oocyte membrane. As a result, water penetrates the perivitelline space, leading to the expansion of the chorion and the formation of PVF

Ocjena rada u tijeku

(Abrams & Mullins, 2009; Fuentes & Fernández, 2010; Mei et al., 2009), which probably contains most of the proteins released by the cortical granules.

Furthermore, the yolk precursor protein, vitellogenin (Vtg), is in oviparous vertebrates produced by the liver of maturing females in response to 17β-E2, which is a strong uncompetitive inhibitor of Oatp1d1 (Popovic et al., 2014). Upon the uptake, Vtg is secreted into the bloodstream and then taken up by growing oocytes to be processed into a suite of yolk proteins that are stored in the ooplasm (Hiramatsu et al., 2005). In another study of *vtg2*-mutant, there were no differences in the number of eggs per spawn, compared to WT females. However, the fertilization rate, hatching rate, and overall survival of *vtg2*-mutant offspring were significantly different than in WT fish. The fertilization rate of eggs from *vtg2*-mutant females was substantially lower than those from WT eggs, and the authors also reported yolk leakage due to vitellin membrane disintegrity and abnormal cell division in mutants (Yilmaz et al., 2023). Vitellogenesis is a specific physiological response to estrogen or estrogenic chemicals. As a result, the mechanisms of vitellogenin (Vtg) production have been extensively studied as a model for steroid hormone action. Vtg naturally appears in the blood of maturing females but not in males or immature fish (Hiramatsu et al., 2005). Therefore, it would be interesting to examine whether there is an up- or downregulation of specific vitellogenins within the multiple Vtg systems, which includes five type I Vtgs, type II Vtgs, and type III Vtg. This is particularly relevant considering previous *in vitro* findings suggesting that Oatp1d1 plays an important role in the transport and balance of steroid hormones. Additionally, according to our observations and the insights available from other similar studies, it is important to emphasize that there are some other possible explanations for the observed phenotype: (i) there could be a leakage or abnormal processing of yolk content and Oatp1d1 potentially participates in the transport of molecules essential for yolk utilization, (ii) particles arise from abnormal secretion processes by the enveloping layer (EVL) due to impaired transporter activity, (iii) considering that mutants show pigment patterning defects, it can be hypothesized that some precursor molecules are mislocalized and pigment-related material is released into PVF space, (iv) some endogenous compounds, e.g., hormones, that are involved in regulation of normal early embryo development are not transported efficiently because of the lack of Oatp1d1 transporter or due to compensation mechanism of other transporters their transport is disturbed. It is also important to take into account that it is something that happens earlier in oocytes and it is

Ocjena rada u tijeku

result of Oatp1d1 mutation in adult females, because this phenotype is something we observed in unfertilized eggs, i.e., due to maternal transfer.

In our toxicity tests, Oatp1d1 mutants appeared more resilient to chemical exposure than WT embryos. One possible explanation was that particles present in mutants might absorb the test compounds, thereby reducing their effective concentration. Although we could not completely rule out this possibility, as no direct chemical analysis was performed, we compared exposures in dechorionated and non-dechorionated embryos and observed identical toxicity outcomes. These results suggest that particle absorption, if it occurred, did not significantly affect the exposure or alter the observed differences between mutant and WT embryos (Figure 38). Based on those data we decided to perform further exposure experiments without dechorionisation, as this process can potentially give false results if it is not performed completely without damaging the embryos. Furthermore, despite the particles in the perivitelline space, the mutant embryos developed normally, apart from the observed lack of yellow pigmentation. Pigment cells develop from a group of stem cells in the embryo called the neural crest cells. During early embryo development, neural crest precursor cells further segregate into neural elements, ectomesenchymal cells and pigment cells which is in parallel with lateral and anterior-posterior migration of neural crest-derived cells and formation of complex pigmentation pattern (Dorsky et al., 2000; García-Castro & Bronner-Fraser, 1999; Le Douarin & Kalcheim, 1999). Differentiation of neural cells, and melanophores, iridophores and xanthophores as pigment cells, is closely linked to the initiation of pteridine synthesis, which begins from GTP and is regulated by the activity of GTP cyclohydrolase I. In zebrafish embryos, *de novo* pteridine synthesis increases during the first 72 hours post-fertilization, leading to the production of H_4-biopterin. This molecule acts as a cofactor for neurotransmitter synthesis in neural cells and for tyrosine production in melanophores. Later, sepiapterin (6-lactoyl-7,8-dihydropterin) starts to accumulate as a yellow pigment in xanthophores, along with other pteridines like 7-oxobiopterin, isoxanthopterin, and 2,4,7-trioxopteridine. Sepiapterin is a key intermediate in the synthesis of 7-oxopteridines, a process that relies on enzymes from the xanthine oxidoreductase family (Ziegler, 2003). Within the pigment cells, pigments are located in specialized organelles such as melanosomes, which contain melanin (Birbeck, 1963; Charles & Ingram, 1959; Drochmans, 1960) and pterinosomes, which contain pteridines in xanthophores (Kamei-Takeuchi & Hama, 1971; Matsumoto, 1965). Pterinosomes, like melanosomes, are derived from the Golgi complex (Obika, 1993). They contain a species-

Ocjena rada u tijeku

specific set of pteridines that appear simultaneously with the differentiation of xanthophores (Hama, 1963; Matsumoto et al., 1960; Obika, 1963).

It is important to emphasise that the pigmentation pattern of embryos is indeed different from that of adults. In the first five days of embryonic development, a larval pigment pattern is formed. A distinctive early larval pattern of pigment cells is essentially complete by 5 dpf and remains unchanged until metamorphosis (Owen et al., 2020). Xanthophores are one of three types of pigment cells found in teleosts and their yellow color is due to pteridines packed into the pterinosomes, subcellular compartments (Guyader & Jesuthasan, 2002). By examining the observed lack in yellow pigmentation in more detail, we observed that the difference in fluorescence intensity of the embryo matrix, measured by spectrophotometry (from 6 hpf to 2 mpf), starts at 24 hpf. That corresponds to the period when the first pteridines are formed (Ziegler, 2003), and this difference becomes more pronounced as the embryos age (Figure 22C). It was previously shown that methylene blue specifically labels xanthophores in zebrafish embryos and this blue staining was seen to primarily localize into pterinosomes. Furthermore, mutant strains like *yobo* and *brie* with abnormal xanthophores did not have blue color of methylene blue localization in xanthophores. Possible explanation is, the color of methylene blue depends on the redox state of the environment which suggests that pterinosomes represent an oxidizing environment (Guyader & Jesuthasan, 2002). In the same paper authors proposed another easy method to visualize xanthophores by their autofluorescence, because most pteridines are fluorescent under UV illumination. We also observed that within a few seconds of exposure to UV light under the fluorescence microscope, xanthophores became fluorescent, and consequently in mutants we observed lack of signal. Unfortunately, we still do not know whether the lack of yellow pigmentation in the mutants is a consequence of abnormal xanthophore development, or perhaps a precursor in the pteridine biosynthetic pathway is not being transported due to the absence of the Oatp1d1-mediated transport. As already mentioned, the evaluation of the mutants according to morphological criteria is not suitable for answering the question of whether the absence of pigment cells, and xanthophores in particular, is caused by a failure of the survival mechanisms, the specification mechanisms or the pteridine pathway itself (Ziegler, 2003). The importance of pteridines lies in their involvement in numerous pathways, as pteridines are required in many organisms for a number of processes such as cell proliferation (He & Rosazza, 2003), immunity (Hamerlinck, 1999), neurotransmitter synthesis, and antioxidant metabolism (Thöny et al., 2000).

Ocjena rada u tijeku

Perturbations in the pigment pattern may therefore be useful for understanding fundamentally important biological processes. In addition, when analyzing the expression levels of *slc22* and *slc21* transporters reported in the Daniocell (online resource that presents single-cell gene expression data generated from the whole-animal wild-type (TL/AB) zebrafish embryos and larvae), it is interesting to note that *oat2a* is only expressed in pigment cells. In addition, Saunders et al. (2019) identified novel xanthophore markers within xanthophore cluster-specific expression, and *slc22a7* or *oat2a* are among them. However, by analyzing gene expression at developmental stages we found that *oat2a* is downregulated in Oatp1d1 embryos compared to WT embryos, which could be one explanation for the absence of yellow pigmentation in embryos. Human SLC22A7 is known as a facilitative transporter of cGMP and other guanine nucleotides (Cropp et al., 2008). In medaka and zebrafish mutations in *slc2a11b* gene show xanthophore pigmentation deficiency at the embryonic stage (T. Kimura et al., 2014). Another example, again in medaka, *slc2a15b* mutants show also xanthophore pigment deficiency in the embryonic stage (T. Kimura et al., 2014). This suggests that Slc proteins most likely transport the substrates for pteridines formation into the xanthophores. However, the specific role of Oat2a in pigment cell development of pigment cells is not well understood yet and should be further investigated.

It is also important to note that in previous studies aimed at understanding of pigment development in zebrafish, the authors not only investigated the expression of specific genes, but have also emphasized the role of thyroid hormones as important regulators of pigmentation patterns (Saunders et al., 2019). In general, it is known that two groups of the pigment cells respond to thyroid hormone in different ways. First, thyroid hormone regulates xanthophores to increase in number, promoting carotenoid-dependent repigmentation in xanthophores. Secondly, release of thyroid hormones at the same time limits the number of melanophores promoting terminal differentiation and proliferative arrest. To further investigate this, we exposed embryos to T3 and T4 hormones known to influence zebrafish development. Our data show that both thyroid hormones cause a visible lack of yellow pigments in 48 hpf old WT embryos and reduced fluorescence of the embryonic matrix in WT embryos (Figures 25 and 26). Since WT embryos exposed to thyroid hormones develop a similar phenotype to Oatp1d1 mutants in terms of pteridine content, the question arises whether there is a link between Oatp1d1, thyroid hormones and yellow pigments in zebrafish. Previous research has already shown that T3 acts as an inhibitor of the Oatp1d1 transporter in the cells, while T4 does not interact with it (Popovic et al., 2013). However,

Ocjena rada u tijeku

the exact mechanism by which thyroid hormones influence pigment cells during embryonic development remains unclear. Furthermore, it is known that thyroid hormones affect pigmentation differently in the larval stage and in adult zebrafish, respectively (Saunders et al., 2019).

In adults, contrary to embryos, both male and female mutants developed more intense pigmentation and appear darker, and these individuals are easily distinguishable from WT fish (Figure 24). Beginning around three weeks of age and over a period of a few weeks, zebrafish generate a robust adult stripe pattern of alternating dark blue stripes and golden interstripes (Frohnhöfer et al., 2013; Parichy et al., 2009). Three different pigment-producing cell types are involved in stripe pattern: melanocytes, containing black melanin; xanthophores containing yellow and orange carotenoids and pteridines; and iridescent iridophores, containing guanine crystals within reflective platelets (Hirata et al., 2003). The majority of adult xanthophores originate directly from embryonic/larval (EL) xanthophores, which first lose their pigmentation and later reacquire it during the late stages of adult pattern formation (McMenamin et al., 2014). For example, thyroid hormone (TH)–mediated regulation of multiple carotenoid pathway genes is essential for this re-pigmentation process in cryptic xanthophores (Saunders et al., 2019). More specifically, adult melanophores arise from transit-amplifying progenitor, but most adult xanthophores develop directly from embryonic/larval EL xanthophores, lose their pigment and regain the color again in adult pattern formation coinciding with rising (TH) levels. Pteridine pigments, carotenoid pigments, or a combination of both contribute to the yellow-orange pigmentation of xanthophores (Granneman et al., 2017; Hahn & Stegeman, 1994; Lister, 2019; Ziegler, 2003). It was assumed that TH mediates a transition from the pteridine-dependent pigmentation present at embryonic/larval stages to carotenoid dependent pigmentation in adults. For example, *scarb1* (*scavenger receptor class B, member 1*) mutants did not show carotenoid accumulation in adult pigment pattern formation, but at embryonical/larval stages mutants lacked xanthophore phenotype (they had yellow coloration). Another, opposite example is where mutants with colors deficiencies in embryonic/larval stages have normal coloration and pigmented adult xanthophores. Interestingly, our observations support the idea that pigment development in embryos, larvae, and adults differs both in biosynthetic pathways and regulatory mechanisms. While embryonic stages show a clear deficiency of yellow pigments in mutants, primarily due to impaired pteridine synthesis, we observed a stronger signal in those mutants during late larval development, around 2 months post-fertilization (mpf), suggesting a partial recovery approaching

Ocjena rada u tijeku

WT levels. In adults, this pattern is completely reversed: mutants exhibit an increased number of xanthophores when compared to WTs, which at this stage are largely dependent on carotenoids rather than pteridines. Unlike pteridines, carotenoids are not synthesized in vertebrates and fish acquire them from the diet. Once they are acquired from food, they are transported and deposited in lipid droplets in xanthophores (T. Kimura, 2021). Through the plasma membrane of xanthophores they are transported by lipoproteins, since they are highly hydrophobic (Toews et al., 2017). We have already mentioned *scarb1* which is one of the scavenger receptors which recognize these lipoproteins and facilitate the movement of carotenoids into xanthophores. Another gene involved in carotenoid transport and deposition i *plin6* (*peripilin 6*) which transports, concentrates carotenoids into lipid droplets in xanthophores and zebrafish *plin6* knockout mutants had reduces carotenoid concentration (Granneman et al., 2017). Next, except the transport, for cleavage of carotenoids, β-carotene oxygenases are shown to be responsible in vertebrates (*e.g.*, *bco1*) (T. Kimura, 2021). Saunders et al. (2019), showed that zebrafish orthologs *bco1* and *bco2* are expressed in xanthophores which suggests that they are related to the production of yellow pigmentation from dietary derived β-carotene (T. Kimura, 2021). Since we observed an increased number of xanthophores in adult fish, we can hypothesise that the transport of thyroid hormones may be disturbed, which in turn affects the regulation of xanthophores and their repigmentation. This would suggest that adult Oatp1d1 fish have an excess of thyroid hormones, similar to Oatp1d1 embryos, a finding consistent with our exposure experiments in which WT embryos exposed to excess T3 and T4 developed a phenotype similar to that of the mutants. Considering that adult pigmentation and its regulation are completely different from embryonic development, we also need to investigate the deposition of carotenoids and assess whether genes involved in carotenoid transport or metabolism show altered expression.

In conclusion, the first data obtained in this study on changes in pigmentation pattern in Oatp1d1 mutant embryos and adults point to a clear need for further investigation of physiological importance of Oatp1d1 membrane transporter. Importantly, general biological significance (both reproductive and ecological) of this phenotype in natural populations should be thoroughly investigated in follow up studies.

Except for the observed pigment changes, red spots (Figure 24) have been observed in adult fish, which appear between 9 and 12 months and occasionally disappear and reappear. It has already

Ocjena rada u tijeku

been noted that hypothyroidism can lead to erythema, which could be the case here. However, this phenomenon could also be an immune response. Interestingly, the appearance of the red spots coincides with an increase in the production of unfertilized and low-quality embryos. Although the observed red spots do not cause mortality in the fish, they clearly have an impact on overall fitness, as reproduction, which occurs in parallel with the appearance of red spots, is reduced along with embryo quality. Further microbiological analyses are required to determine the cause of the red spots.

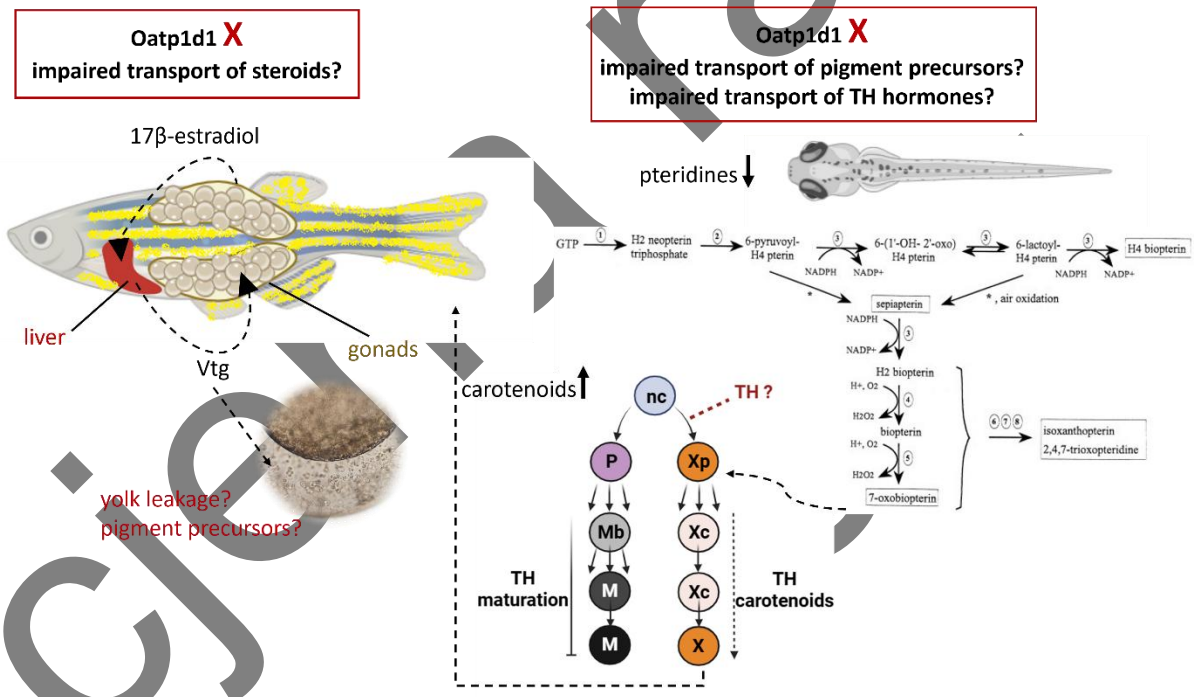

Figure 58. Possible roles of Oatp1d1 transporter in development of pigmentation in zebrafish adults and embryos as well as in the role of normal development of oocytes. Created in BioRender.

4.4. Exposure to model fluorescent substrates reveals reduced uptake and metabolism of compounds in Oatp1d1 mutant embryos

Ocjena rada

Our results indicate that Oatp1d1 embryos probably excrete lucifer yellow more slowly (Figure 27). Possible explanation for this is the reduced absorption of the compound, as they have already developed a mouth at the age of five days and a significant part of the absorption takes place via the mouth and then the intestine. Due to the absence of the Oatp1d1 transporter, LY may not be transported from the intestine to the rest of the body and excreted, but accumulates there instead, as shown by the stronger signal in the intestine. Unfortunately, due to the lack of pigments in the Oatp1d1 mutants and the overlapping fluorescence spectra of pteridines, xanthophores and lucifer yellow, we could not measure the fluorescence in the embryos. Instead, we tried to measure the extrusion of the compound into the surrounding medium. However, the results were not consistent, as data from only one experiment matched the previously observed imaging results (data not shown). The concentration of the excreted compound was very low, which made quantification with an adequate number of embryos difficult.

4.5. Role of Oatp1d1 in ADME – insights from exposure experiments with diclofenac and PFOS

As already emphasized, the presence of Oatp1d1 in the plasma membranes of hepatocytes is crucial for the biotransformation of harmful substances into less toxic metabolites and thus protects zebrafish during embryo development. However, it is well-known that hepatic metabolism can also result in production of metabolites that are more toxic than the original compound. Therefore, this crucial protective mechanism can be impaired, leading to enhancement of developmental deformities and toxicity. Consequently, Oatp1d1 transport activity could also have a dual role in embryonic development, both protective and potentially harmful, depending on the substrates involved (Figure 59). To further explore these opposing roles in zebrafish, we exposed both mutant and WT embryos to environmentally relevant model pollutants shown previously to be strong Oatp1d1 interactors.

Diclofenac. As shown by previous *in vitro* studies in our group, diclofenac was identified as a substrate for Oatp1d1 in HEK cells overexpressed with zebrafish Oatp1d1, and showed competitive inhibition with a K_i value of 0.23 (Popovic et al., 2014). Diclofenac undergoes phase I and phase II biotransformation in hepatocytes and the transport by Oatp1d1 is crucial for its metabolism and excretion in zebrafish. Metabolism of diclofenac leads to the formation of several

Ocjena rada
U tijeku

metabolites, including 4- and 5-hydroxy-diclofenac, diclofenac 1-O-acylglucuronide, diclofenac glutathione thioester, and a more toxic metabolite diclofenac methyl ester (Fu et al., 2020; Syed et al., 2016). Consequently, the formation of more toxic diclofenac metabolites suggests that the presence of Oatp1d1 in hepatocyte membranes may actually enhance the deleterious effects of diclofenac on developing embryos. Conversely, the absence of Oatp1d1 could make the embryos more resistant, in contrast to the protective role of Oatp1d1 in case of xenobiotics that are more toxic than original substances. A similar phenomenon has been reported, in which inhibition of the human organic cation transporter 1 (Oct1) leads to reduced uptake and metabolism of the drug in the liver, resulting in higher concentrations of tropisetron and potentially of ondansetron in the blood, increasing their therapeutic efficacy (Tzvetkov et al., 2012).

Differences between mutant and WT exposed embryos on the developmental level started showing around 3 dpf (2 dpe) with delayed hatching, occurrence of pericardial edemas and blood pooling in the heart area. All these effects indicate already observed nephrotoxicity of diclofenac (Hickey et al., 2001), as with all NSAIDs, diclofenac exerts its action via inhibition of prostaglandin synthesis by inhibiting cyclooxygenase-1 (COX-1) and cyclooxygenase-2 (COX-2) (Gan, 2010) and prostaglandins play an important role in renal functional development (Gleason, 1987).

As embryos develop further, characteristic muscle deformations were visible in diclofenac exposed embryos, especially at higher concentrations (≥20 μM). It is known that diclofenac induces malformations in muscle fiber alignment and disrupts actin organization during early embryogenesis, leading to deformations in spinal curvature. These deformations are most prominently visible at 3 days post-fertilization (48 dpe) (Chen et al., 2011). All observed effects of diclofenac exposure in Oatp1d1 mutant embryos were delayed and occurred at a lower frequency compared to WT embryos (Figure 31). We confirmed this hypothesis by injecting MO-ATG and chose muscle degradation as the endpoint because it is clearly visible. Phalloidin staining of muscle filaments confirmed the differences between WT and mutant embryos (Figures 37 and 38), with the Oatp1d1 mutants showing minimal effects of diclofenac exposure and almost no signs of muscle degradation. Finally, MO-ATG embryos exhibited an intermediate phenotype between mutant and WT embryos, suggesting that Oatp1d1 is essential for diclofenac transport into the liver and subsequent metabolism. Experiments with diclofenac exposure also revealed a possible indication of partial rescue (Figure 54), as injected Oatp1d1 embryos showed slight body

Ocjena rada u tijeku

curvature, haemorrhage and a generally poorer condition compared to Oatp1d1 mutants. However, we cannot be certain that a rescue of the mutant phenotype has occurred as these results were not consistent across all replicates. If the observed resistance is due not only to the absence of Oatp1d1 protein but also to compensatory mechanisms due to the loss of Oatp1d1 function, then injection of *oatp1d1* mRNA may not be sufficient to restore the phenotype, similar to what we observed in attempts to rescue pigmentation. Further studies should attempt to inject mRNA rescue constructs of other transporters which also showed down-regulation in Oatp1d1 mutants and are transporters of diclofenac. The same should be done in the case of the pigment phenotype, developing a construct to rescue *oat2a* expression.

We hypothesise that the lack of Oatp1d1 expression in hepatocyte membranes (in both embryos and adults) is likely responsible for these developmental outcomes (Vujica et al., 2024). Without efficient Oatp1d1-mediated transport of diclofenac into hepatocytes, the metabolism of the substance slows down, delaying the formation of potentially more toxic metabolites (Fu et al., 2020). Consequently, mutant embryos show a delayed and less pronounced toxic response to diclofenac.

In addition, diclofenac exposure induced significant changes in the gene expression patterns in 3 dpf embryos. A modest down-regulation of *oatp1d1* was observed, suggesting a limited feedback effect on the mutant gene. However, *oat1* and *oat3* showed upregulation in mutant embryos exposed to diclofenac, supporting our hypothesis of compensatory mechanisms triggered by the Oatp1d1 mutation. In contrast, *oat2a* and *oatp2b1* showed pronounced downregulation in the mutants, whereas they were only minimally reduced in embryos exposed to diclofenac. This indicates a reduced responsiveness of these genes to diclofenac and implies that they are not involved in compensating for the loss of Oatp1d1 function. (Figure 32). Importantly, data from interaction studies with environmental pollutants showed different patterns than for physiological compounds, such that Oatp1d1 and Oat1 did not overlap with environmental pollutants, while e.g., Oat3 was found to overlap with substrates such as PFOS and diclofenac (Dragojević et al., 2020). Considering these findings, it is possible to expect different and complex compensatory mechanisms in zebrafish with mutated and non-functional Oatp1d1 transporter, leading to complex phenotypic changes.

Ocjena rada u tijeku

In summary, exposure studies with WT and Oatp1d1 mutant embryos confirmed the dual role of Oatp1d1 in the absorption, distribution, metabolism and elimination (ADME) of diclofenac and possibly other compounds with metabolites that are more toxic than their parent molecules (Figure 59). Previous research on the effects of diclofenac in aquatic organisms such as zebrafish has documented developmental abnormalities, reproductive toxicity and endocrine disruption (Memmert et al., 2013; van den Brandhof & Montforts, 2010). Our results are consistent with these reports and show comparable adverse effects of diclofenac exposure (Figure 31.). We calculated an LC_{50} of 23.48 µM for diclofenac (Figure 30), which is consistent with the previously reported value of 26 µM (van den Brandhof & Montforts, 2010). However, in the Oatp1d1 mutants developed here, the LC_{50} shifted to 35.91 µM (Figure 30). This indicates that the mutants exhibit increased resistance to the toxicity of diclofenac, which is probably due to reduced Oatp1d1-mediated uptake of the substance into the embryonic tissue.

Consequently, considering the adverse developmental and physiological effects of diclofenac on zebrafish embryos and the disruption of gene expression that could alter enzyme activity and hormonal pathways, the environmental risks posed by diclofenac must be taken seriously. Although environmental concentrations of diclofenac in surface waters, ranging from nanograms to micrograms per liter (Kumar et al., 2010), are generally lower than the levels found to be harmful to zebrafish embryos in this study, they may still pose a biological risk, as the lipophilic nature of diclofenac (Log Kow = 4.02, EPI Suite) indicates a strong potential for bioaccumulation. Combined with its pseudo-persistent behaviour, diclofenac proves to be an important pollutant that requires closer monitoring and further research into its effects an aquatic organisms. Likewise, a deeper understanding of the exposure of scavengers to NSAIDs and a clearer insight into the mechanisms underlying NSAID toxicity are urgently needed. More knowledge is therefore important to accurately assess the current and potential future impact of NSAIDs on the environment and to find safer alternatives to diclofenac (Swan et al., 2006).

PFOS. Contamination with PFOS in soil and water sources has been well documented (Ahrens & Bundschuh, 2014; DeWitt et al., 2019; Giesy & Kannan, 2001; Z. Wang et al., 2017). PFOS can cause adverse effects in both aquatic and terrestrial organisms, including humans. Some of the reported effects of PFOS exposure are: hepatotoxicity, immunotoxicity, neurotoxicity, developmental delay, behavioral changes, reproductive toxicity, thyroid toxicity and impacts on

Ocjena rada u tijeku

microbiome (J. Chen et al., 2016; DeWitt et al., 2019; Du et al., 2013; Lai et al., 2018; Negri et al., 2017; Sunderland et al., 2019). Due to the unexpected reverse effects observed during diclofenac exposure, in which Oatp1d1 mutant embryos showed greater resistance than wild type, we wanted to test an additional substrate to further investigate this phenomenon. Exposure to PFOS was part of the phenotypic characterisation of the Oatp1d1 mutants, with modulation of toxicity helping to reveal the role of Oatp1d1 in PFOS transport. Important differences were found in the responses of the WT and Oatp1d1 mutant lines to a persistent and bioaccumulative PFAS compound that is of a significant environmental concern, which contributed to the discovery of the importance of the Oatp1d1 protein in PFOS metabolism.

Following exposure to PFOS, distinct differences in mortality rates between WT and Oatp1d1 mutant embryos were observed, highlighting the role of Oatp1d1-mediated transport in modulating sensitivity to this compound. The calculated LC_{50} values, 23.57 μM for WT and 16.71 μM for Oatp1d1 mutants (Figure 38), indicate that mutant embryos exhibit increased susceptibility to PFOS toxicity. These results suggest a potentially critical role for the Oatp1d1 transporter in mitigating PFOS-induced effects, likely through its involvement in detoxification pathways or regulation of PFOS bioavailability. This is in line with previous findings that highlighted the importance of membrane transporters in transport of PFOS (Dragojević et al., 2021; Popovic et al., 2014).

In addition to mortality, phenotypic changes were also observed in embryos exposed to PFOS. It is known that exposure to PFOS causes significant developmental abnormalities in zebrafish embryos, particularly affecting the swim bladder (Hagenaars et al., 2014). This organ is vital for buoyancy and balance and its impairment leads to severe physiological consequences (Mylroie et al., 2021). We observed that PFOS-exposed embryos exhibited reduced swim bladder size, resulting in reduced activity and abnormal positioning, effects that were exacerbated in Oatp1d1 mutants. Which was in accordance with previous results where PFOS was developmentally toxic in all windows of development, but the 97-121 hpf window was the most sensitive, thus the peak malformation frequency and maximum PFOS uptake resulted from exposure during this same window (Huang et al., 2010). The spectrum of PFOS-induced abnormalities, including swim bladder impairment, scoliosis and necrosis, particularly in mutant embryos, emphasizes the need

Ocjena rada u tijeku

for further research into the specific mechanisms by which PFOS disrupts developmental processes (Huang et al., 2010; Lau et al., 2007; S. Wang et al., 2017).

Except the genetic and morphological homology, zebrafish exhibit complex behavior that closely resemble those of mammals, making them a valuable model for studying neurological disorders through behavioral assays (Basnet et al., 2019; Norton, 2013). Measuring locomotor activity of zebrafish embryos is now widely used method for identification of behavioral disturbances caused by chemicals (Ulhaq et al., 2013). Changing of lighting conditions alters the locomotor activity of zebrafish embryos and they are less active during the light compared with the dark (Emran et al., 2008; Irons et al., 2010; MacPhail et al., 2009). Sudden transition to darkness triggers a rapid and pronounced increase in activity and deviations from this behavior are usually recorded after exposure to neurotoxicant (Ulhaq et al., 2013). To investigate whether the observed responses are associated with a locomotor deficit, swimming behavior was monitored at 120 h of exposure to tested samples. Oatp1d1 embryos exposed to PFOS exhibited a significant decrease of locomotor activity during dark phases (Figure 42) compared to WT embryos exposed to PFOS. During light periods there were no significant changes between WT and Oatp1d1 embryos, both exposed and nonexposed to PFOS. The first study to examine the behavioral effects of PFOS in larval zebrafish showed a higher rate of swimming of embryos after 4 days of exposure to 1 μM PFOS than was observed at 0, 0.5 or 2.0 μM (Huang et al., 2010). Authors also emphasize that they did not see a differential swim response between PFOS and control larvae following a sudden light-to dark transition which is not in accordance with results obtained in our study. We clearly see higher locomotor activity in WT embryos when transitioning to the dark phase of measurement period (Figure 42). The reason is probably that we used higher concentrations of PFOS, as we observed that exposed WT embryos clearly react, and the mutants do not, to mechanical and light stimuli.

In our next research phase, a detailed analysis of the changes in gene expression induced by PFOS exposure was performed, focusing on genes coding for other transporters to elucidate possible compensation mechanisms and genes involved in biotransformation processes. In contrast to the lack of changes in *oatp1d1* expression in mutant embryos, we observed the upregulation of *oatp1d1* in WT embryos after PFOS exposure (Figures 43 and 44) similar as in case of diclofenac (Figure 32). In addition, we observed significant modulations in the expression of another important transporter from the same Slc21 family, *oatp2b1* (Dragojević et al., 2021). PFOS

Ocjena rada u tijeku

exposure resulted in upregulation of *oatp2b1*, both in WT and mutant embryos, with the response being slightly more pronounced in Oatp1d1 mutant embryos (Figures 43 and 44). Therefore, Oatp2b1 may also play an important role in mediating the toxic effects of PFOS.

Our results also showed a significant modulation of the expression of several *cyp* genes, shown to play a crucial role in the oxidative metabolism of a variety of endogenous and exogenous compounds (Nawaji et al., 2020), suggesting that PFOS exposure can alter the metabolic capacity of zebrafish embryos. The low expression and weak inducibility of *cyp1a* was expected given the higher expression of *cyp3a*, which is more actively involved in detoxification processes during early zebrafish development. In contrast, *cyp1a* is more prominent in adult zebrafish (Verbueken et al., 2017). The upregulation of *cyp3a* in WT embryos after PFOS exposure indicates an adaptive response aimed at improving detoxification and metabolic processing of PFOS. In particular, the different expression patterns between WT and mutant embryos, with mutants showing a stronger upregulation of *cyp3a*, suggest possible compensatory mechanisms activated in response to PFOS-induced stress. These results are consistent with previous studies demonstrating the induction of cytochrome P450 enzymes in response to chemical stressors, which may enhance an organism's ability to metabolize and eliminate toxins (Stegeman & Hahn, 1994).

Similarly, glutathione S-transferase enzymes encoded by *gst* genes play a key role in detoxification by facilitating the conjugation of glutathione with various substrates and promoting their excretion (Glisic et al., 2015). PFOS exposure led to changes in the expression of the *gstp1-2* and *gstr1* genes. The observed down-regulation of these genes in both WT and mutant embryos indicates a reduced ability to detoxify reactive intermediates generated during PFOS metabolism. This reduced expression may contribute to increased oxidative stress and cell damage, as glutathione conjugation is essential for neutralizing reactive oxygen species and preventing oxidative damage (Hayes & Pulford, 1995). Our results support this, as the Oatp1d1 mutant embryos had higher levels of oxidative stress compared to WT embryos when exposed to DCFH-DA used for detection of ROS (Figure 50). PFOS exposure was shown to produce oxidative stress and induce apoptosis with involvement of caspases in primary cultured tilapia hepatocytes (C. Liu et al., 2007). suggesting that the loss of Oatp1d1 impairs the excretion of PFOS, leading to toxic accumulation in the bloodstream and resulting in severe developmental abnormalities. Here, we introduced MO-splice to determine whether the effects of increased oxidative stress are a consequence of the

Ocjena rada u tijeku

Oatp1d1 protein mutation. The results showed that WT embryos injected with MO-splice exhibit a phenotype closer to the mutants, thus higher levels of oxidative stress (Figure 52). However, this requires further investigation, considering the short time window during which the morpholino is active, (extremely active through 50 hpf), while the effects we are studying after PFOS exposure become more pronounced only after four days. What should be done next is to examine whether MO-splice causes gene expression changes in WT embryos during PFOS exposure that are similar to those observed in mutants, but at earlier developmental stages. Interestingly, when WT embryos were exposed together with 17β-E2 and PFOS, we observed a potential inhibition of the Oatp1d1 protein and consequently more pronounced effects of PFOS exposure in WT embryos.

We have also observed increased apoptosis in the mutant embryos exposed to PFOS after staining with AO (Figure 51). Maintaining a balance between cell proliferation and apoptosis is essential for normal embryonic development and can be disrupted by exposure to toxicants (Cole and Ross, 2001; Ahmadi et al., 2003). Increasing PFOS exposure significantly increased apoptosis in the brain, eye and tail region at 24 hpf embryos (Huang et al., 2010). Another study also found apoptosis occurred in the zebrafish tail and heart of embryos exposed to 5 mg/mL PFOS, both with AO staining and TUNEL and genes related to cell apoptosis such as p53 and Bax were both significantly up-regulated upon exposure to PFOS. Authors propose the mechanisms for zebrafish embryo and larval malformation might occur via activated p53 that triggers Bax transactivation leading to apoptosis (X. Shi et al., 2008).

PFOS exposure led to an upregulation of *hhex* and *pax8*, indicating a potential stimulatory effect of PFOS on early thyroid gland development in zebrafish embryos, although a direct link between the elevated expression of these genes and circulating thyroid hormone (TH) levels remains unclear (Shi et al., 2008). Our preliminary results (the experiment performed only once) showed decreased *pax8* levels in Oatp1d1 mutants when compared to WT embryos with and without PFOS exposure (Figure S8) WT embryos showed induction of *pax8* expression after three days of exposure to 30 µM PFOS. This is particularly interesting, as we also hypothesized that disrupted thyroid hormone levels might contribute to the mutant phenotype. *Pax8* is expressed up to 7 dpf and is generally required for the late differentiation of thyroid follicular cells (Wendl et al., 2002). It would be worthwhile to investigate whether the thyroid gland in Oatp1d1 mutant fish is properly

Ocjena rada u tijeku

developed, what causes the reduced *pax8* expression, and to directly measure thyroid hormone levels.

As previously shown, embryonic PFOS exposures impacted gene expressions and processes involved in adipogenesis and lipid homeostasis within the peroxisome proliferator-activated receptors (PPAR) signaling pathway (Sant et al., 2018). PPAR signaling stimulates processes such as glycolysis, adipogenesis and fatty acid metabolism and synthesis and it is a tissue specific signaling pathway. Unsaturated fatty acids, and to some extent saturated fatty acids, are ligands for PPARs stimulating processes as lipid catabolism or storage (Grygiel-Górniak, 2014; Varga et al., 2011). PFOS indeed impacted fatty acid concentration in exposed embryos (16 and 32 µM PFOS) in a dose dependent manner. Additionally, increased lipid droplets observed in 15 dpf larvae that had been previously exposed (1-5 dpf) suggests that early exposure alone is capable of increasing adipogenesis later in the larval stages (Sant et al., 2021).

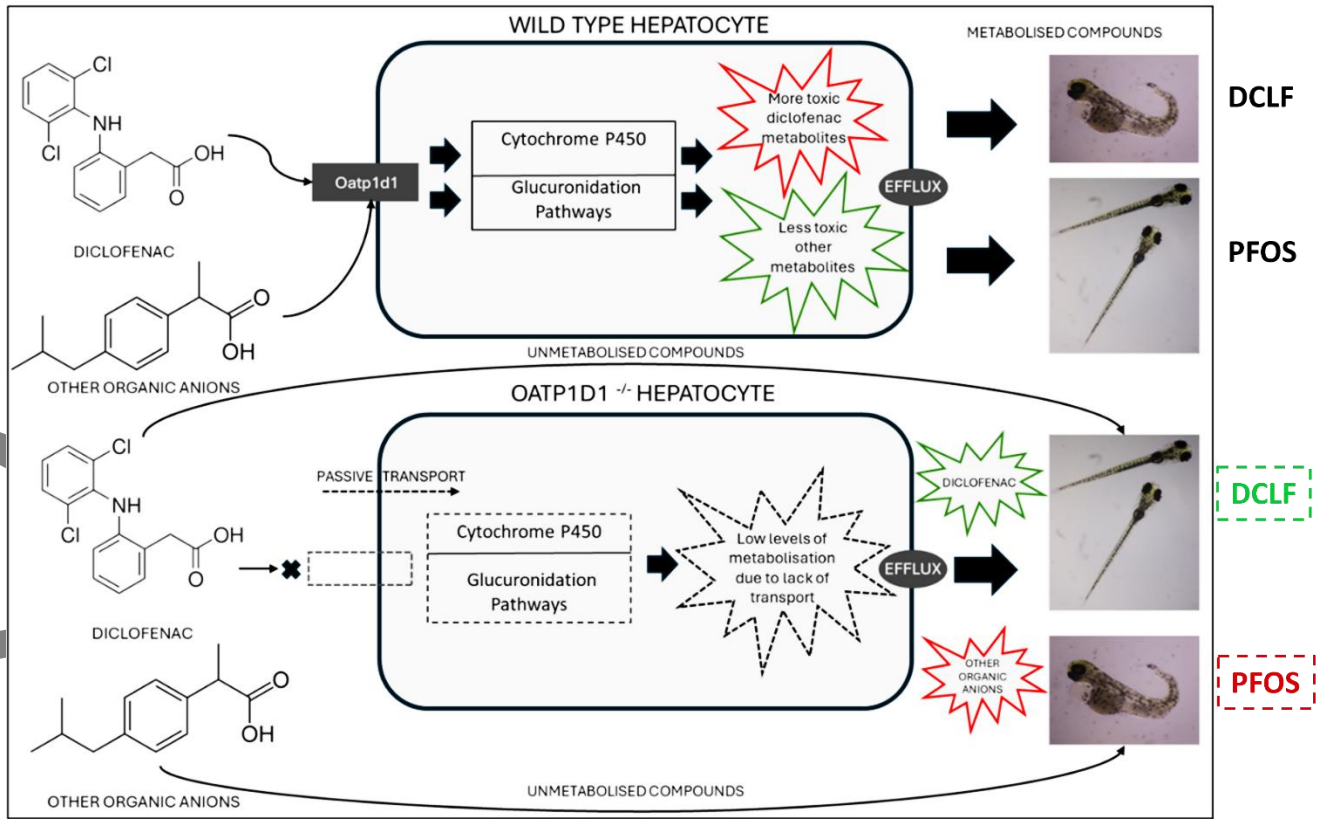

Figure 59. Schematic representation of the possible dual role of Oatp1d1 in the transport and metabolism of diclofenac and PFOS. Diclofenac is metabolised in zebrafish hepatocytes by phase I and II biotransformation enzymes into more toxic metabolites that have deleterious effects

on developing embryos. Consequently, the absence of Oatp1d1 in the mutant embryos leads to less toxic developmental effects. The other part of the Oatp1d1 duality is manifested upon exposure to PFOS, which yield less toxic metabolites and consequently have opposite effects on the development of WT and Oatp1d1 mutant embryos, making the mutant embryos more sensitive.

5. CONCLUSIONS

This study is the first *in vivo* investigation of the functional role of the Oatp1d1 transporter. Loss of function of Oatp1d1 in zebrafish knockouts resulted in significant changes in the bioaccumulation and subsequent toxicity of selected environmental pollutants previously identified as its substrates. These changes were associated with differential phenotypic, behavioural and toxicological responses compared to WT zebrafish, highlighting the physiological and ecotoxicological importance of Oatp1d1 in mediating the transport of xenobiotics. Summarizing the most important findings obtained in this study, we highlight the following:

- Oatp1d1 mutant line was created using CRISPR-Cas9 methodology and verified as a suitable research model to address potential (eco)toxicological role of zebrafish Oatp1d1 *in vivo*.
- Oatp1d1 mutation causes changes in pigmentation pattern in Oatp1d1 mutant embryos and adults, pointing to a clear need for further investigation of physiological importance of Oatp1d1 membrane transporter.
- Given the polyspecific nature of membrane transporters, several organic anion transporters that are likely candidates for compensatory mechanisms and may contribute to the observed mutant phenotypes were identified.
- A range of lethal and sublethal toxicological endpoints in exposures to diclofenac and PFOS were determined.
- WT embryos showed developmental delays and malformations such as spinal curvature, cardiac oedema, and blood pooling at higher diclofenac concentrations, while the Oatp1d1 mutant embryos showed marked resilience, with milder developmental defects and delayed toxic effects.

Ocjena rada u tijeku

- Observed developmental and physiological abnormalities in zebrafish embryos exposed to PFOS highlight the potential risks to aquatic organisms, particularly at higher trophic levels regarding the environmental persistence and bioaccumulative nature of PFOS.
- Observed gene expression changes of membrane transporter genes and I and II biotransformation enzymes between WT and mutant embryos, as well as determined oxidative stress and apoptosis levels, emphasize the complexity of PFOS toxicity and highlight the versatile nature of the organism's response to PFOS-induced stress.
- Two morpholino oligonucleotides, one targeting ATG translation initiation site, and the other targeting exon-intron boundary at the splice donor site, were successfully designed. Both morpholinos, ATG and splice, recapitulated the mutant phenotype upon exposure to diclofenac and PFOS, respectively. This effect was not observed in the mutant phenotype without exposure, which may suggest the involvement of a compensatory mechanism that cause pigment phenotype and particles in PVF in Oatpd1 mutants, which are not triggered by the morpholino itself.
- There is possible dual role of the Oatp1d1 transporter, depending on the toxicants to which embryos and fish are exposed. When a compound is metabolized, for example in the liver, it can produce more toxic metabolites. In the absence of Oatp1d1, these compounds are not transported to the liver for metabolism, making the mutants more resistant. On the other hand, if a compound is not efficiently metabolized, it remains in the organism and causes various toxic effects in the absence of the Oatp1d1 transporter, which would otherwise facilitate its more efficient excretion.

6. FUTURE PLANS

Based largely on data obtained during this study, our future work will include exposure of juvenile and adult zebrafish mutants to established Oatp1d1 substrates and inhibitors to further characterize their phenotypes and investigate stage-specific differences resulting from developmental maturation and sex differentiation between WT and mutant individuals. As shown, our results indicate the activation of compensatory mechanisms in response to the absence of the functional

Ocjena rada u tijeku

Oatp1d1 protein. Therefore, it is highly recommended to perform follow-up transcriptomic analyses to assess the expression of different uptake and efflux transporters as well as phase I and phase II biotransformation enzymes in embryos and subsequently in juvenile and adult fish. This is important not only to better understand the phenotype of the mutants, in particular the presence of particles in the perivitelline fluid (PVF) and impaired pigmentation, but also to elucidate the mechanisms underlying the effects observed after diclofenac and PFOS exposure. Likewise, it would be highly beneficial to expand the scope of this research towards behavioural assessments with adults to capture a broader range of neurological responses. To gain more detailed insights into tissue-specific toxic effects in the absence of Oatp1d1, we also plan to use transgenic zebrafish lines with fluorescently labelled liver and kidney tissue. To confirm observed effects of MO-ATG on diclofenac-caused phenotype of muscle degradation and effects of MO-splice on PFOS-caused ROS production we plan to perform co-injection of Oatp1d1 mRNA together with both morpholinos and to target other transporters which could cause mutant phenotype, e.g. *oat2a*. Finally, we plan to determine the accumulation of test compounds and their metabolites both in zebrafish embryos and in the surrounding medium by analytical chemical determinations using liquid chromatography-tandem mass spectrometry (LC-MS/MS).

Ocjena rada u tijeku

7. REFFERENCES

1. Abrams, E. W., & Mullins, M. C. (2009). Early zebrafish development: It's in the maternal genes. *Current Opinion in Genetics & Development*, *19*(4), 396–403. https://doi.org/10.1016/j.gde.2009.06.002
2. Abramson, J., Adler, J., Dunger, J., Evans, R., Green, T., Pritzel, A., Ronneberger, O., Willmore, L., Ballard, A. J., Bambrick, J., Bodenstein, S. W., Evans, D. A., Hung, C.-C., O'Neill, M., Reiman, D., Tunyasuvunakool, K., Wu, Z., Žemgulytė, A., Arvaniti, E., … Jumper, J. M. (2024). Accurate structure prediction of biomolecular interactions with AlphaFold 3. *Nature*, *630*(8016), 493–500. https://doi.org/10.1038/s41586-024-07487-w
3. Adeyemi, J. A., da Cunha Martins-Junior, A., & Barbosa, F. (2015). Teratogenicity, genotoxicity and oxidative stress in zebrafish embryos (*Danio rerio*) co-exposed to arsenic and atrazine. *Comparative Biochemistry and Physiology Part C: Toxicology & Pharmacology*, *172–173*, 7–12. https://doi.org/10.1016/j.cbpc.2015.04.001
4. Ahrens, L., & Bundschuh, M. (2014). Fate and effects of poly- and perfluoroalkyl substances in the aquatic environment: A review. *Environmental Toxicology and Chemistry*, *33*(9), 1921–1929. https://doi.org/10.1002/etc.2663

5. Aigouy, B., & Mirouse, V. (2013). ScientiFig: A tool to build publication-ready scientific figures. *Nature Methods*, *10*(11), 1048. https://doi.org/10.1038/nmeth.2692
6. Alam, K., Crowe, A., Wang, X., Zhang, P., Ding, K., Li, L., & Yue, W. (2018). Regulation of Organic Anion Transporting Polypeptides (OATP) 1B1- and OATP1B3-Mediated Transport: An Updated Review in the Context of OATP-Mediated Drug-Drug Interactions. *International Journal of Molecular Sciences*, *19*(3), 855. https://doi.org/10.3390/ijms19030855
7. Almazroo, O. A., Miah, M. K., & Venkataramanan, R. (2017). Drug Metabolism in the Liver. *Clinics in Liver Disease*, *21*(1), 1–20. https://doi.org/10.1016/j.cld.2016.08.001
8. Ankley, G. T., Cureton, P., Hoke, R. A., Houde, M., Kumar, A., Kurias, J., Lanno, R., McCarthy, C., Newsted, J., Salice, C. J., Sample, B. E., Sepúlveda, M. S., Steevens, J., & Valsecchi, S. (2021). Assessing the Ecological Risks of Per- and Polyfluoroalkyl Substances: Current State-of-the Science and a Proposed Path Forward. *Environmental Toxicology and Chemistry*, *40*(3), 564–605. https://doi.org/10.1002/etc.4869
9. Annilo, T., Chen, Z.-Q., Shulenin, S., Costantino, J., Thomas, L., Lou, H., Stefanov, S., & Dean, M. (2006). Evolution of the vertebrate ABC gene family: Analysis of gene birth and death. *Genomics*, *88*(1), 1–11. https://doi.org/10.1016/j.ygeno.2006.03.001
10. Asharani, P. V., Lian Wu, Y., Gong, Z., & Valiyaveettil, S. (2008). Toxicity of silver nanoparticles in zebrafish models. *Nanotechnology*, *19*(25), 255102. https://doi.org/10.1088/0957-4484/19/25/255102
11. Badagnani, I., Castro, R. A., Taylor, T. R., Brett, C. M., Huang, C. C., Stryke, D., Kawamoto, M., Johns, S. J., Ferrin, T. E., Carlson, E. J., Burchard, E. G., & Giacomini, K. M. (2006). Interaction of methotrexate with organic-anion transporting polypeptide 1A2 and its genetic variants. *The Journal of Pharmacology and Experimental Therapeutics*, *318*(2), 521–529. https://doi.org/10.1124/jpet.106.104364
12. Bai, X., Moraes ,Trevor F., & and Reithmeier, R. A. F. (2017). Structural biology of solute carrier (SLC) membrane transport proteins. *Molecular Membrane Biology*, *34*(1–2), 1–32. https://doi.org/10.1080/09687688.2018.1448123
13. Banerjee, N., Allen, C., & Bendayan, R. (2012). Differential role of organic anion-transporting polypeptides in estrone-3-sulphate uptake by breast epithelial cells and breast cancer cells. *The Journal of Pharmacology and Experimental Therapeutics*, *342*(2), 510–519. https://doi.org/10.1124/jpet.112.192344
14. Barron, M. G., Schultz, I. R., & Hayton, W. L. (1989). Presystemic branchial metabolism limits di-2-ethylhexyl phthalate accumulation in fish. *Toxicology and Applied Pharmacology*, *98*(1), 49–57. https://doi.org/10.1016/0041-008x(89)90133-6
15. Bartram, A., Winter, M., Huggett, D., McCormack, P., Constantine, L., Hetheridge, M., Hutchinson, T., Kinter, L., Ericson, J., Sumpter, J., & Owen, S. (2012). In vivo and in vitro liver and gill EROD activity in rainbow trout (Oncorhynchus mykiss) exposed to the beta-blocker propranolol. *Environmental Toxicology*, *27*(10), 573–582. https://doi.org/10.1002/tox.20684
16. Basnet, R. M., Zizioli, D., Taweedet, S., Finazzi, D., & Memo, M. (2019). Zebrafish Larvae as a Behavioral Model in Neuropharmacology. *Biomedicines*, *7*(1), 23. https://doi.org/10.3390/biomedicines7010023
17. Belanger, S. E., Rawlings, J. M., & Carr, G. J. (2013). Use of fish embryo toxicity tests for the prediction of acute fish toxicity to chemicals. *Environmental Toxicology and Chemistry*, *32*(8), 1768–1783. https://doi.org/10.1002/etc.2244
18. Benedetti, M. S., Whomsley, R., Poggesi, I., Cawello, W., Mathy, F.-X., Delporte, M.-L., Papeleu, P., & Watelet, J.-B. (2009). Drug metabolism and pharmacokinetics. *Drug Metabolism Reviews*, *41*(3), 344–390. https://doi.org/10.1080/10837450902891295

Osiena rada Utiieku

19. Benotti, M. J., Trenholm, R. A., Vanderford, B. J., Holady, J. C., Stanford, B. D., & Snyder, S. A. (2009). Pharmaceuticals and Endocrine Disrupting Compounds in U.S. Drinking Water. *Environmental Science & Technology*, *43*(3), 597–603. https://doi.org/10.1021/es801845a
20. Bernsel, A., Viklund, H., Hennerdal, A., & Elofsson, A. (2009). TOPCONS: Consensus prediction of membrane protein topology. *Nucleic Acids Research*, *37*(Web Server issue), W465-468. https://doi.org/10.1093/nar/gkp363
21. Berthelot, C., Brunet, F., Chalopin, D., Juanchich, A., Bernard, M., Noël, B., Bento, P., Da Silva, C., Labadie, K., Alberti, A., Aury, J.-M., Louis, A., Dehais, P., Bardou, P., Montfort, J., Klopp, C., Cabau, C., Gaspin, C., Thorgaard, G. H., … Guiguen, Y. (2014). The rainbow trout genome provides novel insights into evolution after whole-genome duplication in vertebrates. *Nature Communications*, *5*, 3657. https://doi.org/10.1038/ncomms4657
22. Bill, B. R., Petzold, A. M., Clark, K. J., Schimmenti, L. A., & Ekker, S. C. (2009). A Primer for Morpholino Use in Zebrafish. *Zebrafish*, *6*(1), 69–77. https://doi.org/10.1089/zeb.2008.0555
23. Birbeck, M. S. (1963). Electron microscopy of melanocytes: The fine structure of hair-bulb premelanosomes. *Annals of the New York Academy of Sciences*, *100*, 540–547. https://doi.org/10.1111/j.1749-6632.1963.tb42871.x
24. Buck, R. C., Franklin, J., Berger, U., Conder, J. M., Cousins, I. T., de Voogt, P., Jensen, A. A., Kannan, K., Mabury, S. A., & van Leeuwen, S. P. J. (2011). Perfluoroalkyl and polyfluoroalkyl substances in the environment: Terminology, classification, and origins. *Integrated Environmental Assessment and Management*, *7*(4), 513–541. https://doi.org/10.1002/ieam.258
25. Burnison, B. K., Meinelt, T., Playle, R., Pietrock, M., Wienke, A., & Steinberg, C. E. W. (2006). Cadmium accumulation in zebrafish (Danio rerio) eggs is modulated by dissolved organic matter (DOM). *Aquatic Toxicology (Amsterdam, Netherlands)*, *79*(2), 185–191. https://doi.org/10.1016/j.aquatox.2006.06.010
26. Cai, S.-Y., Wang, W., Soroka, C. J., Ballatori, N., & Boyer, J. L. (2002). An evolutionarily ancient Oatp: Insights into conserved functional domains of these proteins. *American Journal of Physiology. Gastrointestinal and Liver Physiology*, *282*(4), G702-710. https://doi.org/10.1152/ajpgi.00458.2001
27. Cameron, I. L., & Hunter, K. E. (1984). Regulation of the permeability of the medaka fish embryo chorion by exogeneous sodium and calcium ions. *The Journal of Experimental Zoology*, *231*(3), 447–454. https://doi.org/10.1002/jez.1402310320
28. Chabchoubi, I. B., Bouchhima, R. A., Louhichi, N., Baanannou, A., Masmoudi, S., & Hentati, O. (2023). Short-term effects of various non-steroidal anti-inflammatory drugs (NSAIDs) on *Danio rerio* embryos. *MethodsX*, *10*, 102215. https://doi.org/10.1016/j.mex.2023.102215
29. Chan, L. M. S., Lowes, S., & Hirst, B. H. (2004). The ABCs of drug transport in intestine and liver: Efflux proteins limiting drug absorption and bioavailability. *European Journal of Pharmaceutical Sciences: Official Journal of the European Federation for Pharmaceutical Sciences*, *21*(1), 25–51. https://doi.org/10.1016/j.ejps.2003.07.003
30. Charles, A., & Ingram, J. T. (1959). Electron microscope observations of the melanocyte of the human epidermis. *The Journal of Biophysical and Biochemical Cytology*, *6*(1), 41–44. https://doi.org/10.1083/jcb.6.1.41
31. Chen, J., Wang, X., Ge, X., Wang, D., Wang, T., Zhang, L., Tanguay, R. L., Simonich, M., Huang, C., & Dong, Q. (2016). Chronic perfluorooctanesulphonic acid (PFOS) exposure produces estrogenic effects in zebrafish. *Environmental Pollution (Barking, Essex: 1987)*, *218*, 702–708. https://doi.org/10.1016/j.envpol.2016.07.064
32. Chen, J., Xie, P., Li, L., & Xu, J. (2009). First identification of the hepatotoxic microcystins in the serum of a chronically exposed human population together with indication of hepatocellular

Ocjena rada utijeku

damage. *Toxicological Sciences: An Official Journal of the Society of Toxicology*, *108*(1), 81–89. https://doi.org/10.1093/toxsci/kfp009
33. Chen, J.-B., Gao, H.-W., Zhang, Y.-L., Zhang, Y., Zhou, X.-F., Li, C.-Q., & Gao, H.-P. (2014). Developmental Toxicity of Diclofenac and Elucidation of Gene Regulation in zebrafish (Danio rerio). *Scientific Reports*, *4*(1), 4841. https://doi.org/10.1038/srep04841
34. Chen, Y.-H., Chang, C.-Y., Wang, Y.-H., Wen, C.-C., Chen, Y.-C., Hu, S.-C., Yu, D.-S., & Chen, Y.-H. (2011). Embryonic exposure to diclofenac disturbs actin organization and leads to myofibril misalignment. *Birth Defects Research. Part B, Developmental and Reproductive Toxicology*, *92*(2), 139–147. https://doi.org/10.1002/bdrb.20292
35. Choi, T.-Y., Choi, T.-I., Lee, Y.-R., Choe, S.-K., & Kim, C.-H. (2021). Zebrafish as an animal model for biomedical research. *Experimental & Molecular Medicine*, *53*(3), 310–317. https://doi.org/10.1038/s12276-021-00571-5
36. Ciarimboli, G., Deuster, D., Knief, A., Sperling, M., Holtkamp, M., Edemir, B., Pavenstädt, H., Lanvers-Kaminsky, C., am Zehnhoff-Dinnesen, A., Schinkel, A. H., Koepsell, H., Jürgens, H., & Schlatter, E. (2010). Organic cation transporter 2 mediates cisplatin-induced oto- and nephrotoxicity and is a target for protective interventions. *The American Journal of Pathology*, *176*(3), 1169–1180. https://doi.org/10.2353/ajpath.2010.090610
37. Ciută, A.-D., Nosol, K., Kowal, J., Mukherjee, S., Ramírez, A. S., Stieger, B., Kossiakoff, A. A., & Locher, K. P. (2023). Structure of human drug transporters OATP1B1 and OATP1B3. *Nature Communications*, *14*(1), 5774. https://doi.org/10.1038/s41467-023-41552-8
38. Colas, C., Ung, P. M.-U., & Schlessinger, A. (2016). SLC transporters: Structure, function, and drug discovery. *MedChemComm*, *7*(6), 1069–1081. https://doi.org/10.1039/C6MD00005C
39. Conder, J. M., Hoke, R. A., De Wolf, W., Russell, M. H., & Buck, R. C. (2008). Are PFCAs bioaccumulative? A critical review and comparison with regulatory criteria and persistent lipophilic compounds. *Environmental Science & Technology*, *42*(4), 995–1003. https://doi.org/10.1021/es070895g
40. Consoer, D. M., Hoffman, A. D., Fitzsimmons, P. N., Kosian, P. A., & Nichols, J. W. (2016). Toxicokinetics of perfluorooctane sulfonate in rainbow trout (Oncorhynchus mykiss). *Environmental Toxicology and Chemistry*, *35*(3), 717–727. https://doi.org/10.1002/etc.3230
41. Couto, N., Newton, J. R. A., Russo, C., Karunakaran, E., Achour, B., Al-Majdoub, Z. M., Sidaway, J., Rostami-Hodjegan, A., Clench, M. R., & Barber, J. (2021). Label-Free Quantitative Proteomics and Substrate-Based Mass Spectrometry Imaging of Xenobiotic Metabolizing Enzymes in Ex Vivo Human Skin and a Human Living Skin Equivalent Model. *Drug Metabolism and Disposition*, *49*(1), 39–52. https://doi.org/10.1124/dmd.120.000168
42. Crnčević, D., Krce, L., Brkljača, Z., Cvitković, M., Brčić, S. B., Čož-Rakovac, R., Odžak, R., & Šprung, M. (2025). A dual antibacterial action of soft quaternary ammonium compounds: Bacteriostatic effects, membrane integrity, and reduced in vitro and in vivo toxicity. *RSC Advances*, *15*(2), 1490–1506. https://doi.org/10.1039/D4RA07975B
43. Cropp, C. D., Komori, T., Shima, J. E., Urban, T. J., Yee, S. W., More, S. S., & Giacomini, K. M. (2008). Organic anion transporter 2 (SLC22A7) is a facilitative transporter of cGMP. *Molecular Pharmacology*, *73*(4), 1151–1158. https://doi.org/10.1124/mol.107.043117
44. De la Paz, J. F., Anguita-Salinas, C., Díaz-Celis, C., Chávez, F. P., & Allende, M. L. (2020). The Zebrafish Perivitelline Fluid Provides Maternally-Inherited Defensive Immunity. *Biomolecules*, *10*(9), 1274. https://doi.org/10.3390/biom10091274
45. Dean, M., Rzhetsky, A., & Allikmets, R. (2001). The Human ATP-Binding Cassette (ABC) Transporter Superfamily. *Genome Research*, *11*(7), 1156–1166. https://doi.org/10.1101/gr.184901
46. Deeks, E. D. (2017). Lesinurad: A Review in Hyperuricaemia of Gout. *Drugs & Aging*, *34*(5), 401–410. https://doi.org/10.1007/s40266-017-0461-y

Osijek Univerzitet

47. Devlin, R. H., & Nagahama, Y. (2002). Sex determination and sex differentiation in fish: An overview of genetic, physiological, and environmental influences. *Aquaculture*, *208*(3), 191–364. https://doi.org/10.1016/S0044-8486(02)00057-1
48. DeWitt, J. C., Blossom, S. J., & Schaider, L. A. (2019). Exposure to per-fluoroalkyl and polyfluoroalkyl substances leads to immunotoxicity: Epidemiological and toxicological evidence. *Journal of Exposure Science & Environmental Epidemiology*, *29*(2), 148–156. https://doi.org/10.1038/s41370-018-0097-y
49. Diniz, M. S., Salgado, R., Pereira, V. J., Carvalho, G., Oehmen, A., Reis, M. A. M., & Noronha, J. P. (2015). Ecotoxicity of ketoprofen, diclofenac, atenolol and their photolysis byproducts in zebrafish (*Danio rerio*). *Science of The Total Environment*, *505*, 282–289. https://doi.org/10.1016/j.scitotenv.2014.09.103
50. Domingo, J. L., & Nadal, M. (2019). Human exposure to per- and polyfluoroalkyl substances (PFAS) through drinking water: A review of the recent scientific literature. *Environmental Research*, *177*, 108648. https://doi.org/10.1016/j.envres.2019.108648
51. Dorsky, R. I., Moon, R. T., & Raible, D. W. (2000). Environmental signals and cell fate specification in premigratory neural crest. *BioEssays: News and Reviews in Molecular, Cellular and Developmental Biology*, *22*(8), 708–716. https://doi.org/10.1002/1521-1878(200008)22:8<708::AID-BIES4>3.0.CO;2-N
52. Dragojević, J., Marakovic, N., Popović, M., & Smital, T. (2021). Zebrafish (Danio rerio) Oatp2b1 as a functional ortholog of the human OATP2B1 transporter. *Fish Physiology and Biochemistry*, *47*(6), 1837–1849. https://doi.org/10.1007/s10695-021-01015-7
53. Dragojević, J., Marić, P., Lončar, J., Popović, M., Mihaljević, I., & Smital, T. (2020). Environmental contaminants modulate transport activity of zebrafish organic anion transporters Oat1 and Oat3. *Comparative Biochemistry and Physiology Part C: Toxicology & Pharmacology*, *231*, 108742. https://doi.org/10.1016/j.cbpc.2020.108742
54. Drew, D., & Boudker, O. (2016). Shared Molecular Mechanisms of Membrane Transporters. *Annual Review of Biochemistry*, *85*, 543–572. https://doi.org/10.1146/annurev-biochem-060815-014520
55. Drochmans, P. (1960). Electron microscope studies of epidermal melanocytes, and the fine structure of melanin granules. *The Journal of Biophysical and Biochemical Cytology*, *8*(1), 165–180. https://doi.org/10.1083/jcb.8.1.165
56. Drozdzik, M., Czekawy, I., Oswald, S., & Drozdzik, A. (2020). Intestinal drug transporters in pathological states: An overview. *Pharmacological Reports*, *72*(5), 1173–1194. https://doi.org/10.1007/s43440-020-00139-6
57. Drozdzik, M., Gröer, C., Penski, J., Lapczuk, J., Ostrowski, M., Lai, Y., Prasad, B., Unadkat, J. D., Siegmund, W., & Oswald, S. (2014). Protein abundance of clinically relevant multidrug transporters along the entire length of the human intestine. *Molecular Pharmaceutics*, *11*(10), 3547–3555. https://doi.org/10.1021/mp500330y
58. Du, G., Hu, J., Huang, H., Qin, Y., Han, X., Wu, D., Song, L., Xia, Y., & Wang, X. (2013). Perfluorooctane sulfonate (PFOS) affects hormone receptor activity, steroidogenesis, and expression of endocrine-related genes in vitro and in vivo. *Environmental Toxicology and Chemistry*, *32*(2), 353–360. https://doi.org/10.1002/etc.2034
59. Eimon, P. M. (2014). Studying Apoptosis in the Zebrafish. In *Methods in Enzymology* (Vol. 544, pp. 395–431). Elsevier. https://doi.org/10.1016/B978-0-12-417158-9.00016-9
60. El-Gebali, S., Bentz, S., Hediger, M. A., & Anderle, P. (2013). Solute carriers (SLCs) in cancer. *Molecular Aspects of Medicine*, *34*(2–3), 719–734. https://doi.org/10.1016/j.mam.2012.12.007

Osijek rada u tijeku

61. Emran, F., Rihel, J., & Dowling, J. E. (2008). A behavioral assay to measure responsiveness of zebrafish to changes in light intensities. *Journal of Visualized Experiments: JoVE*, *20*, 923. https://doi.org/10.3791/923
62. Engeszer, R. E., Ryan, M. J., & Parichy, D. M. (2004). Learned social preference in zebrafish. *Current Biology: CB*, *14*(10), 881–884. https://doi.org/10.1016/j.cub.2004.04.042
63. Escapa, C., Torres, T., Neuparth, T., Coimbra, R. N., García, A. I., Santos, M. M., & Otero, M. (2018). Zebrafish embryo bioassays for a comprehensive evaluation of microalgae efficiency in the removal of diclofenac from water. *The Science of the Total Environment*, *640–641*, 1024–1033. https://doi.org/10.1016/j.scitotenv.2018.05.353
64. Estudante, M., Morais, J. G., Soveral, G., & Benet, L. Z. (2013). Intestinal drug transporters: An overview. *Advanced Drug Delivery Reviews*, *65*(10), 1340–1356. https://doi.org/10.1016/j.addr.2012.09.042
65. Evans, D. H., Piermarini, P. M., & Choe, K. P. (2005). The multifunctional fish gill: Dominant site of gas exchange, osmoregulation, acid-base regulation, and excretion of nitrogenous waste. *Physiological Reviews*, *85*(1), 97–177. https://doi.org/10.1152/physrev.00050.2003
66. Evans, R., O'Neill, M., Pritzel, A., Antropova, N., Senior, A., Green, T., Žídek, A., Bates, R., Blackwell, S., Yim, J., Ronneberger, O., Bodenstein, S., Zielinski, M., Bridgland, A., Potapenko, A., Cowie, A., Tunyasuvunakool, K., Jain, R., Clancy, E., … Hassabis, D. (2022). *Protein complex prediction with AlphaFold-Multimer* (p. 2021.10.04.463034). bioRxiv. https://doi.org/10.1101/2021.10.04.463034
67. Ferguson, J. L., & Shive, H. R. (2019). Sequential Immunofluorescence and Immunohistochemistry on Cryosectioned Zebrafish Embryos. *Journal of Visualized Experiments : JoVE*, *147*, 10.3791/59344. https://doi.org/10.3791/59344
68. Ferrada, E., & Superti-Furga, G. (2022). A structure and evolutionary-based classification of solute carriers. *iScience*, *25*(10), 105096. https://doi.org/10.1016/j.isci.2022.105096
69. Fischer, A., Hoeger, S. J., Stemmer, K., Feurstein, D. J., Knobeloch, D., Nussler, A., & Dietrich, D. R. (2010). The role of organic anion transporting polypeptides (OATPs/SLCOs) in the toxicity of different microcystin congeners in vitro: A comparison of primary human hepatocytes and OATP-transfected HEK293 cells. *Toxicology and Applied Pharmacology*, *245*(1), 9–20. https://doi.org/10.1016/j.taap.2010.02.006
70. Fraher, D., Sanigorski, A., Mellett, N. A., Meikle, P. J., Sinclair, A. J., & Gibert, Y. (2016). Zebrafish Embryonic Lipidomic Analysis Reveals that the Yolk Cell Is Metabolically Active in Processing Lipid. *Cell Reports*, *14*(6), 1317–1329. https://doi.org/10.1016/j.celrep.2016.01.016
71. Frank, N. Y., Pendse, S. S., Lapchak, P. H., Margaryan, A., Shlain, D., Doeing, C., Sayegh, M. H., & Frank, M. H. (2003). Regulation of progenitor cell fusion by ABCB5 P-glycoprotein, a novel human ATP-binding cassette transporter. *The Journal of Biological Chemistry*, *278*(47), 47156–47165. https://doi.org/10.1074/jbc.M308700200
72. Frohnhöfer, H. G., Krauss, J., Maischein, H.-M., & Nüsslein-Volhard, C. (2013). Iridophores and their interactions with other chromatophores are required for stripe formation in zebrafish. *Development (Cambridge, England)*, *140*(14), 2997–3007. https://doi.org/10.1242/dev.096719
73. Froschauer, A., Braasch, I., & Volff, J.-N. (2006). Fish Genomes, Comparative Genomics and Vertebrate Evolution. *Current Genomics*, *7*(1), 43–57. https://doi.org/10.2174/138920206776389766
74. Fu, Q., Fedrizzi, D., Kosfeld, V., Schlechtriem, C., Ganz, V., Derrer, S., Rentsch, D., & Hollender, J. (2020). Biotransformation Changes Bioaccumulation and Toxicity of Diclofenac in Aquatic Organisms. *Environmental Science & Technology*, *54*(7), 4400–4408. https://doi.org/10.1021/acs.est.9b07127

Ocjena rada Ujileku

75. Fujiwara, K., Adachi, H., Nishio, T., Unno, M., Tokui, T., Okabe, M., Onogawa, T., Suzuki, T., Asano, N., Tanemoto, M., Seki, M., Shiiba, K., Suzuki, M., Kondo, Y., Nunoki, K., Shimosegawa, T., Iinuma, K., Ito, S., Matsuno, S., & Abe, T. (2001). Identification of thyroid hormone transporters in humans: Different molecules are involved in a tissue-specific manner. *Endocrinology*, *142*(5), 2005–2012. https://doi.org/10.1210/endo.142.5.8115
76. Gan, T. J. (2010). Diclofenac: An update on its mechanism of action and safety profile. *Current Medical Research and Opinion*, *26*(7), 1715–1731. https://doi.org/10.1185/03007995.2010.486301
77. Gao, B., Hagenbuch, B., Kullak-Ublick, G. A., Benke, D., Aguzzi, A., & Meier, P. J. (2000). Organic anion-transporting polypeptides mediate transport of opioid peptides across blood-brain barrier. *The Journal of Pharmacology and Experimental Therapeutics*, *294*(1), 73–79.
78. Gao, B., Huber, R. D., Wenzel, A., Vavricka, S. R., Ismair, M. G., Remé, C., & Meier, P. J. (2005). Localization of organic anion transporting polypeptides in the rat and human ciliary body epithelium. *Experimental Eye Research*, *80*(1), 61–72. https://doi.org/10.1016/j.exer.2004.08.013
79. Gao, B., Vavricka, S. R., Meier, P. J., & Stieger, B. (2015). Differential cellular expression of organic anion transporting peptides OATP1A2 and OATP2B1 in the human retina and brain: Implications for carrier-mediated transport of neuropeptides and neurosteriods in the CNS. *Pflugers Archiv: European Journal of Physiology*, *467*(7), 1481–1493. https://doi.org/10.1007/s00424-014-1596-x
80. García-Castro, M., & Bronner-Fraser, M. (1999). Induction and differentiation of the neural crest. *Current Opinion in Cell Biology*, *11*(6), 695–698. https://doi.org/10.1016/s0955-0674(99)00038-1
81. Garibsingh, R.-A. A., & Schlessinger, A. (2019). Advances and Challenges in Rational Drug Design for SLCs. *Trends in Pharmacological Sciences*, *40*(10), 790–800. https://doi.org/10.1016/j.tips.2019.08.006
82. Giesy, J. P., & Kannan, K. (2001). Global Distribution of Perfluorooctane Sulfonate in Wildlife. *Environmental Science & Technology*, *35*(7), 1339–1342. https://doi.org/10.1021/es001834k
83. Gleason, C. A. (1987). Prostaglandins and the developing kidney. *Seminars in Perinatology*, *11*(1), 12–21.
84. Glisic, B., Mihaljevic, I., Popovic, M., Zaja, R., Loncar, J., Fent, K., Kovacevic, R., & Smital, T. (2015). Characterization of glutathione-S-transferases in zebrafish (Danio rerio). *Aquatic Toxicology (Amsterdam, Netherlands)*, *158*, 50–62. https://doi.org/10.1016/j.aquatox.2014.10.013
85. Goldstone, J. V., Hamdoun, A., Cole, B. J., Howard-Ashby, M., Nebert, D. W., Scally, M., Dean, M., Epel, D., Hahn, M. E., & Stegeman, J. J. (2006). The chemical defensome: Environmental sensing and response genes in the *Strongylocentrotus purpuratus* genome. *Developmental Biology*, *300*(1), 366–384. https://doi.org/10.1016/j.ydbio.2006.08.066
86. Gould, S. B. (2018). Membranes and evolution. *Current Biology*, *28*(8), R381–R385. https://doi.org/10.1016/j.cub.2018.01.086
87. Granneman, J. G., Kimler, V. A., Zhang, H., Ye, X., Luo, X., Postlethwait, J. H., & Thummel, R. (2017). Lipid droplet biology and evolution illuminated by the characterization of a novel perilipin in teleost fish. *eLife*, *6*, e21771. https://doi.org/10.7554/eLife.21771
88. Grunwald, D. J., & Eisen, J. S. (2002). Headwaters of the zebrafish—Emergence of a new model vertebrate. *Nature Reviews. Genetics*, *3*(9), 717–724. https://doi.org/10.1038/nrg892
89. Grygiel-Górniak, B. (2014). Peroxisome proliferator-activated receptors and their ligands: Nutritional and clinical implications - a review. *Nutrition Journal*, *13*(1), 17. https://doi.org/10.1186/1475-2891-13-17
90. Guarin, M., Ny, A., De Croze, N., Maes, J., Léonard, M., Annaert, P., & de Witte, P. A. M. (2021). Pharmacokinetics in Zebrafish Embryos (ZFE) Following Immersion and Intrayolk Administration: A Fluorescence-Based Analysis. *Pharmaceuticals (Basel, Switzerland)*, *14*(6), 576. https://doi.org/10.3390/ph14060576

91. Guyader, S. L., & Jesuthasan, S. (2002). Analysis of Xanthophore and Pterinosome Biogenesis in Zebrafish Using Methylene Blue and Pteridine Autofluorescence. *Pigment Cell Research*, *15*(1), 27–31. https://doi.org/10.1034/j.1600-0749.2002.00045.x
92. Haberkorn, B., Oswald, S., Kehl, N., Gessner, A., Taudte, R. V., Dobert, J. P., Zunke, F., Fromm, M. F., & König, J. (2022). Cancer-type organic anion transporting polypeptide 1B3 (Ct-OATP1B3) is localized in lysosomes and mediates resistance against kinase inhibitors. *Molecular Pharmacology*, *102*(6), MOLPHARM-AR-2022-000539. https://doi.org/10.1124/molpharm.122.000539
93. Hagenaars, A., Stinckens, E., Vergauwen, L., Bervoets, L., & Knapen, D. (2014). PFOS affects posterior swim bladder chamber inflation and swimming performance of zebrafish larvae. *Aquatic Toxicology (Amsterdam, Netherlands)*, *157*, 225–235. https://doi.org/10.1016/j.aquatox.2014.10.017
94. Hagenbuch, B., & Gui, C. (2008). Xenobiotic transporters of the human organic anion transporting polypeptides (OATP) family. *Xenobiotica*, *38*(7–8), 778–801. https://doi.org/10.1080/00498250801986951
95. Hagenbuch, B., & Meier, P. J. (2004). Organic anion transporting polypeptides of the OATP/SLC21 family: Phylogenetic classification as OATP/SLCO superfamily, new nomenclature and molecular/functional properties. *Pflügers Archiv*, *447*(5), 653–665. https://doi.org/10.1007/s00424-003-1168-y
96. Hagenbuch, B., & Stieger, B. (2013). The SLCO (former SLC21) superfamily of transporters. *Molecular Aspects of Medicine*, *34*(2–3), 396–412. https://doi.org/10.1016/j.mam.2012.10.009
97. Hagenbuch, B., Stieger, B., & Locher, K. P. (2025). Organic anion transporting polypeptides: Pharmacology, toxicology, structure, and transport mechanisms. *Pharmacological Reviews*, *77*(2), 100023. https://doi.org/10.1016/j.pharmr.2024.100023
98. Hahn, M. E., & Stegeman, J. J. (1994). Regulation of Cytochrome P4501A1 in Teleosts: Sustained Induction of CYP1A1 mRNA, Protein, and Catalytic Activity by 2,3,7,8-Tetrachlorodibenzofuran in the Marine Fish *Stenotomus chrysops*. *Toxicology and Applied Pharmacology*, *127*(2), 187–198. https://doi.org/10.1006/taap.1994.1153
99. Halpern, M. E., Rhee, J., Goll, M. G., Akitake, C. M., Parsons, M., & Leach, S. D. (2008). Gal4/UAS transgenic tools and their application to zebrafish. *Zebrafish*, *5*(2), 97–110. https://doi.org/10.1089/zeb.2008.0530
100. Hama, T. (1963). The relation between the chromatophores and pterin compounds. *Annals of the New York Academy of Sciences*, *100*, 977–986.
101. Hamerlinck, F. F. (1999). Neopterin: A review. *Experimental Dermatology*, *8*(3), 167–176. https://doi.org/10.1111/j.1600-0625.1999.tb00367.x
102. Hänggi, E., Grundschober, A. F., Leuthold, S., Meier, P. J., & St-Pierre, M. V. (2006). Functional analysis of the extracellular cysteine residues in the human organic anion transporting polypeptide, OATP2B1. *Molecular Pharmacology*, *70*(3), 806–817. https://doi.org/10.1124/mol.105.019547
103. Hayes, J. D., & Pulford, D. J. (1995). The glutathione S-transferase supergene family: Regulation of GST and the contribution of the isoenzymes to cancer chemoprotection and drug resistance. *Critical Reviews in Biochemistry and Molecular Biology*, *30*(6), 445–600. https://doi.org/10.3109/10409239509083491
104. He, A., & Rosazza, J. P. N. (2003). GTP Cyclohydrolase I: Purification, Characterization, and Effects of Inhibition on Nitric Oxide Synthase in Nocardia Species. *Applied and Environmental Microbiology*, *69*(12), 7507–7513. https://doi.org/10.1128/AEM.69.12.7507-7513.2003

Osijek rada Utjeku

105. Hediger, M. A., Clémençon, B., Burrier, R. E., & Bruford, E. A. (2013). The ABCs of membrane transporters in health and disease (SLC series): Introduction. *Molecular Aspects of Medicine*, *34*(2–3), 95–107. https://doi.org/10.1016/j.mam.2012.12.009
106. Hema, T., Poopal, R.-K., Ramesh, M., Ren, Z., & Li, B. (2023). Developmental toxicity of the emerging contaminant cyclophosphamide and the integrated biomarker response (IBRv2) in zebrafish. *Environmental Science: Processes & Impacts*, *25*(8), 1391–1406. https://doi.org/10.1039/D3EM00186E
107. Hickey, E. J., Raje, R. R., Reid, V. E., Gross, S. M., & Ray, S. D. (2001). Diclofenac induced in vivo nephrotoxicity may involve oxidative stress-mediated massive genomic DNA fragmentation and apoptotic cell death. *Free Radical Biology & Medicine*, *31*(2), 139–152. https://doi.org/10.1016/s0891-5849(01)00560-3
108. Hill, R. L., & Janz, D. M. (2003). Developmental estrogenic exposure in zebrafish (Danio rerio): I. Effects on sex ratio and breeding success. *Aquatic Toxicology (Amsterdam, Netherlands)*, *63*(4), 417–429. https://doi.org/10.1016/s0166-445x(02)00207-2
109. Hiramatsu, N., Cheek, A. O., Sullivan, C. V., Matsubara, T., & Hara, A. (2005). Chapter 16 Vitellogenesis and endocrine disruption. In T. P. Mommsen & T. W. Moon (Eds.), *Biochemistry and Molecular Biology of Fishes* (Vol. 6, pp. 431–471). Elsevier. https://doi.org/10.1016/S1873-0140(05)80019-0
110. Hirano, M., Maeda, K., Shitara, Y., & Sugiyama, Y. (2006). Drug-drug interaction between pitavastatin and various drugs via OATP1B1. *Drug Metabolism and Disposition: The Biological Fate of Chemicals*, *34*(7), 1229–1236. https://doi.org/10.1124/dmd.106.009290
111. Hirata, M., Nakamura, K., Kanemaru, T., Shibata, Y., & Kondo, S. (2003). Pigment cell organization in the hypodermis of zebrafish. *Developmental Dynamics: An Official Publication of the American Association of Anatomists*, *227*(4), 497–503. https://doi.org/10.1002/dvdy.10334
112. Hoeger, B., Köllner, B., Dietrich, D. R., & Hitzfeld, B. (2005). Water-borne diclofenac affects kidney and gill integrity and selected immune parameters in brown trout (Salmo trutta f. Fario). *Aquatic Toxicology (Amsterdam, Netherlands)*, *75*(1), 53–64. https://doi.org/10.1016/j.aquatox.2005.07.006
113. Houde, M., Martin, J. W., Letcher, R. J., Solomon, K. R., & Muir, D. C. G. (2006). Biological monitoring of polyfluoroalkyl substances: A review. *Environmental Science & Technology*, *40*(11), 3463–3473. https://doi.org/10.1021/es052580b
114. Howe, K., Clark, M. D., Torroja, C. F., Torrance, J., Berthelot, C., Muffato, M., Collins, J. E., Humphray, S., McLaren, K., Matthews, L., McLaren, S., Sealy, I., Caccamo, M., Churcher, C., Scott, C., Barrett, J. C., Koch, R., Rauch, G.-J., White, S., … Stemple, D. L. (2013). The zebrafish reference genome sequence and its relationship to the human genome. *Nature*, *496*(7446), 498–503. https://doi.org/10.1038/nature12111
115. Huang, H., Huang, C., Wang, L., Ye, X., Bai, C., Simonich, M. T., Tanguay, R. L., & Dong, Q. (2010). Toxicity, uptake kinetics and behavior assessment in zebrafish embryos following exposure to perfluorooctanesulphonicacid (PFOS). *Aquatic Toxicology (Amsterdam, Netherlands)*, *98*(2), 139–147. https://doi.org/10.1016/j.aquatox.2010.02.003
116. Hudziak, R. M., Barofsky, E., Barofsky, D. F., Weller, D. L., Huang, S.-B., & Weller, D. D. (1996). Resistance of Morpholino Phosphorodiamidate Oligomers to Enzymatic Degradation. *Antisense and Nucleic Acid Drug Development*, *6*(4), 267–272. https://doi.org/10.1089/oli.1.1996.6.267
117. Humphrey, W., Dalke, A., & Schulten, K. (1996). VMD: Visual molecular dynamics. *Journal of Molecular Graphics*, *14*(1), 33–38. https://doi.org/10.1016/0263-7855(96)00018-5

Ociena rada Utilieku

118. Hwang, W. Y., Fu, Y., Reyon, D., Maeder, M. L., Tsai, S. Q., Sander, J. D., Peterson, R. T., Yeh, J.-R. J., & Joung, J. K. (2013). Efficient genome editing in zebrafish using a CRISPR-Cas system. *Nature Biotechnology*, *31*(3), 227–229. https://doi.org/10.1038/nbt.2501
119. Ionescu, C., & Caira, M. R. (Eds.). (2005). *Drug Metabolism: Current Concepts*. Springer Netherlands. https://doi.org/10.1007/1-4020-4142-X
120. Irons, T. D., MacPhail, R. C., Hunter, D. L., & Padilla, S. (2010). Acute neuroactive drug exposures alter locomotor activity in larval zebrafish. *Neurotoxicology and Teratology*, *32*(1), 84–90. https://doi.org/10.1016/j.ntt.2009.04.066
121. James, M. O. (2011). Steroid catabolism in marine and freshwater fish. *The Journal of Steroid Biochemistry and Molecular Biology*, *127*(3), 167–175. https://doi.org/10.1016/j.jsbmb.2010.10.003
122. Jantzen, C. E., Annunziato, K. M., & Cooper, K. R. (2016). Behavioral, morphometric, and gene expression effects in adult zebrafish (Danio rerio) embryonically exposed to PFOA, PFOS, and PFNA. *Aquatic Toxicology (Amsterdam, Netherlands)*, *180*, 123–130. https://doi.org/10.1016/j.aquatox.2016.09.011
123. Jumper, J., Evans, R., Pritzel, A., Green, T., Figurnov, M., Ronneberger, O., Tunyasuvunakool, K., Bates, R., Žídek, A., Potapenko, A., Bridgland, A., Meyer, C., Kohl, S. A. A., Ballard, A. J., Cowie, A., Romera-Paredes, B., Nikolov, S., Jain, R., Adler, J., … Hassabis, D. (2021). Highly accurate protein structure prediction with AlphaFold. *Nature*, *596*(7873), 583–589. https://doi.org/10.1038/s41586-021-03819-2
124. Jung, S.-H., Lee, W., Park, S.-H., Lee, K.-Y., Choi, Y.-J., Choi, S., Kang, D., Kim, S., Chang, T.-S., Hong, S.-S., & Lee, B.-H. (2020). Diclofenac impairs autophagic flux via oxidative stress and lysosomal dysfunction: Implications for hepatotoxicity. *Redox Biology*, *37*, 101751. https://doi.org/10.1016/j.redox.2020.101751
125. Kallio, J.-M., Lahti, M., Oikari, A., & Kronberg, L. (2010). Metabolites of the aquatic pollutant diclofenac in fish bile. *Environmental Science & Technology*, *44*(19), 7213–7219. https://doi.org/10.1021/es903402c
126. Kalliokoski, A., & Niemi, M. (2009). Impact of OATP transporters on pharmacokinetics. *British Journal of Pharmacology*, *158*(3), 693–705. https://doi.org/10.1111/j.1476-5381.2009.00430.x
127. Kamei-Takeuchi, I., & Hama, T. (1971). Structural change of pterinosome (pteridine pigment granule) during the xanthophore differentiation of *Oryzias* fish. *Journal of Ultrastructure Research*, *34*(5), 452–463. https://doi.org/10.1016/S0022-5320(71)80058-8
128. Karaica, D., Mihaljević, I., Vujica, L., Bošnjak, A., Dragojević, J., Otten, C., Babić, N., Lončar, J., & Smital, T. (2023). Stage-dependent localization of F-actin and Na+ /K+ -ATPase in zebrafish embryos detected using optimized cryosectioning immunostaining protocol. *Microscopy Research and Technique*, *86*(3), 294–310. https://doi.org/10.1002/jemt.24270
129. Keogh, J. P. (2012). Membrane Transporters in Drug Development. In *Advances in Pharmacology* (Vol. 63, pp. 1–42). Elsevier. https://doi.org/10.1016/B978-0-12-398339-8.00001-X
130. Kielkopf, C. L., Bauer, W., & Urbatsch, I. L. (2020). Bradford Assay for Determining Protein Concentration. *Cold Spring Harbor Protocols*, *2020*(4), 102269. https://doi.org/10.1101/pdb.prot102269
131. Kim, H., & Xue, X. (2020). Detection of Total Reactive Oxygen Species in Adherent Cells by 2',7'-Dichlorodihydrofluorescein Diacetate Staining. *Journal of Visualized Experiments : JoVE*, *160*, 10.3791/60682. https://doi.org/10.3791/60682

Osijek rada Učiteku

132. Kim, K.-T., & Tanguay, R. L. (2014). The role of chorion on toxicity of silver nanoparticles in the embryonic zebrafish assay. *Environmental Health and Toxicology*, *29*, e2014021. https://doi.org/10.5620/eht.e2014021
133. Kimmel, C. B., Ballard, W. W., Kimmel, S. R., Ullmann, B., & Schilling, T. F. (1995). Stages of embryonic development of the zebrafish. *Developmental Dynamics: An Official Publication of the American Association of Anatomists*, *203*(3), 253–310. https://doi.org/10.1002/aja.1002030302
134. Kimura, O., Fujii, Y., Haraguchi, K., Kato, Y., Ohta, C., Koga, N., & Endo, T. (2020). Effects of perfluoroalkyl carboxylic acids on the uptake of sulfobromophthalein via organic anion transporting polypeptides in human intestinal Caco-2 cells. *Biochemistry and Biophysics Reports*, *24*, 100807. https://doi.org/10.1016/j.bbrep.2020.100807
135. Kimura, T. (2021). Pigments in Teleosts and their Biosynthesis. In H. Hashimoto, M. Goda, R. Futahashi, R. Kelsh, & T. Akiyama (Eds.), *Pigments, Pigment Cells and Pigment Patterns* (pp. 127–148). Springer. https://doi.org/10.1007/978-981-16-1490-3_4
136. Kimura, T., Nagao, Y., Hashimoto, H., Yamamoto-Shiraishi, Y., Yamamoto, S., Yabe, T., Takada, S., Kinoshita, M., Kuroiwa, A., & Naruse, K. (2014). Leucophores are similar to xanthophores in their specification and differentiation processes in medaka. *Proceedings of the National Academy of Sciences of the United States of America*, *111*(20), 7343–7348. https://doi.org/10.1073/pnas.1311254111
137. Klaassen, C. D., & Lu, H. (2008). Xenobiotic Transporters: Ascribing Function from Gene Knockout and Mutation Studies. *Toxicological Sciences*, *101*(2), 186–196. https://doi.org/10.1093/toxsci/kfm214
138. Kmieć, Z. (2001). Cooperation of liver cells in health and disease. *Advances in Anatomy, Embryology, and Cell Biology*, *161*, III–XIII, 1–151. https://doi.org/10.1007/978-3-642-56553-3
139. Kobayashi, D., Nozawa, T., Imai, K., Nezu, J., Tsuji, A., & Tamai, I. (2003). Involvement of human organic anion transporting polypeptide OATP-B (SLC21A9) in pH-dependent transport across intestinal apical membrane. *The Journal of Pharmacology and Experimental Therapeutics*, *306*(2), 703–708. https://doi.org/10.1124/jpet.103.051300
140. Koepsell, H. (2011). Substrate recognition and translocation by polyspecific organic cation transporters. *Biological Chemistry*, *392*(1–2), 95–101. https://doi.org/10.1515/BC.2011.009
141. Koepsell, H., Schmitt, B. M., & Gorboulev, V. (2003). Organic cation transporters. *Reviews of Physiology, Biochemistry and Pharmacology*, *150*, 36–90. https://doi.org/10.1007/s10254-003-0017-x
142. König, J., Müller, F., & Fromm, M. F. (2013). Transporters and drug-drug interactions: Important determinants of drug disposition and effects. *Pharmacological Reviews*, *65*(3), 944–966. https://doi.org/10.1124/pr.113.007518
143. Kramer, W. (2011). Transporters, Trojan horses and therapeutics: Suitability of bile acid and peptide transporters for drug delivery. *Biological Chemistry*, *392*(1–2), 77–94. https://doi.org/10.1515/BC.2011.017
144. Kropf, C., Fent, K., Fischer, S., Casanova, A., & Segner, H. (2020). ABC transporters in gills of rainbow trout (Oncorhynchus mykiss). *Journal of Experimental Biology*, *223*(15), jeb221069. https://doi.org/10.1242/jeb.221069
145. Kullak-Ublick, G. A., Stieger, B., & Meier, P. J. (2004). Enterohepatic bile salt transporters in normal physiology and liver disease. *Gastroenterology*, *126*(1), 322–342. https://doi.org/10.1053/j.gastro.2003.06.005
146. Kumar, A., Chang, B., & Xagoraraki, I. (2010). Human Health Risk Assessment of Pharmaceuticals in Water: Issues and Challenges Ahead. *International Journal of Environmental Research and Public Health*, *7*(11), 3929–3953. https://doi.org/10.3390/ijerph7113929

Ocjena rada u tijeku

147. Lai, K. P., Ng, A. H.-M., Wan, H. T., Wong, A. Y.-M., Leung, C. C.-T., Li, R., & Wong, C. K.-C. (2018). Dietary Exposure to the Environmental Chemical, PFOS on the Diversity of Gut Microbiota, Associated With the Development of Metabolic Syndrome. *Frontiers in Microbiology*, *9*. https://doi.org/10.3389/fmicb.2018.02552

148. Langenau, D. M., Feng, H., Berghmans, S., Kanki, J. P., Kutok, J. L., & Look, A. T. (2005). Cre/lox-regulated transgenic zebrafish model with conditional myc-induced T cell acute lymphoblastic leukemia. *Proceedings of the National Academy of Sciences of the United States of America*, *102*(17), 6068–6073. https://doi.org/10.1073/pnas.0408708102

149. Lau, C., Anitole, K., Hodes, C., Lai, D., Pfahles-Hutchens, A., & Seed, J. (2007). Perfluoroalkyl acids: A review of monitoring and toxicological findings. *Toxicological Sciences: An Official Journal of the Society of Toxicology*, *99*(2), 366–394. https://doi.org/10.1093/toxsci/kfm128

150. Lawrence, C., Ebersole, J. P., & Kesseli, R. V. (2007). Rapid growth and out-crossing promote female development in zebrafish (Danio rerio). *Environmental Biology of Fishes*, *81*(2), 239–246. https://doi.org/10.1007/s10641-007-9195-8

151. Le Douarin, N., & Kalcheim, C. (1999). *The Neural Crest* (2nd ed.). Cambridge University Press. https://doi.org/10.1017/CBO9780511897948

152. Lee, K. J., Nallathamby, P. D., Browning, L. M., Osgood, C. J., & Xu, X.-H. N. (2007). In Vivo Imaging of Transport and Biocompatibility of Single Silver Nanoparticles in Early Development of Zebrafish Embryos. *ACS Nano*, *1*(2), 133–143. https://doi.org/10.1021/nn700048y

153. Lee, W., Glaeser, H., Smith, L. H., Roberts, R. L., Moeckel, G. W., Gervasini, G., Leake, B. F., & Kim, R. B. (2005). Polymorphisms in human organic anion-transporting polypeptide 1A2 (OATP1A2): Implications for altered drug disposition and central nervous system drug entry. *The Journal of Biological Chemistry*, *280*(10), 9610–9617. https://doi.org/10.1074/jbc.M411092200

154. Leuthold, S., Hagenbuch, B., Mohebbi, N., Wagner, C. A., Meier, P. J., & Stieger, B. (2009). Mechanisms of pH-gradient driven transport mediated by organic anion polypeptide transporters. *American Journal of Physiology. Cell Physiology*, *296*(3), C570-582. https://doi.org/10.1152/ajpcell.00436.2008

155. Li, L., Lee, T. K., Meier, P. J., & Ballatori, N. (1998). Identification of glutathione as a driving force and leukotriene C4 as a substrate for oatp1, the hepatic sinusoidal organic solute transporter. *The Journal of Biological Chemistry*, *273*(26), 16184–16191. https://doi.org/10.1074/jbc.273.26.16184

156. Li, L., Meier, P. J., & Ballatori, N. (2000). Oatp2 mediates bidirectional organic solute transport: A role for intracellular glutathione. *Molecular Pharmacology*, *58*(2), 335–340. https://doi.org/10.1124/mol.58.2.335

157. Li, T., Jiang, L., Zheng, S., Qiu, C., Zhao, N., Lin, X., Ren, H., Huang, J., Wang, H., & Qiu, L. (2023). Organic anion transporting polypeptide 3a1 is a novel influx pump for Perfluorooctane sulfonate in Sertoli cells and contributes to its reproductive toxicity. *Chemosphere*, *345*, 140428. https://doi.org/10.1016/j.chemosphere.2023.140428

158. Lieschke, G. J., & Currie, P. D. (2007). Animal models of human disease: Zebrafish swim into view. *Nature Reviews. Genetics*, *8*(5), 353–367. https://doi.org/10.1038/nrg2091

159. Lin, L., Yee, S. W., Kim, R. B., & Giacomini, K. M. (2015). SLC transporters as therapeutic targets: Emerging opportunities. *Nature Reviews. Drug Discovery*, *14*(8), 543–560. https://doi.org/10.1038/nrd4626

160. Lister, J. A. (2019). Larval but not adult xanthophore pigmentation in zebrafish requires GTP cyclohydrolase 2 (gch2) function. *Pigment Cell & Melanoma Research*, *32*(5), 724–727. https://doi.org/10.1111/pcmr.12783

Olena Utijeku

161. Liu, C., Yu, K., Shi, X., Wang, J., Lam, P. K. S., Wu, R. S. S., & Zhou, B. (2007). Induction of oxidative stress and apoptosis by PFOS and PFOA in primary cultured hepatocytes of freshwater tilapia (*Oreochromis niloticus*). *Aquatic Toxicology*, *82*(2), 135–143. https://doi.org/10.1016/j.aquatox.2007.02.006
162. Liu, L., & Liu, X. (2019). Contributions of Drug Transporters to Blood-Brain Barriers. *Advances in Experimental Medicine and Biology*, *1141*, 407–466. https://doi.org/10.1007/978-981-13-7647-4_9
163. Liu, P., Luk, K., Shin, M., Idrizi, F., Kwok, S., Roscoe, B., Mintzer, E., Suresh, S., Morrison, K., Frazão, J. B., Bolukbasi, M. F., Ponnienselvan, K., Luban, J., Zhu, L. J., Lawson, N. D., & Wolfe, S. A. (2019). Enhanced Cas12a editing in mammalian cells and zebrafish. *Nucleic Acids Research*, *47*(8), 4169–4180. https://doi.org/10.1093/nar/gkz184
164. Liu, X. (2019). Overview: Role of Drug Transporters in Drug Disposition and Its Clinical Significance. *Advances in Experimental Medicine and Biology*, *1141*, 1–12. https://doi.org/10.1007/978-981-13-7647-4_1
165. Liu, Y. (2023). Zebrafish as a Model Organism for Studying Pathologic Mechanisms of Neurodegenerative Diseases and other Neural Disorders. *Cellular and Molecular Neurobiology*, *43*(6), 2603–2620. https://doi.org/10.1007/s10571-023-01340-w
166. Lomize, A. L., Pogozheva, I. D., & Mosberg, H. I. (2011). Anisotropic Solvent Model of the Lipid Bilayer. 2. Energetics of Insertion of Small Molecules, Peptides, and Proteins in Membranes. *Journal of Chemical Information and Modeling*, *51*(4), 930–946. https://doi.org/10.1021/ci200020k
167. Lomize, A. L., Schnitzer, K. A., & Pogozheva, I. D. (2020). TMPfold: A Web Tool for Predicting Stability of Transmembrane α-Helix Association. *Journal of Molecular Biology*, *432*(11), 3388–3394. https://doi.org/10.1016/j.jmb.2019.10.024
168. Lomize, A. L., Todd, S. C., & Pogozheva, I. D. (2022). Spatial arrangement of proteins in planar and curved membranes by PPM 3.0. *Protein Science*, *31*(1), 209–220. https://doi.org/10.1002/pro.4219
169. Lomize, M. A., Pogozheva, I. D., Joo, H., Mosberg, H. I., & Lomize, A. L. (2012). OPM database and PPM web server: Resources for positioning of proteins in membranes. *Nucleic Acids Research*, *40*(Database issue), D370-376. https://doi.org/10.1093/nar/gkr703
170. Lončar, J., Popović, M., Zaja, R., & Smital, T. (2010). Gene expression analysis of the ABC efflux transporters in rainbow trout (*Oncorhynchus mykiss*). *Comparative Biochemistry and Physiology Part C: Toxicology & Pharmacology*, *151*(2), 209–215. https://doi.org/10.1016/j.cbpc.2009.10.009
171. Long, Y., Li, Q., & Cui, Z. (2011). Molecular analysis and heavy metal detoxification of ABCC1/MRP1 in zebrafish. *Molecular Biology Reports*, *38*(3), 1703–1711. https://doi.org/10.1007/s11033-010-0283-z
172. Long, Y., Li, Q., Li, J., & Cui, Z. (2011). Molecular analysis, developmental function and heavy metal-induced expression of ABCC5 in zebrafish. *Comparative Biochemistry and Physiology. Part B, Biochemistry & Molecular Biology*, *158*(1), 46–55. https://doi.org/10.1016/j.cbpb.2010.09.005
173. Lou, Q.-Q., Zhang, Y.-F., Zhou, Z., Shi, Y.-L., Ge, Y.-N., Ren, D.-K., Xu, H.-M., Zhao, Y.-X., Wei, W.-J., & Qin, Z.-F. (2013). Effects of perfluorooctanesulfonate and perfluorobutanesulfonate on the growth and sexual development of Xenopus laevis. *Ecotoxicology (London, England)*, *22*(7), 1133–1144. https://doi.org/10.1007/s10646-013-1100-y
174. Luckenbach, T., Fischer, S., & Sturm, A. (2014). Current advances on ABC drug transporters in fish. *Comparative Biochemistry and Physiology Part C: Toxicology & Pharmacology*, *165*, 28–52. https://doi.org/10.1016/j.cbpc.2014.05.002

Osijek rada u tijeku

175. Maack, G., & Segner, H. (2003). Morphological development of the gonads in zebrafish. *Journal of Fish Biology*, *62*, 895–906. https://doi.org/10.1046/j.1095-8649.2003.00074.x
176. MacPhail, R. C., Brooks, J., Hunter, D. L., Padnos, B., Irons, T. D., & Padilla, S. (2009). Locomotion in larval zebrafish: Influence of time of day, lighting and ethanol. *Neurotoxicology*, *30*(1), 52–58. https://doi.org/10.1016/j.neuro.2008.09.011
177. Marić, P., Ahel, M., Maraković, N., Lončar, J., Mihaljević, I., & Smital, T. (2021). Selective interaction of microcystin congeners with zebrafish (Danio rerio) Oatp1d1 transporter. *Chemosphere*, *283*, 131155. https://doi.org/10.1016/j.chemosphere.2021.131155
178. Matsumoto, J. (1965). Studies on fine structure and cytochemical properties of erythrophores in swordtail, Xiphophorus helleri, with special reference to their pigment granules (Pterinosomes). *The Journal of Cell Biology*, *27*(3), 493–504. https://doi.org/10.1083/jcb.27.3.493
179. Matsumoto, J., Kajishima, T., & Hama, T. (1960). Relation between the Pigmentation and Pterin Derivatives of Chromatophores during Development in the Normal Black and Transparent Scaled Types of Goldfish (Carassius Auratus). *Genetics*, *45*(9), 1177–1189. https://doi.org/10.1093/genetics/45.9.1177
180. McMenamin, S. K., Bain, E. J., McCann, A. E., Patterson, L. B., Eom, D. S., Waller, Z. P., Hamill, J. C., Kuhlman, J. A., Eisen, J. S., & Parichy, D. M. (2014). Thyroid hormone-dependent adult pigment cell lineage and pattern in zebrafish. *Science (New York, N.Y.)*, *345*(6202), 1358–1361. https://doi.org/10.1126/science.1256251
181. Mehinto, A. C., Hill, E. M., & Tyler, C. R. (2010). Uptake and biological effects of environmentally relevant concentrations of the nonsteroidal anti-inflammatory pharmaceutical diclofenac in rainbow trout (Oncorhynchus mykiss). *Environmental Science & Technology*, *44*(6), 2176–2182. https://doi.org/10.1021/es903702m
182. Memmert, U., Peither, A., Burri, R., Weber, K., Schmidt, T., Sumpter, J. P., & Hartmann, A. (2013). Diclofenac: New data on chronic toxicity and bioconcentration in fish. *Environmental Toxicology and Chemistry*, *32*(2), 442–452. https://doi.org/10.1002/etc.2085
183. Mihaljevic, I., Popovic, M., Zaja, R., & Smital, T. (2016). Phylogenetic, syntenic, and tissue expression analysis of slc22 genes in zebrafish (Danio rerio). *BMC Genomics*, *17*(1), 626. https://doi.org/10.1186/s12864-016-2981-y
184. Mikros, E., & Diallinas, G. (2019). Tales of tails in transporters. *Open Biology*, *9*(6), 190083. https://doi.org/10.1098/rsob.190083
185. Mirdita, M., Schütze, K., Moriwaki, Y., Heo, L., Ovchinnikov, S., & Steinegger, M. (2022). ColabFold: Making protein folding accessible to all. *Nature Methods*, *19*(6), 679–682. https://doi.org/10.1038/s41592-022-01488-1
186. Modzelewski, A. J., Chen, S., Willis, B. J., Lloyd, K. C. K., Wood, J. A., & He, L. (2018). Efficient mouse genome engineering by CRISPR-EZ technology. *Nature Protocols*, *13*(6), 1253–1274. https://doi.org/10.1038/nprot.2018.012
187. Morris, G. M., Huey, R., Lindstrom, W., Sanner, M. F., Belew, R. K., Goodsell, D. S., & Olson, A. J. (2009). AutoDock4 and AutoDockTools4: Automated docking with selective receptor flexibility. *Journal of Computational Chemistry*, *30*(16), 2785–2791. https://doi.org/10.1002/jcc.21256
188. Morris, M. E., & Felmlee, M. A. (2008). Overview of the Proton-coupled MCT (SLC16A) Family of Transporters: Characterization, Function and Role in the Transport of the Drug of Abuse γ-Hydroxybutyric Acid. *The AAPS Journal*, *10*(2), 311. https://doi.org/10.1208/s12248-008-9035-6
189. Moulton, J. D. (2017). Using Morpholinos to Control Gene Expression. *Current Protocols in Nucleic Acid Chemistry*, *68*(1). https://doi.org/10.1002/cpnc.21

Osijena rada u tijeku

190. Muthulakshmi, S., Maharajan, K., Habibi, H. R., Kadirvelu, K., & Venkataramana, M. (2018). Zearalenone induced embryo and neurotoxicity in zebrafish model (*Danio rerio*): Role of oxidative stress revealed by a multi biomarker study. *Chemosphere*, *198*, 111–121. https://doi.org/10.1016/j.chemosphere.2018.01.141
191. Muzzio, A. M., Noyes, P. D., Stapleton, H. M., & Lema, S. C. (2014). Tissue distribution and thyroid hormone effects on mRNA abundance for membrane transporters Mct8, Mct10, and organic anion-transporting polypeptides (Oatps) in a teleost fish. *Comparative Biochemistry and Physiology. Part A, Molecular & Integrative Physiology*, *167*, 77–89. https://doi.org/10.1016/j.cbpa.2013.09.019
192. Mylroie, J. E., Wilbanks, M. S., Kimble, A. N., To, K. T., Cox, C. S., McLeod, S. J., Gust, K. A., Moore, D. W., Perkins, E. J., & Garcia-Reyero, N. (2021). Perfluorooctanesulfonic Acid–Induced Toxicity on Zebrafish Embryos in the Presence or Absence of the Chorion. *Environmental Toxicology and Chemistry*, *40*(3), 780–791. https://doi.org/10.1002/etc.4899
193. Nakagawa, H., Terada, T., Harada, K. H., Hitomi, T., Inoue, K., Inui, K.-I., & Koizumi, A. (2009). Human organic anion transporter hOAT4 is a transporter of perfluorooctanoic acid. *Basic & Clinical Pharmacology & Toxicology*, *105*(2), 136–138. https://doi.org/10.1111/j.1742-7843.2009.00409.x
194. Nasevicius, A., & Ekker, S. C. (2000). Effective targeted gene 'knockdown' in zebrafish. *Nature Genetics*, *26*(2), 216–220. https://doi.org/10.1038/79951
195. Nasiadka, A., & Clark, M. D. (2012). Zebrafish breeding in the laboratory environment. *ILAR Journal*, *53*(2), 161–168. https://doi.org/10.1093/ilar.53.2.161
196. Nawaji, T., Yamashita, N., Umeda, H., Zhang, S., Mizoguchi, N., Seki, M., Kitazawa, T., & Teraoka, H. (2020). Cytochrome P450 Expression and Chemical Metabolic Activity before Full Liver Development in Zebrafish. *Pharmaceuticals (Basel, Switzerland)*, *13*(12), 456. https://doi.org/10.3390/ph13120456
197. Negri, E., Metruccio, F., Guercio, V., Tosti, L., Benfenati, E., Bonzi, R., La Vecchia, C., & Moretto, A. (2017). Exposure to PFOA and PFOS and fetal growth: A critical merging of toxicological and epidemiological data. *Critical Reviews in Toxicology*, *47*(6), 482–508. https://doi.org/10.1080/10408444.2016.1271972
198. Nelson, E. (1961). Kinetics of Drug Absorption, Distribution, Metabolism, and Excretion. *Journal of Pharmaceutical Sciences*, *50*(3), 181–192. https://doi.org/10.1002/jps.2600500302
199. Nies, A. T., Koepsell, H., Winter, S., Burk, O., Klein, K., Kerb, R., Zanger, U. M., Keppler, D., Schwab, M., & Schaeffeler, E. (2009). Expression of organic cation transporters OCT1 (SLC22A1) and OCT3 (SLC22A3) is affected by genetic factors and cholestasis in human liver. *Hepatology (Baltimore, Md.)*, *50*(4), 1227–1240. https://doi.org/10.1002/hep.23103
200. Nishimura, Y., Inoue, A., Sasagawa, S., Koiwa, J., Kawaguchi, K., Kawase, R., Maruyama, T., Kim, S., & Tanaka, T. (2016). Using zebrafish in systems toxicology for developmental toxicity testing. *Congenital Anomalies*, *56*(1), 18–27. https://doi.org/10.1111/cga.12142
201. Noé, J., Portmann, R., Brun, M.-E., & Funk, C. (2007). Substrate-dependent drug-drug interactions between gemfibrozil, fluvastatin and other organic anion-transporting peptide (OATP) substrates on OATP1B1, OATP2B1, and OATP1B3. *Drug Metabolism and Disposition: The Biological Fate of Chemicals*, *35*(8), 1308–1314. https://doi.org/10.1124/dmd.106.012930
202. Norton, W. H. J. (2013). Toward developmental models of psychiatric disorders in zebrafish. *Frontiers in Neural Circuits*, *7*, 79. https://doi.org/10.3389/fncir.2013.00079
203. Nozawa, T., Imai, K., Nezu, J.-I., Tsuji, A., & Tamai, I. (2004). Functional characterization of pH-sensitive organic anion transporting polypeptide OATP-B in human. *The Journal of Pharmacology and Experimental Therapeutics*, *308*(2), 438–445. https://doi.org/10.1124/jpet.103.060194

Universitas Islam Negeri Sunan Gunung Djati Bandung

204. Nozawa, T., Nakajima, M., Tamai, I., Noda, K., Nezu, J.-I., Sai, Y., Tsuji, A., & Yokoi, T. (2002). Genetic polymorphisms of human organic anion transporters OATP-C (SLC21A6) and OATP-B (SLC21A9): Allele frequencies in the Japanese population and functional analysis. *The Journal of Pharmacology and Experimental Therapeutics*, *302*(2), 804–813. https://doi.org/10.1124/jpet.302.2.804
205. Obika, M. (1963). Association of pteridines with amphibian larval pigmentation and their biosynthesis in developing chromatophores. *Developmental Biology*, *6*(1), 99–112. https://doi.org/10.1016/0012-1606(63)90007-1
206. Obika, M. (1993). Formation of pterinosomes and carotenoid granules in xanthophores of the teleost Oryzias latipes as revealed by the rapid-freezing and freeze-substitution method. *Cell and Tissue Research*, *271*(1), 81–86. https://doi.org/10.1007/BF00297544
207. Owen, J. P., Kelsh, R. N., & Yates, C. A. (2020). A quantitative modelling approach to zebrafish pigment pattern formation. *eLife*, *9*, e52998. https://doi.org/10.7554/eLife.52998
208. Pan, G. (2019). Roles of Hepatic Drug Transporters in Drug Disposition and Liver Toxicity. *Advances in Experimental Medicine and Biology*, *1141*, 293–340. https://doi.org/10.1007/978-981-13-7647-4_6
209. Panzica-Kelly, J. M., Zhang, C. X., & Augustine-Rauch, K. A. (2015). Optimization and Performance Assessment of the Chorion-Off [Dechorinated] Zebrafish Developmental Toxicity Assay. *Toxicological Sciences: An Official Journal of the Society of Toxicology*, *146*(1), 127–134. https://doi.org/10.1093/toxsci/kfv076
210. Parichy, D. M., Elizondo, M. R., Mills, M. G., Gordon, T. N., & Engeszer, R. E. (2009). Normal table of postembryonic zebrafish development: Staging by externally visible anatomy of the living fish. *Developmental Dynamics: An Official Publication of the American Association of Anatomists*, *238*(12), 2975–3015. https://doi.org/10.1002/dvdy.22113
211. Parikh, N. D., & Levitsky, J. (2013). Hepatotoxicity and drug interactions in liver transplant candidates and recipients. *Clinics in Liver Disease*, *17*(4), 737–747, x–xi. https://doi.org/10.1016/j.cld.2013.07.013
212. Patel, M., Taskar, K. S., & Zamek-Gliszczynski, M. J. (2016). Importance of Hepatic Transporters in Clinical Disposition of Drugs and Their Metabolites. *Journal of Clinical Pharmacology*, *56 Suppl 7*, S23-39. https://doi.org/10.1002/jcph.671
213. Perland, E., & Fredriksson, R. (2017). Classification Systems of Secondary Active Transporters. *Trends in Pharmacological Sciences*, *38*(3), 305–315. https://doi.org/10.1016/j.tips.2016.11.008
214. Petzinger, E., & Geyer, J. (2006). Drug transporters in pharmacokinetics. *Naunyn-Schmiedeberg's Archives of Pharmacology*, *372*(6), 465–475. https://doi.org/10.1007/s00210-006-0042-9
215. Pizzagalli, F., Hagenbuch, B., Stieger, B., Klenk, U., Folkers, G., & Meier, P. J. (2002). Identification of a novel human organic anion transporting polypeptide as a high affinity thyroxine transporter. *Molecular Endocrinology (Baltimore, Md.)*, *16*(10), 2283–2296. https://doi.org/10.1210/me.2001-0309
216. Pizzagalli, M. D., Bensimon, A., & Superti-Furga, G. (2021). A guide to plasma membrane solute carrier proteins. *The Febs Journal*, *288*(9), 2784–2835. https://doi.org/10.1111/febs.15531
217. Popovic, M., Zaja, R., Fent, K., & Smital, T. (2013). Molecular Characterization of Zebrafish Oatp1d1 (*Slco1d1*), a Novel Organic Anion-transporting Polypeptide*. *Journal of Biological Chemistry*, *288*(47), 33894–33911. https://doi.org/10.1074/jbc.M113.518506
218. Popovic, M., Zaja, R., Fent, K., & Smital, T. (2014). Interaction of environmental contaminants with zebrafish organic anion transporting polypeptide, Oatp1d1 (Slco1d1).

Osijek rada Učiteljski

Toxicology and Applied Pharmacology, *280*(1), 149–158. https://doi.org/10.1016/j.taap.2014.07.015

219. Popovic, M., Zaja, R., & Smital, T. (2010). Organic anion transporting polypeptides (OATP) in zebrafish (Danio rerio): Phylogenetic analysis and tissue distribution. *Comparative Biochemistry and Physiology Part A: Molecular & Integrative Physiology*, *155*(3), 327–335. https://doi.org/10.1016/j.cbpa.2009.11.011
220. Post, G. B., Cohn, P. D., & Cooper, K. R. (2012). Perfluorooctanoic acid (PFOA), an emerging drinking water contaminant: A critical review of recent literature. *Environmental Research*, *116*, 93–117. https://doi.org/10.1016/j.envres.2012.03.007
221. Postlethwait, J. H., Yan, Y. L., Gates, M. A., Horne, S., Amores, A., Brownlie, A., Donovan, A., Egan, E. S., Force, A., Gong, Z., Goutel, C., Fritz, A., Kelsh, R., Knapik, E., Liao, E., Paw, B., Ransom, D., Singer, A., Thomson, M., … Talbot, W. S. (1998). Vertebrate genome evolution and the zebrafish gene map. *Nature Genetics*, *18*(4), 345–349. https://doi.org/10.1038/ng0498-345
222. Povey, S., Lovering, R., Bruford, E., Wright, M., Lush, M., & Wain, H. (2001). The HUGO Gene Nomenclature Committee (HGNC). *Human Genetics*, *109*(6), 678–680. https://doi.org/10.1007/s00439-001-0615-0
223. Praskova, E., Plhalova, L., Chromcova, L., Stepanova, S., Bedanova, I., Blahova, J., Hostovsky, M., Skoric, M., Maršálek, P., Voslarova, E., & Svobodova, Z. (2014). Effects of Subchronic Exposure of Diclofenac on Growth, Histopathological Changes, and Oxidative Stress in Zebrafish (Danio rerio). *The Scientific World Journal*, *2014*, 645737. https://doi.org/10.1155/2014/645737
224. Pressler, H., Sissung, T. M., Venzon, D., Price, D. K., & Figg, W. D. (2011). Expression of OATP family members in hormone-related cancers: Potential markers of progression. *PloS One*, *6*(5), e20372. https://doi.org/10.1371/journal.pone.0020372
225. Prevedouros, K., Cousins, I. T., Buck, R. C., & Korzeniowski, S. H. (2006). Sources, fate and transport of perfluorocarboxylates. *Environmental Science & Technology*, *40*(1), 32–44. https://doi.org/10.1021/es0512475
226. Pritchard, V. L. (2001). *Behaviour and morphology of the zebrafish, danio rerio* [Phd, University of Leeds]. https://etheses.whiterose.ac.uk/id/eprint/323/
227. Pyron, M. (2003). Female preferences and male–male interactions in zebrafish (Danio rerio). *Canadian Journal of Zoology*, *81*(1), 122–125. https://doi.org/10.1139/z02-229
228. Rauwerda, H., Wackers, P., Pagano, J. F. B., Jong, M. de, Ensink, W., Dekker, R., Nehrdich, U., Spaink, H. P., Jonker, M., & Breit, T. M. (2016). Mother-Specific Signature in the Maternal Transcriptome Composition of Mature, Unfertilized Zebrafish Eggs. *PLOS ONE*, *11*(1), e0147151. https://doi.org/10.1371/journal.pone.0147151
229. Rawson, D., Zhang, T., Kalicharan, D., & Jongebloed, W. (2000). Field emission scanning electron microscopy and transmission electron microscopy studies of the chorion, plasma membrane and syncytial layers of the gastrula-stage embryo of the zebrafish Brachydanio rerio: A consideration of the structural and functional relationships with respect to cryoprotectant penetration. *Aquaculture Research*, *31*(3), 325–336.
230. Redzic, Z. (2011). Molecular biology of the blood-brain and the blood-cerebrospinal fluid barriers: Similarities and differences. *Fluids and Barriers of the CNS*, *8*(1), 3. https://doi.org/10.1186/2045-8118-8-3
231. Rombough, P. (2007). The functional ontogeny of the teleost gill: Which comes first, gas or ion exchange? *Comparative Biochemistry and Physiology Part A: Molecular & Integrative Physiology*, *148*(4), 732–742. https://doi.org/10.1016/j.cbpa.2007.03.007
232. Rosenmai, A. K., Taxvig, C., Svingen, T., Trier, X., van Vugt-Lussenburg, B. M. A., Pedersen, M., Lesné, L., Jégou, B., & Vinggaard, A. M. (2016). Fluorinated alkyl substances and technical

Ocjena rada Utjeku

mixtures used in food paper-packaging exhibit endocrine-related activity in vitro. *Andrology*, *4*(4), 662–672. https://doi.org/10.1111/andr.12190
233. Rossi, A., Kontarakis, Z., Gerri, C., Nolte, H., Hölper, S., Krüger, M., & Stainier, D. Y. R. (2015a). Genetic compensation induced by deleterious mutations but not gene knockdowns. *Nature*, *524*(7564), 230–233. https://doi.org/10.1038/nature14580
234. Rossi, A., Kontarakis, Z., Gerri, C., Nolte, H., Hölper, S., Krüger, M., & Stainier, D. Y. R. (2015b). Genetic compensation induced by deleterious mutations but not gene knockdowns. *Nature*, *524*(7564), 230–233. https://doi.org/10.1038/nature14580
235. Roth, M., Araya, J. J., Timmermann, B. N., & Hagenbuch, B. (2011). Isolation of modulators of the liver-specific organic anion-transporting polypeptides (OATPs) 1B1 and 1B3 from Rollinia emarginata Schlecht (Annonaceae). *The Journal of Pharmacology and Experimental Therapeutics*, *339*(2), 624–632. https://doi.org/10.1124/jpet.111.184564
236. Roth, M., Obaidat, A., & Hagenbuch, B. (2012). OATPs, OATs and OCTs: The organic anion and cation transporters of the SLCO and SLC22A gene superfamilies. *British Journal of Pharmacology*, *165*(5), 1260–1287. https://doi.org/10.1111/j.1476-5381.2011.01724.x
237. Rueden, C. T., Schindelin, J., Hiner, M. C., DeZonia, B. E., Walter, A. E., Arena, E. T., & Eliceiri, K. W. (2017). ImageJ2: ImageJ for the next generation of scientific image data. *BMC Bioinformatics*, *18*(1), 529. https://doi.org/10.1186/s12859-017-1934-z
238. Sacher, F., Lange, F. T., Brauch, H. J., & Blankenhorn, I. (2001). Pharmaceuticals in groundwaters analytical methods and results of a monitoring program in Baden-Württemberg, Germany. *Journal of Chromatography. A*, *938*(1–2), 199–210. https://doi.org/10.1016/s0021-9673(01)01266-3
239. Saier, M. H., Reddy, V. S., Moreno-Hagelsieb, G., Hendargo, K. J., Zhang, Y., Iddamsetty, V., Lam, K. J. K., Tian, N., Russum, S., Wang, J., & Medrano-Soto, A. (2021). The Transporter Classification Database (TCDB): 2021 update. *Nucleic Acids Research*, *49*(D1), D461–D467. https://doi.org/10.1093/nar/gkaa1004
240. Sanchez-Covarrubias, L., Slosky, L. M., Thompson, B. J., Davis, T. P., & Ronaldson, P. T. (2014). Transporters at CNS barrier sites: Obstacles or opportunities for drug delivery? *Current Pharmaceutical Design*, *20*(10), 1422–1449. https://doi.org/10.2174/13816128113199990463
241. Sant, K. E., Annunziato, K., Conlin, S., Teicher, G., Chen, P., Venezia, O., Downes, G. B., Park, Y., & Timme-Laragy, A. R. (2021). Developmental exposures to perfluorooctanesulfonic acid (PFOS) impact embryonic nutrition, pancreatic morphology, and adiposity in the zebrafish, *Danio rerio*. *Environmental Pollution*, *275*, 116644. https://doi.org/10.1016/j.envpol.2021.116644
242. Sant, K. E., Sinno, P. P., Jacobs, H. M., & Timme-Laragy, A. R. (2018). Nrf2a modulates the embryonic antioxidant response to perfluorooctanesulfonic acid (PFOS) in the zebrafish, *Danio rerio*. *Aquatic Toxicology*, *198*, 92–102. https://doi.org/10.1016/j.aquatox.2018.02.010
243. Sant, K. E., & Timme-Laragy, A. R. (2018). Zebrafish as a Model for Toxicological Perturbation of Yolk and Nutrition in the Early Embryo. *Current Environmental Health Reports*, *5*(1), 125–133. https://doi.org/10.1007/s40572-018-0183-2
244. Satlin, L. M., Amin, V., & Wolkoff, A. W. (1997). Organic anion transporting polypeptide mediates organic anion/HCO3- exchange. *The Journal of Biological Chemistry*, *272*(42), 26340–26345. https://doi.org/10.1074/jbc.272.42.26340
245. Sato, I., Kawamoto, K., Nishikawa, Y., Tsuda, S., Yoshida, M., Yaegashi, K., Saito, N., Liu, W., & Jin, Y. (2009). Neurotoxicity of perfluorooctane sulfonate (PFOS) in rats and mice after single oral exposure. *The Journal of Toxicological Sciences*, *34*(5), 569–574. https://doi.org/10.2131/jts.34.569
246. Saunders, L. M., Mishra, A. K., Aman, A. J., Lewis, V. M., Toomey, M. B., Packer, J. S., Qiu, X., McFaline-Figueroa, J. L., Corbo, J. C., Trapnell, C., & Parichy, D. M. (2019). Thyroid hormone

Oglena Rada Utleku

regulates distinct paths to maturation in pigment cell lineages. *eLife*, *8*, e45181. https://doi.org/10.7554/eLife.45181

247. Schneider, C. A., Rasband, W. S., & Eliceiri, K. W. (2012). NIH Image to ImageJ: 25 years of image analysis. *Nature Methods*, *9*(7), 671–675. https://doi.org/10.1038/nmeth.2089

248. Scholz, S., Ortmann, J., Klüver, N., & Léonard, M. (2014). Extensive review of fish embryo acute toxicities for the prediction of GHS acute systemic toxicity categories. *Regulatory Toxicology and Pharmacology*, *69*(3), 572–579. https://doi.org/10.1016/j.yrtph.2014.06.004

249. Schulze, R. J., Schott, M. B., Casey, C. A., Tuma, P. L., & McNiven, M. A. (2019). The cell biology of the hepatocyte: A membrane trafficking machine. *The Journal of Cell Biology*, *218*(7), 2096–2112. https://doi.org/10.1083/jcb.201903090

250. Schwaiger, J., Ferling, H., Mallow, U., Wintermayr, H., & Negele, R. D. (2004). Toxic effects of the non-steroidal anti-inflammatory drug diclofenac. Part I: Histopathological alterations and bioaccumulation in rainbow trout. *Aquatic Toxicology (Amsterdam, Netherlands)*, *68*(2), 141–150. https://doi.org/10.1016/j.aquatox.2004.03.014

251. Schwede, T., Sali, A., Honig, B., Levitt, M., Berman, H. M., Jones, D., Brenner, S. E., Burley, S. K., Das, R., Dokholyan, N. V., Dunbrack, R. L., Fidelis, K., Fiser, A., Godzik, A., Huang, Y. J., Humblet, C., Jacobson, M. P., Joachimiak, A., Krystek, S. R., … Wilson, I. A. (2009). Outcome of a workshop on applications of protein models in biomedical research. *Structure (London, England: 1993)*, *17*(2), 151–159. https://doi.org/10.1016/j.str.2008.12.014

252. Shan, Z., Yang, X., Liu, H., Yuan, Y., Xiao, Y., Nan, J., Zhang, W., Song, W., Wang, J., Wei, F., & Zhang, Y. (2023). Cryo-EM structures of human organic anion transporting polypeptide OATP1B1. *Cell Research*, *33*(12), 940–951. https://doi.org/10.1038/s41422-023-00870-8

253. Shang, E. H. H., Yu, R. M. K., & Wu, R. S. S. (2006). Hypoxia affects sex differentiation and development, leading to a male-dominated population in zebrafish (Danio rerio). *Environmental Science & Technology*, *40*(9), 3118–3122. https://doi.org/10.1021/es0522579

254. Shen, H., Lai, Y., & Rodrigues, A. D. (2017). Organic Anion Transporter 2: An Enigmatic Human Solute Carrier. *Drug Metabolism and Disposition: The Biological Fate of Chemicals*, *45*(2), 228–236. https://doi.org/10.1124/dmd.116.072264

255. Shi, X., Du, Y., Lam, P. K. S., Wu, R. S. S., & Zhou, B. (2008). Developmental toxicity and alteration of gene expression in zebrafish embryos exposed to PFOS. *Toxicology and Applied Pharmacology*, *230*(1), 23–32. https://doi.org/10.1016/j.taap.2008.01.043

256. Shi, X., Yeung, L. W. Y., Lam, P. K. S., Wu, R. S. S., & Zhou, B. (2009). Protein profiles in zebrafish (Danio rerio) embryos exposed to perfluorooctane sulfonate. *Toxicological Sciences: An Official Journal of the Society of Toxicology*, *110*(2), 334–340. https://doi.org/10.1093/toxsci/kfp111

257. Shi, X., & Zhou, B. (2010). The role of Nrf2 and MAPK pathways in PFOS-induced oxidative stress in zebrafish embryos. *Toxicological Sciences: An Official Journal of the Society of Toxicology*, *115*(2), 391–400. https://doi.org/10.1093/toxsci/kfq066

258. Shi, Y. (2013). Common folds and transport mechanisms of secondary active transporters. *Annual Review of Biophysics*, *42*, 51–72. https://doi.org/10.1146/annurev-biophys-083012-130429

259. Shin, J. T., & Fishman, M. C. (2002). From Zebrafish to human: Modular medical models. *Annual Review of Genomics and Human Genetics*, *3*, 311–340. https://doi.org/10.1146/annurev.genom.3.031402.131506

260. Shúilleabháin, S. N., Davoren, M., Mothersill, C., Sheehan, D., Hartl, M. G. J., Kilemade, M., O'Brien, N. M., O'Halloran, J., Van Pelt, F. N. A. M., & Lyng, F. M. (2005). Identification of a multixenobiotic resistance mechanism in primary cultured epidermal cells from *Oncorhynchus*

mykiss and the effects of environmental complex mixtures on its activity. *Aquatic Toxicology*, *73*(2), 115–127. https://doi.org/10.1016/j.aquatox.2005.03.014

261. Singer, S. J., & Nicolson, G. L. (1972). The fluid mosaic model of the structure of cell membranes. *Science (New York, N.Y.)*, *175*(4023), 720–731. https://doi.org/10.1126/science.175.4023.720

262. Skinner, A. M. J., & Watt, P. J. (2007). Strategic egg allocation in the zebra fish, Danio rerio. *Behavioral Ecology*, *18*(5), 905–909. https://doi.org/10.1093/beheco/arm059

263. Spitsbergen, J. M., & Kent, M. L. (2003). The State of the Art of the Zebrafish Model for Toxicology and Toxicologic Pathology Research—Advantages and Current Limitations. *Toxicologic Pathology*, *31*(Suppl), 62–87.

264. Stein, W. D., & Litman, T. (2015). Chapter 6—Primary Active Transport Systems. In W. D. Stein & T. Litman (Eds.), *Channels, Carriers, and Pumps (Second Edition)* (pp. 247–328). Elsevier. https://doi.org/10.1016/B978-0-12-416579-3.00006-X

265. Steiner, K., Hagenbuch, B., & Dietrich, D. R. (2014). Molecular cloning and functional characterization of a rainbow trout liver Oatp. *Toxicology and Applied Pharmacology*, *280*(3), 534–542. https://doi.org/10.1016/j.taap.2014.08.031

266. Steiner, K., Zimmermann, L., Hagenbuch, B., & Dietrich, D. (2016). Zebrafish-Oatp mediated transport of Microcystin-congeners. *Archives of Toxicology*, *90*(5), 1129–1139. https://doi.org/10.1007/s00204-015-1544-3

267. Strazielle, N., & Ghersi-Egea, J. F. (2013). Physiology of blood-brain interfaces in relation to brain disposition of small compounds and macromolecules. *Molecular Pharmaceutics*, *10*(5), 1473–1491. https://doi.org/10.1021/mp300518e

268. Sukardi, H., Chng, H. T., Chan, E. C. Y., Gong, Z., & Lam, S. H. (2011). Zebrafish for drug toxicity screening: Bridging the in vitro cell-based models and in vivo mammalian models. *Expert Opinion on Drug Metabolism & Toxicology*, *7*(5), 579–589. https://doi.org/10.1517/17425255.2011.562197

269. Summerton, J., & Weller, D. (1997). Morpholino Antisense Oligomers: Design, Preparation, and Properties. *Antisense and Nucleic Acid Drug Development*, *7*(3), 187–195. https://doi.org/10.1089/oli.1.1997.7.187

270. Sunderland, E. M., Hu, X. C., Dassuncao, C., Tokranov, A. K., Wagner, C. C., & Allen, J. G. (2019). A review of the pathways of human exposure to poly- and perfluoroalkyl substances (PFASs) and present understanding of health effects. *Journal of Exposure Science & Environmental Epidemiology*, *29*(2), 131–147. https://doi.org/10.1038/s41370-018-0094-1

271. Swan, G. E., Cuthbert, R., Quevedo, M., Green, R. E., Pain, D. J., Bartels, P., Cunningham, A. A., Duncan, N., Meharg, A. A., Lindsay Oaks, J., Parry-Jones, J., Shultz, S., Taggart, M. A., Verdoorn, G., & Wolter, K. (2006). Toxicity of diclofenac to Gyps vultures. *Biology Letters*, *2*(2), 279–282. https://doi.org/10.1098/rsbl.2005.0425

272. Syed, M., Skonberg, C., & Hansen, S. H. (2016). Mitochondrial toxicity of diclofenac and its metabolites via inhibition of oxidative phosphorylation (ATP synthesis) in rat liver mitochondria: Possible role in drug induced liver injury (DILI). *Toxicology in Vitro: An International Journal Published in Association with BIBRA*, *31*, 93–102. https://doi.org/10.1016/j.tiv.2015.11.020

273. Takenaka, S., Itoh, T., & Fujiwara, R. (2013). Expression pattern of human ATP-binding cassette transporters in skin. *Pharmacology Research & Perspectives*, *1*(1). https://doi.org/10.1002/prp2.5

274. Talevi, A., & Bellera, C. L. (2022). Solute Carrier (SLC) Transporters: An Overview. In A. Talevi (Ed.), *The ADME Encyclopedia: A Comprehensive Guide on Biopharmacy and*

Ocjena rada Utilleku

Pharmacokinetics (pp. 1082–1087). Springer International Publishing. https://doi.org/10.1007/978-3-030-84860-6_83

275. Tamai, I., Nezu, J., Uchino, H., Sai, Y., Oku, A., Shimane, M., & Tsuji, A. (2000). Molecular identification and characterization of novel members of the human organic anion transporter (OATP) family. *Biochemical and Biophysical Research Communications*, *273*(1), 251–260. https://doi.org/10.1006/bbrc.2000.2922

276. Tauxe-Wuersch, A., De Alencastro, L. F., Grandjean, D., & Tarradellas, J. (2005). Occurrence of several acidic drugs in sewage treatment plants in Switzerland and risk assessment. *Water Research*, *39*(9), 1761–1772. https://doi.org/10.1016/j.watres.2005.03.003

277. Teorell, T. (1937). Kinetics of distribution of substances administered to the body, II: The intravascular modes of administration. *Archives Internationales de Pharmacodynamie et de Thérapie*. https://www.semanticscholar.org/paper/Kinetics-of-distribution-of-substances-administered-Teorell/dc46f2dc7a632c352f50972903b564acc6e570dd

278. Thakkar, N., Kim, K., Jang, E. R., Han, S., Kim, K., Kim, D., Merchant, N., Lockhart, A. C., & Lee, W. (2013). A cancer-specific variant of the SLCO1B3 gene encodes a novel human organic anion transporting polypeptide 1B3 (OATP1B3) localized mainly in the cytoplasm of colon and pancreatic cancer cells. *Molecular Pharmaceutics*, *10*(1), 406–416. https://doi.org/10.1021/mp3005353

279. Thomas, J. R., Frye, W. J. E., Robey, R. W., & Gottesman, M. M. (2024). Progress in characterizing ABC multidrug transporters in zebrafish. *Drug Resistance Updates*, *72*, 101035. https://doi.org/10.1016/j.drup.2023.101035

280. Thöny, B., Auerbach, G., & Blau, N. (2000). Tetrahydrobiopterin biosynthesis, regeneration and functions. *The Biochemical Journal*, *347 Pt 1*(Pt 1), 1–16.

281. Tischer, S., & Fontana, R. J. (2014). Drug-drug interactions with oral anti-HCV agents and idiosyncratic hepatotoxicity in the liver transplant setting. *Journal of Hepatology*, *60*(4), 872–884. https://doi.org/10.1016/j.jhep.2013.11.013

282. Toews, D. P. L., Hofmeister, N. R., & Taylor, S. A. (2017). The Evolution and Genetics of Carotenoid Processing in Animals. *Trends in Genetics: TIG*, *33*(3), 171–182. https://doi.org/10.1016/j.tig.2017.01.002

283. Triebskorn, R., Casper, H., Heyd, A., Eikemper, R., Köhler, H.-R., & Schwaiger, J. (2004). Toxic effects of the non-steroidal anti-inflammatory drug diclofenac. Part II: Cytological effects in liver, kidney, gills and intestine of rainbow trout (Oncorhynchus mykiss). *Aquatic Toxicology (Amsterdam, Netherlands)*, *68*(2), 151–166. https://doi.org/10.1016/j.aquatox.2004.03.015

284. Trott, O., & Olson, A. J. (2009). AutoDock Vina: Improving the speed and accuracy of docking with a new scoring function, efficient optimization, and multithreading. *Journal of Computational Chemistry*, NA-NA. https://doi.org/10.1002/jcc.21334

285. Truong, L., Reif, D. M., St Mary, L., Geier, M. C., Truong, H. D., & Tanguay, R. L. (2014). Multidimensional in vivo hazard assessment using zebrafish. *Toxicological Sciences: An Official Journal of the Society of Toxicology*, *137*(1), 212–233. https://doi.org/10.1093/toxsci/kft235

286. Turner, J. R. (2009). Intestinal mucosal barrier function in health and disease. *Nature Reviews. Immunology*, *9*(11), 799–809. https://doi.org/10.1038/nri2653

287. Tzvetkov, M. V., Saadatmand, A. R., Bokelmann, K., Meineke, I., Kaiser, R., & Brockmöller, J. (2012). Effects of OCT1 polymorphisms on the cellular uptake, plasma concentrations and efficacy of the 5-HT(3) antagonists tropisetron and ondansetron. *The Pharmacogenomics Journal*, *12*(1), 22–29. https://doi.org/10.1038/tpj.2010.75

288. Uchida, D., Yamashita, M., Kitano, T., & Iguchi, T. (2004). An aromatase inhibitor or high water temperature induce oocyte apoptosis and depletion of P450 aromatase activity in the gonads of genetic female zebrafish during sex-reversal. *Comparative Biochemistry and Physiology.*

Ocjena rada Utjeku

Part A, Molecular & Integrative Physiology, *137*(1), 11–20. https://doi.org/10.1016/s1095-6433(03)00178-8

289. Ulhaq, M., Orn, S., Carlsson, G., Morrison, D. A., & Norrgren, L. (2013). Locomotor behavior in zebrafish (Danio rerio) larvae exposed to perfluoroalkyl acids. *Aquatic Toxicology (Amsterdam, Netherlands)*, *144–145*, 332–340. https://doi.org/10.1016/j.aquatox.2013.10.021
290. van den Brandhof, E.-J., & Montforts, M. (2010). Fish embryo toxicity of carbamazepine, diclofenac and metoprolol. *Ecotoxicology and Environmental Safety*, *73*(8), 1862–1866. https://doi.org/10.1016/j.ecoenv.2010.08.031
291. van der Deure, W. M., Peeters, R. P., & Visser, T. J. (2010). Molecular aspects of thyroid hormone transporters, including MCT8, MCT10, and OATPs, and the effects of genetic variation in these transporters. *Journal of Molecular Endocrinology*, *44*(1), 1–11. https://doi.org/10.1677/JME-09-0042
292. Varga, T., Czimmerer, Z., & Nagy, L. (2011). PPARs are a unique set of fatty acid regulated transcription factors controlling both lipid metabolism and inflammation. *Biochimica et Biophysica Acta (BBA) - Molecular Basis of Disease*, *1812*(8), 1007–1022. https://doi.org/10.1016/j.bbadis.2011.02.014
293. Varshney, G. K., Sood, R., & Burgess, S. M. (2015). Understanding and Editing the Zebrafish Genome. *Advances in Genetics*, *92*, 1–52. https://doi.org/10.1016/bs.adgen.2015.09.002
294. Verbueken, E., Alsop, D., Saad, M. A., Pype, C., Van Peer, E. M., Casteleyn, C. R., Van Ginneken, C. J., Wilson, J., & Van Cruchten, S. J. (2017). In Vitro Biotransformation of Two Human CYP3A Probe Substrates and Their Inhibition during Early Zebrafish Development. *International Journal of Molecular Sciences*, *18*(1), 217. https://doi.org/10.3390/ijms18010217
295. Visentin, M., Chang, M.-H., Romero, M. F., Zhao, R., & Goldman, I. D. (2012). Substrate- and pH-specific antifolate transport mediated by organic anion-transporting polypeptide 2B1 (OATP2B1-SLCO2B1). *Molecular Pharmacology*, *81*(2), 134–142. https://doi.org/10.1124/mol.111.074823
296. von Hellfeld, R., Brotzmann, K., Baumann, L., Strecker, R., & Braunbeck, T. (2020). Adverse effects in the fish embryo acute toxicity (FET) test: A catalogue of unspecific morphological changes versus more specific effects in zebrafish (Danio rerio) embryos. *Environmental Sciences Europe*, *32*(1), 122. https://doi.org/10.1186/s12302-020-00398-3
297. von Hofsten, J., & Olsson, P.-E. (2005). Zebrafish sex determination and differentiation: Involvement of FTZ-F1 genes. *Reproductive Biology and Endocrinology : RB&E*, *3*, 63. https://doi.org/10.1186/1477-7827-3-63
298. Vujica, L., Lončar, J., Mišić, L., Lučić, B., Radman, K., Mihaljević, I., Bertoša, B., Mesarić, J., Horvat, M., & Smital, T. (2023). Environmental contaminants modulate transport activity of zebrafish (*Danio rerio*) multidrug and toxin extrusion protein 3 (Mate3/Slc47a2.1). *Science of The Total Environment*, *901*, 165956. https://doi.org/10.1016/j.scitotenv.2023.165956
299. Vujica, L., Mihaljević, I., Dragojević, J., Lončar, J., Karaica, D., Dananić, A., Bošnjak, A., & Smital, T. (2024). Functional knockout of the Oatp1d1 membrane transporter affects toxicity of diclofenac in zebrafish embryos. *Aquatic Toxicology (Amsterdam, Netherlands)*, *273*, 107031. https://doi.org/10.1016/j.aquatox.2024.107031
300. Wang, H., Yan, Z., Dong, M., Zhu, X., Wang, H., & Wang, Z. (2012). Alteration in placental expression of bile acids transporters OATP1A2, OATP1B1, OATP1B3 in intrahepatic cholestasis of pregnancy. *Archives of Gynecology and Obstetrics*, *285*(6), 1535–1540. https://doi.org/10.1007/s00404-011-2183-4
301. Wang, P., Hata, S., Xiao, Y., Murray, J. W., & Wolkoff, A. W. (2008). Topological assessment of oatp1a1: A 12-transmembrane domain integral membrane protein with three N-linked

Ocjena rada Utjecaj

carbohydrate chains. *American Journal of Physiology. Gastrointestinal and Liver Physiology*, *294*(4), G1052-1059. https://doi.org/10.1152/ajpgi.00584.2007

302. Wang, S., Zhuang, C., Du, J., Wu, C., & You, H. (2017). The presence of MWCNTs reduces developmental toxicity of PFOS in early life stage of zebrafish. *Environmental Pollution*, *222*, 201–209. https://doi.org/10.1016/j.envpol.2016.12.055
303. Wang, Y.-Q., Hu, L.-X., Liu, T., Zhao, J.-H., Yang, Y.-Y., Liu, Y.-S., & Ying, G.-G. (2022). Per- and polyfluoralkyl substances (PFAS) in drinking water system: Target and non-target screening and removal assessment. *Environment International*, *163*, 107219. https://doi.org/10.1016/j.envint.2022.107219
304. Wang, Z., DeWitt, J. C., Higgins, C. P., & Cousins, I. T. (2017). A Never-Ending Story of Per- and Polyfluoroalkyl Substances (PFASs)? *Environmental Science & Technology*, *51*(5), 2508–2518. https://doi.org/10.1021/acs.est.6b04806
305. Watson, H. (2015). Biological membranes. *Essays in Biochemistry*, *59*, 43–69. https://doi.org/10.1042/bse0590043
306. Wendl, T., Lun, K., Mione, M., Favor, J., Brand, M., Wilson, S. W., & Rohr, K. B. (2002). Pax2.1 is required for the development of thyroid follicles in zebrafish. *Development (Cambridge, England)*, *129*(15), 3751–3760. https://doi.org/10.1242/dev.129.15.3751
307. Westerfield, M. (1995). *The zebrafish book: A guide for the laboratory use of zebrafish (Danio rerio)*. https://www.semanticscholar.org/paper/The-zebrafish-book-%3A-a-guide-for-the-laboratory-use-Westerfield/5ff1aefdada5bdfe8900e782f8c6a3a45777908f
308. Wiegand, C., Pflugmacher, S., Giese, M., Frank, H., & Steinberg, C. (2000). Uptake, toxicity, and effects on detoxication enzymes of atrazine and trifluoroacetate in embryos of zebrafish. *Ecotoxicology and Environmental Safety*, *45*(2), 122–131. https://doi.org/10.1006/eesa.1999.1845
309. Willi, R. A., & Fent, K. (2018). Interaction of environmental steroids with organic anion transporting polypeptide (Oatp1d1) in zebrafish (Danio rerio). *Environmental Toxicology and Chemistry*, *37*(10), 2670–2676. https://doi.org/10.1002/etc.4231
310. Williams, C. J., Headd, J. J., Moriarty, N. W., Prisant, M. G., Videau, L. L., Deis, L. N., Verma, V., Keedy, D. A., Hintze, B. J., Chen, V. B., Jain, S., Lewis, S. M., Arendall, W. B., Snoeyink, J., Adams, P. D., Lovell, S. C., Richardson, J. S., & Richardson, D. C. (2018). MolProbity: More and better reference data for improved all-atom structure validation. *Protein Science: A Publication of the Protein Society*, *27*(1), 293–315. https://doi.org/10.1002/pro.3330
311. Xue, Y., Ma, C., Hanna, I., & Pan, G. (2019). Intestinal Transporter-Associated Drug Absorption and Toxicity. *Advances in Experimental Medicine and Biology*, *1141*, 361–405. https://doi.org/10.1007/978-981-13-7647-4_8
312. Yang, X., & Han, L. (2019). Roles of Renal Drug Transporter in Drug Disposition and Renal Toxicity. *Advances in Experimental Medicine and Biology*, *1141*, 341–360. https://doi.org/10.1007/978-981-13-7647-4_7
313. Yilmaz, O., Com, E., Pineau, C., & Bobe, J. (2023). Genomic disturbance of vitellogenin 2 (vtg2) leads to vitellin membrane deficiencies and significant mortalities at early stages of embryonic development in zebrafish (Danio rerio). *Scientific Reports*, *13*(1), 18795. https://doi.org/10.1038/s41598-023-46148-2
314. Zaïr, Z. M., Eloranta, J. J., Stieger, B., & Kullak-Ublick, G. A. (2008). Pharmacogenetics of OATP (*SLC21* / *SLCO*), OAT and OCT (*SLC22*) and PEPT (*SLC15*) Transporters in the Intestine, Liver and Kidney. *Pharmacogenomics*, *9*(5), 597–624. https://doi.org/10.2217/14622416.9.5.597
315. Zhang, K., Yuan, G., Werdich, A. A., & Zhao, Y. (2020). Ibuprofen and diclofenac impair the cardiovascular development of zebrafish (Danio rerio) at low concentrations. *Environmental Pollution (Barking, Essex: 1987)*, *258*, 113613. https://doi.org/10.1016/j.envpol.2019.113613

Orientada Utieku

316. Zhao, C., Tang, C. Y., Li, P., Adrian, P., & Hu, G. (2016). Perfluorooctane sulfonate removal by nanofiltration membrane—The effect and interaction of magnesium ion / humic acid. *Journal of Membrane Science*, *503*, 31–41. https://doi.org/10.1016/j.memsci.2015.12.049
317. Ziegler, I. (2003). The Pteridine Pathway in Zebrafish: Regulation and Specification during the Determination of Neural Crest Cell-Fate. *Pigment Cell Research*, *16*(3), 172–182. https://doi.org/10.1034/j.1600-0749.2003.00044.x
318. Zuber, R., Anzenbacherová, E., & Anzenbacher, P. (2002). Cytochromes P450 and experimental models of drug metabolism. *Journal of Cellular and Molecular Medicine*, *6*(2), 189–198. https://doi.org/10.1111/j.1582-4934.2002.tb00186.x

Ocjena rada u tijeku

8. SUMMARY

The primary function and physiological purpose of all components involved in the ADME processes (adsorption, distribution, metabolism, excretion) is to eliminate endogenous and/or xenobiotic compounds that may pose a toxic threat to the cell or organism, or that are simply not useful as energy sources, structural components or signalling molecules. Since most endo- or xenobiotics are not soluble enough in the cell or body fluids, they cannot pass through the cell membrane by simple diffusion and specific transmembrane proteins are required for this transport. These membrane transporters play a key role in the uptake, distribution and excretion of nutrients, xenobiotics and metabolites. Organic Anion Transporting Polypeptides (OATPs) are membrane proteins that belong to the SLC (Solute Carrier) superfamily of transporters and mediate the uptake of a wide range of structurally unrelated organic anions, cations and even neutral compounds into the cytoplasm. This study was specifically aimed at the *in vivo* characterisation of the fish-specific organic anion-transporting polypeptide 1d1 (Oatp1d1), using zebrafish as a model organism. To achieve this main research goal, we (i) developed specific antibodies to characterise the Oatp1d1 mutant line; (ii) analysed the phenotype of the Oatp1d1 mutants; (iii) analysed the changes in the *oatp1d1* gene expression as well as the transcripts of other transporters and biotransformation enzymes caused by the Oatp1d1 mutation; (iv) exposed the embryos to diclofenac and PFOS,

model contaminants that have been shown to be Oatp1d1 substrates, to observe differences in the phenotypic and toxic responses in the WT and Oatp1d1 mutant embryos.

Using methods such as immunohistochemistry, Western blot and qPCR, we confirmed the absence of a functional Oatp1d1 protein, but also a lower transcription of the *oatp1d1* gene in the mutants generated by the CRISP-Cas9 method. We obtained the AF3 structure of the Oatp1d1 protein and used molecular docking to verify the binding of substrates and inhibitors and to get more insight into the mechanism of transport. Observing the phenotypic changes in the mutants, we found a lack of yellow pigments in all embryonic stages, which we confirmed by measuring the fluorescence of the embryonic matrix and analysing the autofluorescence of xanthophores. We exposed the embryos to methylene blue, which specifically stains pterinosomes, and crossed adult mutants with WT fish to reverse the pigment phenotype of the mutants. Next, we exposed the embryos to thyroid hormones (T4 and T3), which regulate the transition of pigmentation from larvae to adults, and found that the WT embryos lacked yellow pigments, suggesting that thyroid hormones regulate pigmentation in embryos as well and that Oatp1d1 may play a role in the transport of pigment precursors or in the regulation of thyroid hormones. In addition, we observed particles in the perivitelline fluid (PVF) that only appeared in mutant embryos and were dependent on the mutant mothers.

To investigate possible compensatory mechanisms due to the mutation, we analysed the expression of the *Slc21* and *Slc22* genes in embryos and adult tissues. The lower expression of *oat2a* is interesting due to its specific expression during embryonic development - only in xanthophores. Besides *oat2a*, *oat1*, *oat3*, *oat2d* and *oatp2b1* showed altered gene expressions in mutant embryos and may contribute to the overall phenotype and the results of the exposure experiments.

Furthermore, exposure experiments with diclofenac and PFOS have revealed a possible dual role of Oatp1d1 in embryonic development, which can be both protective and potentially harmful when exposed to different Oatp1d1 substrates. In addition, we have designed two morpholino oligonucleotides to knockdown Oatp1d1 protein in WTs and monitor phenotypic changes due to exposure. Exposure of embryos to diclofenac showed a higher resistance of mutant embryos with a delayed onset of sublethal effects. Mortality rates (LC_{50}) differed between WT and mutant embryos, with a calculated LC_{50} of 35.91 for WT and 23.48 µM for Oatp1d1 mutants. All observed effects and malformations caused by diclofenac exposure in the Oatp1d1 mutant embryos were

Ocjena rada u tijeku

delayed and occurred at a lower frequency compared to the WT embryos. Apart from pericardial oedema, blood accumulation in the heart area and body curvature, muscle degradation was prominent in WT embryos, so we further analysed the malformations in muscle fibre alignment by phalloidin staining. Phalloidin staining confirmed that muscle degradation was almost absent in the mutant embryos, and in this case the MO-ATG embryos showed a similar phenotype to the mutant embryos, confirming that the observed effect was due to the Oatp1d1 mutation. To confirm that the observed lack of phenotype in the mutants was due to the absence of the functional Oatp1d1 protein, a rescue experiment was performed in which the mutant embryos were injected with *oatp1d1* mRNA. The upregulation of *oat1* and *oat3* in diclofenac-exposed mutants supports our suggestion of possible compensatory mechanisms, while the downregulation of *oat2a* and *oatp2b1* suggests limited inducibility by diclofenac in the mutants and a lack of involvement in compensation for the Oatp1d1 mutation.

Given the unexpected reverse effects observed during diclofenac exposure, in which the Oatp1d1 mutant embryos showed greater resistance than the WT embryos, we used an additional substrate to further explore this phenomenon. Interestingly, the mutant embryos show increased susceptibility to PFOS toxicity with the calculated LC_{50} values of 23.57 µM for WT and 16.71 µM for Oatp1d1 mutants. Phenotypic changes due to PFOS exposure, reduced swim bladder size, abnormal embryo positioning, scoliosis and necrosis were all more pronounced and occurred earlier in the mutant embryos. When locomotor activity was measured, the PFOS- exposed Oatp1d1 embryos also showed a significant decrease in activity during the dark conditions suggesting that PFOS is neurotoxic and has greater effects on the mutant embryos. A detailed analysis of the changes in gene expression induced by PFOS exposure was performed, and we hypothesise that Oatp2b1 may play an important role in mediating the toxic effects of PFOS due to its upregulation in both WTs and mutants. To quantify the level of oxidative stress in embryos exposed to PFOS, we used DCFH-DA, a common dye for the detection of ROS. Oatp1d1 mutant embryos exhibited higher levels of oxidative stress compared to WT embryos. Furthermore, the use of MO-splice resulted in WT embryos being more sensitive to PFOS and therefore exhibiting higher levels of oxidative stress closer to those of the mutants. In addition, we observed increased apoptosis in the PFOS-exposed mutant embryos after staining with AO.

Ocjena rada u tijeku

In summary, this is the first *in vivo* study on Oatp1d1 mutants that provides a comprehensive analysis of the role and potential ecotoxicological relevance of a fish membrane transporter. The initial data obtained in this study on changes in the pigmentation pattern in Oatp1d1 mutant embryos and adults indicate a clear physiological importance of the Oatp1d1 membrane transporter that needs to be further investigated. Exposure experiments revealed a possible dual role of Oatp1d1 depending on the substrates to which the embryos and fish are exposed. When a compound is metabolised, as in the case of diclofenac, more toxic metabolites are not transported to the liver because the Oatp1d1 transporter is absent, and the mutants are more resistant. In other cases, a compound that is not efficiently metabolised is also not efficiently excreted, causing various toxic effects in mutant embryos. In conclusion, the complexity of the transport network and ADME processes in zebrafish needs further investigation, and with the results obtained in this study we provide the basis for further *in vivo* research on embryos and adults using CRISPR/Cas mutants that lack transport activity mediated by targeted membrane transporters.

9. SAŽETAK

Primarna funkcija i fiziološka svrha svih komponenti uključenih u ADME procese (apsorpcija, distribucija, metabolizam i ekskrecija) jest eliminacija endogenih i/ili ksenobiotskih spojeva koji mogu predstavljati toksičnu prijetnju za stanicu ili organizam, ili nisu korisni kao izvor energije, građevni materijal ili signalne molekule. Prijenos različitih organskih i anorganskih molekula, koje se međusobno razlikuju po kemijskoj i strukturnoj građi, preko stanične membrane ključan je za održavanje staničnog metabolizma i opće homeostaze organizma. Budući da većina endo- i ksenobiotika ne može pasivno proći kroz staničnu membranu zbog niske topljivosti u tjelesnim tekućinama, nužna je prisutnost specifičnih transmembranskih proteina. Membranski prijenosnici imaju ključnu ulogu u unosu, distribuciji i izlučivanju nutrijenata, ksenobiotika i metabolita. OATP-i (eng., Organic Anion Transporting Polypeptides; OATPs) su membranski proteini koji pripadaju SLC (eng., Solute Carrier) superobitelji prijenosnika te posreduju u unosu velikog broja strukturno nepovezanih organskih aniona, kationa, pa čak i neutralnih spojeva u citoplazmu.

Ovo istraživanje bilo je usmjereno na *in vivo* karakterizaciju prijenosnika organskih aniona Oatp1d1 koristeći zebricu (*Danio rerio*) kao modelni organizam. Kako bismo ostvarili ciljeve istraživanja: (i) razvili smo specifična protutijela za karakterizaciju Oatp1d1mutantne linije; (ii)

Ocjena rada u tijeku

analizirali smo fenotip mutanata; (iii) ispitali promjene u ekspresiji *oatp1d1* gena i drugih transportera i enzima biotransformacije izazvane mutacijom; (iv) proveli izlaganja modelnim zagađivalima koja su supstrati Oatp1d1 prijenosnika, kako bismo usporedili odgovore embrija divljeg tipa (WT) i Oatp1d1 mutiranih embrija, promatrajući fenotipske, ali i promjene na molekularnoj razini.

Korištenjem imunohistokemije, Western blot-a i qPCR-a, potvrdili smo odsutnost funkcionalnog Oatp1d1 proteina te smanjenu transkripciju *oatp1d1* gena kod mutanata dobivenih CRISPR-Cas9 metodom. AF3 struktura Oatp1d1 proteina korištena je za molekulsko uklapanje s kojim smo ispitali vezanje supstrata i inhibitora te dobili bolji uvid u mehanizam prijenosa. Uočili smo izostanak žutih pigmenata u svim razvojnim fazama kod mutanata, što je potvrđeno mjerenjem fluorescencije i analizom autofluorescencije ksantofora. Izlaganjem metilenskom modrilu i križanjem odraslih mutanata s WT jedinkama djelomično smo vratili pigmentni fenotip. Izlaganjem embrija T3 i T4 hormonima, koji reguliraju promjene pigmentacije prilikom razvoja iz larvi u odrasle ribe, utvrđeno je da i WT embriji pokazuju smanjenu pigmentaciju, što upućuje na ulogu hormona štitnjače i u embrionalnim stadijima te moguću ulogu Oatp1d1 u prijenosu pigmentnih prekursora.

Kod mutanata smo u perivitelinskom prostoru uočili čestice koje su isključivo rezultat nasljeđivanja preko majki. Moguće je da Oatp1d1 sudjeluje u prijenosu steroida koji reguliraju prijenos vitelogenina, ili se radi o curenju pigmentnih prekursora. Za razliku od embrija, odrasli mutanti imaju više ksantofora, te su potrebne daljnje analize gena uključenih u metabolizam i prijenos karotenoida ili regulaciju hormona štitnjače. Ispitali smo ekspresiju gena iz *Slc21* i *Slc22* obitelji u embrijima i tkivima odraslih riba. Smanjena ekspresija *oat2a*, koji je specifično eksprimiran samo u ksantoforima tijekom embrionalnog razvoja, te promjene u ekspresiji *oat1*, *oat3*, *oat2d* i *oatp2b1* ukazuju na njihov potencijalni doprinos fenotipu i odgovorima na izlaganje.

Eksperimentima izlaganja s modelnim zagađivalima, diklofenakom i PFOS-om, otkrili smo moguću dvostruku ulogu Oatp1d1 prijenosnika ovisno o supstratu kojem su embriji izloženi. Kod diklofenaka, mutanti su pokazali veću otpornost i kasniju pojavu subletalnih učinaka. LC_{50} vrijednosti iznosile su 35,91 µM za WT embrije i 23,48 µM za Oatp1d1 embrije. Malformacije mišićnih vlakana bile su izraženije kod WT embrija, što je potvrđeno faloidinskim bojanjem. Sličan fenotip opažen je i kod MO-ATG embrija, potvrđujući povezanost s nedostatkom

Ocjena rada u tijeku

funkcionalnog proteina Oatp1d1. U *rescue* eksperimentima opažena je djelomična obnova WT fenotipa kod izlaganja diklofenaku.

Povećana ekspresija *oat1* i *oat3* kod mutanata izloženih diklofenaku podupire postojanje kompenzacijskih mehanizama putem regulacija prijenosnika s koji se prema sutpstratnoj specifičnosti djelomično preklapaju s Oatp1d1 prijenosnikom, dok pad ekspresije *oat2a* i *oatp2b1* ukazuje na nedostatak inducibilnosti uzrokovane diklofenakom.

Zbog opažene neočekivano više otpornosti mutanata na diklofenak, odlučili smo izlagati embrije i drugom modelnom zagađivalu, PFOS-u. Mutanti su pokazali veću osjetljivost na PFOS, s LC_{50} vrijednostima od 23,57 µM za WT embrije i 16,71 µM za Oatp1d1 embrije. Fenotipske promjene (skolioza, nekroza, položaj embrija, smanjen plivaći mjehur) bile su izraženije kod mutanata. Mutanti su također pokazali smanjenu motoričku aktivnost u uvjetima tame, upućujući na izraženiju neurotoksičnost PFOS-a kod mutanata. Ekspresijska analiza gena ukazala je na potencijalno važnu ulogu Oatp2b1 prijenosnika, čiji je transkript bio induciran u oba genotipa. Za kvantifikaciju oksidativnog stresa korišten je DCFH-DA, pri čemu su mutanti pokazali višu razinu ROS-a. Injektiranjem MO-splice u WT embrije opažena je povećana osjetljivost WT embrija. Korištenjem boje AO uočena je i povećana apoptoza kod mutanata izlaganih PFOS-u.

Zaključno, ovo je prvo istraživanje koje pruža sveobuhvatnu analizu uloge membranskog prijenosnika Oatp1d1 u zaštiti organizma. Promjene u pigmentaciji jasno upućuju na fiziološki značaj ovog prijenosnika. Eksperimenti izlaganja ukazuju na njegovu dvostruku ulogu u obrani organizma, ovisno o vrsti supstrata. U slučaju metaboliziranih spojeva, poput diklofenaka čiji su metabolite toksičniji od izvornog spoja, odsutnost Oatp1d1 rezultira manjom toksičnošću spoja za embrije zbog smanjenog unosa i posljedičnog metabolizma dikofenaka, dok kod nemetaboliziranih spojeva, poput PFOS-a, dolazi do akumulacije i izraženije toksičnosti kod mutanata zbog smanjenog izbacivanja spoja te njegovog nakupljanja u organizmu. Zaključno, kompleksnost mreže staničnih membranskih prijenosnika i njihova uloge u ADME procesima treba biti detaljnije istraživana, a rezultati predstavljeni u ovoj doktorskoj disertaciji postavljaju temelje za daljnja *in vivo* istraživanja uloge membranskih prijenosnika u embrijima i odraslim ribama, posebice korištenjem CRISPR/Cas mutantnih linija kojima ciljano nedostaje transportna aktivnost posredovana istraživanim prijenosnicima.

Ocjena rada u tijeku

10. SUPPLEMENT

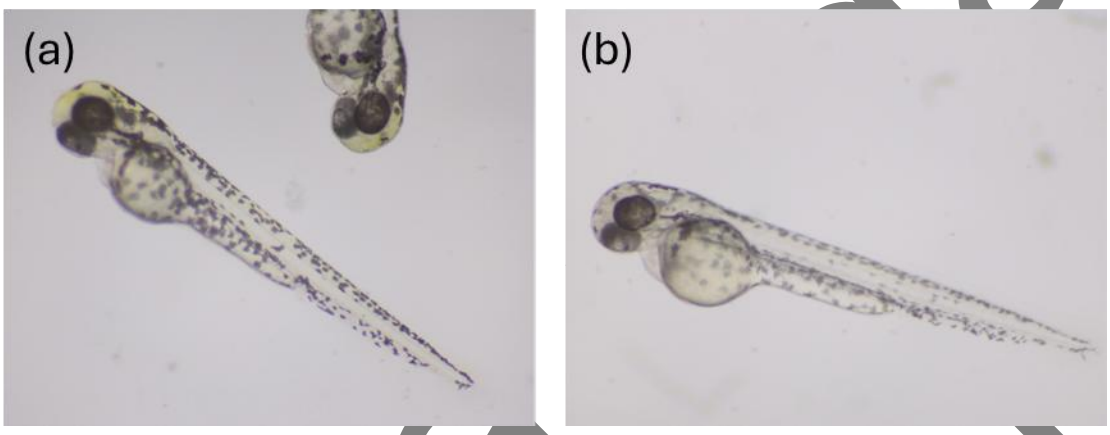

Figure S1. Images of 4 dpf DMSO treated control embryos. (a) WT, (b) Oatp1d1 mutant.

Membrane 1

Parameters of Protein in Membrane

Depth/Hydrophobic Thickness	$\Delta G_{transfer}$	Tilt Angle
33.8 ± 1.8 Å	-99.8 kcal/mol	3 ± 0°

Membrane Embedded Residues (in Hydrocarbon Core)

Subunits	Tilt	Segments
		Embedded residues:
A	4	16-40,42,50-74,78-101,103-104,158-182,197-220,222,246-268,321,325,329,331-359,363,367-393,401-424,529-555,566-591,617-643
		Transmembrane secondary structure segments:
A	3	1(18- 42), 2(50- 72), 3(81- 101), 4(159- 182), 5(198- 220), 6(247- 267), 7(331- 359), 8(367- 393), 9(402- 424),10(529- 552),11(567- 591),12(618- 642)

Figure S2. Predicted positions of TM segments when positioned in the membrane of zebrafish Oatp1d1 protein with 689 residues positioned in the membrane using the method PPM 3.0 (A. L.

Lomize et al., 2022), starting from the AlphaFold3 algorithm. Amino acid residue numbering corresponds to the complete sequence.

Table S1 Predicted positions of TM-helices (position from residue no. 1) of zebrafish Oatp1d1 protein by the top performing models and their consensus developed for predicting the structure and topology of membrane proteins. The positions of TM segments predicted by the TOPCONS method are marked in blue and those obtained by PPM 3.0 in red rectangles.

TOPCONS	**TM1:** 13-33,	**TM2:** 53-73,	**TM3:** 83-103,	**TM4:** 160-180,	**TM5:** 195-215,	**TM6:** 248-268,	**TM7:** 332-352,	**TM8:** 372-392,	**TM9:** 402-422,	**TM10:** 532-552,	**TM11:** 569-589,	**TM12:** 620-640
OCTOPUS	**TM1:** 15-35,	**TM2:** 52-72,	**TM3:** 82-102,	**TM4:** 196-216,	**TM5:** 239-253,	**TM6:** 255-269,	**TM7:** 331-351,	**TM8:** 373-393,	**TM9:** 402-422,	**TM10:** 532-552,	**TM11:** 569-589,	**TM12:** 618-638
Philius	**TM1:** 14-32,	**TM2:** 53-74,	**TM3:** 83-104,	**TM4:** 164-185,	**TM5:** 195-218,	**TM6:** 246-268,	**TM7:** 332-354,	**TM8:** 370-392,	**TM9:** 401-424,	**TM10:** 534-556,	**TM11:** 567-590,	**TM12:** 622-640
PolyPhobius	**TM1:** 13-31,	**TM2:** 52-76,	**TM3:** 83-104,	**TM4:** 160-181,	**TM5:** 195-220,	**TM6:** 245-268,	**TM7:** 333-354,	**TM8:** 370-393,	**TM9:** 402-424,	**TM10:** 531-555,	**TM11:** 567-588,	**TM12:** 620-641
SCAMPI	**TM1:** 10-30,	**TM2:** 58-78,	**TM3:** 83-103,	**TM4:** 153-173,	**TM5:** 195-215,	**TM6:** 249-269,	**TM7:** 334-354,	**TM8:** 368-388,	**TM9:** 406-426,	**TM10:** 529-549,	**TM11:** 572-592,	**TM12:** 621-641
SPOCTOPUS	**TM1:** 15-35,	**TM2:** 52-72,	**TM3:** 82-102	**TM4:** 195-215,	**TM5:** 245-265	**TM6:** 331-351	**TM7:** 373-393	**TM8:** 402-422	**TM9:** 533-553	**TM10:** 569-589	**TM11:** 618-638	
AF3-PPM3	**TM1** 18- 42	**TM2** 50- 72	**TM3** 81-101	**TM4** 159-182	**TM5** 198-220	**TM6** 247-267	**TM7** 331-359	**TM8** 367-393	**TM9** 402-424	**TM10** 529-552	**TM11** 567-591	**TM12** 618-642

```
Seq.          MSTEKKKEPC CSKLKMFLAA MCFVFFAKAF QGSYMKSSVT QIERRFDVPS
TOPCONS       iiiiiiiiii iiMMMMMMMM MMMMMMMMMM MMMooooooo ooooooooo
OCTOPUS       iiiiiiiiii iiiiMMMMMM MMMMMMMMMM MMMMMooooo ooooooooo
Philius       iiiiiiiiii iiiMMMMMMM MMMMMMMMMM MMooooooo ooooooooo
PolyPhobius   iiiiiiiiii iiMMMMMMMM MMMMMMMMMM Mooooooooo ooooooooo
SCAMPI        iiiiiiiiiM MMMMMMMMMM MMMMMMMMMM ooooooooo ooooooooo
SPOCTOPUS     ooooooooo oooMMMMMMM MMMMMMMMMM MMMMMiiiii iiiiiiiii

                        51                                  91
Seq.          SLIGFIDGSF EIGNLFVIAF VSYFGAKLHR PRLIAAGCLV MSAGSFITAM
TOPCONS       ooMMMMMMM MMMMMMMMMM MMMiiiiiii iiMMMMMMM MMMMMMMMMM
OCTOPUS       oMMMMMMMM MMMMMMMMMM MMiiiiiiii iMMMMMMMM MMMMMMMMMM
Philius       ooMMMMMMM MMMMMMMMMM MMMMiiiiii iiMMMMMMM MMMMMMMMMM
PolyPhobius   oMMMMMMMM MMMMMMMMMM MMMMMMiiii iiMMMMMMM MMMMMMMMMM
SCAMPI        ooooooMMM MMMMMMMMMM MMMMMMMMii iiMMMMMMM MMMMMMMMMM
SPOCTOPUS     iMMMMMMMM MMMMMMMMMM MMooooooooo oMMMMMMMM MMMMMMMMMM

                        101                                 141
```

Ocjena rada tijekom

```
Seq.          PHFFQGQYKY ESTISHFSAS VNGTENVLPC LTNASLAQDS EIPTVESQAE
TOPCONS       MMMooooooo oooooooooo oooooooooo oooooooooo oooooooooo
OCTOPUS       MMoooooooo oooooooooo oooooooooo oooooooooo oooooooooo
Philius       MMMMooooooo oooooooooo oooooooooo oooooooooo oooooooooo
PolyPhobius   MMMMooooooo oooooooooo oooooooooo oooooooooo oooooooooo
SCAMPI        MMMooooooo oooooooooo oooooooooo oooooooooo oooooooooo
SPOCTOPUS     MMiiiiiiiii iiiiiiiiii iiiiiiiiii iiiiiiiiii iiiiiiiiii

              151                                           191
Seq.          CEKASSSSLW LFVFLGNMLR GIGETPVMPL GLSYLDDFSR EENTAFYLAL
TOPCONS       oooooooooM MMMMMMMMMM MMMMMMMMMM iiiiiiiiii iiiiMMMMMM
OCTOPUS       oooooooooo oooooooooo oooooooooo oooooooooo oooooMMMMM
Philius       oooooooooo oooMMMMMMM MMMMMMMMMM MMMMMiiiii iiiiMMMMMM
PolyPhobius   ooooooooooM MMMMMMMMMM MMMMMMMMMM Miiiiiiiii iiiiMMMMMM
SCAMPI        ooMMMMMMMM MMMMMMMMMM MMMiiiiiii iiiiiiiiii iiiiMMMMMM
SPOCTOPUS     iiiiiiiiii iiiiiiiiii iiiiiiiiii iiiiiiiiii iiiiMMMMMM

              201                                           241
Seq.          IQTVGIMGPM FGFMLGSFCA KLYVDIGTVD LDSITINYKD SRWVGAWWLG
TOPCONS       MMMMMMMMMM MMMMMooooo oooooooooo oooooooooo ooooooMMM
OCTOPUS       MMMMMMMMMM MMMMMMiiii iiiiiiiiii iiiiiiiiMM MMMMMMMMMM
Philius       MMMMMMMMMM MMMMMMMMoo oooooooooo oooooooooo oooooMMMMM
PolyPhobius   MMMMMMMMMM MMMMMMMMMM oooooooooo oooooooooo ooooMMMMMM
SCAMPI        MMMMMMMMMM MMMMMooooo oooooooooo oooooooooo oooooooMM
SPOCTOPUS     MMMMMMMMMM MMMMMooooo oooooooooo oooooooooo ooooMMMMMM

              251                                           291
Seq.          FLVTGGVMLL AGIPFWFLPK SLTRQGEPES EKKPGAPEGG EQERFIPDNN
TOPCONS       MMMMMMMMMM MMMMMMMMii iiiiiiiiii iiiiiiiiii iiiiiiiiii
OCTOPUS       MMMoMMMMMM MMMMMMMMMi iiiiiiiiii iiiiiiiiii iiiiiiiiii
Philius       MMMMMMMMMM MMMMMMMMii iiiiiiiiii iiiiiiiiii iiiiiiiiii
PolyPhobius   MMMMMMMMMM MMMMMMMMii iiiiiiiiii iiiiiiiiii iiiiiiiiii
SCAMPI        MMMMMMMMMM MMMMMMMMMi iiiiiiiiii iiiiiiiiii iiiiiiiiii
SPOCTOPUS     MMMMMMMMMM MMMMMiiiii iiiiiiiiii iiiiiiiiii iiiiiiiiii

              301                                           341
Seq.          KHNPPASKPA PVTMSALAKD FLPSLKKLFS NTIYVLLVCT GLIQVSGFIG
TOPCONS       iiiiiiiiii iiiiiiiiii iiiiiiiiii iMMMMMMMMM MMMMMMMMMM
OCTOPUS       iiiiiiiiii iiiiiiiiii iiiiiiiiii MMMMMMMMMM MMMMMMMMMM
Philius       iiiiiiiiii iiiiiiiiii iiiiiiiiii iMMMMMMMMM MMMMMMMMMM
PolyPhobius   iiiiiiiiii iiiiiiiiii iiiiiiiiii iiMMMMMMMM MMMMMMMMMM
SCAMPI        iiiiiiiiii iiiiiiiiii iiiiiiiiii iiiMMMMMMM MMMMMMMMMM
SPOCTOPUS     iiiiiiiiii iiiiiiiiii iiiiiiiiii MMMMMMMMMM MMMMMMMMMM

              351                                           391
Seq.          MITFKPKFME QVYGQSASRA IFLIGIMNLP AVALGIVTGG FIMKRFKVNV
TOPCONS       MMooooooooo oooooooooo oMMMMMMMMM MMMMMMMMMM MMiiiiiiii
OCTOPUS       Mooooooooo oooooooooo ooMMMMMMMM MMMMMMMMMM MMMiiiiiii
Philius       MMMMooooooo ooooooooooM MMMMMMMMMM MMMMMMMMMM MMiiiiiiii
PolyPhobius   MMMMooooooo ooooooooooM MMMMMMMMMM MMMMMMMMMM MMMiiiiiii
SCAMPI        MMMMooooooo ooooooooMMM MMMMMMMMMM MMMMMMMMii iiiiiiiiii
SPOCTOPUS     Mooooooooo oooooooooo ooMMMMMMMM MMMMMMMMMM MMMiiiiiii

              401                                           441
Seq.          LGAAKICIVA SVLAFCSMLI QYFLQCDNSQ VAGLTVTYQG APEVSYQTET
TOPCONS       iMMMMMMMMM MMMMMMMMMM MMooooooooo oooooooooo oooooooooo
OCTOPUS       iMMMMMMMMM MMMMMMMMMM MMooooooooo oooooooooo oooooooooo
Philius       MMMMMMMMMM MMMMMMMMMM MMMMooooooo oooooooooo oooooooooo
PolyPhobius   iMMMMMMMMM MMMMMMMMMM MMMMooooooo oooooooooo oooooooooo
SCAMPI        iiiiiMMMMM MMMMMMMMMM MMMMMMooooo oooooooooo oooooooooo
```

```
SPOCTOPUS     iMMMMMMMMM MMMMMMMMMM MMoooooooo oooooooooo oooooooooo

              451                                          491
Seq.          LISQCNIGCS CSLKHWDPIC ASNGVTYTSP CLAGCQTSTG IGKEMVFHNC
TOPCONS       oooooooooo oooooooooo oooooooooo oooooooooo oooooooooo
OCTOPUS       oooooooooo oooooooooo oooooooooo oooooooooo oooooooooo
Philius       oooooooooo oooooooooo oooooooooo oooooooooo oooooooooo
PolyPhobius   oooooooooo oooooooooo oooooooooo oooooooooo oooooooooo
SCAMPI        oooooooooo oooooooooo oooooooooo oooooooooo oooooooooo
SPOCTOPUS     oooooooooo oooooooooo oooooooooo oooooooooo oooooooooo

              501                                          541
Seq.          SCIGEALLPY TNMSAVLGQC PRKSDCDFMF KIYMAVTVIG AFFSAVGATP
TOPCONS       oooooooooo oooooooooo oooooooooo oMMMMMMMMM MMMMMMMMMM
OCTOPUS       oooooooooo oooooooooo oooooooooo oMMMMMMMMM MMMMMMMMMM
Philius       oooooooooo oooooooooo oooooooooo oooMMMMMMM MMMMMMMMMM
PolyPhobius   oooooooooo oooooooooo oooooooooo MMMMMMMMMM MMMMMMMMMM
SCAMPI        oooooooooo oooooooooo ooooooooMM MMMMMMMMMM MMMMMMMMMi
SPOCTOPUS     oooooooooo oooooooooo oooooooooo ooMMMMMMMM MMMMMMMMMM

              551                                          591
Seq.          GYIILLRSIT PELKSLALGM HTLIVRTLGG IPPPIYFGAL IDKTCLKWGL
TOPCONS       MMiiiiiiii iiiiiiiiMM MMMMMMMMMM MMMMMMMMMo oooooooooo
OCTOPUS       MMiiiiiiii iiiiiiiiMM MMMMMMMMMM MMMMMMMMMo oooooooooo
Philius       MMMMMMiiii iiiiiiMMMM MMMMMMMMMM MMMMMMMMMM oooooooooo
PolyPhobius   MMMMMiiiii iiiiiiMMMM MMMMMMMMMM MMMMMMMMoo oooooooooo
SCAMPI        iiiiiiiiii iiiiiiiiii iMMMMMMMMM MMMMMMMMMM MMoooooooo
SPOCTOPUS     MMMiiiiiii iiiiiiiiMM MMMMMMMMMM MMMMMMMMMo oooooooooo

              601                                          641
Seq.          KQCGGRGACR IYDSGAFRNA FLGLIYALYS SSYLLFGLLY NRLSHREKKQ
TOPCONS       oooooooooo oooooooooM MMMMMMMMMM MMMMMMMMMM iiiiiiiiii
OCTOPUS       oooooooooo oooooooMMM MMMMMMMMMM MMMMMMMMii iiiiiiiiii
Philius       oooooooooo oooooooooo oMMMMMMMMM MMMMMMMMMM iiiiiiiiii
PolyPhobius   oooooooooo oooooooooM MMMMMMMMMM MMMMMMMMMM Miiiiiiiii
SCAMPI        oooooooooo oooooooooo MMMMMMMMMM MMMMMMMMMM Miiiiiiiii
SPOCTOPUS     oooooooooo oooooooMMM MMMMMMMMMM MMMMMMMMii iiiiiiiiii
```

Figure S3. Sequences and predicted 2D topologies: (i: inside the membrane, o: outside the membrane, M: membrane region) of zebrafish Oatp1d1 protein determined by several top performing methods developed for membrane protein topology prediction and their consensus prediction. The topologies determined by the TOPCONS method are highlighted in blue. In the line corresponding to the protein sequence, the topology prediction of the PPM 3.0 method (A. L. Lomize et al., 2022) is marked with red rectangles based on the 3D structure of protein determined by AlphaFold 3.

A

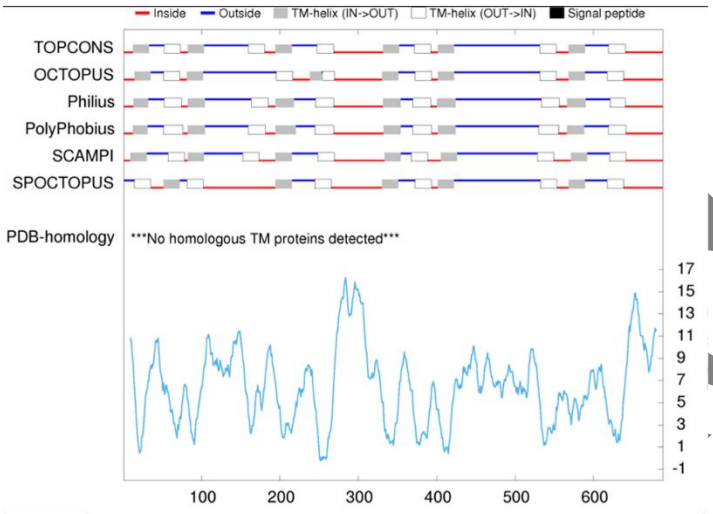

B

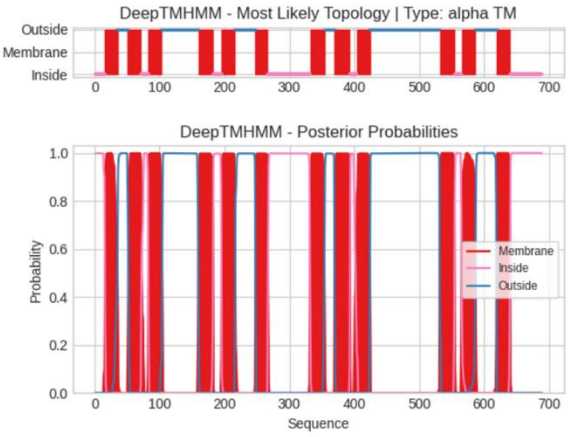

C

Membrane embeded form and evaluation of AlphaFold structure

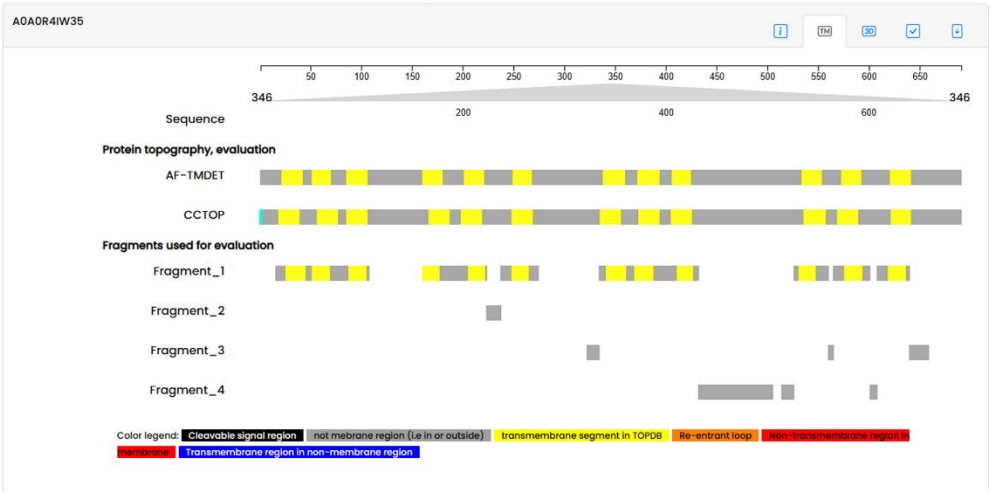

Ocr

Figure S4. Predicted topologies by the TOPCONS (A) (consensus) method and other individual methods, and predicted ΔG values for the zebrafish Oatp1d1. Predicted topologies by the DeepTMHMM (B) and TMDET (C).

A

Helix-helix association free energies - Subunit A

TMH	1	2	3	4	5	6	7	8	9	10	11	12
1	0.0	-3.5	-1.7	-6.9	-9.7	-8.3	-0.1	-1.5	0.4	-0.4	0.8	-0.5
2	-3.5	0.0	-1.3	-14.1	-0.6	0.8	-2.0	0.5	-0.4	0.4	-9.4	0.7
3	-1.7	-1.3	0.0	-14.7	1.0	-10.3	0.4	-0.5	0.2	-0.3	0.6	-0.2
4	-6.9	-14.1	-14.7	0.0	-1.2	0.8	-0.4	0.5	-0.3	0.3	-1.0	0.3
5	-9.7	-0.6	1.0	-1.2	0.0	-4.0	1.1	-9.4	0.5	-0.8	0.6	-0.4
6	-8.3	0.8	-10.3	0.8	-4.0	0.0	-0.5	0.8	-0.2	0.3	-0.4	0.3
7	-0.1	-2.0	0.4	-0.4	1.1	-0.5	0.0	-3.6	1.0	-1.9	-6.6	-7.0
8	-1.5	0.5	-0.5	0.5	-9.4	0.8	-3.6	0.0	-2.0	-8.5	-0.7	0.9
9	0.4	-0.4	0.2	-0.3	0.5	-0.2	1.0	-2.0	0.0	-10.3	0.9	-11.6
10	-0.4	0.4	-0.3	0.3	-0.8	0.3	-1.9	-8.5	-10.3	0.0	-0.9	1.3
11	0.8	-9.4	0.6	-1.0	0.6	-0.4	-6.6	-0.7	0.9	-0.9	0.0	-1.4
12	-0.5	0.7	-0.2	0.3	-0.4	0.3	-7.0	0.9	-11.6	1.3	-1.4	0.0

B

TM Helix Assembly Pathway

Step	ΔG_{assoc}	Assembly
1	-14.7	3+4
2	-30.0	2+(3+4)
3	-42.1	1+(2+(3+4))
4	-52.7	(1+(2+(3+4)))+5
5	-73.8	((1+(2+(3+4)))+5)+6
6	-10.3	9+10
7	-20.8	8+(9+10)
8	-25.3	7+(8+(9+10))
9	-110.3	(((1+(2+(3+4)))+5)+6)+(7+(8+(9+10)))
10	-126.5	((((1+(2+(3+4)))+5)+6)+(7+(8+(9+10))))+11
11	-144.1	(((((1+(2+(3+4)))+5)+6)+(7+(8+(9+10))))+11)+12
Pathway		((((((1+(2+(3+4)))+5)+6)+(7+(8+(9+10))))+11)+12)

Figure S5. Free association energies of TM α-helical (TMH) segments (A) and their most likely association pathway **(B)**, estimated using the TMPfold method/server (Lomize et al., 2020) for zebrafish Oatp1d1 protein.

Table S2 Coordinates of the grid centers and sizes of grids used for docking calculations.

Docking	X	Y	Z
Blind docking	-0.415	0.382	-0.314
Central pore	-1.165	-7.681	3.357
Size of grid (Å)			
Blind docking	126	126	126
Central pore	48	68	50

Table S3 Analysis summary of multiple unpaired t test of *oatp1d1* expression in embryonal stages. Normality of data was tested using Shapiro-Wilk test (alpha=0.05). Statistically significant differences marked in pink.

stage	Discovery?	P value	Mean of WT	Mean of Oatp1d1	Difference	SE of difference	t ratio	df	q value
6 hpf	No	0.014365	2157	4203	-2046	247.9	8.253	2	0.021763
1 dpf	Yes	0.004477	80001	1682	78319	550.8	142.2	1	0.009044
2 dpf	No	0.685221	7730	8082	-351.9	818.7	0.4298	5	0.519055
3 dpf	Yes	0.000464	9652	4150	5502	968.2	5.682	8	0.001405
4 dpf	Yes	0.000027	12054	5607	6446	563.2	11.45	6	0.000162
5 dpf	No	0.029488	33236	4095	29141	7430	3.922	3	0.03162
6 dpf	No	0.031307	5630	4493	1137	454.3	2.503	10	0.03162
7 dpf	No	0.195387	7322	24463	-17141	11765	1.457	6	0.169149

Table S4 Analysis summary of multiple unpaired t test of *oatp1d1* expression in males. Normality of data was tested using Shapiro-Wilk test (alpha=0.05). Statistically significant differences marked in pink.

Tissue	Discovery?	P value	Mean of WT	Mean of Oatp1d1	Difference	SE of difference	t ratio	df	q value
liver	Yes	0.00548	349618	30766	318851	23700	13.45	2	0.009685
kidney	No	0.061362	1403	875.6	527.4	137	3.849	2	0.054229
gut	Yes	0.001068	47217	6340	40876	1337	30.57	2	0.003777
brain	Yes	0.000278	69704	15962	53742	896.4	59.95	2	0.001966
testis	No	0.425804	3768	3876	-108	108.9	0.9918	2	0.301043

Ocjena rada u tijeku

gills	No	0.014593	54662	1492	53170	6494	8.187	2	0.014739
eye	No	0.013385	11626	2345	9281	1085	8.557	2	0.014739
skin	Yes	0.002968	1973	571.5	1402	76.53	18.31	2	0.006995
muscle	No	0.096225	6565	3620	2945	986.3	2.986	2	0.07559
heart	No	0.007751	2912	394.2	2518	223	11.29	2	0.010959

Table S5. Analysis summary of multiple unpaired t test of *oatp1d1* expression in females. Normality of data was tested using Shapiro-Wilk test (alpha=0.05). In each tissue *oatp1d1* expression was significantly lower in Oatp1d1 mutant females.

Tissue	Discovery?	P value	Mean of WT	Mean of Oatp1d1	Difference	SE of difference	t ratio	df	q value
liver	Yes	0.000898	72698	2806	69892	2096	33.35	2	0.000227
kidney	Yes	0.054845	2230	1456	774.6	189.3	4.092	2	0.006155
gut	Yes	0.000024	59638	4567	55071	271.3	203	2	0.000025
brain	Yes	0.00165	61178	15494	45684	1858	24.59	2	0.000278
ovaries	Yes	0.004832	5814	1394	4420	308.4	14.33	2	0.00061
gills	Yes	0.000131	26426	1449	24976	285.7	87.43	2	0.000066
eye	Yes	0.000688	15708	2756	12952	340	38.1	2	0.000227
skin	Yes	0.003272	4921	2240	2681	153.8	17.44	2	0.000472
muscle	Yes	0.001452	20071	1876	18196	694	26.22	2	0.000278

Table S6 Analysis summary of multiple unpaired t test of fluorescence signal of the matrix of zebrafish embryos. Normality of data was tested using Shapiro-Wilk test (alpha=0.05). At each stage, the fluorescence of the matrix of Oatp1d1 embryos differed significantly from the fluorescence of the matrix of WT embryos.

stage	Discovery?	P value	Mean of WT	Mean of Oatp1d1	Difference	SE of difference	t ratio	df	q value
6 hpf	Yes	0.015585	11	14.5	-3.5	0.866	4.041	4	0.001431
1 dpf	Yes	0.000621	130.5	15	115.5	11.85	9.747	4	0.000070
2 dpf	Yes	<0.000001	5826	26	5800	89.99	64.45	4	<0.000001
2 dpf PTU	Yes	0.005363	1831	18.33	1813	330.2	5.49	4	0.000542
4 dpf	Yes	0.000108	19378	27.67	19350	1269	15.25	4	0.000018
5 dpf	Yes	0.000335	24508	44.5	24463	2142	11.42	4	0.000042

Ocjena rada u tijeku

6 dpf	Yes	0.000160	19438	35	19403	1407	13.79	4	0.000023
11 dpf	Yes	<0.000001	10188	45.33	10142	105	96.62	4	<0.000001
12 dpf	Yes	0.000021	11926	37.5	11888	514.5	23.11	4	0.000004
18 dpf	Yes	0.000020	3694	85.17	3609	154.8	23.31	4	0.000004
2 mpf	Yes	0.000002	12261	1202	11060	276.4	40.01	4	<0.000001

Table S7 Analysis summary of Ordinary one-way ANOVA, Tukey`s multiple comparisons test of changes in the locomotor activity of Oatp1d1 mutant embryos (5 dpf) exposed to PFOS. Statistically significant differences marked in pink.

Tukey's multiple comparisons test	Mean Diff.	95.00% CI of diff.	Below threshold?	Summary	Adjusted P Value
wt ctrl dan vs. 1d1 ctrl dan	53.64	-117.1 to 224.4	No	ns	0.9739
wt ctrl dan vs. wt+pfos dan	44.01	-126.7 to 214.8	No	ns	0.9917
wt ctrl dan vs. 1d1+ pfos dan	20.11	-156.6 to 196.9	No	ns	>0.9999
wt ctrl dan vs. wt ctrl noc	-436.8	-607.6 to -266.0	Yes	****	<0.0001
wt ctrl dan vs. 1d1 ctrl noc	-230.3	-401.0 to -59.51	Yes	**	0.002
wt ctrl dan vs. wt + pfos noc	-275.3	-446.0 to -104.5	Yes	***	0.0001
wt ctrl dan vs. 1d1+ pfos noc	17.64	-159.1 to 194.4	No	ns	>0.9999
1d1 ctrl dan vs. wt+pfos dan	-9.63	-180.4 to 161.1	No	ns	>0.9999
1d1 ctrl dan vs. 1d1+ pfos dan	-33.54	-210.3 to 143.2	No	ns	0.9988
1d1 ctrl dan vs. wt ctrl noc	-490.4	-661.2 to -319.7	Yes	****	<0.0001
1d1 ctrl dan vs. 1d1 ctrl noc	-283.9	-454.7 to -113.2	Yes	****	<0.0001
1d1 ctrl dan vs. wt + pfos noc	-328.9	-499.7 to -158.2	Yes	****	<0.0001
1d1 ctrl dan vs. 1d1+ pfos noc	-36	-212.8 to 140.8	No	ns	0.9981
wt+pfos dan vs. 1d1+ pfos dan	-23.91	-200.7 to 152.8	No	ns	0.9999
wt+pfos dan vs. wt ctrl noc	-480.8	-651.6 to -310.1	Yes	****	<0.0001
wt+pfos dan vs. 1d1 ctrl noc	-274.3	-445.0 to -103.5	Yes	***	0.0001
wt+pfos dan vs. wt + pfos noc	-319.3	-490.1 to -148.5	Yes	****	<0.0001
wt+pfos dan vs. 1d1+ pfos noc	-26.37	-203.1 to 150.4	No	ns	0.9997
1d1+ pfos dan vs. wt ctrl noc	-456.9	-633.7 to -280.2	Yes	****	<0.0001

Ojena rada

1d1+ pfos dan vs. 1d1 ctrl noc	-250.4	-427.1 to -73.62	Yes	**	0.001
1d1+ pfos dan vs. wt + pfos noc	-295.4	-472.1 to -118.6	Yes	****	<0.0001
1d1+ pfos dan vs. 1d1+ pfos noc	-2.464	-185.0 to 180.1	No	ns	>0.9999
wt ctrl noc vs. 1d1 ctrl noc	206.5	35.77 to 377.3	Yes	**	0.0079
wt ctrl noc vs. wt + pfos noc	161.5	-9.243 to 332.3	No	ns	0.0763
wt ctrl noc vs. 1d1+ pfos noc	454.4	277.7 to 631.2	Yes	****	<0.0001
1d1 ctrl noc vs. wt + pfos noc	-45.02	-215.8 to 125.7	No	ns	0.9905
1d1 ctrl noc vs. 1d1+ pfos noc	247.9	71.16 to 424.7	Yes	**	0.0012
wt + pfos noc vs. 1d1+ pfos noc	292.9	116.2 to 469.7	Yes	****	<0.0001

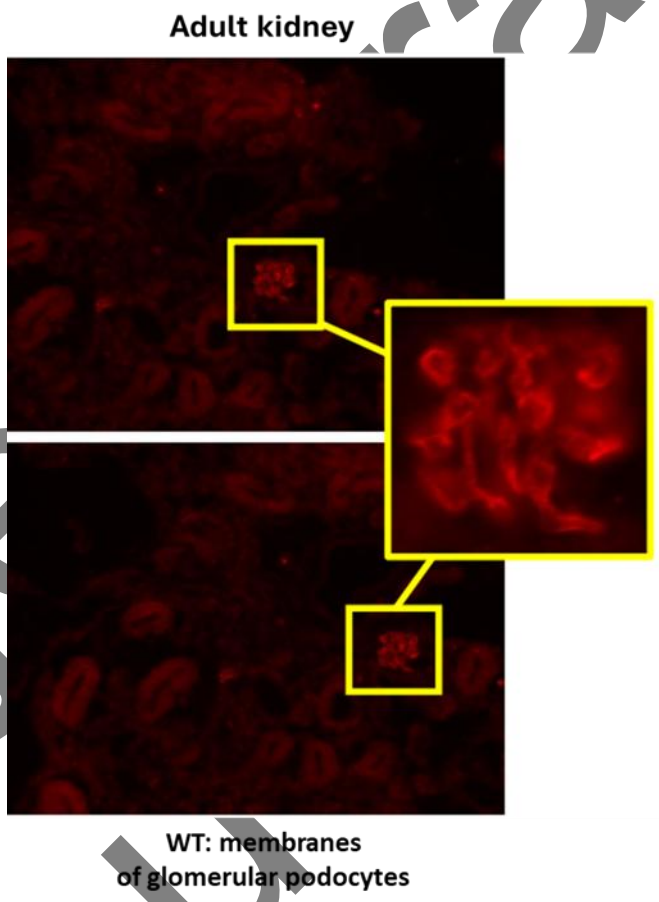

Figure S6. Immunohistological localization of Oatp1d1 in adult kidney of wild type zebrafish. Localization of positive (Cy3) signal in membranes of glomerular podoytes.

Ociejus.gu.se

Family	Gene	WT	mutant	WT	mutant	WT	mutant	WT	mutant	WT	mutant
slc21	*oatp1d1*	5601 ± 4350	6766 ± 4594	9147 ± 339	2527 ± 475	9539 ± 475	6117 ± 2113	18309 ± 5994	11547 ± 4454	65512 ± 21906	5528 ± 1358
	oatp2b1	2574 ± 1572	4877 ± 2282	8784 ± 150	3687 ± 636	46757 ± 3098	19628 ± 651	45446 ± 2705	28876 ± 10646	46186 ± 1541	27252 ± 982
	oatp5a2	n/a	n/a	145 ± 19	110 ± 19	171 ± 19	196 ± 19	200 ± 19	215 ± 19	254 ± 19	76 ± 19
	oatp1f2	56 ± 31	452 ± 47	40 ± 5	67 ± 22	488 ± 134	214 ± 49	115 ± 24	142 ± 36	199 ± 62	117 ± 27
slc22	*oat1*	13443 ± 7582	6486 ± 1954	662 ± 137	313 ± 19	1922 ± 587	2232 ± 756	1247 ± 411	3908 ± 1573	2430 ± 585	1252 ± 71
	oat2a	9645 ± 6259	8111 ± 1506	17761 ± 1123	7154 ± 2842	36675 ± 1777	13296 ± 4072	29064 ± 7453	14969 ± 4828	21517 ± 1085	9463 ± 1510
	oat2c	296 ± 71	874 ± 118	99 ± 18	152 ± 20	583 ± 123	154 ± 7	925 ± 166	3106 ± 212	1829 ± 81	2307 ± 270
	oat2d	1098 ± 104	7382 ± 1019	537 ± 169	2232 ± 220	2358 ± 333	577 ± 139	425 ± 31	1058 ± 373	1980 ± 874	1863 ± 357
	oat2e	602 ± 51	1573 ± 386	2589 ± 315	1204 ± 183	3285 ± 232	1873 ± 337	1811 ± 129	6803 ± 214	4072 ± 909	1704 ± 274
	oat3	271 ± 207	761 ± 516	39 ± 8	46 ± 3	341 ± 104	311 ± 105	863 ± 284	3078 ± 1238	2264 ± 545	2123 ± 121
Developmental stage		1 dpf		2 dpf		3 dpf		4 dpf		5 dpf	

Transcript expression levels

Minimal	1 - 999 *10^6
Low	1000 - 4999
Mild	5000 - 8999
Moderate	9000 - 19999
Moderately high	20000 - 29999
High	30000 - 49999
Very high	50000 -

Figure S7. Transcript expression patterns of *oatp1d1, oatp2b1, oatp5a2, oatp1f2, oat1, oat2a, oat2c, oat2d, oat2e* and *oat3* in WT and mutant embryos during initial five days of development. Heatmap representation of gene expression differences between WT and mutant embryos. Results of two to three independent determinations for each developmental stage (pools of 10 embryos) are presented. Data represents MNE (mean normalized expression) ± SE normalized to the ATP50.

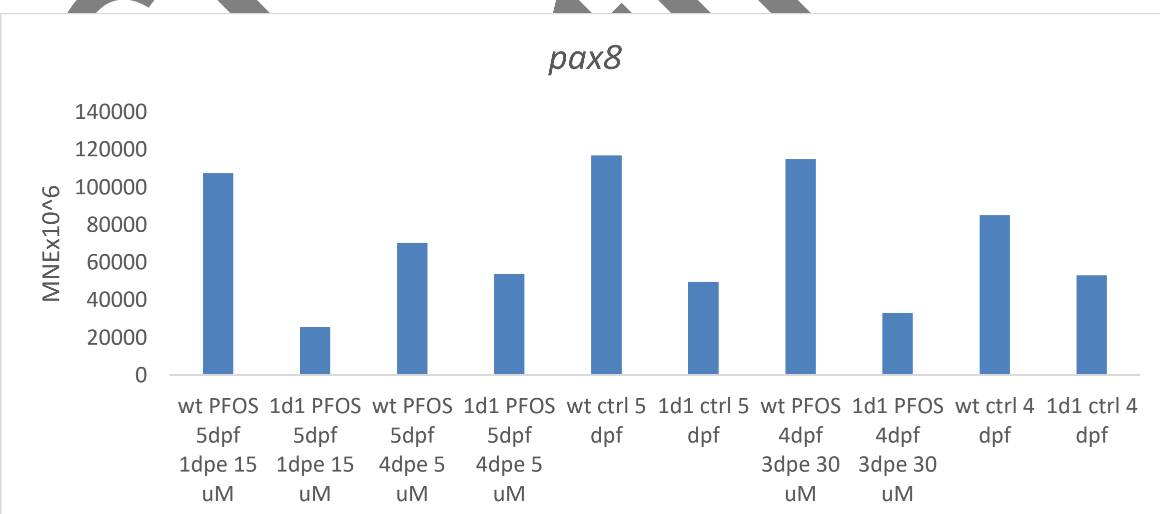

Figure S8. Preliminary results of pax8 expression in WT and Oatp1d1 embryos, with and without exposure to PFOS.

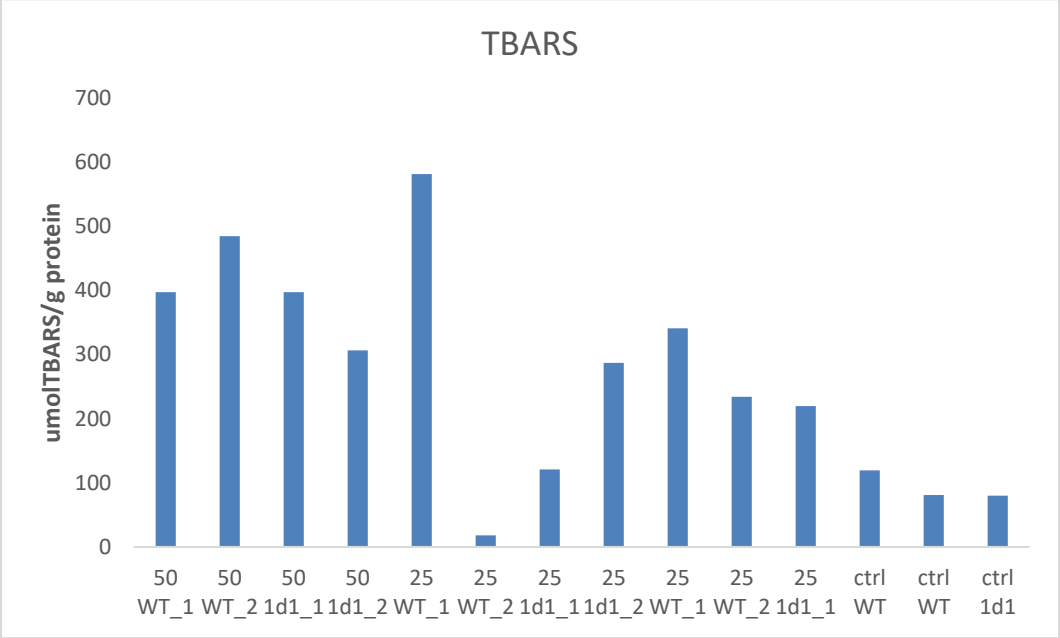

Figure S9. Optimisation of TBARS assay. Embryos WT and Oatp1d1 exposed to diclofenac (50 and 25 µM). Difference between exposed and unexposed embryos is evident. Data was not reproducible.

Ocjena u tijeku

11. AUTHOR BIOGRAPHY

Name: Lana Vujica
E-mail: lana.vujica@irb.hr
Date and place of birth: 12.12.1996.

Education:

2020 – **University Postgraduate Interdisciplinary Doctoral Study**, Molecular Biosciences.
J. J. Strossmayer University of Osijek, University of Dubrovnik, Ruđer Bošković Institute, Zagreb.

2018. — 2020. **mag. oecol., Prirodoslovno-matematički fakultet, Sveučilište u Zagrebu, Biološki odsjek, Zagreb, Croatia.** „Distribution of rare earth elements in fruiting bodies of summer truffle (*Tuber aestivum*)" master thesis

2015. — 2018. **univ. bacc. oecol, univ. bacc. oecol., Faculty of Science, Department of Biology, (GPA)** "Alpine newt (*Ichthyosaura alpestris*)", bachelor degree

Publications:

1. **Vujica, Lana**; Mihaljević, Ivan; Dragojević, Jelena; Lončar, Jovica; Karaica, Dean; Dananić, Ana; Bošnjak, Arvena; Smital, Tvrtko Functional knockout of the Oatp1d1 membrane transporter affects toxicity of diclofenac in zebrafish embryos, Aquatic Toxicology, Volume 273, 2024. https://doi.org/10.1016/j.aquatox.2024.107031.

2. **Vujica, Lana**; Lončar, Jovica; Mišić, Lana; Lučić, Bono; Radman, Katarina; Mihaljević, Ivan; Bertoša, Branimir; Mesarić, Josip; Horvat, Marina; Smital, Tvrtko Environmental contaminants modulate transport activity of zebrafish (Danio rerio) multidrug and toxin extrusion protein 3 (Mate3/Slc47a2.1) // Science of the total environment, 901 (2023), doi:0.1016/j.scitotenv.2023.165956.

3. Karaica, Dean; Mihaljević, Ivan; **Vujica, Lana**; Bošnjak, Arvena; Dragojević, Jelena; Otten, Cecile; Babić, Nency; Lončar, Jovica; Smital, Tvrtko, Stage-dependent localization of F-actin and <scp> Na ⁺ /K ⁺ </scp> - <scp>ATPase</scp> in zebrafish embryos detected using optimized cryosectioning immunostaining protocol // Microscopy research and technique, 2022 (2022), 1-17. doi: 10.1002/jemt.24270

4. Mihaljević, Ivan; **Vujica, Lana**; Dragojević, Jelena; Lončar, Jovica; Smital, Tvrtko Differential Toxicity of Perfluorooctane Sulfonate (PFOS) in Wild-Type and Oatp1d1 Mutant Zebrafish Embryos, bioRxiv 2024.06.28.601146; doi: https://doi.org/10.1101/2024.06.28.601146 (*bioarchive*)

Conferences:

1. **Vujica, Lana**; Mihaljević, Ivan; Dragojević, Jelena; Lončar, Jovica; Smital, Tvrtko Phenotype changes in zebrafish Oatp1d1 mutants, PRIMO 22; 26. – 29.05.2024., Nantes, France. **(poster)**

Ocjena rada u tijeku

2. **Vujica, Lana** Karakterizacija SLC i MATE transportnih proteina zebrice (*Danio rerio*), 1.Skup mladih znanstvenika ZIMO-a; 11.12.2023. (oral presentation)

3. **Vujica, Lana**; Lončar, Jovica; Mišić, Lana; Lučić, Bono; Radman, Katarina; Mihaljević, Ivan; Bertoša, Branimir; Mesarić, Josip; Horvat, Marina; Smital, Tvrtko First in vitro and in silico characterization of zebrafish (*Danio rerio*) multidrug and toxin extrusion protein 3 (Mate3/Slc47a2.1), 12th European Zebrafish Meeting July 09. – 13.07.2023; Krakow, Poland. (oral presentation)

4. **Vujica, Lana**; Mišić, Lana; Horvat, Marina; Lončar, Jovica; Mihaljević, Ivan; Smital, Tvrtko Interaction of Environmental Contaminants with Zebrafish (*Danio rerio*) Multidrug and Toxin Extrusion Protein 3 (Mate3/Slc47a2.1), HDBMB22: From Science to Knowledge 28.09. – 01. 10. 2022, Brela, Croatia. (poster)

5. **Vujica, Lana**; Mišić, Lana; Horvat, Marina; Lončar, Jovica; Mihaljević, Ivan; Smital, Tvrtko: Interaction of environmental contaminants with zebrafish (*Danio rerio*) multidrug and toxin extrusion protein 3 (Mate3/Slc47a3). PRIMO21, The 21th International Symposium on Pollutant Responses in Marine Organisms, Gothenburg, Sweeden, 22. – 25.05.2022. (poster)

6. **Vujica, Lana**: Establishment of complete oct1 and oatp1d1 knockout mutants in zebrafish. Transporttage 2021., Greiswald, Njemačka. 01. – 03.2021.(oral presentation)

Awards:

1. **Best poster award: Vujica, Lana**; Mihaljević, Ivan; Dragojević, Jelena; Lončar, Jovica; Smital, Tvrtko Phenotype changes in zebrafish Oatp1d1 mutants, PRIMO 22; 26. – 29.05.2024., Nantes, France.
2. **12th European Zebrafish Meeting Grant** (12th European Zebrafish Meeting July 09. – 13.07.2023; Krakow, Poljska)
3. **PRIMO21 Student Travel Grant 2022 (**PRIMO21, The 21th International Symposium on Pollutant Responses in Marine Organisms, Gothenburg, Švedska, 22. – 25.05.2022.)

Proffesional experiences and training:

1. **Laboratory practice at the Ruđer Bošković Institute,** Laboratory for inorganic environmental geochemistry and chemodynamics of nanoparticles, 2019–2020.
2. **Laboratory practice at Aquatika – Freshwater Aquarium, Karlovac,** 2018.
3. **Teaching Assistant in Vertebrata Practicum** 2017./2018.
   Faculty of Science, University of Zagreb – Department of Biology

Courses:

1. Tečaj primijenjene statistike za mlade znanstvenike ZIMO-a, Ruđer Bošković Institute, 18.10, 25.10, 30.10., 8.11., 15.11.2024.
2. Young leaders 2024: Empowering young group leaders for scientific leadership, Ruđer Bošković Institute, 10.10.-11. 10., 08.11.-09.11., 09.12.-10.12.2024.
3. Zašto ići putem inovacija i komercijalizacije?, Croatian Association for Cancer Research (CACR) and Ruđer Bošković Institute 27. 03. 2023.
4. Uvod u molekulsko modeliranje, Croatian Association for Cancer Research and Ruđer Bošković Institute, 8., 9., 12.12.2022.
5. EMBO Workshop on Research Integrity, Ruđer Bošković Institute, 20.10.2022**.**

Ocjena rada u tijeku

Science popularization:

1. **Otvoreni dan (Frizbijada)** – Ruđer Bošković Institute, student guide, 02.06.2023.
2. **MUZZA 3. Tjedan znanosti** Open Mind 12. - 14.04.2024. Presenter.

Participation in organizing committees:

1. **Workshop organization** - Zebrafish (Danio rerio) as a model organism in biological, biomedical and environmental research, Institute for Medical Research and Occupational Health, Zagreb, 5.6.2024.
2. **Organization of guest talks and pub quiz at IRB as member of Union**

Memberships:

Penkala
Young Researchers
Independent Union of Science and Higher Education Employees of Croatia
Croatian Association for Cancer Research (CACR)
The Croatian Society of Biochemistry and Molecular Biology
Croatian Biophysical Society
Croatian Genetic Society

Ocjena rada u tijeku